

*Comprehensive Nuclear Model Calculations:  
Introduction to the Theory  
and Use of the GNASH Code*

*P. G. Young  
E. D. Arthur  
M. B. Chadwick*

MASTER

Los Alamos Los Alamos National Laboratory  
Los Alamos, New Mexico 87545

## CONTENTS

ABSTRACT .....	1
I. THE GNASH NUCLEAR THEORY CODE - OVERVIEW AND THEORETICAL MODELS.....	1
A. Introduction .....	1
B. Summary Description of GNASH.....	2
C. General Theoretical and Computational Approach.....	3
1. Hauser-Feshbach formulation.....	3
2. Computational structure.....	7
3. Corrections.....	8
D. Nuclear Models Utilized by GNASH.....	9
1. Optical model particle transmission coefficients.....	9
2. Gamma-ray strength functions.....	10
a. Weisskopf approximation.....	10
b. Brink-Axel standard Lorentzian.....	11
c. Kopecky-Uhl generalized Lorentzian.....	11
3. Level density models.....	13
a. Gilbert-Cameron model.....	14
b. Backshifted Fermi-gas model.....	16
c. Ignatyuk form of Fermi-gas model.....	16
4. Preequilibrium and direct reaction effects.....	17
a. Nucleon preequilibrium.....	18
b. Photon preequilibrium emission.....	21
c. Composite particle preequilibrium.....	22
d. Flux adjustment for preequilibrium contributions.....	23
e. Correction for direct reactions.....	24
5. Description of the fission barrier model in GNASH.....	24
II. DESCRIPTION OF THE INPUT DATA AND OUTPUT RESULTS FROM GNASH.....	26
A. General Comments on Input and Output .....	26
B. Description of Necessary Auxiliary Parameter Files.....	27
1. Ground-state spins, parities, and masses (TAPE13).....	27
2. Nuclear structure data (TAPE8).....	28
3. Particle transmission coefficients (TAPE10).....	28
C. Input or Calculation Directory File (INPUT).....	29

D.	Optional Auxiliary File for Inputting Direct Reaction Cross Sections, Width Fluctuation Corrections, and Tabulated Gamma-Ray Strength Functions (TAPE33)..	31
E.	Description of Output Data.....	32
1.	Main OUTPUT file from $n + {}^{93}\text{Nb}$ .....	32
a.	Nuclear masses, reaction sequencing, and parentage information.....	32
b.	Gamma-ray strength function information.....	33
c.	Preequilibrium spectra.....	33
d.	Ratios of preequilibrium to reaction cross sections.....	33
e.	Binary reaction cross sections.....	34
f.	Angle-integrated emission spectra for individual reactions.....	34
g.	Composite particle and gamma-ray angle-integrated spectra.....	35
h.	Discrete level cross sections: primary capture gamma-ray, level excitation, discrete gamma, and isomer production cross sections.....	36
i.	Level density parameters and matching data.....	37
2.	Binary output of continuum and level populations.....	39
3.	Auxiliary output files of discrete level and preequilibrium gamma-ray data.....	39
F.	Utility Codes for Analyzing GNASH Output.....	39
III.	DESCRIPTION OF THE STRUCTURE OF THE GNASH CODE.....	39
A.	General Description of the Computational Approach.....	39
B.	Identification and Description of the Most Important Subroutines .....	40
C.	Discussion of the SPECTRA Subroutine.....	43
D.	Summary of General Guidelines for Calculations with GNASH.....	44
E.	Examples of Calculations with GNASH.....	45
1.	Examples of discrete/continuum level density matching.....	45
2.	Neutron-, proton-, and alpha-induced reactions near $A = 56$ .....	45
3.	$n + {}^{93}\text{Nb}$ reactions.....	45
4.	$n + {}^{238}\text{U}$ and $p + {}^{238}\text{U}$ results.....	45
5.	Neutron-induced reactions on Pb isotopes.....	46
IV.	HIGHLIGHTS OF THE MULTIBARRIER FISSION MODEL IN GNASH, AND PLANS FOR FUTURE DEVELOPMENTS OF THE CODE.....	46
A.	Fission Model.....	46
1.	Description of the fission model in GNASH.....	46
2.	Input example for fission cross section calculation.....	46
3.	Output example from fission calculation.....	47
a.	Input data.....	47
b.	Reaction labeling, reaction parentage, masses, buffer numbers.....	47

c.	Fission barrier parameters.....	48
d.	Direct reaction cross section data.....	48
e.	Preequilibrium information.....	48
f.	Binary cross sections.....	48
g.	Individual reaction spectra for $n + {}^{238}\text{U}$ calculations.....	49
h.	Composite spectra for emission particles and gamma rays.....	49
i.	Level density information for $n + {}^{238}\text{U}$ calculations.....	49
B.	Plans for Future Developments.....	50
1.	Cross sections from multiple preequilibrium processes.....	50
2.	Automation of calculation of collective effects.....	50
3.	Photon-induced reactions.....	50
4.	Fission fragment calculations.....	50
5.	Increase user friendliness and generally tidy up coding.....	50
REFERENCES	.....	51
FIGURES	.....	56
APPENDICES	.....	96
Appendix 1.	Sample of Data in Ground-State Mass, $J^\pi$ File (TAPE13).....	96
Appendix 2.	Discrete Level File (TAPE8) Input Parameters.....	97
Appendix 3.	Transmission Coefficient File (TAPE10).....	99
Appendix 4.	GNASH Input File Description.....	101
Appendix 5.	$n + {}^{93}\text{Nb}$ Problem Sample Input.....	114
Appendix 6.	TAPE 33 Input Description.....	116
Appendix 7.	Selected Portions of Main Output File from $n + {}^{93}\text{Nb}$ Calculation.....	118
Appendix 8.	$n + {}^{238}\text{U}$ Problem Sample Input.....	139
Appendix 9.	Selected Portions of Output File from $n + {}^{238}\text{U}$ Calculation.....	145

# COMPREHENSIVE NUCLEAR MODEL CALCULATIONS: INTRODUCTION TO THE THEORY AND USE OF THE GNASH CODE

P. G. Young, E. D. Arthur, and M. B. Chadwick

## ABSTRACT

A user's manual describing the theory and operation of the GNASH nuclear reaction computer code is presented. This work is based on a series of lectures describing the statistical Hauser-Feshbach plus preequilibrium version of the code with full angular momentum conservation. This version is expected to be most applicable for incident particle energies between 1 keV and 50 MeV. General features of the code, the nuclear models that are utilized, input parameters needed to perform calculations, and the output quantities from typical problems are described in detail. The computational structure of the code and the subroutines and functions that are called are summarized as well. Two detailed examples are considered: 14-MeV neutrons incident on  $^{93}\text{Nb}$  and 12-MeV neutrons incident on  $^{238}\text{U}$ . The former example illustrates a typical calculation aimed at determining neutron, proton, and alpha emission spectra from 14-MeV reactions, and the latter example demonstrates use of the fission model in GNASH.

---

## I. THE GNASH NUCLEAR THEORY CODE - OVERVIEW AND THEORETICAL MODELS

### A. Introduction

The first version of the GNASH nuclear theory code was completed in 1974. The code has been developed continually since that time and has been used often to supply various types of nuclear data for applications. While the original structure of the code has remained largely unchanged, many improvements have been made over the years, including the addition of preequilibrium corrections and a multiple barrier fission model. Several versions of the code are in use, including one adapted for use in generating activation cross sections for the Japanese fusion program,<sup>1</sup> and two versions with modifications and approximations suitable for higher energy calculations.<sup>2</sup> The code described here is referred to as the statistical Hauser-Feshbach plus preequilibrium version with full angular momentum conservation.

The first documentation of GNASH occurred in 1977.<sup>3</sup> The present work summarizes a series of lectures and computer exercises presented by Young at the International Centre for Theoretical Physics (ICTP) in Trieste.<sup>4</sup> A similar set of lectures was given by Arthur in 1988.<sup>5</sup>

Section I summarizes general features of the GNASH code, the computational approach, and the nuclear models used in the code. Section II describes in detail the input parameters required for the code and explains the various quantities that appear in the GNASH output. An input setup and the resulting output for  $n + {}^{93}\text{Nb}$  reactions are used as examples. Section III provides a detailed description of the structure of the code, including summaries of the major subroutines and algorithms that are used. The final section (Sec. IV) covers the fission model in GNASH and details the input and output from calculations of  $n + {}^{238}\text{U}$  reactions. Also included in the final section is a discussion of future improvements planned for the code.

Four computer exercise sessions were held in conjunction with the ICTP lectures, and input and output files from these exercises are available from the Radiation Shielding Information Center at Oak Ridge and from the Nuclear Energy Agency Data Bank in Paris. In addition to the examples described here, sample inputs and outputs are included for calculation of  $(n,\gamma)$ ,  $(n,n')$ ,  $(n,p)$ , and  $(n,\alpha)$  cross sections from neutron interactions with  ${}^{93}\text{Nb}$  at lower energies, calculations for incident neutrons, protons, and alpha particles up to 40 MeV on  ${}^{56}\text{Fe}$  and  ${}^{55}\text{Mn}$ , and proton-induced calculations on  ${}^{238}\text{U}$ . Using these examples, simple exercises can be performed such as observing the effects on calculations of varying level densities,  $\gamma$ -ray strength functions, and preequilibrium parameters. Additionally, the code capabilities for handling more complicated reaction chains that are required at higher energies are illustrated by the examples.

## B. Summary Description of GNASH

GNASH implements Hauser-Feshbach theory in an open-ended sequence of reaction chains, limited in number only by the memory and speed of the computer being utilized. The version of the code used in the ICTP exercises is dimensioned for 10 primary compound nuclei. Up to 6 types of radiation can be emitted from each compound system, so that a maximum of 60 reaction paths can be handled in a single calculation. The reaction chain followed in the  $n + {}^{93}\text{Nb}$  calculations of Exercise 1 is illustrated in Fig. 1. Note that the chains involving deuteron emission are dashed because they are not included in the sample calculation but their addition would be straightforward. (Much more complicated configurations have been calculated at higher energies using a faster evaporation version of the code.) Width fluctuation and preequilibrium corrections including surface effects can be applied to the decay channels of the initial compound nucleus. Three model choices are available for continuum level densities and for gamma-ray strength functions. Maximum use is made of experimental structure information for all residual nuclei

occurring in a given calculation. For actinide studies, the code contains a rather detailed fission model, allowing use of up to three uncoupled fission barriers.

The primary output from GNASH are absolute angle-integrated particle and gamma-ray spectra plus excitation and deexcitation cross sections of discrete states. The calculated spectra are integrated and summed, so that absolute reaction cross sections are readily obtained. The present configuration of the code permits the following incident particle types: neutrons, protons, deuterons, tritons,  $^3\text{He}$ , and  $^4\text{He}$ . The same particles are permitted in decay channels as well as gamma rays. Examples of reactions for which cross sections and emission spectra can be calculated are  $(n,p)$ ,  $(n,d)$ ,  $(n,\alpha)$ ,  $(n,xn)$ ,  $(n,xn\gamma)$ ,  $(p,xn\gamma)$ ,  $(\alpha, px\alpha\gamma)$ , etc. In Fig. 2, a schematic is given that illustrates in more detail the first several reactions possible from the  $n + ^{93}\text{Nb}$  example of Fig. 1. In particular, an energy diagram is given that shows the binary and  $(n,2n)$  reactions from the main compound nucleus.

The code has been used for calculations at energies as low as 0.1 keV and as high as 100 MeV. The models utilized are expected to be most applicable for the energy range 1 keV to 50 MeV. Angular effects are not included in the calculations, as the results are normally used in combination with the systematics-based parameterization of Kalbach<sup>6</sup> to determine angular distributions. For that purpose, the code provides tables of ratios of preequilibrium to total emission cross sections as functions of emission energy for all outgoing particles, which are required for applying the Kalbach relations.

GNASH has been used at Los Alamos to support data evaluations for a number of materials, including ENDF/B-V and VI evaluations for  $^{182,183,184,186}\text{W}$ ,  $^{151,153}\text{Eu}$ ,  $^{165}\text{Ho}$ ,  $^{185,187}\text{Re}$ ,  $^{237}\text{Np}$ ,  $^{235,238}\text{U}$ , and  $^{239,240}\text{Pu}$  (Ref. 7). It was utilized for comprehensive analyses of neutron-induced reactions with  $^{89}\text{Y}$  and  $^{90}\text{Zr}$  (Ref. 8), and for calculations up to 40 MeV for  $^{56}\text{Fe}$  (Ref. 9), to 50 MeV for  $^{59}\text{Co}$  (Ref. 10), and to 100 MeV for  $^{208}\text{Pb}$  (Ref. 11). Additionally, the full angular momentum version was used extensively up to about 50 MeV in generating neutron- and proton-induced transport libraries to higher energies for  $^{27}\text{Al}$ ,  $^{28}\text{Si}$ ,  $^{56}\text{Fe}$ ,  $^{184}\text{W}$ , and  $^{238}\text{U}$  (Ref. 12). When GNASH is used for data evaluation work, a series of utility codes are normally used to extract and format data from the outputs, as summarized in Sec. II.F.

## C. General Theoretical and Computational Approach

### 1. Hauser-Feshbach formulation

Although many theoretical models are utilized, the Hauser-Feshbach statistical model provides the basic underpinning for the GNASH code. The discussion here follows closely the description and nomenclature of Uhl<sup>13</sup> and the references contained therein. The principal assumption used in the calculation of cross sections and emission spectra from complex reaction

processes is that the reaction proceeds in a series of binary reaction stages, and at each stage particle and gamma ray emission are calculated. The energetics of this process are illustrated schematically in Fig 3. An initial compound nucleus is formed with excitation energy  $U$ , spin  $J$ , and parity  $\Pi$ . This process (and all others occurring in the calculation) is subject to constraints imposed by the following conservation laws:

$$\begin{aligned}
 \varepsilon + B_a &= \varepsilon' + E' + B_{a'} = U && \text{[energy]} \\
 i + I + \ell &= i' + I' + \ell' = J && \text{[spin]} \\
 p * P * (-1)^\ell &= p' * P' * (-1)^{\ell'} = \Pi && \text{[parity]}
 \end{aligned}
 \tag{1}$$

where  $\varepsilon$  and  $\varepsilon'$  are center of mass energies of incoming and outgoing particles  $a$  and  $a'$ ;  $B_a$  and  $B_{a'}$  are binding energies of the particles relative to the compound system;  $i$ ,  $I$ ,  $p$ , and  $P$  are spins and parities associated with light particles and the heavier target or residual nucleus; and  $\ell$  is the orbital angular momentum. The primed quantities indicate the outgoing channel.

The statistical model predicts reaction cross sections averaged over many resonances in the intermediate nuclei. The mean angle-integrated cross section for formation of the final state ( $E'$ ,  $I'$ ,  $P'$ ) by means of the ( $a, a'$ ) reaction is given as

$$\sigma_{a,a'}(\varepsilon, I, P; E', I', P') = \sum_{J, \pi} \sigma_a(\varepsilon, I, P; U, J, \pi) \frac{\Gamma_{a'}(U, J, \pi; E', I', P')}{\Gamma(U, J, \pi)} ,
 \tag{2}$$

where  $(U, J, \pi)$  are the quantum numbers of the compound states through which the reactions proceed;  $\sigma_a(\varepsilon, I, P; U, J, \pi)$  is the reaction cross section for formation of the compound nucleus with quantum numbers  $(U, J, \pi)$ ; and  $\Gamma_{a'}(U, J, \pi; E', I', P')$  is the decay width of the compound nucleus into the state ( $E', I', P'$ ) of the residual nucleus by emission of the particle  $a'$ . The quantity  $\Gamma(U, J, \pi)$  is the total decay width of the compound nucleus state  $(U, J, \pi)$  and is the sum of all possible decay widths,

$$\Gamma(U, J, \pi) = \sum_{a''} \sum_{E'', I'', P''} \Gamma_{a''}(U, J, \pi; E'', I'', P'') ,
 \tag{3}$$

where the summation over  $a''$  includes all particles and gamma rays whose emission is energetically possible from  $(U, J, \pi)$ , and the second summation includes all possible states ( $E'', I'', P''$ ) in the various residual nuclei that result, consistent with the conservation laws given in Eq. (1).

The reaction cross section for formation of the compound nucleus can be expressed in terms of optical model transmission coefficients,  $T_l^a(\varepsilon)$ , as follows:



$$\sigma_a(\epsilon, I, P; U, J, \pi) = \frac{\pi}{k^2} \frac{(2J+1)}{(2I+1)(2i+1)} \sum_{S=|I-i|}^{I+i} \sum_{\ell=|J-S|}^{J+S} f_{\ell}(\ell, \pi) T_{\ell}^a(\epsilon), \quad (4)$$

where  $k$  is the wave number of relative motion,  $S$  indicates channel spin, and the function  $f(\ell, \pi)$  is unity if parity is conserved and zero otherwise, as provided by Eq. (1). Through use of the reciprocity theorem (detailed balance) of nuclear reactions, the decay widths can be related to the transmission coefficients:

$$\Gamma_a(U, J, \pi; E', I', P') = \frac{1}{2\pi\rho(U, J, \pi)} \sum_{S=|I'-I|}^{I'+I} \sum_{\ell=|J-S|}^{J+S} f_{\ell}(\ell, \pi) T_{\ell}^{a'}(U-E'-B_a) \quad (5)$$

where  $\rho(U, J, \pi)$  is the nuclear level density of the intermediate nucleus having the quantum numbers  $(U, J, \pi)$ . To obtain Eq. (5), the assumption is made that the optical model transmission coefficients, determined from analysis of experimental data on the ground states of nuclei, also describe the inverse reactions on excited states of the residual nuclei.

In general, the energies covered in GNASH calculations exceed the range where there is detailed information concerning discrete excited states. Thus, each nucleus occurring in a given calculation is assumed to be comprised of a series of known discrete levels having quantum numbers  $(E_k, J_k, P_k)$ , above which exists a continuum of levels described by a level density function,  $\rho(E, I, P)$ . Therefore, the summations in the above equations must be modified to include transitions in the continuum region. For example, the expression for the total decay width [Eq. (3)] becomes

$$\Gamma(U, J, \pi) = \sum_{a'} \sum_{I, P} \int_{E_c}^{U-B_a} dE \Gamma_{a'}(U, J, \pi; E, I, P) \rho(E, I, P) + \sum_k \Gamma_{a'}(U, J, \pi; E_k, I_k, P_k) \quad (6)$$

where the  $E_c$  is the lower excitation energy bound of the continuum region, and the  $k$  summation extends over the discrete states from  $E_x = 0$  to  $E_x = E_c$ .

In GNASH analyses, detailed calculations are made of the populations of discrete and continuum levels for all possible spins and parities. If  $\mathcal{P}^{(n)}(U, J, \pi)$  is the level population at excitation energy  $U$  in the  $n^{\text{th}}$  compound system, then the population in the  $(n+1)^{\text{th}}$  compound system formed by emission of particle ( $a'$ ) is given by

$$\mathcal{P}^{(n+1)}(U', J', \pi') = \rho^{(n+1)}(U', J', \pi') \sum_{J, \pi} \int_{U'+B_{a'}}^{U_{\max}} dU \mathcal{P}^{(n)}(U, J, \pi) \frac{\Gamma_{a'}^{(n)}(U, J, \pi; U', J', \pi')}{\Gamma(U, J, \pi)} \quad (7)$$

where  $U_{\max}$  is the maximum excitation energy attainable in the  $n^{\text{th}}$  compound nucleus, which depends on the incident projectile energy and the reaction path to that nucleus. The summation includes those values of  $(J, \pi)$  that can couple via Eq. (1) to form  $(J', \pi')$  levels in the compound nucleus  $(n+1)$ . It is understood that the integral in Eq. (7) also includes a sum over any discrete states in the  $n^{\text{th}}$  nucleus that are energetically able to contribute to  $\mathcal{P}^{(n+1)}(U', J', \pi')$ . Note that Eq. (7) also allows the explicit calculation of gamma-ray cascades if one considers the  $(n+1)^{\text{th}}$  and  $(n)^{\text{th}}$  compound systems to be the same, with emission channel ( $a'$ ) indicating gamma-ray emission.

The initialization of any decay sequence begins with the calculation of the cross section for formation of the first or primary compound nucleus. This cross section is determined from Eq. (4), and the population of the initial levels in the first compound nucleus is given simply by

$$\mathcal{P}^{(1)}(U, J, \pi) = \sigma_a(\epsilon, I, P; U, J, \pi) \delta(U - \epsilon - B_a) \quad (8)$$

The quantity  $\Gamma_{a'}^{(n)}(U, J, \pi; U', J', \pi')/\Gamma(U, J, \pi)$  in Eq. (7) represents the branching ratio of the partial width for decay by a given channel to a given  $(J, \pi)$  level relative to the total width for all possible decays. This branching ratio can be simply expressed in terms of transmission coefficients as follows:

$$\frac{\Gamma_{a'}^{(n)}(U, J, \pi; U', J', \pi')}{\Gamma(U, J, \pi)} = \frac{1}{N(U, J, \pi)} \sum_{S' = |i - J'|}^{i + J'} \sum_{\ell = |J - S'|}^{J + S'} f(\ell, \pi) T_{\ell}^{a'}(U - U' - B_{a'}) \quad (9)$$

where  $B_{a'}$  is the binding energy associated with the decay of interest (zero for gamma-ray emission), and the summations are over the channel spins and orbital angular momenta that can connect the levels  $(U, J, \pi)$  and  $(U', J', \pi')$ . The denominator in Eq. (9),  $N(U, J, \pi)$ , is proportional to the total decay width and can be expressed in terms of transmission coefficients:

$$\begin{aligned}
N(U, J, \pi) = & \sum_{a'} \sum_{I', P'} \sum_{S' = |i' - I'|}^{i' + I'} \sum_{\ell = |J - S'|}^{J + S'} \int_{E_c'}^{U - B_{a'}} dU' f(\ell, \pi) T_{\ell}^{a'}(U - U' - B_{a'}) \rho(U', I', P') + \\
& + \sum_k f(\ell, \pi) T_{\ell}^{a'}(U - U'_k - B_{a'}) \quad (10)
\end{aligned}$$

where the primed quantities are associated with the nucleus formed by emission of the  $a'$  particle or gamma-ray.

## 2. Computational structure

In this section a summary is given of how the Hauser-Feshbach equations of the previous section are applied in the GNASH code. A detailed description of the structure of the code is reserved for Sec. III.

Equations (1), (4), and (7)-(10) are applied directly in the calculations. Referring back to Fig. 3, the incident particle brings in a certain amount of energy, exciting the main compound nucleus to an excitation energy of  $U_0 = \epsilon_0 + B_0$ , where  $\epsilon_0$  is the center of mass energy of the projectile and  $B_0$  is the projectile binding energy in the compound nucleus. The level population that occurs in the main compound nucleus is computed by mean of Eqs. (4) and (8). (Note that the level populations have the units of cross section; in GNASH the standard units used are barns for cross sections and MeV for energies.) The initial energy brought into the compound system determines, of course, the maximum energies that can be reached in all reaction chains being considered. The available excitation energy range of each residual nucleus in a calculation is split into continuum and discrete level energy ranges, depending upon the amount of discrete level information included. The continua of the various products are divided into a series of equally spaced energy bins for the calculation, as illustrated in Fig. 4. The continuum occurs in the shaded areas of the figure, and the discrete levels are indicated schematically at the lowest excitation energies. The figure shows the various decays possible from the  $K^{\text{th}}$  energy bin in the  $I^{\text{th}}$  compound nucleus, with the continuum-to-continuum (C-C) and continuum-to-discrete level (C-D) transitions indicated. The energy bin index begins with  $K=1$  at the maximum excitation energy reached in the main compound nucleus;  $K$  increases with decreasing excitation energy in each compound system that is permitted to decay. The populations in each energy bin and discrete level that can be reached by decays in a given compound nucleus are incremented as each energy bin is permitted to decay, beginning from the top. These calculations are carried out using Eqs. (9) and (10). The population increments are indicated schematically in Fig. 4 but in practice are stored as functions of residual nucleus number, excitation energy, spin, and parity.

The calculations proceed systematically through all the compound nuclei considered in a given analysis. The deexcitation of levels in compound nucleus K shown in Fig. 4, which is formed by one of the decay channels from compound nucleus I, is not calculated until nucleus I has been completely deexcited. In practice, a residual nucleus such as K in a complicated calculation might be formed through several different reaction sequences. The code has the option to combine all the level population in a given residual nucleus from all sources, or to keep each reaction sequence separate. This situation is illustrated in Fig. 3 for the product nucleus labelled "U<sub>3,4</sub>".

As the various energy bins and discrete levels are permitted to decay, center-of-mass spectra are accumulated ( $\Delta\mathcal{P}/\Delta U$ ), and level excitation and deexcitation cross sections are accumulated, both by individual reaction and grouped according to radiation type (neutrons, protons, gamma rays, etc.) These quantities comprise the bulk of the calculated output from the GNASH code.

### 3. Corrections

When the GNASH code was first written, its main anticipated use was for calculations in the MeV energy range for medium-to-heavy targets, and no provision was made for direct calculation of width fluctuation corrections. In subsequent years, however, increasing use of the code has been made at lower energies where such corrections are important. Therefore, as an interim solution (still in use) to this problem, provision was made to read in a table of correction factors as functions of incident energy. We normally utilize a modified version of the COMNUC code<sup>14</sup> to calculate the table, utilizing the integral method by Moldauer<sup>15</sup> and an approximation from Tebel et al.<sup>16</sup> to calculate the correction factors. The further approximation is made in GNASH that a single averaged correction factor can be used at each incident energy for each emitted radiation type; that is, at each energy there a single correction factor for gamma rays, one for neutrons, one for protons, etc.

The second major correction that is made to the basic Hauser-Feshbach calculations is for nonequilibrium reactions. The exciton model of Kalbach<sup>17</sup> is utilized for calculating preequilibrium cross sections for each particle emitted in binary reactions,\* and the compound nucleus cross section for each binary reaction as well as the continuum level populations of residual nuclei that can further decay is modified to account for the corrections. A more complete discussion of preequilibrium corrections is given below in the section on nuclear models.

---

\* Versions of GNASH used in higher energy calculations also include preequilibrium effects from tertiary reactions.<sup>2,4</sup>

## D. Nuclear Models Utilized by GNASH

Summaries are given in this section of the major nuclear models used either directly in the GNASH code or indirectly by means of input quantities. Additional discussion of some of the models occurs in Secs. II-IV.

### 1. Optical model particle transmission coefficients

All particle transmission coefficients are introduced into the GNASH calculations from an external input file (TAPE10) that is obtained from either spherical or coupled-channel optical model calculations. Because of the presence of spin-orbit coupling terms in optical potentials, such transmission coefficients normally depend on orbital angular momentum,  $\ell$ , and total angular momentum,  $\mathbf{j} = \ell + \mathbf{i}$ . As implied in the Eqs. (3)-(10) above, we normally ignore spin-orbit coupling in GNASH calculations, using transmission coefficients that depend only on the orbital angular momentum quantum number. That is, the transmission coefficients  $T_{\ell}^a(\epsilon)$  are weighted averages of the  $T_{\ell, \mathbf{j}}^a(\epsilon)$ . In the case of spin 1/2 particles (neutrons, protons, tritons,  $^3\text{He}$ ), the  $\ell$ -dependent transmission coefficients are obtained from the optical model calculations as follows:<sup>13</sup>

$$T_{\ell}^a(\epsilon) = \frac{1}{(2\ell+1)} \left[ (\ell+1) T_{\ell, \ell+1/2}^a(\epsilon) + \ell T_{\ell, \ell-1/2}^a(\epsilon) \right]. \quad (11)$$

Because of their spin 0 nature, transmission coefficients for alpha particles only depend on  $\ell$ . Although deuterons have spin = 1, they are usually treated as spin 0 particles in GNASH calculations, depending on the optical model code used to determine the transmission coefficients.

A version of GNASH exists that includes spin-orbit coupling in the various summations. We have verified that the effects on calculated cross sections and spectra of including spin-orbit effects by use of  $T_{\ell, \mathbf{j}}^a(\epsilon)$  transmission coefficients are small.

Spherical optical model transmission coefficients for GNASH calculations are usually determined with the nonrelativistic SCAT code by Bersillon.<sup>18</sup> We have an early version at Los Alamos that produces transmission coefficients in the required format for GNASH. If we require transmission coefficients calculated with a relativistic optical model, we use the SNOOPY code developed by Madland.<sup>19</sup> SNOOPY treats the deuteron as a spin 1 particle, whereas the original version of SCAT makes the spin 0 approximation for the deuteron. A more recent version of SCAT, described by Bersillon during this workshop, treats the deuteron as a spin 1 particle.

For calculations with incident neutrons or protons on nuclei that are strongly deformed such as rare earths and actinides, we usually use coupled-channel optical model calculations with the

ECIS code<sup>20</sup> to obtain transmission coefficients. The required transmission coefficients are obtained by combining elements of the S-matrix, as formulated by Lagrange, Madland, and Bersillon.<sup>21</sup> Use of transmission coefficients derived in this manner automatically accounts for direct reaction components of the calculated cross sections, and no ad hoc renormalization is needed of the reaction cross sections calculated from the transmission coefficients.

## 2. Gamma-ray strength functions

Gamma-ray transmission coefficients are calculated using one of several possible forms for gamma-ray strength functions. The transmission coefficients are obtained using detailed balance, exploiting the inverse photoabsorption process. The Brink-Axel<sup>22</sup> hypothesis is used, permitting the cross section for photoabsorption by an excited state to be equated with that of the ground state. The transmission coefficients for gamma-ray emission are obtained from the expression:

$$T^{X\ell}(\epsilon_\gamma) = 2\pi f_{X\ell}(\epsilon_\gamma) \epsilon_\gamma^{2\ell+1} \quad (12)$$

where  $\epsilon_\gamma$  denotes gamma-ray energy,  $X\ell$  indicates the multipolarity of the gamma-ray, and  $f_{X\ell}(\epsilon_\gamma)$  is the energy-dependent gamma-ray strength function.

GNASH has three options available for calculating gamma-ray strength functions from built-in models, in addition to a fourth option of simply inputting a table of  $f_{E1}(\epsilon_\gamma)$  values. The three choices of built-in models are the Weisskopf single-particle model,<sup>23</sup> the Brink-Axel giant dipole model,<sup>22</sup> and the Kopecky-Uhl generalized Lorentzian model.<sup>24</sup> In practice, the latter two models are most often used.

### a. Weisskopf approximation

The gamma-ray strength function with the Weisskopf approximation<sup>23</sup> is simply

$$f_{X\ell}(\epsilon_\gamma) = C_{X\ell} = \text{constant} \quad (13)$$

where the default value for electric dipole transitions is based on systematics from Kopecky and Uhl<sup>25</sup> compiled for  $\langle \epsilon_\gamma \rangle = 7$  MeV:

$$C_{E1} = (4.6 \times 10^{-12}) A^{1.91} [\text{MeV}^{-3}] \quad (14)$$

In practice, the Weisskopf option is rarely used and almost always is normalized using  $2\pi \langle \Gamma_\gamma \rangle / \langle D_0 \rangle$  data, as described below.

### b. Brink-Axel standard Lorentzian

When the Brink-Axel<sup>22</sup> option is chosen in GNASH, a standard Lorentzian form is used to describe the giant dipole resonance shape, and the gamma-ray strength function is obtained from the expression:

$$f_{E1}(\epsilon_\gamma) = K_{E1} \frac{\sigma_0 \epsilon_\gamma \Gamma^2}{(\epsilon_\gamma^2 - E^2)^2 + \epsilon_\gamma^2 \Gamma^2} \quad (15)$$

where  $\sigma_0$ ,  $\Gamma$ , and  $E$  are the standard giant dipole resonance parameters, usually taken from the tables of Dietrich and Berman,<sup>26</sup> and  $K_{E1} = 8.68 \times 10^{-8} \text{ mb}^{-1} \text{ MeV}$  (nominally). Again, the constant  $K_{E1}$  is frequently obtained by normalization to  $2\pi \langle \Gamma_{\gamma 0} \rangle / \langle D_0 \rangle$  data, as described below.

### c. Kopecky-Uhl generalized Lorentzian

The third built-in option in GNASH utilizes the generalized Lorentzian form obtained by Kopecky and Uhl<sup>24</sup> to calculate the gamma-ray strength function:

$$f_{E1}(\epsilon_\gamma T) = K_{E1} \left[ \frac{\epsilon_\gamma \Gamma(\epsilon_\gamma)}{(\epsilon_\gamma^2 - E^2)^2 + \epsilon_\gamma^2 \Gamma(\epsilon_\gamma)^2} + \frac{0.7 \Gamma 4\pi^2 T^2}{E^5} \right] \sigma_0 \Gamma \quad (16)$$

where  $\Gamma(\epsilon_\gamma)$  is an energy-dependent damping width based on Fermi liquid theory

$$\Gamma(\epsilon_\gamma) = \Gamma \frac{\epsilon_\gamma^2 + 4\pi^2 T^2}{E^2} \quad (17)$$

and  $T$  is the nuclear temperature given by

$$T = \sqrt{\frac{B_n - \epsilon_\gamma}{a}} \quad (18)$$

and  $K_{E1}$  is the same as for the Brink-Axel model but again can be determined from normalization to  $2\pi \langle \Gamma_{\gamma 0} \rangle / \langle D_0 \rangle$  data. The quantities  $B_n$  and  $a$  are the neutron binding energy and Fermi gas level density parameter, respectively. The Lorentzian parameters of the giant-dipole resonance,  $E$  and  $\Gamma$ , are the same as with the Brink-Axel option.

In addition to E1 radiation, M1 and E2 as well as higher order components can also be included in GNASH calculations. For M1, a standard Lorentzian expression is used for the gamma-ray strength function with built-in resonance parameters. When the Brink-Axel option is chosen for M1 transitions, the default parameters are  $\sigma_0 = 1$  mb,  $E = 8$  MeV, and  $\Gamma = 5$  MeV, although  $\sigma_0$  can be input directly. When the Kopecky-Uhl option is chosen, slightly different M1 resonance parameters are used, in particular, those recommended by Kopecky and Uhl:<sup>24</sup>  $E = 41 A^{-1/3}$  (MeV) and  $\Gamma = 4$  MeV.

Except when the Kopecky-Uhl formulation is used, a Weisskopf form (or constant) is used for the E2 gamma-ray strength function. When the Kopecky-Uhl formulation is employed, a giant resonance formulation is also used to calculate the E2 strength function, as follows:

$$f_{E2}(\epsilon_\gamma) = K_{E2} \frac{\sigma_0 \epsilon_\gamma^{-1} \Gamma^2}{(\epsilon_\gamma^2 - E^2)^2 + \epsilon_\gamma^2 \Gamma^2} \quad (19)$$

where  $K_{E2} = 5.22 \times 10^{-8}$  (mb<sup>-1</sup> MeV<sup>-2</sup>),  $E = 63 A^{-1/3}$  (MeV),  $\Gamma = (6.11 - 0.12A)$  (MeV), and  $\sigma_0 = 1.5 \times 10^{-4} Z^2 E^2 A^{-1/3} / \Gamma$  (mb).

As mentioned above, GNASH has the option of renormalizing any of the gamma-ray strength functions that are chosen. When this option is chosen, the constants in the Eqs. (13)-(16) are determined by renormalizing the gamma-ray strength function to match low-energy s-wave resonance data. The normalization can be carried out either by directly inputting relative contributions of  $X\ell$  components (for example, E1, M1, and E2), in which case each  $f_{X\ell}$  is normalized separately, or by using the absolute values of the individual components as calculated by the code to establish the relative contributions and then just determining one overall normalization constant. The normalization is carried out as follows:

$$\frac{2\pi \langle \Gamma_\gamma \rangle}{\langle D_0 \rangle} = \sum_{J\pi} \sum_{X\ell} \sum_{j=|J-\ell|}^{J+\ell} \left[ \int_0^{S_n - E_c} d\epsilon_\gamma T^{X\ell}(\epsilon_\gamma) f(\ell, J, j') \rho(S_n - \epsilon_\gamma, j', \pi') + \sum_{k=1} T_k^{X\ell}(\epsilon_\gamma) f(\ell, J, j') \right] \quad (20)$$

where the  $J\pi$  sum is over the possible compound nucleus states that can be formed with s-wave incident particles, the  $X\ell$  sum is over the multipole radiations included in the calculation, the  $j'$  sum is over the spins in the final state, the  $f(\ell, J, j')$  is a factor of 1 or 0 to force compliance with multipole radiation selection rules, and  $S_n$  is the separation energy of the projectile in the



compound system. The mean gamma width  $\langle \Gamma_\gamma \rangle$  and mean level spacing  $\langle D_0 \rangle$  for s-wave incident neutrons are usually obtained from the compilation of Mughabghab et al.<sup>27</sup>

The present version of GNASH is dimensioned for up to 6 values of gamma-ray multipolarity. The absolute contributions to Eq. (20) for each multipolarity can be input into the code. Alternatively, one can use the absolute gamma-ray strength functions in Eqs. (13)-(18) above to calculate the relative contributions. If one uses multipole radiation other than E1, M1, and E2, then the relative contributions are estimated in GNASH as follows:

$$\frac{R(M\ell)}{R(E\ell)} \equiv 10 \left( \frac{\hbar}{m_N c R} \right)^2 = 0.45 \text{ fm}^2 \left( \frac{1}{r_0 A^{1/3}} \right)^2 \quad (21)$$

and

$$\frac{R(E\ell+1)}{R(E\ell)} \equiv \frac{R(M\ell+1)}{R(M\ell)} \equiv 8 \times 10^{-4} \quad (22)$$

where  $R(X\ell)$  indicates the relative amounts of each multipolarity.

### 3. Level density models

The continuum level density function  $\rho(U, J, \pi)$ , introduced in Eq. (5) above, has the following form in GNASH:

$$\rho(U, J, \pi) = F_\pi(\pi) F_J(J, U) \rho(U) \quad (23)$$

where the spin and parity components are given by<sup>28</sup>

$$F_\pi(\pi) = \frac{1}{2} \quad (24)$$

and

$$F_J(J, U) = \frac{(2J+1)}{2\sigma(U)} \exp \left[ -\frac{(J+\frac{1}{2})^2}{2\sigma(U)^2} \right] \quad (25)$$

The quantity  $\sigma(U)$  is a spin cutoff function given by the expression

$$\sigma(U)^2 = C_{SC} A^{2/3} \sqrt{aU} \quad (26)$$

with  $C_{SC}$  being a constant equal to either 0.0888 (Ref. 28) or 0.146 (Ref. 29).

Three built-in models of the energy-dependent level density,  $\rho(U)$ , are available in the GNASH code. Historically, the Gilbert and Cameron<sup>28</sup> model has been utilized most often in GNASH, although some use has been made of the backshifted Fermi-gas model,<sup>30</sup> and in recent years the extension of GNASH calculations to higher energies has motivated our use of the Ignatyuk form of the Fermi-gas model.<sup>31</sup> Use of either the Gilbert-Cameron or the Ignatyuk models is reasonably well automated in GNASH with internal defaults that usually produce reasonable results. In the case of the backshifted Fermi-gas model, all parameters must be input. A description of the  $\rho(U)$  models follows.

#### a. Gilbert-Cameron model

The Gilbert and Cameron level density formulation consists of a constant temperature form for use at lower excitation energies and a Fermi gas form for use at higher energies. The constant temperature form is given by

$$\rho_T(U) = \frac{1}{T} \exp[(U + \Delta - E_0)/T] \quad (27)$$

where  $T$  is the nuclear temperature and  $E_0$  is a normalization factor. The quantity  $U$  is related to the excitation energy by  $U = E - \Delta$ , where  $\Delta$  is the pairing energy. The Fermi gas form of the level density is

$$\rho_F(U) = \frac{\exp(2\sqrt{aU})}{12\sqrt{2} \sigma(U)U(aU)^{1/4}} \quad (28)$$

where 'a' is the level density parameter.

The constant temperature and Fermi gas functions are illustrated schematically in Fig. 5. The quantities  $N_T(E)$  and  $N_F(E)$  are the cumulative number of levels in the two level density regions, obtained by integrating Eqs. (27) and (28). The temperature level density is matched to the cumulative number of known discrete levels ( $N_{\text{exp}}$ ) in the excitation energy interval  $E_L$  to  $E_c$ , as follows:

$$N_{\text{exp}}(E_c) = N_{\text{exp}}(E_L) + \int_{E_L}^{E_c} dE \rho_T(E) \quad (29)$$

Two different options are available for utilizing Eq. (29) in the matching. The original formulation simply assumes that  $N_{\text{exp}}(E_1 = -\infty) = 0$ , which leads to the expression

$$N_{\text{exp}}(E_c) = \exp\left(\frac{E_c - E_0}{T}\right) \quad (29a)$$

Eq. (29a) is very convenient in that it can be used in circumstances where the structure of a nucleus is completely unknown, that is, where we only know that there is a ground state. In this case  $N_{\text{exp}}(E_c = 0) = 1$  is the only information available, but the matching can be done with Eq. (29a). (This leads, of course, to the result that  $E_0 = 0$ .)

For cases where there is significant information concerning the structure of a nucleus, however, the above simple treatment can lead to a slight distortion of the continuum temperature expression, mainly near the matching point. In such cases it is better to set the lower integration limit around the 2<sup>nd</sup> - 4<sup>th</sup> excited state, and Eq. (29a) must be replaced by

$$N_{\text{exp}}(E_c) = N_{\text{exp}}(E_1) + \left[ \exp\left(\frac{E_c}{T}\right) - \exp\left(\frac{E_1}{T}\right) \right] \exp\left(\frac{-E_0}{T}\right) \quad (29b)$$

Eq. (29b) is the usual option used in GNASH for calculations of non-fissile target nuclei. For fission calculations, the matching routines for the transition states use Eq. (29a) (see Section I.D.5 below).

The constant temperature and Fermi-gas expressions are matched at excitation energy  $E_m$  by requiring that

$$\rho_T(E_m) = \rho_F(E_m)$$

and

$$\frac{d\rho_T}{dE}(E_m) = \frac{d\rho_F}{dE}(E_m) \quad (30)$$

The combination of matchings in Eqs. (29) and (30) determines the constants  $T$ ,  $E_0$ , and  $E_m$ .

The pairing energy  $\Delta$  that relates  $U$  and  $E$  is the sum of proton and neutron pairing corrections,  $P(Z)$  and  $P(N)$ , and is determined in GNASH from the Cook<sup>32</sup> tabulation. The default values of the Fermi gas level density parameter in the GNASH code are from Gilbert and Cameron<sup>28</sup> as follows:

$$\frac{a}{A} = 0.00917 [S(Z) + S(N)] + C \quad (31)$$

where  $S(Z)$  and  $S(N)$  are shell factors again taken from the Cook parameter set.<sup>32</sup> The constant  $C$  is equal to  $0.142 \text{ MeV}^{-1}$  for spherical nuclei and  $0.120 \text{ MeV}^{-1}$  for deformed nuclei.

### b. Backshifted Fermi-gas model

With the backshifted Fermi-gas model of Dilg,<sup>30</sup> a single formulation describes the level density at all excitation energies, as follows:

$$\rho(U) = \frac{1}{12\sqrt{2}} \frac{1}{\sigma(U) a^{1/4}} \frac{\exp(\sqrt{2aU})}{(U+t)^{5/4}} \quad (32)$$

where the spin cutoff expression is evaluated in this case by

$$\sigma^2(U) = 0.015 t A^{5/3} \quad (33)$$

and the nuclear temperature  $t$  is defined by

$$U = at^2 - t \quad (34)$$

### c. Ignatyuk form of Fermi-gas model

The Gilbert and Cameron and the back-shifted Fermi gas level density formulations utilize an energy-independent level density parameter,  $a$ , which somewhat restricts flexibility at higher energies. This difficulty is compounded by the effects of shell closures on the Fermi gas level density parameter and on their propagation to higher energies. To address these problems, we implemented the phenomenological level density model developed by Ignatyuk et al.<sup>31</sup> In this model the Fermi gas parameter is assumed to be energy dependent and is given as a function of excitation energy  $U$  by the expression

$$a(U) = \alpha [1 + f(U) \delta W/U], \quad (35)$$

where  $\alpha$  is the asymptotic value occurring at high energies. Shell effects are included in the term  $\delta W$ , which is determined via  $\delta W = M_{\text{exp}}(Z,A) - M_{\text{ld}}(Z,A,\beta)$ . In our calculations we determine the experimental masses,  $M_{\text{exp}}(Z,A)$ , through use of a preliminary version of the 1988 Wapstra et al. mass compilation,<sup>32</sup> and we calculate liquid drop masses,  $M_{\text{ld}}(Z,A,\beta)$ , through use of standard

liquid drop expressions evaluated at a deformation  $\beta$ . Additional energy dependence in  $a(U)$  occurs via the term  $f(U)$  which is given by

$$f(U) = 1 - \exp(-\gamma U) \quad (36)$$

where  $\gamma = 0.05$  MeV was determined by Ignatyuk et al.

Thus, this model permits shell effects to be included at low excitation energies while at higher energies such effects disappear as  $a(U)$  reaches the asymptotic value  $\alpha$ . This form is in better agreement with results from microscopic Fermi gas models than the assumption of energy independence for  $a$ . The asymptotic value of  $a(U) \rightarrow \alpha$  is given by Ignatyuk et al. as a function of mass by the expression

$$\frac{\alpha}{A} = \eta + \beta A \quad (37)$$

with  $\eta = 0.154$  and  $\beta = 6.3 \times 10^{-5}$ , and with  $\alpha$  in units of MeV<sup>-1</sup> and  $A$  in amu. In the default option in the GNASH code, however, we utilize Arthur's parameterization<sup>11</sup> of Eq. (37), which is based on fits to s-wave resonance data<sup>27</sup> and which resulted in the parameters  $\eta = 0.1375$  and  $\beta = -8.36 \times 10^{-5}$ .

The Ignatyuk et al. level density model is implemented in the GNASH code using exactly the same Fermi gas and constant temperature formulas as are applied with the Gilbert and Cameron representation, that is, Eqs. (23)-(30) above, and the continuum matching and matching to the discrete levels is done in the same manner. The only difference is the energy and shell dependence of the level density parameter,  $a(U)$ , as specified in Eqs. (35)-(37).

#### 4. Preequilibrium and direct reaction effects

After calculation of populations of the first compound nucleus using the Hauser-Feshbach expressions discussed here, corrections for nonequilibrium reaction mechanisms (preequilibrium and direct-reaction effects on populations and particle emission spectra) can be made. The major part of these contributions is calculated using the exciton preequilibrium model as formulated by Natta and CO-B.<sup>33</sup> The corrections are applied after the initial Hauser-Feshbach calculation has been made. The logic for doing this will be addressed later in the discussion of the normalization of spectra and population increments.

### a. Nucleon preequilibrium

The exciton model assumes that, after the initial interaction between the incident particle and the target nucleus, the excited system can pass through a series of stages of increasing complexity before equilibrium is reached, and emission may occur from these stages, giving the preequilibrium particles. This process is illustrated schematically in Fig. 6, together with a sample particle-emission spectrum showing the regions of importance of compound nucleus, preequilibrium, and direct reaction emission. The different stages of complexity are classified according to the number of particles and holes excited, and the exciton model calculations involve solving a series of master equations that describe the equilibration of an excited system through a series of two-body collisions producing more complex configurations of particle-hole pairs. The master equation is

$$\frac{dP}{dt}(n,t) = \lambda^+(n-2)P(n-2,t) + \lambda^-(n+2)P(n+2,t) - [\lambda^+(n) + \lambda^-(n) + W(n)]P(n,t), \quad (38)$$

where

$P(n,t)$  = probability that the excited nuclear system exists in the exciton state  $n$  ( $n \equiv p+h$ , the number of particles plus holes excited) at time  $t$ ;

$\lambda^+, \lambda^-$  = internal transition rates for  $n \rightarrow n+2$  and  $n \rightarrow n-2$ , respectively;

$W(n)$  = total particle emission rate from stage  $n$  summed over all outgoing particles and energies.

The initial condition for solution of these equations is

$$P(p,h,0) = \delta(p,p_0) \delta(h,h_0), \quad (39)$$

where the initial particle number is  $p_0 = 2$  and initial hole number is  $h_0 = 1$  for nucleon-induced reactions. Angle integrated cross sections are calculated from the relation

$$\frac{d\sigma}{d\varepsilon}(a,b) = \sigma_a \sum_n W_b(n,\varepsilon) \tau(n), \quad (40)$$

where, as before,  $\sigma_a$  is the reaction cross section, and  $\tau(n)$  is the mean lifetime for the exciton state, defined by

$$\tau(n) = \int_{t=0}^{\infty} P(n,t) dt , \quad (41)$$

and  $W_b(n,\epsilon)$  is the average rate for emission of particle  $b$  with energy  $\epsilon$  from the  $n^{\text{th}}$  exciton stage.

The transition rates are calculated using Fermi's Golden Rule:

$$\lambda = \frac{2\pi}{\hbar} M^2 Y , \quad (42)$$

where

$M^2$  = averaged squared matrix element for two-body interactions between specific initial and final states (parameterized according to the Kalbach<sup>34</sup> systematics);

$Y$  = accessible phase space for the transition.

To calculate the accessible phase space, the equidistant single-particle state density expression of Williams<sup>35</sup> is used as follows:

$$\omega(p,h,E) = \frac{g^n (E - A_{p,h})^{n-1}}{p! h! (n-1)!} , \quad (43)$$

where

$A_{p,h}$  = factor restricting the number of allowed states due to the Pauli exclusion principle;

$E$  = excitation energy of the system;

$g$  = inverse of the single-particle level spacing, related to the Fermi gas level density parameter by  $g = 6a/\pi^2$ , or frequently calculated simply as  $A/13$ .

The factor  $A_{p,h}$  is given by

$$A_{p,h} = E_p(p,h) - \frac{p^2 + h^2 + n}{4g} \quad (44a)$$

with  $E_p$  being the minimum energy required for the configuration by the Pauli exclusion principle, given by  $E_p = [\max(p,h)]^2/g$ . It should be noted that an alternative expression has also been used for  $A_{p,h}$ , namely,<sup>36</sup>

$$A_{p,h} = \frac{p^2 + h^2 + p - 3h}{4g} \quad (44b)$$

Rates for transitions allowed by the assumption of binary collisions ( $\Delta n=0,\pm 2$ ) are

$$\lambda^+(p,h,E) = \frac{2\pi}{h} M^2 \frac{g^3 [E - E_p(p+1,h+1)]^2}{2(n+1)} \quad (45)$$

$$\lambda^-(p,h,E) = \frac{2\pi}{h} M^2 \frac{gph(n-2)}{2} \left[ 1 - \frac{(n-1)(p-1)(p-2) + (h-1)(h-2)}{(n-2)8g[E - E_p(p,h)]} \right],$$

where  $M^2$  is the matrix element for two-body interaction between a specific initial and final state and  $E_p$  is the Pauli energy for the indicated configuration. In GNASH,  $M^2$  is parameterized as a function of  $e=E/n$  as follows:

$$\begin{aligned} M^2 &= \frac{k}{A^3 e} \sqrt{\frac{e}{7 \text{ MeV}}} \sqrt{\frac{e}{2 \text{ MeV}}} & e < 2 \text{ MeV} \\ &= \frac{k}{A^3 e} \sqrt{\frac{e}{7 \text{ MeV}}} & 2 < e < 7 \text{ MeV} \\ &= \frac{k}{A^3 e} & 7 < e < 15 \text{ MeV} \\ &= \frac{k}{A^3 e} \sqrt{\frac{15 \text{ MeV}}{e}} & e > 15 \text{ MeV} \end{aligned} \quad (46)$$

with 'e' in MeV. The constant k is usually set equal to 130-160 MeV<sup>3</sup>.

The emission rate for particles of type b and emission energy e is obtained by considering a detailed balance of the emission channel and the analogous absorption channel of particles b:

$$W_b(n,\epsilon) = \frac{(2s_b + 1)}{\pi^2 h^3} \mu_b \sigma_b(e) \epsilon \frac{\omega(p-p_b, h, U)}{\omega(p, h, E)} Q_b(p), \quad (47)$$

where



$s_b, \mu_b, p_b$  = spin, reduced mass, and nucleon number of the emitted particle,

$U$  = residual nucleus excitation energy,

$\sigma_b(\epsilon)$  = inverse cross section evaluated at the emission energy of  $b$ ,

$Q_b(p)$  = factor that takes into account the distinguishability of neutrons and protons in the intranuclear cascade.<sup>37</sup>

Two methods are employed in GNASH to calculate  $Q_b(p)$ . The first is based upon the assumption that in each pair-creation interaction, protons and neutrons are created with the relative probabilities  $Z/A$  and  $N/A$ . The second form assumes the neutron and proton  $p$ - $h$  pairs are excited in proportion to the state densities of the configurations formed.<sup>38</sup>

### b. Photon preequilibrium emission

The GNASH code also allows preequilibrium configurations to decay by E1 photon emission, through the giant dipole resonance (GDR). This preequilibrium photon decay mechanism allows a simple estimate of the direct-semidirect capture spectrum within the framework of the exciton model.<sup>39</sup> Eq. (40) is used for the preequilibrium photon emission spectrum (with the summation now started at the configuration  $p_0=1, h_0=0$ ), and  $W_b(n, \epsilon)$  being the photon decay rate from the  $n^{\text{th}}$  exciton stage. This is determined by applying detailed balance using the Brink-Axel hypothesis, and is found to be

$$W_{\gamma}(n, \epsilon_{\gamma}) = \left[ \frac{\epsilon_{\gamma}^2 \sigma_{\gamma}(\epsilon_{\gamma})}{\pi^2 \hbar^3 c^2 \omega(p, h, E)} \right] \left( \frac{g^2 \epsilon_{\gamma} \omega(p-1, h-1, E-\epsilon_{\gamma})}{g(n-2) + g^2 \epsilon_{\gamma}} + \frac{g n \omega(p, h, E-\epsilon_{\gamma})}{g n + g^2 \epsilon_{\gamma}} \right) \quad (48)$$

where  $\sigma_{\gamma}(\epsilon)$  is the photoabsorption cross section for a photon of energy  $\epsilon$  on the residual nucleus, and is obtained using a Lorentzian parameterization from the tables of Dietrich and Berman.<sup>26</sup> The inverse spacing of single particle levels is  $g = A/13$ .

The two terms within the round brackets describe photon emission processes in which the total number of excitons changes by either  $\Delta n = -2$  (particle-hole annihilation), or  $\Delta n = 0$ . The dominant mechanism in the preequilibrium photon emission process corresponds to an initial  $1p$  state decaying through the GDR to a  $1p$  state of lower energy, and the photon emission spectrum peaks for photon energies in the region of the GDR. The GDRs which are built upon the final  $1p$  states are of a  $2p1h$  nature, though according to the Brink-Axel hypothesis they have a state density corresponding to that of a  $1p$  state. This explains why the dominant mechanism is determined by  $1p$  state densities even though the formation of intermediate  $2p1h$  GDR states is implicitly included.

### c. Composite particle preequilibrium

In addition to the preequilibrium cross sections and spectral contributions calculated using the exciton model, a second, more general class of nonequilibrium contributions, is included automatically in GNASH nonequilibrium calculations. These are contributions arising from particle pickup, knockout, stripping, etc., which are calculated using a phenomenology developed by Kalbach.<sup>17</sup> In particular, these expressions are used to calculate composite-particle emission rather than using exciton model expressions, which would be modified to include "fit parameters" such as preformation constants.

To determine contributions due to pickup/stripping processes the semiempirical expression

$$\frac{d\sigma^{p-s}}{d\epsilon}(a,b) = (2s_b + 1) p_b \epsilon \sigma_b(\epsilon) \omega_F(U) (20)^{\delta_\alpha} f \left( \frac{E_a}{P_a} \right)^{-2\Delta} \left( \frac{780}{A} \right)^\Delta 1.4 \times 10^{-4} (\text{MeV})^{2\Delta-1} \quad (49)$$

is used. Here  $\Delta$  is the number of transferred particles, and  $\delta_\alpha = 1$  if an alpha is formed,  $\delta_\alpha = -1$  if an alpha is destroyed, and zero otherwise. The function  $f$  is

$$f(N,Z,\Delta_\pi,\Delta_\nu) = \left( \frac{2Z}{A} \right)^{6\Delta_\pi} \left( \frac{2N}{A} \right)^{(1-\Delta_\pi)\Delta_\nu(\Delta_\nu+1)/2} \quad (50)$$

where  $\Delta_\pi$  and  $\Delta_\nu$  are the number of transferred protons and neutrons respectively. The density of states is determined from

$$\omega_F^{p-s}(U) = \frac{\Delta!}{\Delta_\pi! \Delta_\nu!} \sum_{i=1}^{\Delta} \omega(0,i,U) \quad (51)$$

A second contribution describing knockout and inelastic processes involving alpha clusters is calculated from

$$\frac{d\sigma^{K-I}}{d\epsilon}(a,b) = \frac{\sigma_a}{p_a \epsilon_a^3} (2s_b + 1) p_b \epsilon \sigma_b(\epsilon) \frac{\omega_F^{K-I}(U)}{A} F_a [0.12 \text{ MeV}^2 \text{ mb}^{-1}] \quad (52)$$

where  $F_\alpha = 1$ ,  $F_n = F_p = fZ/2A$ . The density function  $\omega_F^{K-I}$  has the following forms depending upon the process involved:

$$\omega_{F1}^{K-1}(U) = g_i g_\alpha \left( U - \frac{1}{2g_i} - \frac{1}{2g_\alpha} \right) \quad (53a)$$

where  $i=n$  or  $p$  ( $p,\alpha$ ) or ( $n,\alpha$ ) knockout or ( $\alpha,p$ ) or ( $\alpha,n$ ) knockout;

$$\omega_{F2}^{K-1}(U) = g_\alpha^2 U \quad (53b)$$

for elastic scattering with excitation of an alpha particle-hole pair; and,

$$\omega_{F3}^{K-1}(U) = g_n^2 U + g_p^2 U \quad (53c)$$

for ( $\alpha,\alpha'$ ) inelastic scattering exciting a nucleon pair. In these expressions  $g_p = Z/(13 \text{ MeV})$ ,  $g_n = N/(13 \text{ MeV})$ , and  $g_\alpha = A/(52 \text{ MeV})$ .

#### d. Flux adjustment for preequilibrium contributions

Once preequilibrium and other nonequilibrium contributions are computed, they are used to renormalize calculated spectra and continuum populations. The renormalization of calculated spectra for primary emission is accomplished in the following manner:

$$\begin{aligned} \frac{d\sigma}{d\varepsilon} &= F \left( \frac{d\sigma}{d\varepsilon} \right)_{\text{CN}} + \left( \frac{d\sigma}{d\varepsilon} \right)_{\text{NONEQ}} \\ &= F \left( \frac{d\sigma}{d\varepsilon} \right)_{\text{CN}} + \left[ \left( \frac{d\sigma}{d\varepsilon} \right)_{\text{PE}} + \left( \frac{d\sigma}{d\varepsilon} \right)_{\text{K-I}}^{\text{P-S}} \right] \end{aligned} \quad (54)$$

where  $F$  is the fractional reduction of the original compound nucleus cross section that is required to conserve flux, given by

$$F = 1 - \frac{1}{\sigma_{\text{CN}}} \sum_i \left[ \int d\varepsilon \left( \frac{d\sigma}{d\varepsilon} \right)_{\text{NONEQ}}^i \right] \quad (55)$$

and the sum runs over all the nonequilibrium cross sections. It should be noted that if the compound nucleus cross section for a given energy bin is zero (corresponding to cases where

widely spaced discrete levels occur in the residual nucleus), then the calculated preequilibrium cross section is also set to zero.

To correct the spin-dependent populations,  $\mathcal{P}(U, J, \pi)$ , computed from continuum-continuum decay of the first compound nucleus for preequilibrium effects, the assumption is made that the preequilibrium contribution (which is spin independent in this model) has the same spin distribution as the Hauser-Feshbach results. Therefore, the correction is:

$$\mathcal{P}(U, J, \pi) = \mathcal{P}_{\text{CN}}(U, J, \pi) \left[ F + \frac{\left( \frac{d\sigma}{d\epsilon}(U) \right)_{\text{NONEQ}}}{\left( \frac{d\sigma}{d\epsilon}(U) \right)_{\text{CN}}} \right] \quad (56)$$

#### e. Correction for direct reactions

In addition to the nonequilibrium cross sections and spectral calculations described above, GNASH also has provision for accounting for direct-reaction contributions to inelastic scattering. These contributions are determined by means of external coupled-channel calculations using a code such as ECIS<sup>20</sup> or through distorted wave Born approximation calculations made using a code such as DWUCK.<sup>40</sup> There is no need to renormalize the reaction cross sections computed in GNASH when coupled-channel calculations are used to provide the direct cross sections, because the direct contributions are automatically removed from the transmission coefficients provided by ECIS. When DWBA calculations are used to provide direct reaction cross sections, however, the original reaction cross section in GNASH must be reduced by the amount of direct reaction cross section added in order to keep the total reaction cross section constant. This renormalization is accomplished automatically by the code.

### 5. Description of the fission barrier model in GNASH

Within the Hauser-Feshbach portion of GNASH, fission can be included as a "decay" path as follows. Up to three uncoupled barriers can be used to represent the fissioning system and each barrier has the characteristics illustrated in Fig. 7a. At each barrier transition states occur that are characterized by an energy,  $E^{\text{TS}}$ , above the barrier as well as by spin and parity  $J^{\pi}$ . At higher energies above the barrier, discrete transition states are replaced by a continuum of such states which is described by the Gilbert-Cameron level density model. Fission transmission coefficients are determined through use of the Hill-Wheeler expression<sup>41</sup> for penetration through a parabolic barrier of height  $E_b$  and curvature  $\kappa\omega$ , as follows:

$$P_f = \frac{1}{1 + \exp\left[-\frac{2\pi}{\hbar\omega}(U - E_b)\right]} \quad (57)$$

Because both discrete transition states and a continuum of such states occur, the total fission transmission coefficient is made up of two contributions, the first describing discrete transition states,

$$T_F^{TS}(U, J, \pi) = \sum_{i=1}^N \frac{1}{1 + \exp\left[-\frac{2\pi}{\hbar\omega}(U - E_b - E_i^{TS})\right]} \quad (58a)$$

and the second gives the continuum of such states,

$$T_F^c(U, J, \pi) = \int_{E_{MAX}^{TS}}^{\infty} d\varepsilon' \rho(\varepsilon', J, \pi) \frac{1}{1 + \exp\left[-\frac{2\pi}{\hbar\omega}(U - E_b - \varepsilon')\right]} \quad (58b)$$

The summation limit  $N$  in Eq. (58a) is the number of transition states having spin and parity  $J^\pi$ . The integration variable  $\varepsilon'$  in Eq. (58b) runs from the excitation energy of the highest transition state built on the fission barrier under consideration, that is, where the continuum region begins, to an excitation energy high enough that contributions to the integral become negligible. In practice, the upper energy limit of the integral in Eq. (58b) is set in GNASH to be  $\varepsilon' = U - E_b + M\hbar\omega$ , where  $M$  can be input but the default value of  $M=5$  is usually used.

The fission model implemented in GNASH assumes the fully damped limit so that the total fission width is determined from the expression

$$T_F^{total}(U, J, \pi) = \frac{T_F^A (T_F^B + T_F^C)}{T_F^A + T_F^B + T_F^C} \quad (59)$$

In this limit no account is made of complications due to states existing in other wells. Width fluctuation correction factors (when used) are set to one for the fission channels.

The specification of the transition state spectrum at each barrier can be made with either of two options. On the one hand the actual states can be specified  $(E_x, J, \pi)$  by the user in which case the same spectrum of discrete levels is assumed to exist at each barrier. Alternatively, different sets

of bandhead parameters can be provided for each barrier and the transition state spectrum is automatically constructed by

$$E^{TS} = E_{\text{band}} + \frac{\hbar^2}{2I} [J(J+1) - K(K+1)] \quad (60)$$

At higher energies above the barrier where a continuum of transition states occurs, the Gilbert-Cameron level density model is used to calculate  $\rho^{TS}(U)$ . Provision is made for matching of the Fermi gas and constant temperature portions of this model using information provided or generated for discrete fission transition states. Finally, the fission transition state density is modified through externally provided factors which account for symmetry conditions existing at each barrier.<sup>42</sup> Enhancements thus arise from the breaking of nuclear symmetries. Such enhancements can be related to the spin cutoff parameters and thus its dependence upon the energy above the barrier has been implemented in GNASH as varying as  $E^{1/4}$  above 1 MeV. Thus, the transition state density is modified from the value calculated with the Gilbert-Cameron expressions by

$$\rho^{TS}(U) = \left( f_0 U^{1/4} \right) \rho^{GC}(U) \quad (61)$$

where  $f_0$  is the inputted density factor. (Below 1 MeV, the enhancement factor varies linearly from 2 to  $f_0$ .) At energies above 15 MeV, the enhancement is assumed to saturate, as indicated (approximately) by the microscopic calculations of Jensen.<sup>43</sup> At still higher energies, the enhancement is assumed to decrease to unity.

The behavior of the enhancement factor with excitation energy is illustrated in Fig. 7b for the case where the input factor is  $f_0 = 4$  (DFAC in Fig. 7b). The energies where the enhancement factor saturates (USMAX), starts decreasing (USMAX1), and then returns to unity (USMAX2) are set in a DATA statement in the code.

## II. DESCRIPTION OF THE INPUT DATA AND OUTPUT RESULTS FROM GNASH

### A. General Comments on Input and Output

The key concern in devising the GNASH input was to keep problem-specific input as simple as possible while permitting maximum flexibility in terms of parameter detail that may be desired

for a specific problem at hand. The general philosophy is to provide bulk data that frequently remains fixed for a given problem in separate input files, together with a much simpler calculational directory file (INPUT) that defines the reaction sequences to be calculated and the model options and parameters to be used. More specifically, atomic mass and ground-state spin and parity data, nuclear structure data, and optical model transmission coefficients are provided on separate files, that is, TAPE13, TAPE8, and TAPE10, respectively. These files contain data that can be shared jointly among several problem types and thus do not have to be altered for each specific calculation. A simpler INPUT file is then used to direct the calculation and to modify parameters as needed from run to run. The TAPE8, TAPE10, and TAPE13 files, together with the INPUT calculational directory file, must be present in the local file space for any calculation. A fifth file, TAPE33, can be used to provide additional optional input information, as outlined below. A schematic illustration of the GNASH input and output information is given in Fig. 8.

A brief description of problem setup is given in this section along with some details concerning the additional data files that are required. The specific input setup described here is for  $n + {}^{93}\text{Nb}$  reactions at 14 MeV, which is one of the available computer exercises.

As summarized in Sec. I, the primary output from GNASH are absolute angle-integrated particle and gamma-ray spectra plus excitation and deexcitation cross sections of discrete states. The calculated spectra are integrated and summed, so that absolute reaction cross sections and average secondary particle and gamma-ray energies are given. The present configuration of the code permits incident particle types to be neutrons, protons, deuterons, tritons,  ${}^3\text{He}$ , and  ${}^4\text{He}$ , with the same particles (as well as gamma rays) permitted in decay channels. The output described here is for the 14-MeV  $n + {}^{93}\text{Nb}$  input case.

## B. Description of Necessary Auxillary Parameter Files

### 1. Ground-state spins, parities, and masses (TAPE13)

Masses and ground state spins and parities for all GNASH calculations are obtained from the input file TAPE13. The current mass values are based upon an interim set from Wapstra<sup>44</sup> obtained prior to the 1988 publication<sup>32</sup> and supplemented in the case of unmeasured masses with values from the Möller and Nix<sup>45</sup> calculations. Unknown spins and parities are flagged during execution, and  $J^\pi = 0^+$  (even A) and  $J^\pi = 1/2^+$  (odd A) are used as defaults in the unknown cases.

A sample of the TAPE13 file is given in Appendix 1. This file includes data from the neutron ( $ZA = 1$  where  $ZA = 1000 \cdot Z + A$ ) to a heavy nucleus with  $ZA = 100274$ , corresponding to a total of 3846 entries of input. Three words of data are read for each entry, with 5 entries per line of data. The quantities read are LZA, ENER, SPNPAR, where LZA is the fixed point "ZA", ENER is the mass excess in MeV, and SPNPAR is the floating point value of  $100 \pm J$ , where the sign of J

is given by the parity, and the sign of SPNPAR indicates the parity. Note that the complete data file has 4795 entries, corresponding to  $ZA = 122318$ , but only 3846 entries are read by GNASH. The additional masses are available if ever needed.

## 2. Nuclear structure data (TAPE8)

Although discrete level data can be read from the input file, the preferred method is to read such data from TAPE8. Thus, a universal library for nuclear structure data can be used in many problems. In practice, however, we usually use a smaller subset of the structure file because of the length of a universal file. The structure file prepared for the computer exercises contains data for a wide range of nuclides in the neighborhood of  $^{56}\text{Fe}$ ,  $^{93}\text{Nb}$ , and  $^{238}\text{U}$ , which are involved in the sample problems.

The sequence of card image types required to construct the structure file appears in Appendix 2, together with a sampling of the structure data for  $^{93}\text{Nb}$ . Note that the parity of levels is indicated by the sign of the spin. Therefore, a spin and parity of  $J^\pi = 0^-$  is indicated by setting  $AJ = -0$ . Considering possible problems of machine independence, if there is any question regarding the parity in the  $J^\pi = 0^-$  case, the quantity AT can be set negative and it will then be used to set the parity when  $J = 0$ .

## 3. Particle transmission coefficients (TAPE10)

Particle transmission coefficients are generally provided to GNASH from an external file, usually TAPE10. This procedure is followed to permit maximum flexibility in providing such input for calculations. To date, we have utilized the nonrelativistic spherical optical model codes TCCAL (developed from routines in the COMNUC code<sup>14</sup>) and SCAT,<sup>18</sup> the relativistic spherical optical model code SNOOPY,<sup>19</sup> and the coupled channel deformed optical model code ECIS<sup>20</sup> for calculating transmission coefficients. A version of GNASH has also been developed that includes an internal optical model routine but it is not in frequent use.

When GNASH was being developed in the early 1970s, the COMNUC code was in common use, so we adopted its format for the transmission coefficient file. The format is described in Appendix 3, including a sample of data from a TAPE10 file. Note that transmission coefficients for the various particles appearing in a calculation can be provided in arbitrary particle order. Also, if the NPART flag of Appendix 3 is negative, then total, shape elastic, and reaction cross sections from the optical model calculations can be provided for each energy on the transmission coefficient grid. This feature is useful in providing a complete set of cross sections in addition to those resulting from the GNASH calculations.



### C. Input or Calculation Directory File (INPUT)

The primary purposes of the INPUT file are to define the problem to be calculated, that is, the incident particle, the target, and the reaction sequences to follow, and to specify the models to be used, together with appropriate parameters as needed. Appendix 4 gives a complete description of input options available for setting up a problem. Appendix 5 presents a specific problem setup for a nonfissionable nucleus ( $n + {}^{93}\text{Nb}$ ) that is included in the computer exercises. Additional sample cases are included in the computer exercises, and a second example involving neutron reactions on  ${}^{238}\text{U}$  is included in Sec. IV to cover the input for a fission case.

The input example in App. 5 is a calculation of neutron, proton, and alpha emission cross sections and spectra from 14-MeV neutron bombardment of  ${}^{93}\text{Nb}$ . (This problem was chosen because a similar one was the subject of a model code comparison study sponsored by the Nuclear Energy Agency in 1983.) Under each of the input lines or groups of lines are given the variable names that are being read. (Note that due to space limitations, some variables at the end of several of the lines have been omitted.) Definitions of all the variables are given in App. 4. While there are a number of input quantities included in the input, many of the variables can simply be left blank or zero to set code defaults, or the values shown here can be used. In this discussion only the most important or frequently varied variables will be mentioned.

The first two lines of the input in App. 5 provide alphanumeric descriptive information regarding the calculation. The third line gives various print options plus the flag ILD, which is very often used to modify the default level density parameters used in a calculation. In the sample case of App. 5, ILD is not set, but if it were  $>0$ , then additional lines would follow specifying new level density parameters to override default values, as described in App. 4. The fourth line specifies the INPOPT parameter, which defines the input option to be used for directing the reaction sequences to be calculated. The choice used in the example is probably the most frequently used one, in that it permits one to tell at a glance what reaction sequences are being followed (lines 10-17), yet does permit some flexibility with parameters (using the ILD flag). The second variable on line 4 that should be mentioned is NLDIR, which gives the number of states for which direct reaction cross sections are read from TAPE33. In this case NLDIR is set to zero for simplicity, but its use is required in some of the computer exercises.

Line 5 gives many of the nuclear model option flags, and several of these are often varied. NI is the number of compound nuclei that will be followed in the calculation, NMP and LGROPT are used to define the gamma-ray strength function options, and LPEQ is a switch to turn the preequilibrium correction on or off. Similarly, IFIS must be turned on to include fission in a calculation, IBSF specifies the level density option to use, and IWFC must be set to read width-fluctuation correction factors from TAPE33. The flag ICAPT must be set equal to one to calculate

radiative capture cross sections and emission spectra. For calculations above a few MeV, where capture is not important, it is recommended to set  $ICAPT = 0$  to speed up calculations. (In the case of  $ICAPT = 0$ , gamma-ray cascades are not calculated in the initial or main compound nucleus.)

Line 6 of the input in App. 5 gives the ZAs for the incident particle and the target nucleus, as well as the important DE parameter, which is the energy bin width to use in the calculation. In the example in App. 5, a bin width of 1 MeV is used simply to keep running time short and to keep the output reasonably short; a more typical bin width for a 14-MeV calculation would be 0.25 MeV. Note that the incident particle ZAP is 1.0 for the neutron. If, for example, the incident particle were an alpha particle, then ZAP would be set equal to 2004.

Line 7 designates spin cutoff parameters, and lines 8 and 9 define the incident particle energies to be calculated. Lines 10-17 define the reaction sequences to calculate, under the input option  $INPOPT = -1$ . The ordering of the ZACN is important. The initial or main compound nucleus is given first (line 10), and every compound nucleus listed subsequently must have been formed in a previous reaction. For the cases shown, every compound nucleus decays by gamma ray, neutron, proton, and alpha emission.

Lines 18-20 in App. 5 specify that E1, M1, and E2 gamma-ray multipolarities are included in the calculations, using default values for relative values of the gamma-ray strength functions. Minimal input is included in lines 21 and 22 for the giant-dipole-resonance shape parameters, and the preequilibrium normalization and composite system state density are given in line 23.

By way of general comments, it should be mentioned that in specifying the decay sequence for emission of particles and gamma rays from a compound system, gamma-ray emission must always be given first. While this is done internally by GNASH when automatic setup options are used ( $INPOPT = -1, 1, 2, \text{ or } 3$ ), this ordering must be specified manually when  $INPOPT = 0$  is specified. Also, when manual setup ( $INPOPT = 0$ ) is used, the reaction parentage parameters, CNPI and CNPIP, must be specified. These parameters define the parent reaction that produces the new compound system. In the example given here, that is, with  $INPOPT = -1$ , the code automatically determines the parent reaction(s) and lumps them together. This feature is discussed further in Section II.E describing outputs.

For specification of parameters dealing with gamma-ray strength function shapes and normalizations, several comments are appropriate. Firstly, regarding the shape when the giant-dipole resonance (GDR) Brink-Axel option is used, the parameters EG1, GG1, EG2, GG2, G2NORM, XNFE1, EGCONM1, GDSTEP, GDELS, GDFLSL, EGCON, EG3, GG3, G3NORM, and GDELE all can be used to tailor the strength function shape, as needed. These parameters are described in detail in Appendix 4 and are indicated schematically in Fig. 9. In actual practice, however, the parameters other than the resonance energies and widths are seldom required, and frequently the only parameters needed for the  $LGROPT = 2$  or 3 cases are a single

GDR energy (EG1) and width (GG1), as used in the present example. For the greatest flexibility in specifying a gamma-ray strength function (E1 only), a tabulated E1 relative strength function can be input using the XNFE1 parameter and TAPE33.

Finally, the Kopecky-Uhl<sup>24</sup> gamma-ray strength function option is chosen in the example case (LGROPT = 3), using the model to calculate the relative strengths of the E1, M1, and E2 functions (RE1 = 0. and GGD NORM = 0. for default model values). The overall strength function is normalized to  $2\pi\langle\Gamma_{\gamma 0}\rangle/\langle D_0\rangle = |SWS| = 0.0118$  (line 10), as described in Sec. I.D.2. With the negative value of SWS on line 10, a single factor is applied to the model values for the E1, M1, and E2 gamma-ray strength functions to accomplish the desired normalization.

Discussion of the fission input option is reserved for Sec. IV.

#### **D. Optional Auxiliary File for Inputting Direct Reaction Cross Sections, Width Fluctuation Corrections, and Tabulated Gamma-Ray Strength Functions (TAPE33)**

As mentioned above, TAPE33 can be used to provide three additional types of information pertinent to a given problem:

1. if the XNFE1 flag is set on the problem input, then a tabulated shape appropriate to the E1 gamma-ray strength function can be provided;
2. if width fluctuation corrections are desired, the IWFC flag (line 5 of sample input in App. 5) can be set to indicate the appropriate input on TAPE33;
3. the most common use of this file is to provide direct reaction cross section contributions to inelastic scattering from discrete states by setting the NLDIR parameter greater than 1.

The input description appearing in App. 6 provides instructions for formats appropriate to TAPE33. Note that when DWBA results are used to determine direct reaction contributions and these are used with reaction cross sections determined from spherical optical model calculations, the reaction cross section available for use in Hauser-Feshbach or preequilibrium calculations are renormalized downward as described in Sec. I. However if coupled-channel calculations are used to produce the desired transmission coefficients, then the direct-reaction components are already removed from the transmission coefficients, that is, the reaction cross section obtained by summing the transmission coefficients already excludes the direct reaction component. Therefore no renormalization is necessary. In this latter case, NLDIR in the input should be incremented as NLDIR+100 to indicate no renormalization is required.

## E. Description of Output Data

Selected portions of the output from the  $n + {}^{93}\text{Nb}$  input given in App. 5 are presented in App. 7. The shortened output of App. 7 is broken into sections given below for the purpose of discussion.

### 1. Main OUTPUT file from $n + {}^{93}\text{Nb}$ calculation

#### a. Nuclear mass, reaction sequencing, and parentage information

The first item appearing in a GNASH output (not shown in App. 7) is a mirror listing of the INPUT file. Next is a listing of the Hollerith information at the beginning of the ground-state mass file (TAPE13), which is reproduced as item 1.A in App. 7. Item 1.B is a labelled listing of all the input variables, including the dimensions for major arrays used in the calculations. Note that all these dimensions are set in a PARAMETER statement and are easily increased or decreased, depending on the available computer memory. Two constraints were imposed for the present calculations as compared to our more usual configuration: the number of compound nuclei (NIDIM) and buffers (NIBDIM) were decreased from 16 to 10, and the number of possible energy bins (NKDIM) was decreased from 240 to 100. These changes result in a considerable reduction in storage requirements.

Item 1.C of App. 7 gives a description of the decay chains and lists other data determined from the problem setup, such as atomic masses and separation energies for each channel. Several items are important to note in this section of output. Notice that (lower case)  $I$  is used to index the various compound nuclei that are included in the calculation, running from 1 to 8 in this case. Similarly, the index  $IP$  is used to label each outgoing radiation channel from the various compound nuclei. For this problem  $IP$  runs from 1 to 4 in all cases, indicating gamma, neutron, proton, and alpha emission. A third index,  $IR$ , is used as a running index for all reaction channels, running from 1 to 32 in this problem. The columns labeled  $ZA1$  and  $ZA2$  give the  $ZA$  of the light and heavy reaction products, and  $XMR$ , and  $S$  give the mass of the heavy (residual) nucleus and the separation energy for each channel.

Beginning with the second compound nucleus ( $I = 2$ ,  $ZACN = 41093$ .), the " $I=...$ " and " $IP=...$ " statements just under  $ZACN$  indicate the  $I$  and  $IP$  of the parent reaction whose decay leads to this  $ZACN$ . Note that for the compound nucleus 40092. ( $I = 5$ ), the parentage indicators are " $I=204$ ." and " $IP=302$ ." These numbers mean that this compound nucleus (40092.) was formed in two preceding reactions, defined by  $I=2$ ,  $IP=3$  and  $I=4$ ,  $IP=2$ . Also note that the "buffer number" on the far right of the listing is the same for the two parent reactions as well as the gamma-ray emission channel of the  $I = 5$  compound nucleus. This simply means that the population data for the 40092 compound nucleus are accumulated in one buffer from all reactions

that form it. For this problem, the compound nuclei indicated by I = 5-8 all come from two parent reactions. Finally, it should be noted that using the more manual input INPOPT = 0 it is possible to avoid combining populations from multiple preceding reactions leading to a given compound nucleus. This latter capability can be useful in isolating contributions from specific channels.

In a complete output, item 1.C is followed by other input information, such as cross sections from the transmission coefficient file, width-fluctuation correction factors if that option is used, and direct cross sections (if included) interpolated at the particular incident energy being calculated.

#### **b. Gamma-ray strength function information**

In Sec. 2 of App. 7 details of the gamma-ray strength function input and normalization are given. This printing occurs in each of the major "I" or compound nucleus loops in the SPECTRA subroutine, which is discussed further in Sec. III. The column labeled "Constant" gives the normalization constant applied to each strength function, followed by the  $2\pi\langle\Gamma_{\gamma 0}\rangle/\langle D_0\rangle$  integral [see Eq. (20) of Sec. I] for each of the multipolarities, prior to normalization.

Note that messages beginning with "++++" are given in this part of the output to indicate that it was not possible to carry out the level density matching prescribed by Eqs. (29) and (30) for the reactions flagged. When this occurs, GNASH simply sets the matching energy between the Fermi-gas and temperature level density regions to a low value, so that use of the Fermi-gas formula begins at a lower-than-usual energy. Frequently, this results in the temperature region being eliminated altogether, that is, only the discrete levels and the Fermi-gas level density are used without precise matching.

#### **c. Preequilibrium spectra**

The preequilibrium parameters and results are printed in the first compound nucleus loop of the SPECTRA subroutine. The spectra that result are included in Section 3 of App. 7, tabulated for the outgoing neutrons (ID = 1), protons (ID = 2), and alpha particles (ID = 6). In the second column for each ID are the tabulated emission energies (midpoints of the energy bins), followed by the preequilibrium component, the equilibrium component (suitably adjusted to account for the preequilibrium flux), and the total emission spectrum value.

#### **d. Ratios of preequilibrium to reaction cross sections**

The main parameter required in the Kalbach systematics<sup>6</sup> for predicting particle angular distributions for a given emitted particle is the ratio of the preequilibrium cross section to the total emission cross section as a function of emission energy. These ratios are provided in the GNASH output just before the close of the compound nucleus loops in the SPECTRA subroutine. The

ratios, which are shown in Sec. 4 of App. 7, are small (or zero) at low emission energies and approach unity at the highest energies, as expected.

#### **e. Binary reaction cross sections**

Next in the GNASH output are the binary reaction and preequilibrium cross section summaries, as shown in Section 5 of App. 7. The first cross sections listed (with the x/s indicator) are mainly those obtained from the transmission coefficient file, or a combination of those results with the compound nucleus calculations. For example, the total, shape elastic, and reaction cross sections that are listed come from TAPE10, but the elastic and nonelastic cross sections also involve GNASH results. Note that, because the radiative capture flag was turned off for the example case, the "radiat. capture x/s" has a different meaning, that is, it is the radiative capture cross section plus the cross section for (n, $\gamma$ n') reactions, as the latter have not been removed. In fact, the radiative capture cross section at this energy is essentially equal to the direct-semidirect capture cross section, computed to be 0.82 mb in this case.

Next in the output are the "binary reaction summaries", which result entirely from the GNASH calculations using the particle transmission coefficients. Note that in the example shown the GNASH reaction cross section is almost, but not exactly, the same as the reaction cross section that comes on TAPE10 directly from the optical model code. This difference is reasonable because of differences in the integration routines in GNASH and in SCAT (in this case).

Finally, the preequilibrium and compound nucleus cross sections for binary reactions are summarized for all outgoing particles.

#### **f. Angle-integrated emission spectra for individual reactions**

Following the integrated cross sections are the angle-integrated emission spectra for individual reactions (Sec. 6, App. 7). These results are given in columns for each reaction channel, tabulated at each particle emission energy and given in the center of mass system of the outgoing particle plus nucleus. At the top of each column are given the ZA of the compound nucleus prior to decay, followed by the ZAs of the light and heavy reaction products. Discrete-level decay and excitation cross sections are given, mainly for diagnostic purposes, followed by the total production cross section and average emission energy for each channel. The latter two quantities are obtained by direct integration of the tabulated spectra that follow.

The individual reaction spectra are given for all 32 reaction channels included in the calculation. The ordering of the spectra is the same as the reaction ordering in the input.

It is within this portion of the output that cross sections for specific reaction paths can be determined. To do so, all particle paths leading to a specific compound nucleus must be summed together. From this sum cross sections for further decay by particle emission or fission must be

subtracted in order to obtain the desired reaction cross section. For the case of incident neutrons, some specific relations are as follows:

$$\begin{aligned}
 \sigma_{n,p} &= S_p(Z,A+1) - \sum_{i=n,p,\alpha} S_i(Z-1,A) \\
 \sigma_{n,\alpha} &= S_\alpha(Z,A+1) - \sum_{i=n,p,\alpha} S_i(Z-2,A-3) \\
 \sigma_{n,n'} &= S_n(Z,A+1) - \sum_{i=n,p,\alpha} S_i(Z,A) - \sigma_{\text{elas}} \\
 \sigma_{n,2n} &= S_n(Z,A) - \sum_{i=n,p,\alpha} S_i(Z,A-1) \\
 \sigma_{n,xn} &= S_n(Z,A+2-X) - \sum_{i=n,p,\alpha} S_i(Z,A+1-X) \\
 \sigma_{n,np} &= S_p(Z,A) + S_n(Z-1,A) - \sum_{i=n,p,\alpha} S_i(Z-1,A-1) \\
 \sigma_{n,n\alpha} &= S_\alpha(Z,A) + S_n(Z-2,A-3) - \sum_{i=n,p,\alpha} S_i(Z-2,A-4)
 \end{aligned} \tag{62}$$

where  $S_i(Z_{CN}, A_{CN})$  is the integrated cross section for particle  $i$ ,  $Z_{CN}$  and  $A_{CN}$  are given by the  $ZACN$  value at the top of each column ( $ZACN = 1000 Z_{CN} + A_{CN}$ ), and  $Z$  and  $A$  are the charge and mass of the target nucleus ( $Z = 41$  and  $A = 93$  in the example here). Analogous equations can be written for incident charged particles.

Note that if gamma decay of the residual nucleus produced by the reaction of interest is included in the calculation, then summation of the yield of the ground state and any long-lived isomeric states, which are listed in the discrete level section, should provide a similar cross section value as Eq. (62), provided that enough multiplicities are included in the gamma-ray decays to prevent "trapping" of cross section in the continuum cascade calculations. See Sec. II.E.1.h below for more on cross section trapping.

#### g. Composite particle and gamma-ray angle-integrated spectra

Following the section dealing with cross sections and spectra for individual reaction paths are similar data for composite spectra produced by summing contributions over all reaction paths for each outgoing radiation type (Sec. 7, App. 7). In this instance particle emission cross sections have multiplicities included. Note that all spectra are angle integrated and spectra from individual reactions are given in the center of mass system of the recoiling nucleus plus particle or gamma ray.

The integrated cross sections, average energies, and spectra are given in the same manner as for individual reactions, with the emission radiation types labelled at the top of each column. The final column on the right, labelled "g.neutr", is the spectrum of neutrons emitted following radiative capture, that is, from  $(n,\gamma')$  reactions. It is only activated if the radiative capture flag, ICAPT, is turned on, so only zeros appear in the example of App. 7.

#### **h. Discrete level cross sections: primary capture gamma-ray, level excitation, discrete gamma, and isomer production cross sections**

Following the spectral data in the output of App. 7 are discrete level cross sections computed for both particle and gamma ray emission (assuming IPRTLEV=1). These results follow the same order as the individual particle spectra, that is, they follow the order that the reaction sequence is input. The first quantities printed (Sec. 8.A) are the gamma-ray cross sections corresponding to transitions from the capturing state in the main compound nucleus to the discrete levels in the compound nucleus, that is, the cross sections for the primary capture gamma-ray lines. Obviously, these are small for 1- MeV incident neutrons and not of much significance in the example case. Under item 8.B are given the discrete gamma-ray cross sections from radiative capture in the main compound nucleus resulting from cascades among the discrete states, having the reaction index IR = 1. Again, because ICAPT = 0 for the present calculation, the continuum cascades for the main compound nucleus were not included in the calculation, so the actual numbers in item B have little meaning. The table has the same form, however, as for the ICAPT = 1 case and is explained further for the  $(n,n'\gamma)$  case described below.

Section 8.C of the App. 7 output contains all the rest of the discrete level data. The first three sets of information, consisting of 5 columns in the output, are discrete level excitation or production cross sections for the channel identified at the top of each set. For example, the first set of data under item C corresponds to the reaction identified by the labels I=1, IP=2, IR=2, and the emitted particle has ZA = 1 (a neutron) and the residual nucleus has ZA = 41093, and by inference the compound nucleus that emitted the neutron has ZA = 41094. Obviously, this is the  $^{93}\text{Nb}(n,n')^{93}\text{Nb}^*$  reaction to discrete states. Similarly, the next two sets of data under item C correspond to  $^{93}\text{Nb}(n,p)^{93}\text{Zr}^*$  (IR = 3) and the  $^{93}\text{Nb}(n,\alpha)^{90}\text{Y}^*$  (IR = 4) reactions to discrete states. Note, that these are excitation cross sections only, that is, there is no gamma cascading yet.

The fourth set of data in Sec. 8.C is for gamma-ray decay of  $^{93}\text{Nb}$  discrete states (I = 2, IP = 1, IR = 5) following  $(n,n')$  reactions, that is, these results are for  $(n,n'\gamma)$  reactions. The discrete states are populated by the neutron reactions in the parent channel I = 1, IP = 2, given above. In all instances of gamma-ray decay, the output includes both level excitation cross sections (4<sup>th</sup> column in the output) and gamma-ray level decay cross sections (12<sup>th</sup> or last column in the listing).



The discrete levels are populated from both the continuum region and from higher lying discrete levels. For isomeric states, that is, states whose decay is somehow impeded, the level excitation cross section (column 4) is the isomeric state cross section. For example, the excitation cross section for level number 2 in the IR = 5 data section (55.5 mb) is the calculated cross section for the well known  $^{93}\text{Nb}(n,n')^{93m}\text{Nb}$  reaction that produces the  $J^\pi = 1/2^-$ , 14-year isomeric state. In calculations involving nuclei with isomeric states, one must be careful to correct the decay scheme for longer-lived states that do not decay "promptly". The definition of "promptly" depends on, for example, the time scale of the measurement that is under comparison.

As pointed out in Sec. II.E.1.f above, the cross section for excitation of the ground-state level after deexcitation of all higher levels gives the production cross section for the residual nucleus. In the present example, this value (427 mb) corresponds to the  $^{93}\text{Nb}(n,n')$  integrated cross section. In general, this value should be consistent with  $\sigma_{n,n'}$  that is obtained using Eq. (62) above, providing that the spin distribution of the discrete states in the calculation is broad enough that no cross section is "trapped" in the continuum energy bins with no possibility of decay. Trapping of cross section in the continuum region occurs when the angular momentum change required for decay of continuum states to the discrete levels is inconsistent with the available gamma-ray multiplicities and can usually be avoided by adding more discrete levels or by adding additional gamma-ray multiplicities.

The next three discrete data sections give neutron, proton, and alpha deexcitation cross sections from the continuum region of  $^{93}\text{Nb}$  (IR = 6, 7, and 8), followed by a section giving the gamma-ray decay of  $^{92}\text{Nb}$  (IR = 9). The latter reaction corresponds to discrete gamma rays from  $^{93}\text{Nb}(n,2n\gamma)^{92}\text{Nb}$  reactions. In an actual output, discrete cross section results would be given for all other residual nuclei formed in the calculation, but for brevity these are omitted from App. 7.

#### i. Level density parameters and matching data

Finally, the last section of the output (Sec. 9, App. 7) provides information on the various level density parameters used for all residual nuclei in the calculation (assuming that the print control parameter is set as in the present case, IPRTC = 1). Again, the results follow the same order as the reaction sequence was input. Two tables of information are given covering the following parameters:

- I,IP,IR = Reaction indexes defined earlier;
- IZA1,IZA2 = ZA numbers for the emitted radiation and residual nucleus in each channel. The level density parameters correspond to the residual nucleus;
- A = Fermi-gas level density parameter;
- TEMP = Temperature in the temperature level density model;

- E0 =** Constant in the temperature level density model;
- EMATCH =** Energy at the boundary between the temperature and Fermi-gas level density regions;
- ECUT =** Energy at which the discrete level region is joined to the temperature level density region. Usually ECUT is the excitation energy of the highest discrete level used in the calculation;
- LEVELS AT ECUT =** Number of the highest discrete level used in the calculation, including the ground state.
- ECUTL =** Excitation energy of the lowest level used in the calculation;
- LEVELS AT ECUTL =** Number of the level at ECUTL (1 = ground state, 2 = first excited state, etc.)
- SIG2 =** Average value of the spin cutoff parameter,  $\sigma^2$ , in the discrete level region when the control parameter ISIG2 = 1;
- Q =** Q-value for the reaction or channel;
- PAIR =** Pairing energy,  $\Delta$ , used in level density calculations [for example, see Eq. (27)], usually determined from: PAIR = PZ + PN (see below), but PAIR can be directly input;
- DO =** Mean level spacing for s-wave neutrons, computed from the Fermi-gas level density expression using the parameters given here;
- PN =** Neutron pairing energy [P(N)];
- PZ =** Proton pairing energy [P(Z)];
- SN =** Neutron shell factor from the Cook tables;<sup>32</sup>
- SP =** Proton shell factor from the Cook tables;
- S =** Separation energy of the emitted radiation for the compound nucleus of each channel;
- SAC =** "Accumulated" separation for the compound nucleus of each channel relative to the initial or primary compound nucleus.
- ID =** Identification index for the various emitted radiation types, that is,
- ID = 1 for neutrons
  - ID = 2 for protons
  - ID = 3 for deuterons
  - ID = 4 for tritons
  - ID = 5 for <sup>3</sup>He
  - ID = 6 for <sup>4</sup>He
  - ID = 7 for gamma rays;
- SEPN =** Separation energy for neutrons relative to the residual nucleus (ZA2);

**SPINT =** Spin of the nucleus that results from separating a neutron from ZA2 (used with SEPN to calculate D0 for each channel).

The asterisks that appear in the "ECUTL" column indicate that either discrete level data are not present in the TAPE8 input for that ZA2, or that only the ground state is given. In either case the determination of the matching parameters is necessarily done differently (note that  $E0 = 0$  in the flagged channels) from the case where discrete levels are known. See the discussion in Sec. I.D.3.a, particularly Eqs. (29a) and (29b).

## **2. Binary output of continuum and level populations**

All GNASH calculations of continuum and discrete level populations are output in binary format on TAPE12. These data are used in the RECOIL code<sup>46</sup> to unfold the calculations to give, for example, neutron spectra from specific (n,xn) reactions for use in ENDF/B evaluations.

## **3. Auxiliary output files of discrete level and preequilibrium gamma-ray data**

Direct-semidirect radiative capture cross sections and photon emission spectra are output on TAPE59. These results are mainly used for checking purposes.

Detailed cross section information on all discrete level reactions calculated in GNASH are output on TAPE60. These results are used in the undocumented Los Alamos code F6GAM that produces ENDF/B-6 formatted gamma-ray production data.

## **F. Utility Codes for Analyzing GNASH Output**

A number of utility codes have been developed at Los Alamos to convert GNASH output files to other forms (ENDF/B files, thick target cross sections, etc.). Some of these codes are illustrated in Fig. 10, including summary remarks regarding their functions. Most of these codes are undocumented.

# **III. DESCRIPTION OF THE STRUCTURE OF THE GNASH CODE**

## **A. General Description of the Computational Approach**

The approach followed in GNASH is to use a main driver program to orchestrate input, problem setup, and output of results. A set of subroutines and functions perform the various model calculations and parameter manipulations. The basic Hauser-Feshbach calculations are

carried out in one large subroutine, described below, that calls in the major model subroutines and is essentially the heart of the code. The output from the code is provided in a standard form that has remained essentially unchanged for many years. Conversion or modification of the output to other formats, such as ENDF/B-6, is accomplished by external utility codes, as outlined in Sec. II.

## **B. Identification and Description of the Most Important Subroutines**

The structure of GNASH is illustrated in Fig 11. The main program module reads in problem-specific information from the INPUT file. It also determines the masses and binding energies as well as ground-state spins and parities through calls to the function ENERGY. A call to LEVPREP reads in discrete level information from TAPE8, while a call to TCPREP reads the particle transmission data from TAPE10. A call to SETUP initializes level density, direct reaction, width fluctuation, and spline parameters. This completes the portion of problem setup that is independent of incident energy.

A DO loop over incident energy is next executed in the main program, and for each incident laboratory energy the following sequence occurs. SETUP2 is called to determine energies and integration end points as well as transmission coefficients for the incident channel. Direct reaction cross sections are also evaluated at the specified incident energy. The SPECTRA subroutine, which is described in detail below, is then called to carry out the major Hauser-Feshbach cross section calculations. If preequilibrium corrections are desired, the PRECMP subroutine is called by SPECTRA after calculations for the first compound nucleus have been completed. Following the Hauser-Feshbach continuum and discrete level calculations, the subroutine GRLINES is called to calculate the deexcitation of all discrete levels by gamma-ray emission until the ground state is reached. After completion of the calculations in SPECTRA, the main program calls PREGAM1 to perform the direct-semidirect radiative capture calculation and to combined those results with the SPECTRA output. Finally, the subroutine DATAOUT is called to print output results. This whole process is then repeated for the next incident energy.

Listed below are the subroutines and functions (indicated with asterisks) comprising GNASH:

1. LCSPACE - Sets up storage, determines parent reactions for decay sequences, and assigns buffers for the various compound nuclei.
2. CHAINS - Constructs optional automatic reaction sequences.
3. ENERGY - Reads mass and ground state spin, parity for TAPE13.
4. LEVPREP - Reads in level data from INPUT or more commonly from TAPE8. Prepares level data as needed for calculation. Calls SORTS.

5. SORTS - Sorts ZA data into ascending order.
6. TCPREP - Reads in particle transmission coefficient from input or more commonly from TAPE10. Eliminates j-dependence of spin 1/2 arrays.
7. SETUP - Determines accumulated separation energies for decaying nuclei and identifies secondary reaction particles and photons. Initializes level density parameters and reads direct reaction cross sections and width fluctuation factors (if desired) from TAPE33.
8. SETUP2 - Determines energies appropriate to problem execution and integration end points. Generates transmission coefficients for incident channel at a given lab energy and also determines direct reaction cross sections appropriate for that energy.
9. SPECTRA - Main cross section calculation routine which is described in detail later. Calls LCMLOAD, GAMSET, INTERPI, PRECMP, and GRLINES. If fission is included calls RHOFIS, BAND, and TFIS.
10. INTERPI - Finds indices for interpolation.
11. TFIS\* - Computes Hill-Wheeler penetrability.
12. BAND - Builds fission transition states from bandhead information.
13. RFIS\* - Computes fission transition state densities.
14. LEVDSET - Determines pairing and Fermi gas parameters. Calls GILCAM for Gilbert-Cameron constant temperature and matching parameters and DOGET to compute  $D_{\text{observed}}$ .
15. DEFN\* - Function that provides deformation energies for computations with Ignatyuk level density.
16. AIGN\* - Function that provides the Fermi-gas level density parameter for calculations with the Ignatyuk level density formulation.
17. GILCAM - Determines constant temperature level density parameters by matching with discrete states data and Fermi-gas level density.
18. LCMLOAD - Computes and stores transmission coefficients on energy grid required for  $I^{\text{th}}$  compound nucleus. Similarly, calculates level density and Yrast values. Provides a print of these quantities on integration grid if desired.
19. GAMSET - Sets up gamma ray cascade calculation. Determines Weisskopf, Brink-Axel, or Kopecky-Uhl strength function parameters and calculates gamma-ray transmission coefficients on integration grid. Provides printout if desired. Calls FXCAL.
20. FXCAL - Computes gamma-ray strength function.

21. WEISSKF - Computes normalization factor for gamma-ray transmission coefficients. Calls FXCAL.
22. INCHSUM - Performs sum over  $s$  and  $l$  of incident channel for a given compound nucleus spin and parity.
23. GRLINES - Calculates discrete gamma-ray cross sections, sums spectra to produce integrated cross sections, computes particle emission from particle unstable levels. Reads level data from TAPE9 scratch file. Calls ISERCH.
24. DATAOUT - Main output routine, calls LINEW2.
25. LINEW2 - Utility for BCD single line writes, calls CXFP.
26. CXFP - Allows more efficient E-formatted writes.
27. ISERCH\* - Function that finds the necessary parameters for spline interpolation.
28. PRECMP - Main calling routine for preequilibrium corrections. Calls PRECOC. Renormalizes spectra, cross sections, and populations.
29. PRECOC - Based on PRECO-B program of Kalbach. Calls COMDEN, TTRANS, EMISS, RESOL, PICNOC, PRESPEC.
30. COMDEN - Determines composite nucleus state densities using Williams expressions. Calls WELL, OMEGA.
31. TTRANS - Computes  $\lambda_+$ ,  $\lambda_-$ ,  $\lambda_0$ .
32. QBETA\* - Determines  $Q_b$  for proton neutron distinguishability.
33. OMEGA\* - Calculated (p,h) state densities.
34. PRESPEC - Determine preequilibrium emission spectra; prints results.
35. RESOL - Solves master equation as well as determines closed-form preequilibrium results.
36. EMISS - Calculates particle emission rates for a given p-h configuration. Determines total emission rate. Calls WELL, OMEGA, QBETA.
37. PICNOC - Determines contributions due to pickup, knockout, and alpha particle reaction processes. Calls FACTOR, FF, OMEGA2.
38. FACTOR\* - Computes factorial.
39. FF\* - Computes  $f$  function needed for pickup, knockout.
40. OMEGA2\* - Computes state densities required for pickup, knockout, etc.
41. PREGAMI - Calculates preequilibrium gamma-ray emission cross sections using detailed balance and the prescription of Akkermans and Gruppelaar.<sup>39</sup>
42. INTERP - Interpolation function.
43. SPLINE - Spline subroutine.
44. FUNDAK\* - Used by spline subroutine.
45. CUT - Used to infer average spin cutoff from distribution of discrete states.

- 46. AGET - Calculated Gilbert-Cameron Fermi gas parameters for  $D_{(j)}$ .
- 47. D0GET - Calculates  $D_{(j)}$  from Gilbert-Cameron level density 'a' parameter.
- 48. WELL - Calculates finite well depth correction factors for use in determining surface effects in preequilibrium model.
- 49. GDR\* - Function that calculates giant-dipole-resonance gamma-ray strength functions for PREGAM1 subroutine.
- 50. NFACT\* - Computes factorials for PREGAM1 subroutine.
- 51. STATEDEN\* - Function that calculates state densities for the PREGAM1 subroutine using the unrestricted Williams expression.

### C. Discussion of the SPECTRA Subroutine

The SPECTRA subroutine is the main calculational portion of the program and is where partial and total widths, continuum population increments, and discrete level populations are computed for all compound systems occurring in a specified decay chain. Fig. 4 (Sec. 1.C.2) illustrates schematically the technique used to accumulate populations during these decay processes, while Fig. 12 provides a simplified description of the coding used to compute binary reaction processes involved in particle or gamma-ray decay.

Several nested DO loops are used to handle the entire reaction sequence. As illustrated in Fig. 12 the outermost loop sums over all compound nuclei appropriate for the problem. The next loop sums over all energy bins (specified by K) in the decaying compound nucleus defined by the first loop. Once a continuum bin is identified, a third loop sums over all decay channels specified for that compound nucleus. The decay type defines the residual nucleus reached so that within this loop contributions from the decay of the continuum bin K to discrete levels in the residual nucleus are accumulated. Increments to the partial and total widths for the specific  $J^\pi$  compound nucleus state are also determined.

After the calculation is completed for decay of the continuum bin K into discrete levels in all residual systems, then the calculation for continuum to continuum transitions is made. For a given energy bin K, the sum over all  $J^\pi$  states begins. For each compound nucleus state specified by  $(U, J, \pi)$ , the sum over all decay channels (in a manner analogous to the method used for population of discrete levels) begins. For each decay process (reaction type), a sum over the allowed range of energy bins in the residual nucleus defined by the decay is made. Within this sum contributions to both partial and total widths are obtained. Note that for both continuum-level and continuum-continuum transitions, the same methodology is used to compute decays no matter what the specific radiation type (gamma rays, particle decay, fission).

After the calculation of partial and total widths has been completed, a series of similar loops is used to normalize each partial width by the total width for the compound nucleus state specified by  $(U, J, \pi)$ . Contributions to spectra are computed and the total population reached by any combination of decay paths and continuum bin decay are stored. Level population arrays are also incremented. If preequilibrium corrections are to be made (for the first compound nucleus), then PRECMP is called. Afterwards the loop over compound nuclei continues until all compound system decays that are energetically possible have been computed. Finally, GRLINES is called to compute discrete gamma ray cross sections after cascades have occurred and these are then added to computed gamma ray spectra.

#### **D. Summary of General Guidelines for Calculations with GNASH**

In this section we list some guidelines that will help avoid problems when running the GNASH code:

1. When setting up reaction decay sequences, it is essential that the first decay channel in each compound nucleus be for gamma rays.
2. It is recommended that the second decay channel for the main compound nucleus be inelastic scattering, that is, emission of the incident particle from the main compound nucleus.
3. No compound nucleus should be put into the reaction sequence until all reactions that decay to it have already been entered.
4. When setting up reaction sequences for higher energy calculations, that is, ones that involve formation of compound nuclei from multiple reactions paths with different Q-values, the reactions with the largest (most positive) Q-values should generally appear first in the input file.
5. When running neutron-induced reactions, our usual procedure regarding gamma-ray strength function normalization is to input  $2\pi\langle\Gamma_{\gamma 0}\rangle/\langle D_0\rangle$  (SWS in the input) using experimental data for the main compound system, and then to set SWS to zero for the remaining compound nuclei. When this is done, the code uses the same normalization factors for the gamma-ray strength functions for all compound systems. These factors have been found to be slowly varying for nearby nuclei.
6. Concerning gamma-ray strength functions for incident charged particles, we usually use normalization constants from a nearby neutron-induced calculation. In this way we are able to utilize  $2\pi\langle\Gamma_{\gamma 0}\rangle/\langle D_0\rangle$  or  $\sigma_{n,\gamma}(E_n)$  results from experiments in determining the gamma-ray strength functions.



7. It is recommended that  $ICAPT = 0$  be used in all calculations except those specifically addressed to  $(n,\gamma)$  radiative capture cross sections and spectra. The main reason for this recommendation is that including the photon cascade in the first compound nucleus ( $ICAPT = 1$ ) greatly increases computation time at higher energies, and the  $(n,\gamma)$  cross section is usually negligible compared to  $(n,n'\gamma)$  and  $(n,xn\gamma)$  reactions at higher energies.

## **E. Examples of Calculations with GNASH**

In this section examples of calculations with GNASH are illustrated, including results from the example calculations used in the computer exercises.

### **1. Examples of discrete/continuum level density matching**

Figure 13 shows some typical examples of matching discrete level structure with the temperature level density function, Eq. (27). In these cases Eq. (29b) was used for the matching. A comparison is given in Fig. 14 of matching the same discrete levels for  $^{239}\text{Pu}$  with the two forms of the temperature function given in Eqs. (29a) and (29b).

### **2. Neutron-, proton-, and alpha-induced reactions near $A = 56$**

Results from calculations of several  $n + ^{56}\text{Fe}$  cross sections as functions of incident energy using the input parameters from the computer exercises are compared with experimental data<sup>47</sup> in Figs. 15-17. Additionally, calculations of  $(p,n)$ ,  $(p,2n)$ , and  $(\alpha,n)$  cross sections on targets in the neighborhood of  $^{56}\text{Fe}$  are illustrated in Figs. 18-20. These latter calculations involve parameterizations similar to but not identical with those used in the computer exercises.

### **3. $n + ^{93}\text{Nb}$ reactions**

Several comparisons to experimental data<sup>47</sup> of calculations of  $n + ^{93}\text{Nb}$  cross sections using the present parameters (App. 5) are given in Figs. 21-24.

### **4. $n + ^{238}\text{U}$ and $p + ^{238}\text{U}$ results**

Results from GNASH calculations of the  $^{238}\text{U}(n,f)$  cross section using model parameters from the computer exercises are illustrated with experimental data<sup>47</sup> in Fig. 25. A similar comparison for the  $^{238}\text{U}(p,f)$  cross section is given in Fig. 26.

## 5. Neutron-induced reactions on Pb isotopes

Results from an extensive set of calculations of neutron-induced reactions on Pb isotopes between  $E_n = 0.01$  and  $100 \text{ MeV}^{11}$  are reproduced in Figs. 27-39. These results illustrate the wide range of experimental data<sup>47</sup> that can be represented in a consistent analysis.

## IV. HIGHLIGHTS OF THE MULTIBARRIER FISSION MODEL IN GNASH, AND PLANS FOR FUTURE DEVELOPMENTS OF THE CODE

### A. Fission Model

#### 1. Description of the fission model in GNASH

The theory associated with the fission model used in GNASH is described in Sec. I.D.5.

#### 2. Input example for fission cross section calculation

The input for the  $n + {}^{238}\text{U}$  calculation covered in the computer exercise examples is given in App. 8. The input is similar to the  $n + {}^{93}\text{Nb}$  case in App. 5 except, of course, the fission flag (IFIS) is set, and an additional line of input is required to input the number of fission barriers to use (line 6). In the example shown here,  $\text{NBAR} = 2$ , that is, a double-humped barrier is used.

The case shown is for 12-MeV incident neutrons, with a relatively straightforward decay sequence, that is, only the gamma-ray, neutron, and fission channels are considered. Note that the fission channels are defined by setting  $\text{ZAI} = 99$  in the decay sequences. At high enough incident energy, proton competition might become significant, but this setup should be adequate up to a least 20 MeV. A more complicated input option ( $\text{INPOPT} = 0$ ) is used in this case to specify the reaction sequence. We typically use this setup for fission problems, because there is usually an interest in specifying more of the level density and matching parameters, and  $\text{INPOPT} = 0$  is convenient for this purpose. Additionally, we already need to input a relatively large amount of fission barrier and transition state data, so being concise is not possible. In the case shown, the level density parameter, the number of discrete levels, the associated excitation energy to match, and the pairing energy are directly input for a number of the channels.

The  $\text{LGROPT} = 2$  option was set in line 5, directing use of the Brink-Axel gamma-ray strength function (GSF). On lines 32-34, the  $\text{REI}(\text{MP})$  are directly input for E1 and M1 and are used with  $\text{SWS}(1) = +0.0063$  to set the normalization constants  $\text{GGDNORM}(\text{MP})$ . Because  $\text{SWS}(\text{MP} > 1)$  are zero, the same GSF normalization constants are used for all compound nuclei. Note that even though finite values for  $\text{GGDNORM}(\text{MP})$  are given in lines 32-34 of the input, the normalization is determined by  $\text{SWS}(1)$ . If, on the other hand,  $\text{SWS}(1)$  were to be set to zero, then the inputted values of  $\text{GGDNORM}(\text{MP})$  would be used for all compound nuclei, as described

in the input description of App. 4. A double peak is used for the GDR Lorentzian (line 35), and the E1 GSF is held constant below  $EGCON = 0.5$  MeV (line 36).

The fission barrier parameters begin on line 38, just following the preequilibrium model input, where nominal values are used. The fission parameters are given in the exact same order as the reaction sequences input in lines 11-31, that is, there is a set of barrier parameters for each compound nucleus appearing in lines 11-31 that has a fission ( $ZA1 = 99.$ ) decay mode. Therefore, lines 38-77 give fission barrier input for  $ZACN = 92239.$ , lines 78-91 for  $ZACN = 92238.$ , etc. (The parameters given here are ones used in calculations for the ENDF/B-VI analysis of  $n + {}^{238}\text{U}$  data.)

Considering the input for  $ZACN = 92239.$ , the barrier heights are given in MeV in line 38, the values of  $\hbar\omega$  (MeV) for the barriers in line 39, and the level density enhancement factors for the two barriers in line 40. The barrier transition states appear next in the input (lines 41-77). Because a positive value of FSTS is used, the actual excitation energies, spins, and parities of the transition states are read in this case, and the same set of transition states (lines 42-77) are used for both barriers. Looking at the input for the second compound system,  $ZACN = 92238.$ , a negative value of FSTS is input (line 81), which means that bandhead information is input with separate bandhead data for each barrier (lines 82-91). In this case, the code automatically constructs the transition states for the bandhead data, using Eq. (60) of Sec. I.

### **3. Output example from fission calculation.**

Excerpts from the output obtained for the  $n + {}^{238}\text{U}$  calculation using the input described above (Sec. IV.A.2) are given in App. 9.

#### **a. Input data**

The first section of any GNASH output is a reproduction of the input data used for the calculation. Following the first section, the input options are listed again with the variables explicitly defined, as shown in Sec. 1 of App. 9. Note that for this case  $NLDIR = 119$  is used, which means that direct reaction cross sections are expected for  ${}^{238}\text{U}$  states through level number 19 on TAPE33. Because  $NLDIR$  is greater than 100, the input direct reaction data are (predominantly) from coupled-channel calculations, so no reaction cross section renormalization is made by the code.

#### **b. Reaction labeling, reaction parentage, masses, buffer numbers**

The reaction sequences are given in Sec. 2 of App. 9, together with the parentage indices, masses, separation energies, and compound nuclei buffers. This section of output is similar to the previous example given in App. 7.

### c. Fission barrier parameters

Section 3 of App. 9 reproduces the portion of the output that gives the fission barrier parameters for the various compound nuclei in the calculations, including all the transition-state data. The data are listed in the same order as the reaction sequence was input, namely,  $^{239}\text{U}$  first barrier,  $^{239}\text{U}$  second barrier,  $^{238}\text{U}$  first barrier, etc. For  $^{239}\text{U}$ , the discrete transition state data is directly input, and the same data are used for both barriers, except different barrier heights are added. In the cases of  $^{238}\text{U}$  and subsequent compound nuclei, the transition states are constructed from the separate bandhead information input for each barrier. The actual transition state data was constructed using Eq.(60) of Sec. 1, and the data for  $^{238}\text{U}$  are shown in Sec. 3 of App.9.

### d. Direct reaction cross section data

As mentioned above, the control parameter NLDIR is set to 119, which means that direct reaction cross section data are read for the first 19 levels of the target nucleus from TAPE33. Section 4 of App. 9 reproduces part of the output concerned with the direct reaction cross sections. The results shown lie inside the incident energy loop, and include a printing of the direct reaction cross sections interpolated to the incident energy, 12 MeV in this case. The direct reaction input data in TAPE33 must include all states up to the highest level with direct reaction data. Therefore, several of the cross sections have zero values. Also, because NLDIR is greater than 100, these direct cross sections are from coupled-channel calculations (predominantly), and the reaction cross section resulting from the transmission coefficients is not renormalized downward by GNASH. In actual fact, only the direct cross section for states numbered 2-5 are from coupled channel calculations, corresponding to the  $2^+$ ,  $4^+$ ,  $6^+$ , and  $8^+$  states of the ground-state rotational band. The cross sections for higher excitation states result from DWBA calculations of vibrational states but are small compared to the coupled-channel cross sections.

### e. Preequilibrium information

More details of the output from the preequilibrium model calculations are included in Sec. 5 of App. 9 than were shown in the previous example in App. 7. In particular, Sec. 5 begins with a table of the particle-hole occupation probabilities, followed by the preequilibrium and unadjusted Hauser-Feshbach spectra. Finally, the corrected inelastic neutron spectra are given.

### f. Binary cross sections

The binary reaction cross sections from the  $n + ^{238}\text{U}$  calculation are given in Sec. 6 of App. 9. Again, the first set of integrated cross sections (adjacent to "lab neutron energy = 1.2000e+01") comes mainly from the optical model cross sections on TAPE10 and the direct cross sections on TAPE33, with some integration of GNASH results. Although annotated remarks are supplied

(bold face), it should be mentioned that under the "binary reaction summaries" section (which only includes GNASH results), the reaction cross section is obtained entirely from the incident particle transmission coefficients. Because NLDIR is set greater than 100, no correction was made in GNASH to remove the DWBA component of the direct cross sections from the GNASH reaction cross sections (although the coupled-channel direct component is automatically removed from the transmission coefficients).

#### **g. Individual reaction spectra for $n + {}^{238}\text{U}$ calculations**

In Sec. 7 of App. 9 the energy spectra of emitted particles and gamma rays are given, together with integrated cross sections and average spectral energies. These results are similar to the output example for  ${}^{93}\text{Nb}$  (App. 7), except in this case the spectral data have no meaning for the fission case ( $\text{ZA1} = 99$ ), because only a cross section is computed in GNASH. The one entry in the spectrum column is simply the fission cross section divided by DE, the bin width. Note that the fission cross sections given in this section correspond to multichance fission, that is, the first-chance fission cross section is 0.352 b, second-chance is 0.647 b, and third-chance fission is 0.210 b for the case shown.

#### **h. Composite spectra for emission particles and gamma rays**

Composite particle-emission spectra, average energies, and integrated cross sections are given in Sec. 8 of App. 9. Again, the spectrum print has no meaning for the fission channel, as the only entry in the spectral part of the fission column is the total fission cross section divided by the energy bin width. It should be noted, however, that while the other columns are valid, neutrons and gamma rays from fission fragments are not included in GNASH calculations such as those discussed here. In order to compute emission spectra from fission fragments, a separate set of GNASH calculations must be made that combines results from calculations like the present ones with additional modeling for the distributions, excitation energies, etc., of the fission fragments.

#### **i. Level density information for $n + {}^{238}\text{U}$ calculations**

The level density parameters for the present problem are given in Sec. 9 of App. 9. The various quantities in the output tables are the same as defined in Sec. II.E.1.i. Note that asterisks appear for all residual nuclei in the "ECUTL" column, indicating that the simple model [Eq. (29a) of Sec. I.D.3.a] was used for matching the temperature level density with the discrete level data.

## **B. Plans for Future Developments**

### **1. Cross sections from multiple preequilibrium processes**

One of the authors (M.B.C) has developed a simple module for calculating cross sections from multiple preequilibrium reactions. Such effects can be important in calculating certain reaction cross sections, even at fairly low incident energies (30-40 MeV). We have found that  $(n,2n\gamma)$  cross sections can be particularly sensitive to secondary nucleon preequilibrium processes, and we plan to incorporate the new coding into the full Hauser-Feshbach version of GNASH.

### **2. Automation of calculation of collective effects**

The technique demonstrated here of including direct reaction effects from external calculations has been used often and has provided meaningful additions to many GNASH analyses. However, it would clearly benefit users of the code to have an internal routine installed in the code to permit the calculation of cross sections from collective effects in an automated fashion. Accordingly, we plan to install a routine for estimating cross sections from vibrational levels based on a simple model described by Kalka et al.<sup>48</sup>

### **3. Photon-induced reactions**

The present versions of GNASH do not provide for incident photon calculations. Most of the modeling required for such calculations is already in GNASH, and we plan to make the required changes to permit this option in the future.

### **4. Fission fragment calculations**

As mentioned above, GNASH can be used to calculate both primary fission cross sections (as described above), and the neutron and gamma-ray emission cross sections from fission fragments formed in the primary fission reactions. At present, the latter can only be calculated in an automated fashion with the evaporation version of GNASH. We plan to develop a version of the full Hauser-Feshbach statistical/preequilibrium code to perform such calculations.

### **5. Increase user friendliness and generally tidy up coding**

The GNASH code was developed originally as a calculational tool for providing evaluated nuclear data, with little concern for a wider distribution of the code than just the authors. While many improvements in user friendliness have been made, there are clearly many more that might be incorporated. We plan to gradually build in more automation and to clarify some of the ambiguities associated with setting up calculations.

## REFERENCES

1. N. Yamamuro, "Nuclear Cross Section Calculations with a Simplified-Input Version of ELIESE-GNASH Joint Program," Proc. Int. Conf. on *Nuclear Data for Science and Technology*, Mito (1988) p.489; *ibid.*, Japanese Atomic Energy Research Institute report JAERI-M 90-006 (1990).
2. P. G. Young, E. D. Arthur, M. Bozoian, T. R. England, G. M. Hale, R. J. LaBauve, R. C. Little, R. E. MacFarlane, D. G. Madland, R. T. Perry, and W. B. Wilson, "Transport Data Libraries for Incident Proton and Neutron Energies to 100 MeV," *Trans. Am. Nucl. Soc.* **60**, 271 (1989); *ibid.*, Los Alamos National Laboratory report LA-11753-MS (1990).
3. P. G. Young and E. D. Arthur, "GNASH: A Preequilibrium, Statistical Nuclear Model Code for Calculation of Cross Sections and Emission Spectra," Los Alamos National Laboratory report LA-6947 (1977).
4. P. G. Young, E. D. Arthur, and M. B. Chadwick, "Comprehensive Nuclear Model Calculations: Introduction to the Theory and Use of the GNASH Code," Proc. ICTP Workshop on *Computation and Analysis of Nuclear Data Relevant to Nuclear Energy and Safety*, 10 February - 13 March, 1992, Trieste, Italy.
5. E. D. Arthur, "The GNASH Preequilibrium Statistical Model Code," Proc. ICTP Workshop on *Applied Nuclear Theory and Nuclear Model Calculations for Nuclear Technology Applications*, 15 February - 18 March, 1988, Trieste, Italy.
6. C. Kalbach, "Systematics of Continuum Angular Distributions: Extensions to Higher Energies," *Phys. Rev. C* **37**, 2350 (1988); see also C. Kalbach and F. M. Mann, "Phenomenology of Continuum Angular Distributions. I. Systematics and Parameterization," *Phys. Rev. C* **23**, 112 (1981).
7. P. Rose, "ENDF-201: ENDF/B Summary Documentation," 4<sup>th</sup> Edition (ENDF/B-VI), Brookhaven National Laboratory report BNL-NCS-17541 [ENDF-201] (1992).
8. E. D. Arthur, "Calculation of Neutron Cross Sections on Isotopes of Yttrium and Zirconium," Los Alamos National Laboratory report LA-7789-MS (1979).

9. E. D. Arthur and P. G. Young, "Evaluation of Neutron Cross Sections to 40 MeV for  $^{54,56}\text{Fe}$ ," Proc. Sym. on *Neutron Cross Sections from 10 to 50 MeV*, Brookhaven National Laboratory, Upton, N.Y., 12-14 May 1980 [Ed: M. R. Bhat and S. Pearlstein, BNL-NCS-51245 (1980)] v. II, p. 731; *ibid*, Los Alamos National Laboratory report LA-8626-MS (1980).
10. E. D. Arthur, P. G. Young, and W. K. Matthes, "Calculation of  $^{59}\text{Co}$  Neutron Cross Sections between 3 and 50 MeV," Proc. Sym. on *Neutron Cross Sections from 10 to 50 MeV*, Brookhaven National Laboratory, Upton, N.Y., 12-14 May 1980 [Ed: M. R. Bhat and S. Pearlstein, BNL-NCS-51245 (1980)] v. II, p. 751.
11. P. G. Young, R. C. Haight, R. O. Nelson, S. A. Wender, C. M. Laymon, G. L. Morgan, D. M. Drake, M. Drogg, H. Vonach, A. Pavlik, S. Tagesen, D. C. Larson, and D. S. Dale, "Calculation of (n,xy) Cross Sections between Threshold and 100 MeV for Fe and Pb Isotopes: Comparisons with Experimental Data," IAEA Coord. Res. Prog. Meeting on Methods for the Calculation of Neutron Nuclear Data for Structural Materials of Fast and Fusion Reactors, Vienna, Austria, 20-22 June 1990 [Compiler: D. W. Muir, INDC(NDS)-247 (1991)] p. 239.
12. P. G. Young, E. D. Arthur, M. Bozoian, T. R. England, G. M. Hale, R. J. LaBauve, R. C. Little, R. E. MacFarlane, D. G. Madland, R. T. Perry, and W. B. Wilson, "Transport Data Libraries for Incident Proton and Neutron Energies to 100 MeV," *Trans. Amer. Nucl. Soc.* **60**, 271 (1989) and Los Alamos National Laboratory report LA-11753-MS (1990).
13. M. Uhl, "Calculations of Reaction Cross Sections on the Basis of a Statistical Model, with Allowance for Angular Momentum and Parity Conservation," *Acta Physica. Austri.* **31**, 245 (1970).
14. C. L. Dunford, "A Unified Model for Analysis of Compound Nucleus Reactions," Atomic International report AI-AEC-12931 (1970).
15. P. A. Moldauer, "Evaluation of the Fluctuation Enhancement Factor," *Phys. Rev. C* **14**, 764 (1976).
16. J. W. Tepel, H. M. Hofmann, and W. A. Weidenmüller, "Hauser-Feshbach Formulas for Medium and Strong Absorption," *Phys. Lett.* **49B**, 1 (1974).



17. C. Kalbach, "The Griffin Model, Complex Particles and Direct Nuclear Reactions," *Z. Phys. A* **283**, 401 (1977).
18. O. Bersillon, "SCAT2 - A Spherical Optical Model Code," in *Progress Report of the Nuclear Physics Division, Bruyeres-le-Chatel 1977* CEA-N-2037, p. 111 (1978).
19. D. G. Madland, Los Alamos National Laboratory, personal communication (1990).
20. J. Raynal, "Optical Model and Coupled-Channel Calculations in Nuclear Physics," International Atomic Energy Agency report IAEA SMR-9/8 (1970) p. 281.
21. Ch. Lagrange, O. Bersillon, and D. G. Madland, "Coupled-Channel Optical-Model Calculations for evaluating Neutron Cross Sections of Odd-Mass Actinides," *Nucl. Sci. Engr.* **83**, 396 (1983).
22. D. M. Brink, "Some Aspects of the Interaction of Fields with Matter," D.Ph. Thesis, Oxford (1955); D. M. Brink, "Individual Particle and Collective Aspects of the Nuclear Photoeffect," *Nucl. Phys.* **4**, 215 (1957); P. Axel, "Electric Dipole Ground State Transition Width Strength Function," *Phys. Rev.* **126**, 671 (1962).
23. J. M. Blatt and V. Weisskopf, *Theoretical Nuclear Physics* (John Wiley and Sons, Inc., New York, 1952).
24. J. Kopecky and M. Uhl, "Test of Gamma-Ray Strength Functions in Nuclear Reaction Model Calculations," *Phys. Rev. C* **42**, 1941 (1990).
25. J. Kopecky and M. Uhl, "Present Status of Gamma-Ray Strength Functions and Their Impact on Statistical Model Calculations," Stichting Energieonderzoek Centrum Nederland report ECN-RX-90-024 (1990).
26. S. S. Dietrich and B. L. Berman, "Atlas of Photoabsorption Cross Sections Obtained with Monoenergetic Photons," *Atomic Data and Nuclear Data Tables* **38**, 199 (1988).
27. S. F. Mughabghab, M. Divadeenam, and N. E. Holden, *Neutron Cross Sections, V. 1, Part A, Z = 1-60* (Academic Press Inc., 1981); S. F. Mughabghab, *Neutron Cross Sections, V. 1, Part B, Z = 61-100* (Academic Press Inc., 1984).

28. A. Gilbert and A. G. W. Cameron, "A Composite Nuclear-Level Density formula with Shell Corrections," *Can. J. Phys.* **43**, 1446 (1965).
29. U. E. Facchini and E. Sacta-Menichella, "Level Density Parameter Values from Neutron and Proton Resonances," *Energ. Nucl.* **15**, 54 (1968).
30. W. Dilg, W. Schantl, H. Vonach, and M. Uhl, "Level Density Parameters for the Back-Shifted Fermi Gas Model in the Mass Range  $40 < A < 250$ ," *Nucl. Phys.* **A217**, 269 (1973).
31. A. V. Ignatyuk, G. N. Smirenkin, and A. S. Tishin, "Phenomenological Description of the Energy Dependence of the Level Density Parameter," *Sov. J. Nucl. Phys.* **21**, 255 (1975).
32. A. H. Wapstra, G. Audi, and R. Hoekstra, "Atomic Masses from (Mainly) Experimental Data," *At. Data and Nucl. Data Tables* **39**, 281 (1988).
33. C. Kalbach, "PRECO Program for Calculating Preequilibrium Particle Energy Spectra," Centre d'Etudes Nucléaires de Saclay Rapport Interne DPh-N/BE/74/3 (1974).
34. C. Kalbach, "Surface Effects in the Exciton Model of Preequilibrium Nuclear Reactions," *Phys. Rev. C* **32**, 1157 (1985).
35. F. C. Williams, Jr., "Particle-Hole State Density in the Uniform Spacing Model," *Nucl. Phys.* **A166**, 231 (1971).
36. H. Gruppelaar, "Level Density in Unified Preequilibrium and Equilibrium Models," Stichting Energieonderzoek Centrum Nederland report ECN-83-064 (1983).
37. J. Dobes and E. Betak, "Two-Component Exciton Model," *Z. Phys. A* **310**, 329 (1983).
38. C. Kalbach, "PRECO-D2: Program for Calculating Preequilibrium and Direct Reaction Double Differential Cross Sections," Los Alamos National Laboratory report LA-10248-MS (1985).
39. J. M. Akkermans and H. Gruppelaar, "Analysis of Continuum Gamma-Ray Emission in Precompound-Decay Reactions," *Phys. Lett.* **157B**, 95 (1985).

40. P. D. Kunz, "DWUCK - A Distorted Wave Born Approximation Program," (1970) unpublished.
41. D. L. Hill and J. A. Wheeler, "Nuclear Constitution and the Interpretation of Fission Phenomena," *Phys. Rev.* **89**, 1102 (1953).
42. S. Bjørnholm and J. E. Lynn, "The Double-Humped Fission Barrier," *Rev. Mod. Phys.* **52**, 725 (1980); S. Bjørnholm, IAEA-SM 174, V.1 (1974) p.367.
43. A. Jensen, "Recent Developments in the Theory of Nuclear Level Densities," *Proc. Int. Conf. on Neutron Physics and Nuclear Data*, Harwell (1978) p.378.
44. A. H. Wapstra, personal communication through D. G. Madland, 1986; see also A. H. Wapstra and K. Bos, "The 1977 Atomic Mass Evaluation," *At. Data and Nucl. Data Tables* **19**, 175 (1977).
45. P. Möller and J. R. Nix, "Atomic Masses and Nuclear Ground-State Deformations Calculated with a New Macroscopic-Microscopic Model," *At. Data and Nucl. Data Tables* **26**, 165 (1981).
46. R.E. MacFarlane and D.G. Foster, Jr., "Advanced Nuclear Data for Radiation Damage Calculations," *J. Nucl. Mat.* **123**, 1047 (1984).
47. Experimental data obtained from the National Nuclear Data Center, Brookhaven National Laboratory, Upton, New York.
48. H. Kalka, M. Torjman, and D. Seeliger, "Statistical Multistep Reactions: Applications," *Phys. Rev. C* **40**, 1619 (1989).

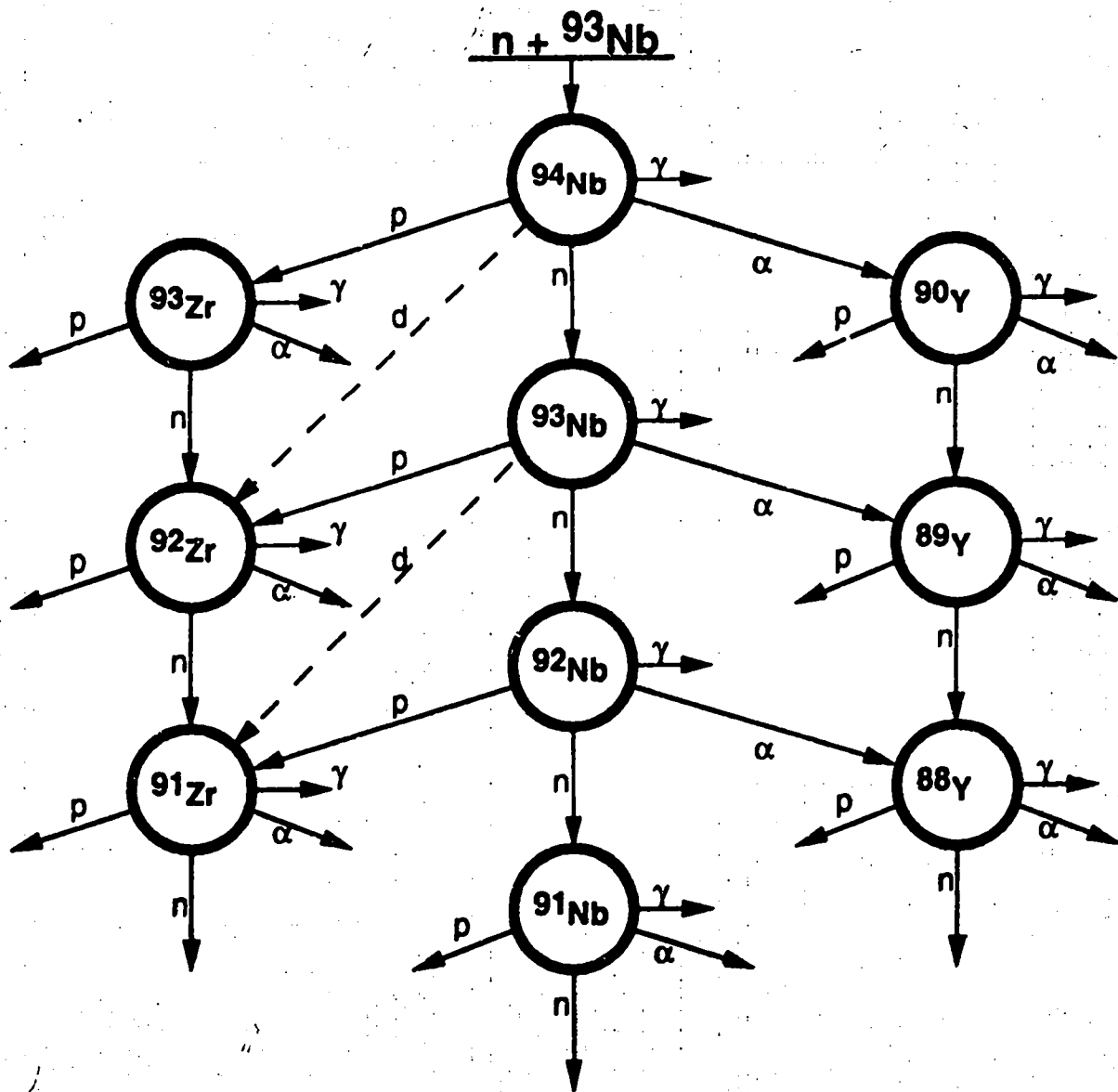


Fig. 1. Reaction chain for calculations of neutron-induced reactions on  ${}^{93}\text{Nb}$ .

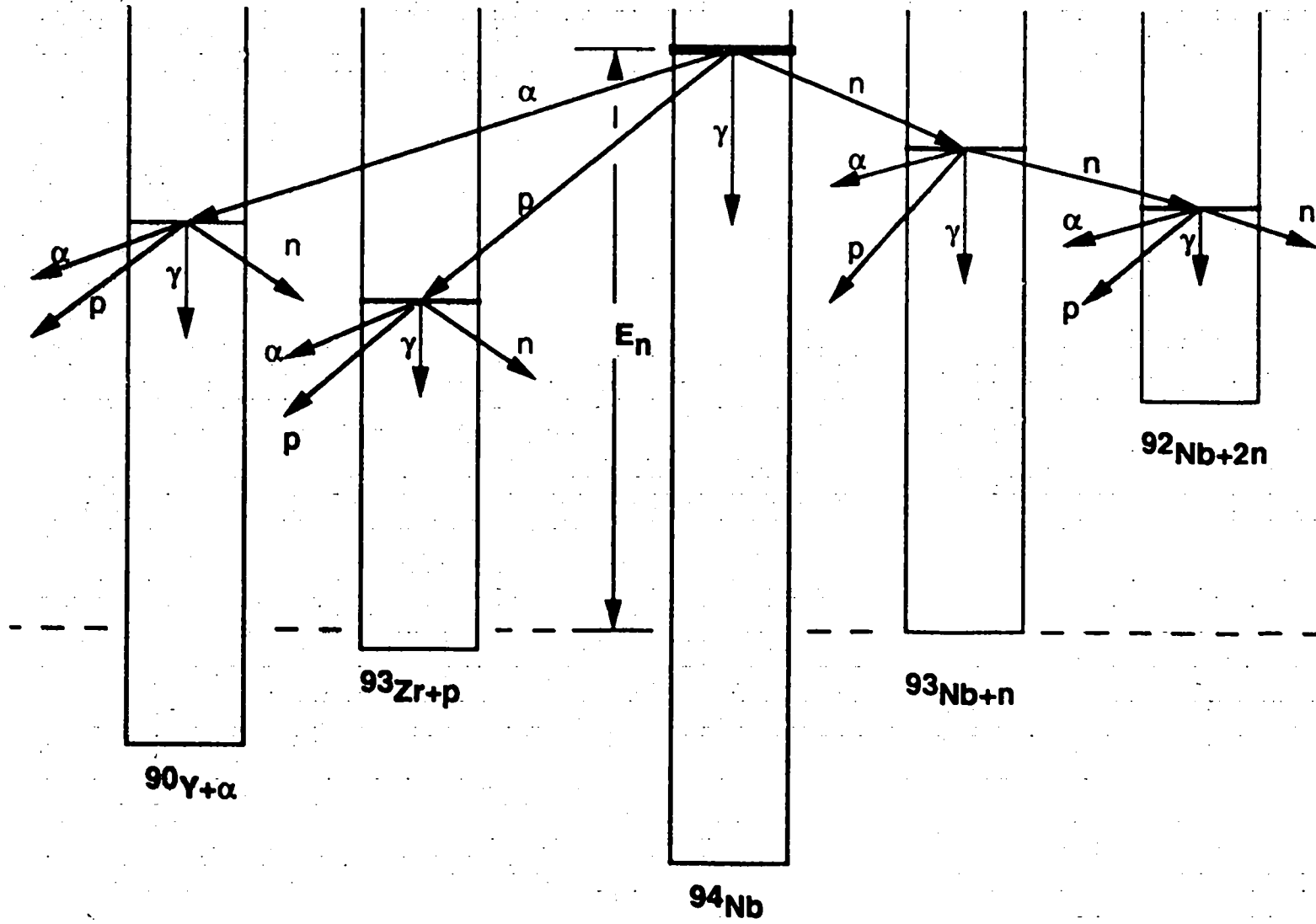


Fig. 2. Schematic diagram showing the first several reactions included in the GNASH calculation of the  $n + {}^{93}\text{Nb}$  interaction.

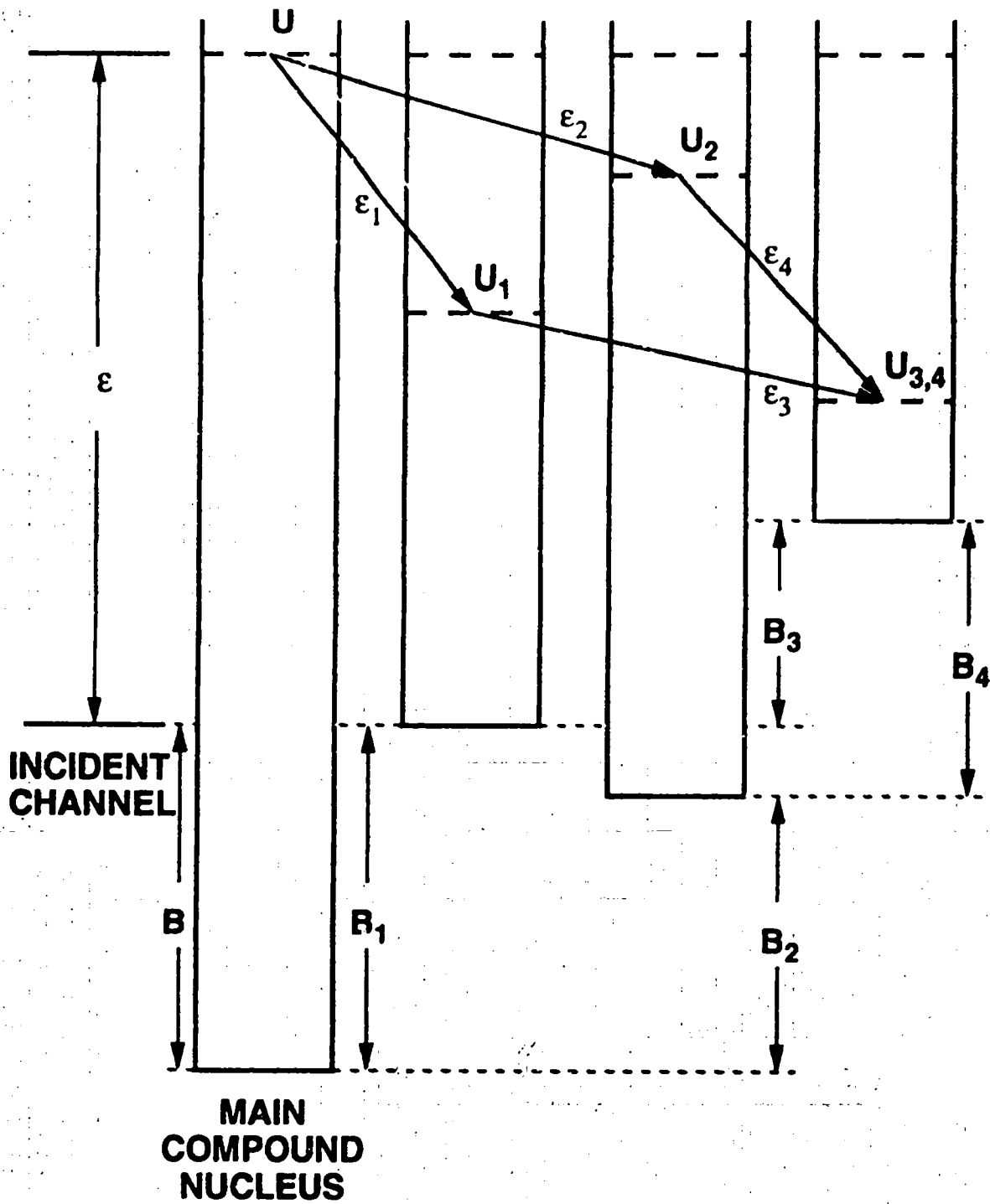


Fig. 3. Schematic illustration of the energetics of reaction sequences included in GNASH.

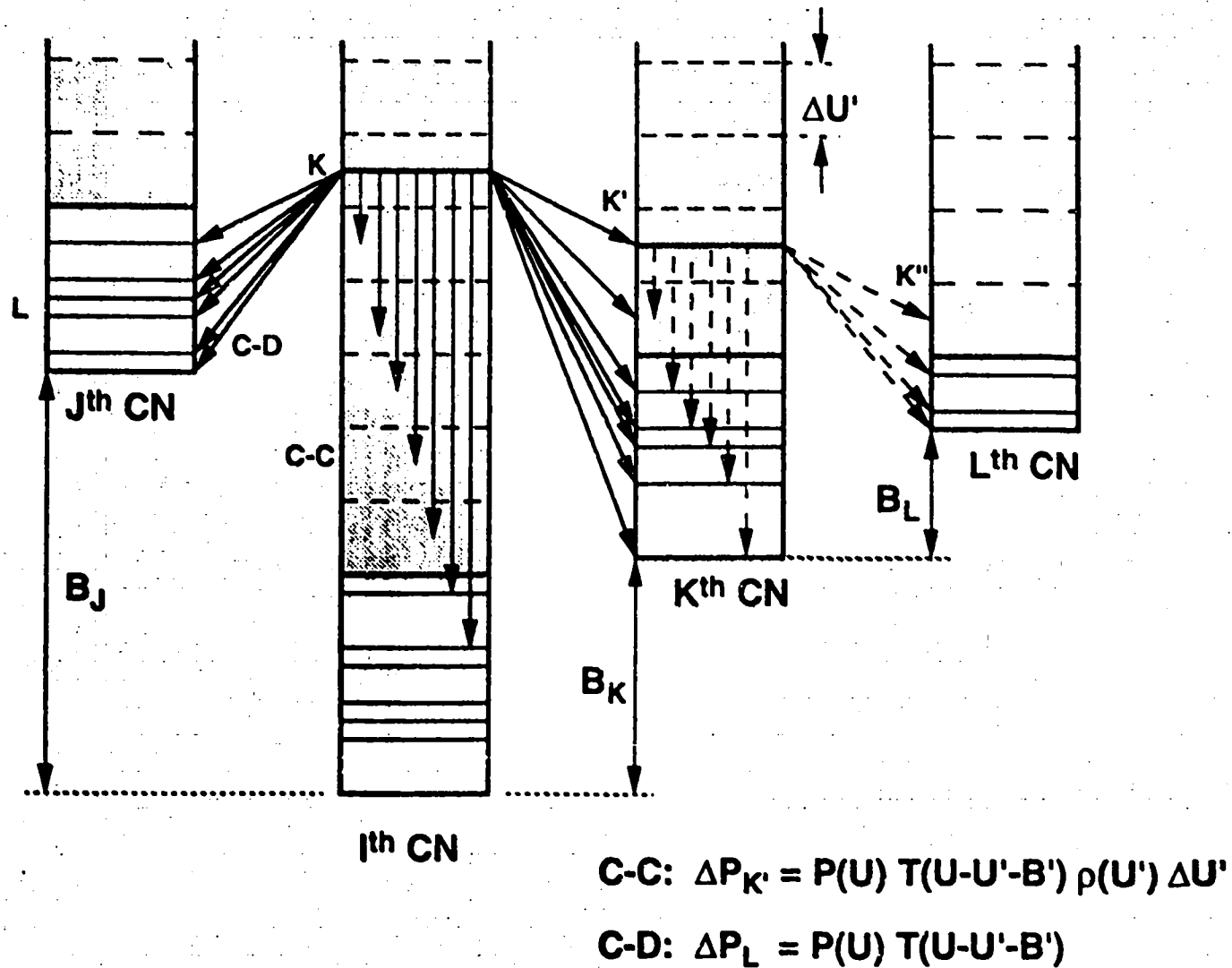


Fig. 4. Illustration of the decay of a continuum energy bin in the  $I^{\text{th}}$  compound nucleus to continuum (C - C) and discrete (C - D) states in the  $J^{\text{th}}$  and  $K^{\text{th}}$  compound systems. Also indicated is the subsequent decay of the  $K'$  energy bin in the  $K^{\text{th}}$  compound nucleus to the continuum and discrete states in the  $I^{\text{th}}$  compound system. Simplified equations depicting the continuum to continuum and continuum to discrete population increments are given.

# Level Diagram

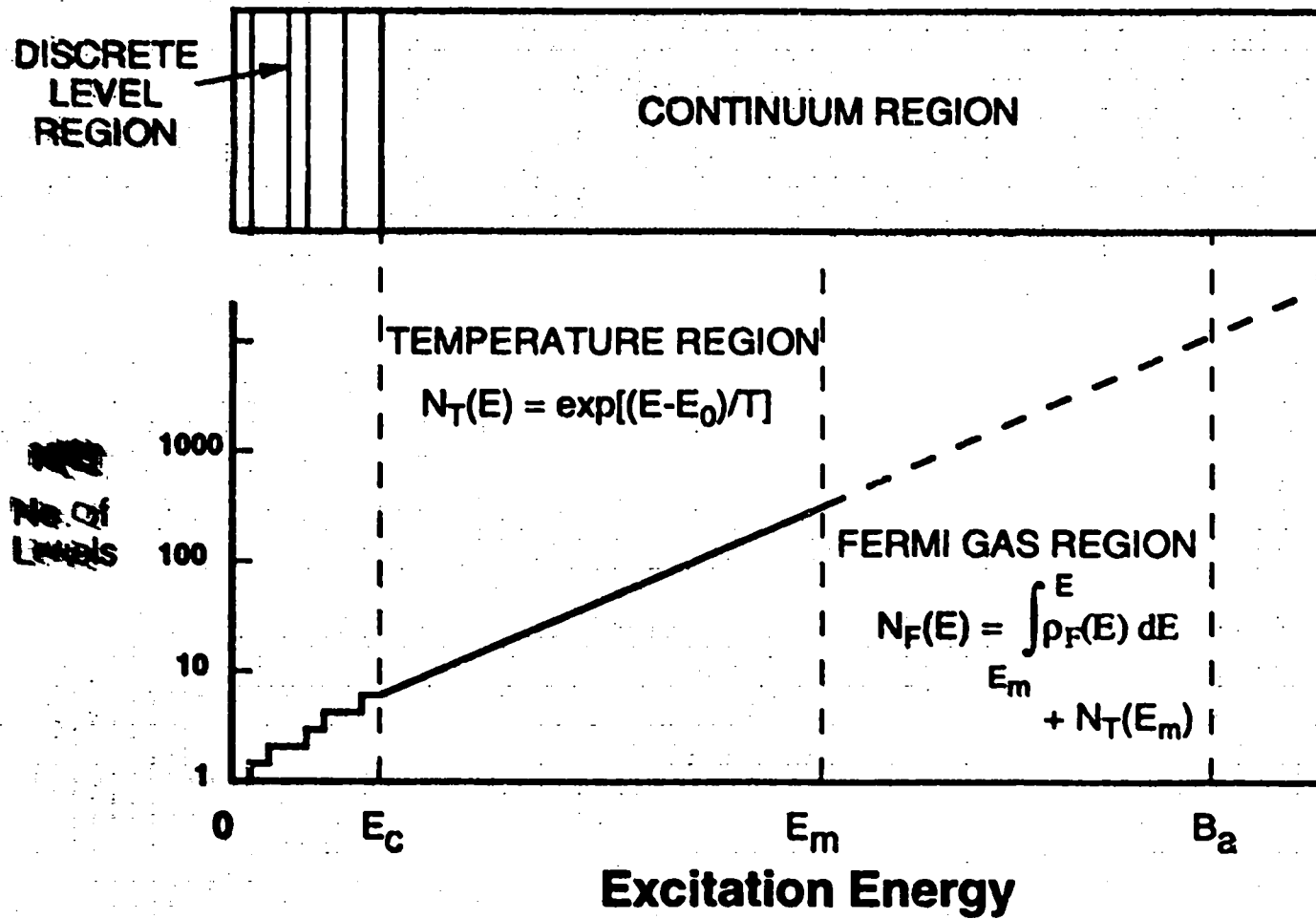


Fig. 5. Schematic energy level diagram indicating the discrete, temperature model, and Fermi-gas energy regions used in the level density formulations of GNASH. The energy  $E_c$  is the boundary between the discrete level and temperature continuum regions,  $E_m$  is the boundary between the temperature and Fermi-gas regions, and  $B_a$  is a typical location for the neutron binding energy, that is, in the Fermi-gas region.



## Preequilibrium reactions

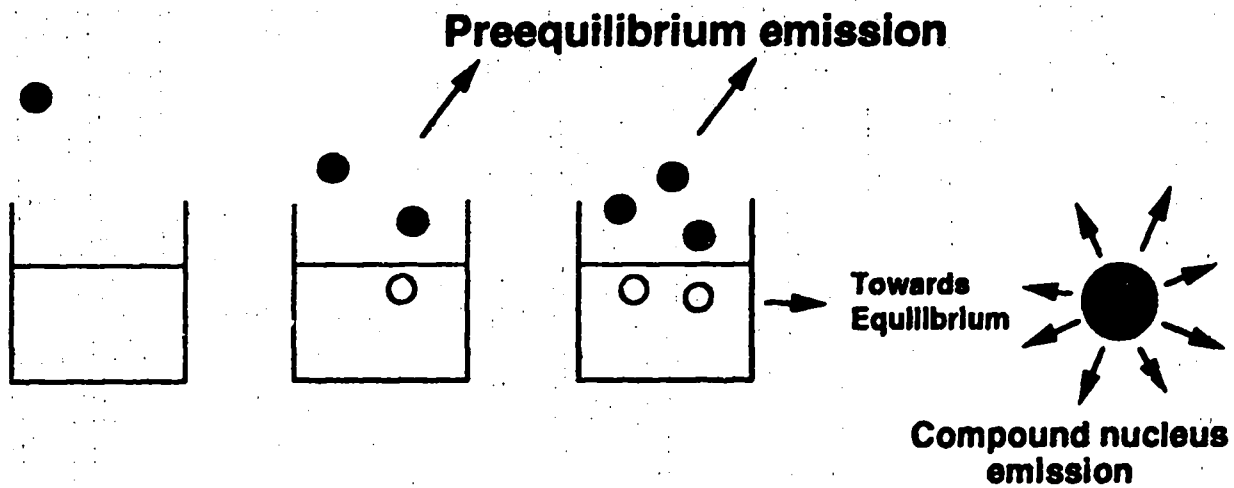
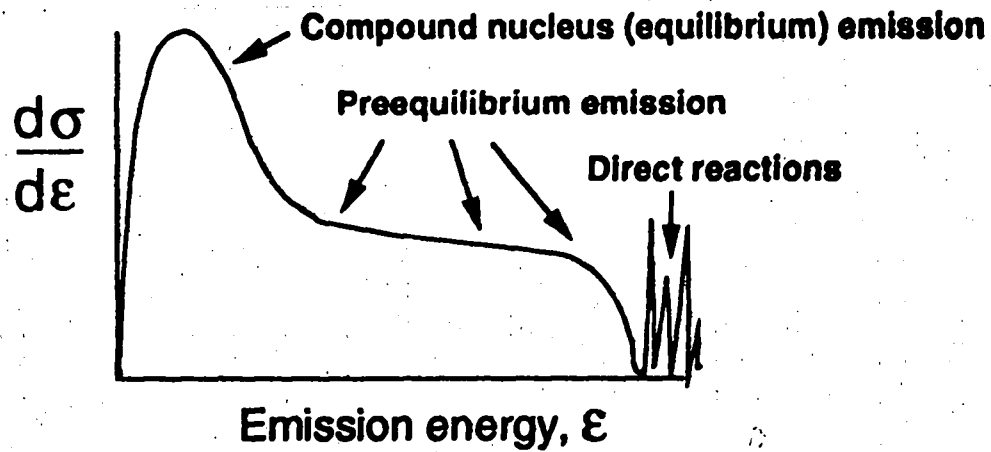


Fig. 6. Schematic representation showing the compound nucleus, preequilibrium, and direct reaction regions of a particle-emission spectrum, and the beginning of the preequilibrium reaction sequences that lead to equilibrium.

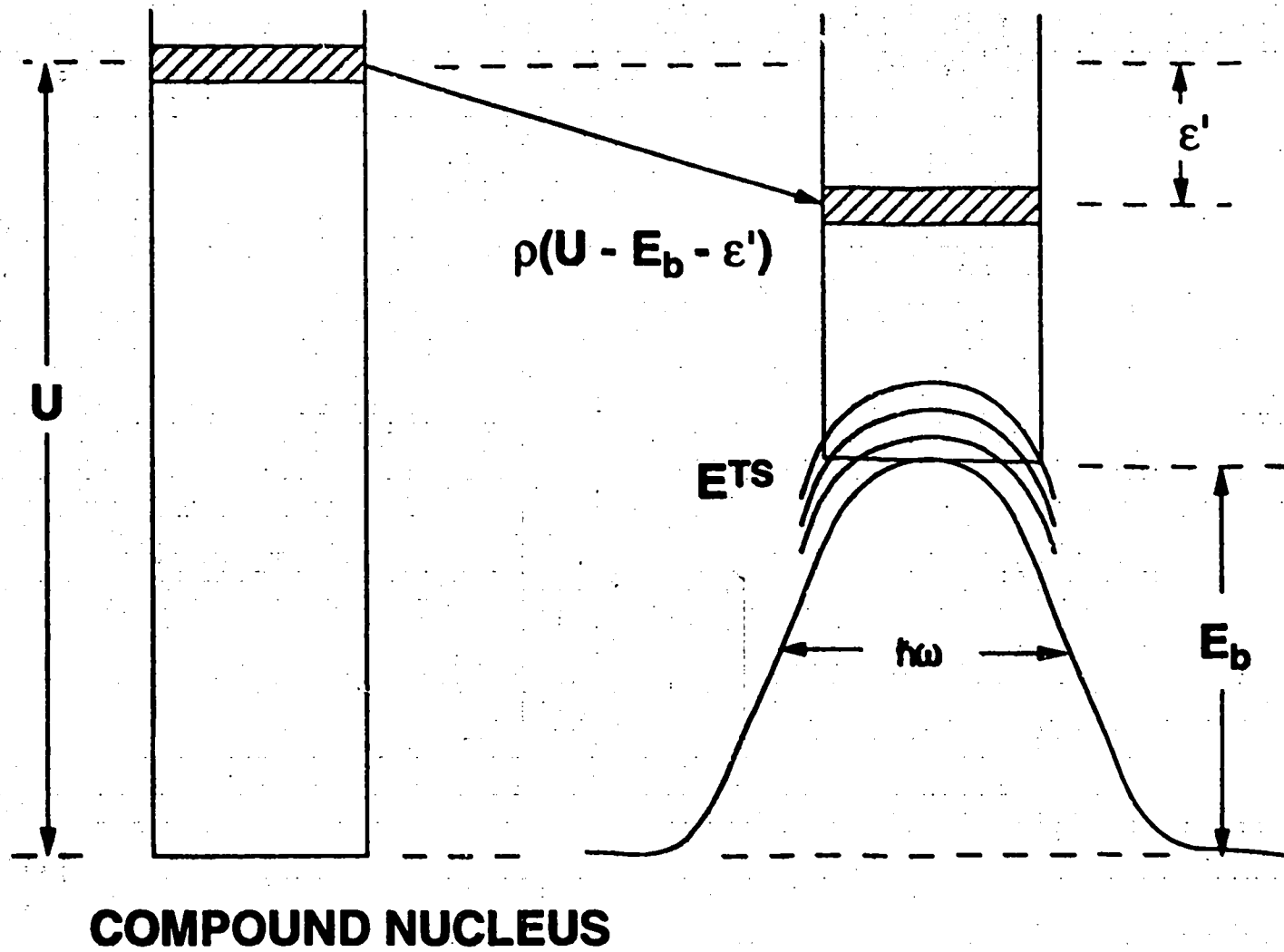


Fig. 7a. Schematic illustration of a fission barrier showing discrete and continuum transition states above the barrier.

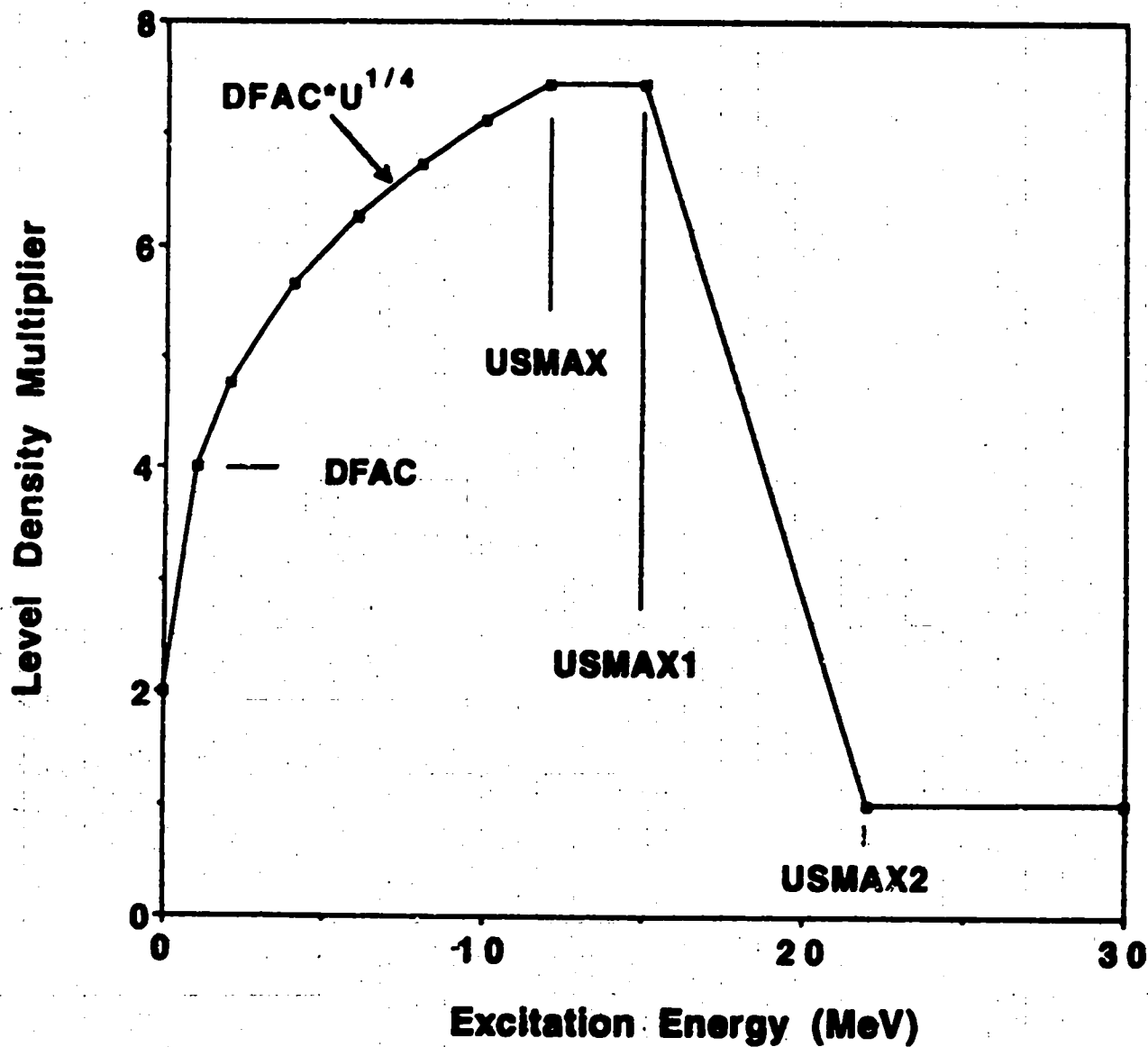


Fig. 7b. Example graph of the level density multiplier applied to fission transition state continuum level densities as a function of excitation energy. An input value of  $DFAC=4$  is assumed in this case; the parameters  $USMAX$ ,  $USMAX1$ , and  $USMAX2$  are set in a `DATA` statement in the `GNASH` code.

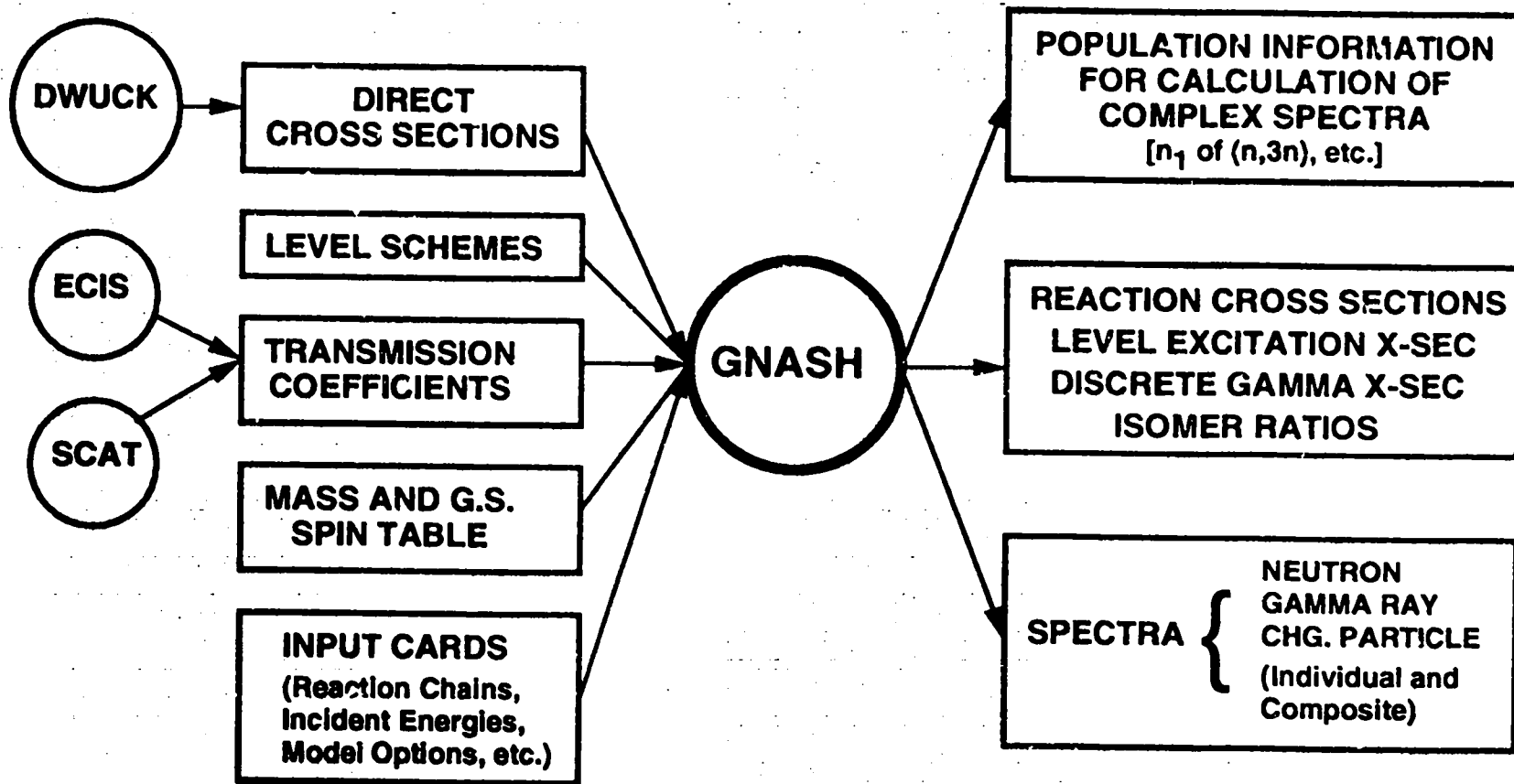


Fig. 8. Schematic representation of the input and output capabilities of the GNASH code.

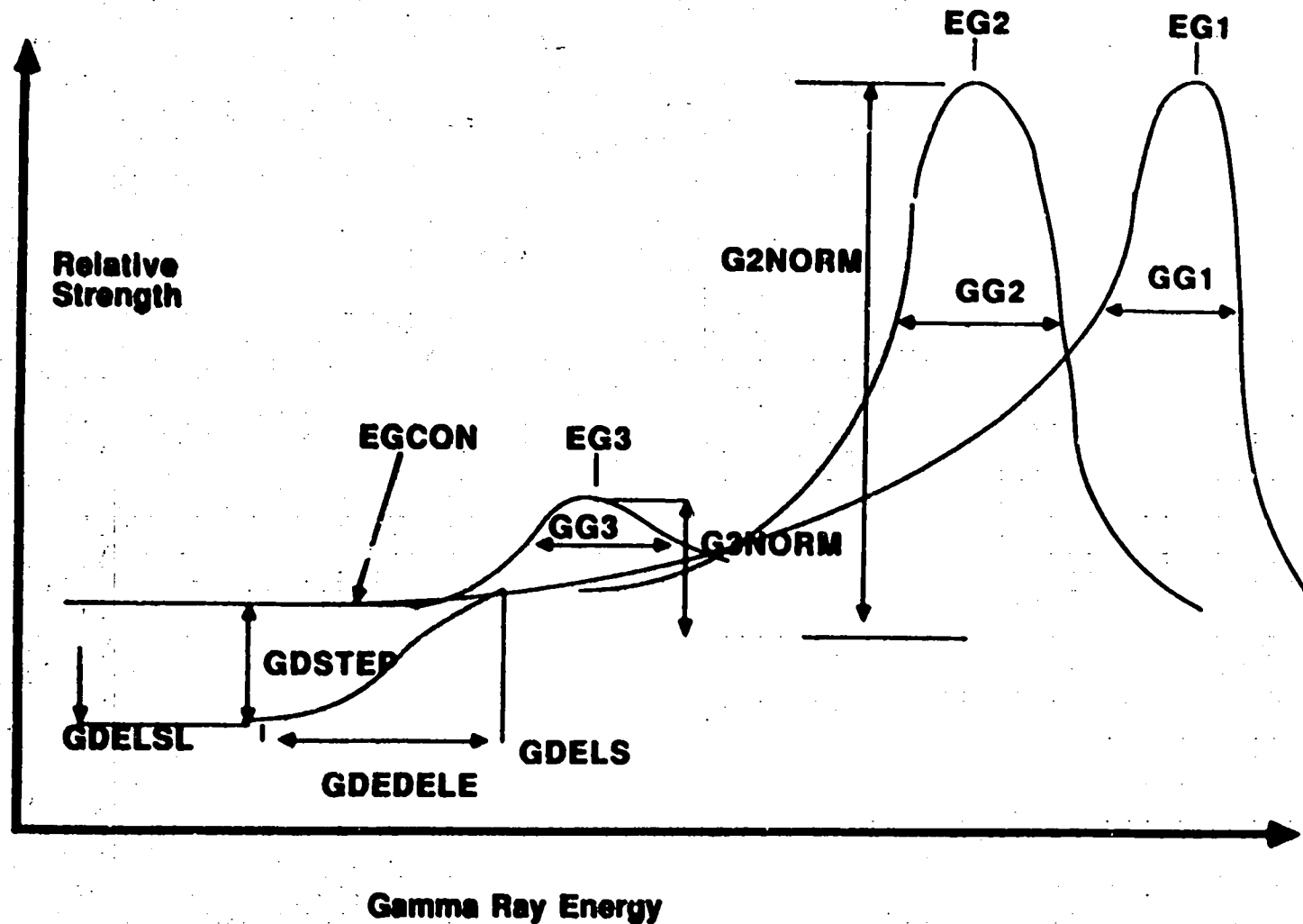


Fig. 9. Schematic representation of gamma-ray strength function shapes in the framework of the giant-dipole-resonance model. The GNASH input parameters that determine the shape of the E1 strength function are illustrated schematically.

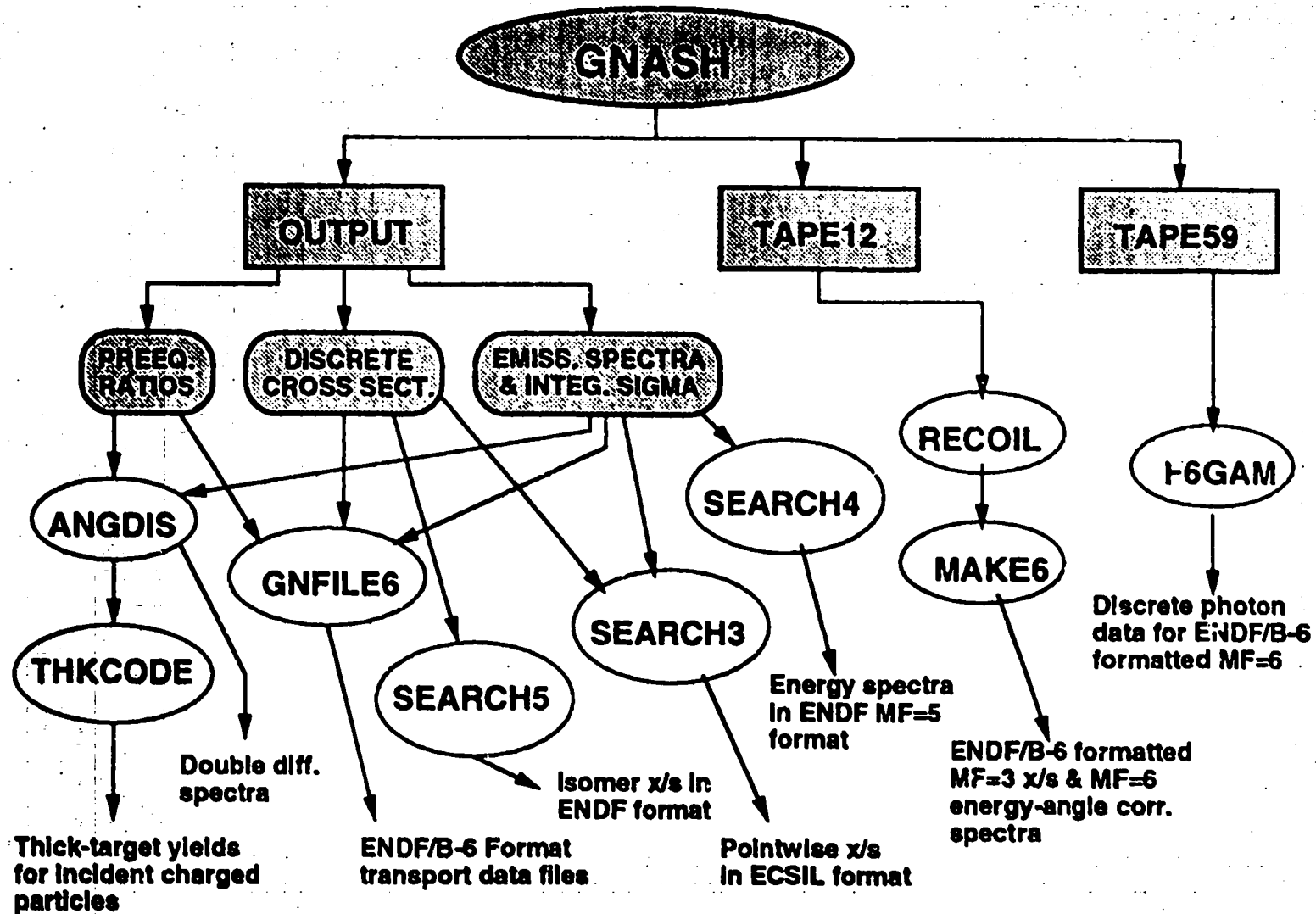


Fig. 10. Diagram illustrating several of the utility codes that operate on GNASH output files to produce data for different applications.

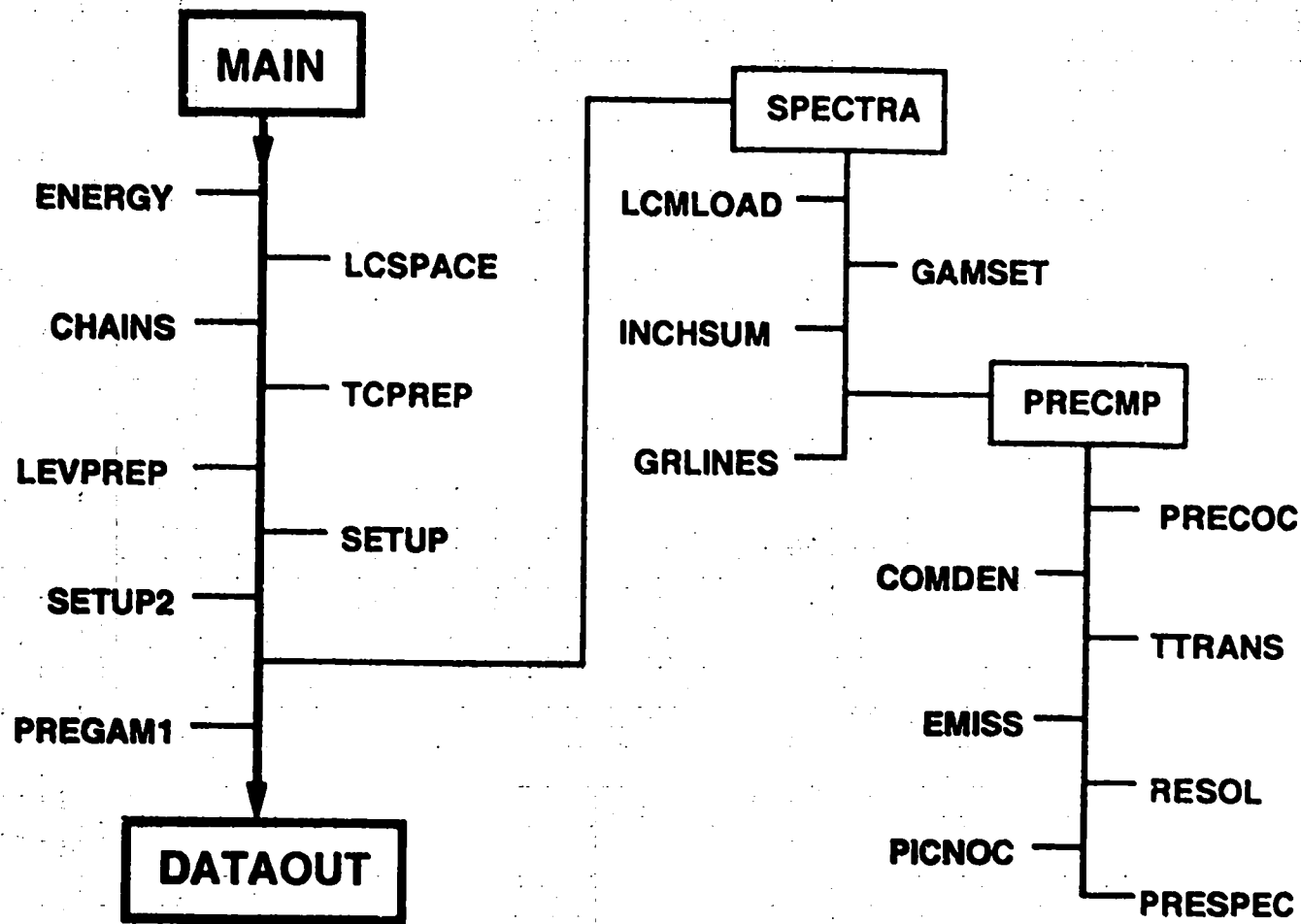


Fig. 11. Schematic illustration of the structure of the GNASH subroutines.

Do 500 I=1,NI Loop on NI CN involved in calculation  
 Do 400 K=1,NKCN For Ith CN begin loop on energy bin K  
 Do 301 IP=1,NIP For each K bin loop over possible decay channels  
 Do 200 N=1,NLEV2 For each residual system loop over discrete levels  
     Accumulate populations and increment total width sum  
     (gamma-ray and particle emission, fission)  
 End N and IP loops

Initial Continuum-  
Level Transition  
Calculation

Do 300 IP=1,NIP Loop over possible decays  
 For a CN state of E, spin, and parity loop over l and s sums  
 Do 180 KP = KLOW,KUP For a given K and IR, loop over  
     all continuum bins available in the residual system  
     Accumulate populations for continuum-continuum transitions  
     and increment total width sum  
 END IP, spins, and KP loops

Initial Continuum-  
Continuum Transition  
Calculation

Total width  
calculation completed,  
all population increments obtained

Do 851 IP=1,NIP Sum over possible decays  
 Do 685 KP = KLOW,NK2 Loop over continuum bins in residual system  
     Normalize populations for continuum-continuum  
     transitions by total width, accumulate spectral contributions  
     Store populations needed for subsequent CN's  
 END KP loop  
 Do 800 N=1,NLEV2 Loop over levels in each residual system  
     Normalize level population increments by total width  
     Add into spectra  
 END N loop  
 END loop over decays  
 END compound nucleus K loop  
 END loop over decaying CN

Normalize all  
populations by total  
width

Fig. 12. Outline of the coding of the SPECTRA subroutine.



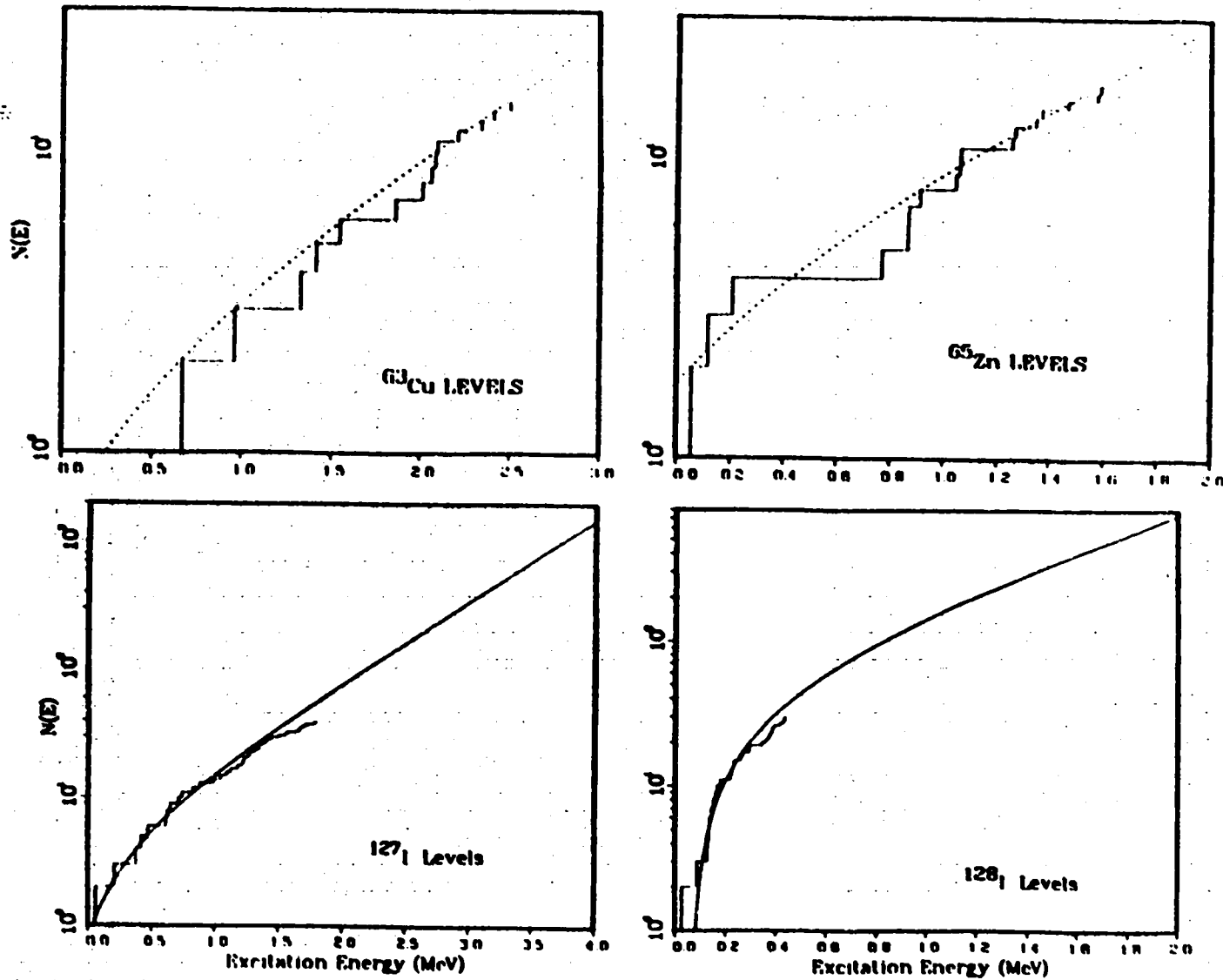


Fig. 13. Examples of matching of discrete level structure with the temperature level density expression. These fits were made using Eq. (29b) of the text.

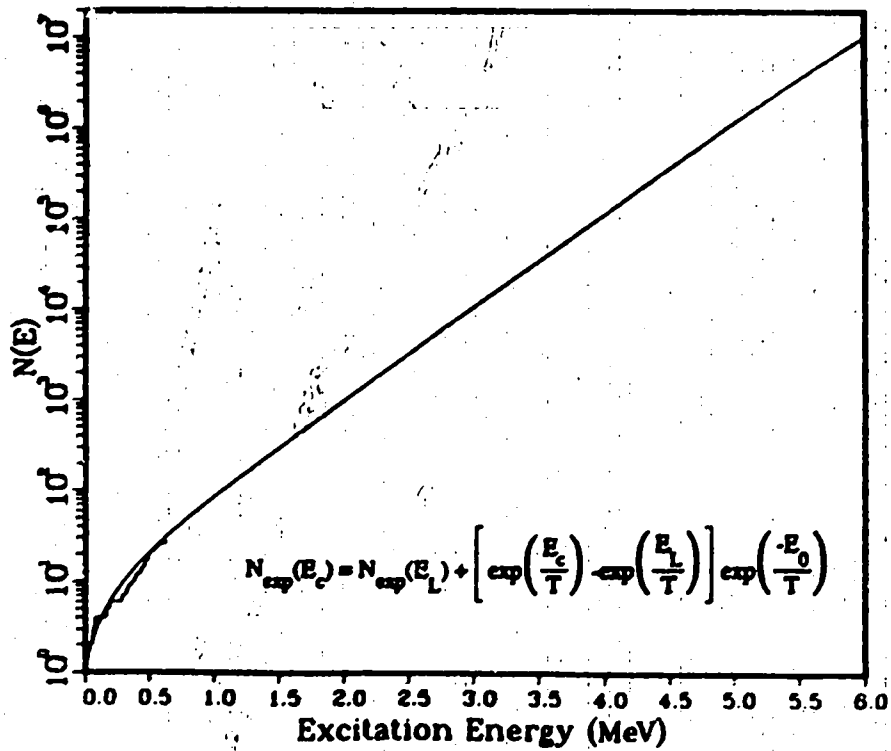
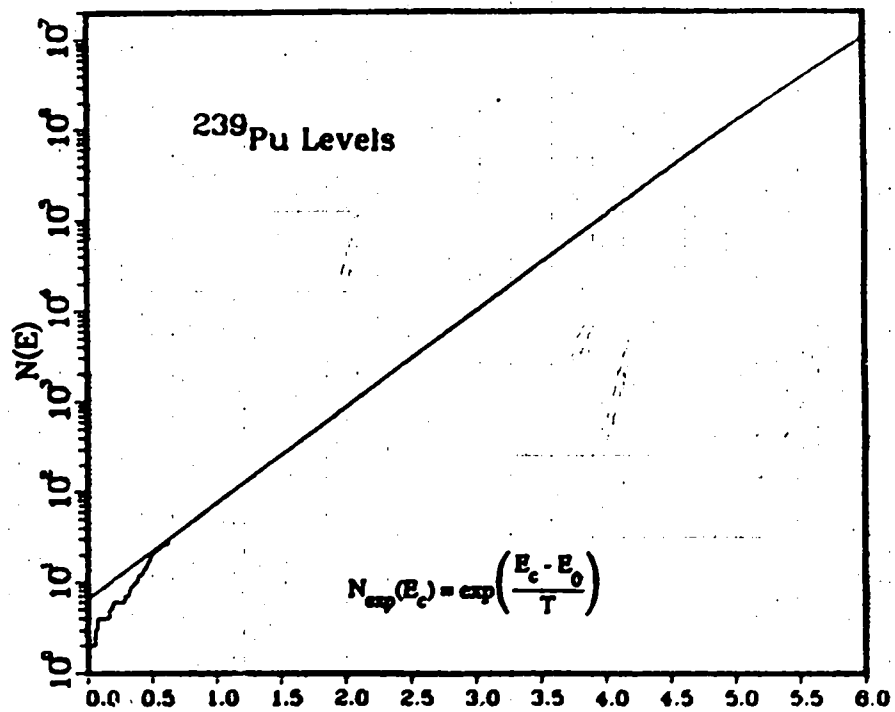


Fig. 14. Comparison of discrete level matching for <sup>239</sup>Pu using Eqs. (29a) and (29b) of the text.

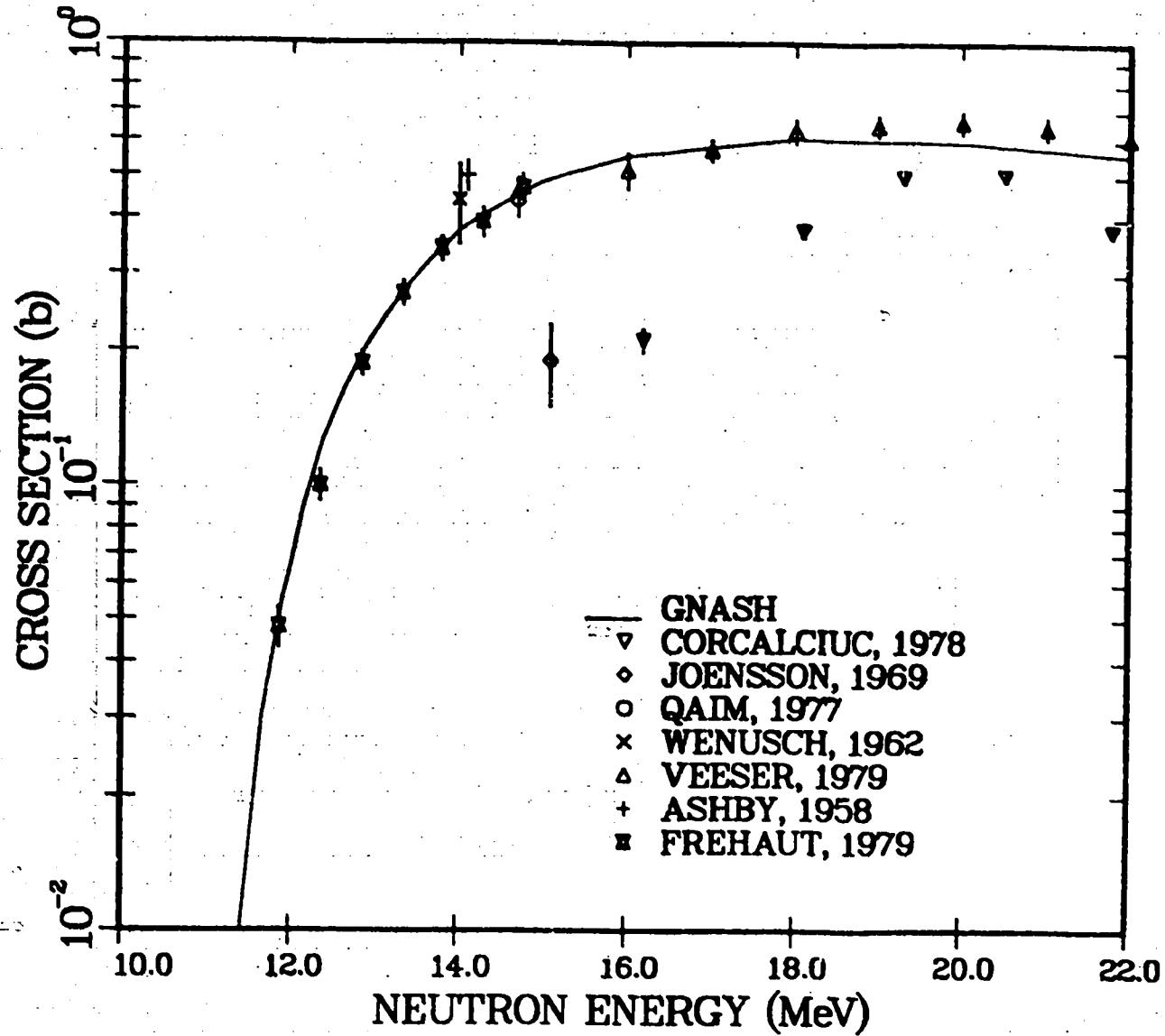


Fig. 15. Calculated and measured values of the  $^{56}\text{Fe}(n,2n)^{55}\text{Fe}$  cross section. The calculations use parameters from the computer exercises.

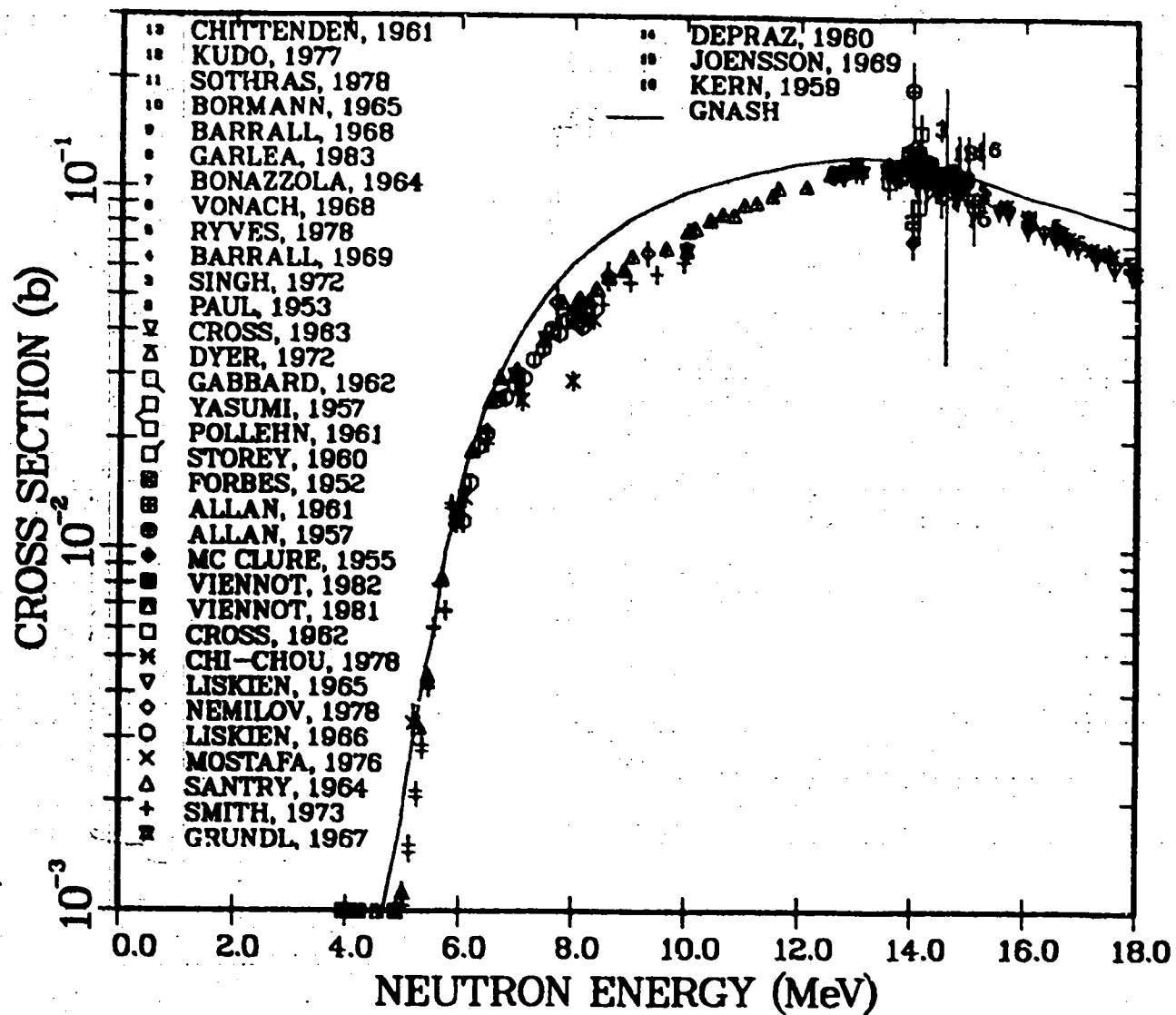


Fig. 16. Calculated and measured values of the  $^{56}\text{Fe}(n,p)^{56}\text{Mn}$  cross section. The calculations use parameters from the computer exercises.

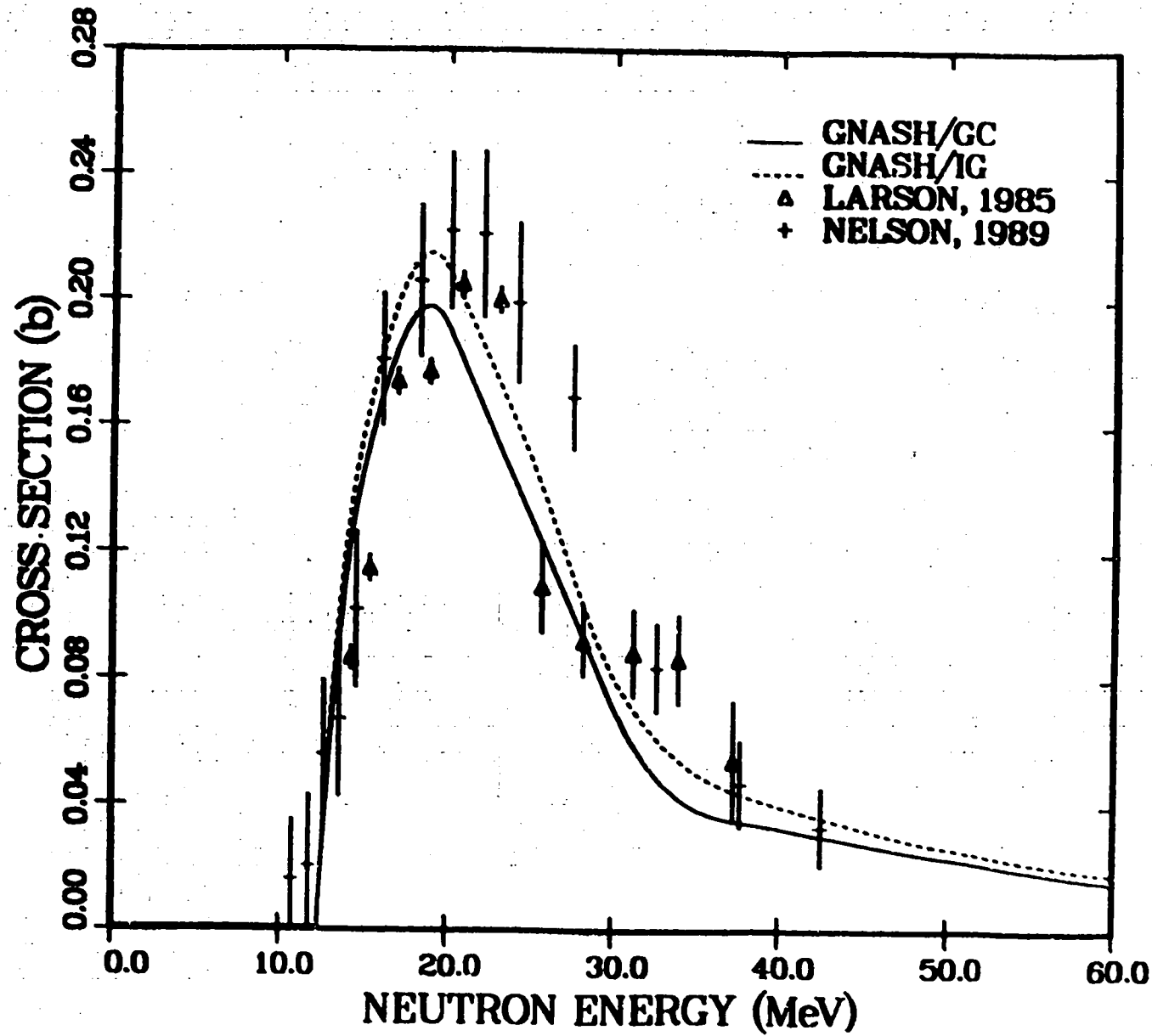


Fig. 17. Comparison of experimental results for the  $^{56}\text{Fe}(n,2n)$  cross section for the 0.931-MeV gamma ray with GNASH calculations. The calculations use parameters similar to those utilized in the computer exercises.

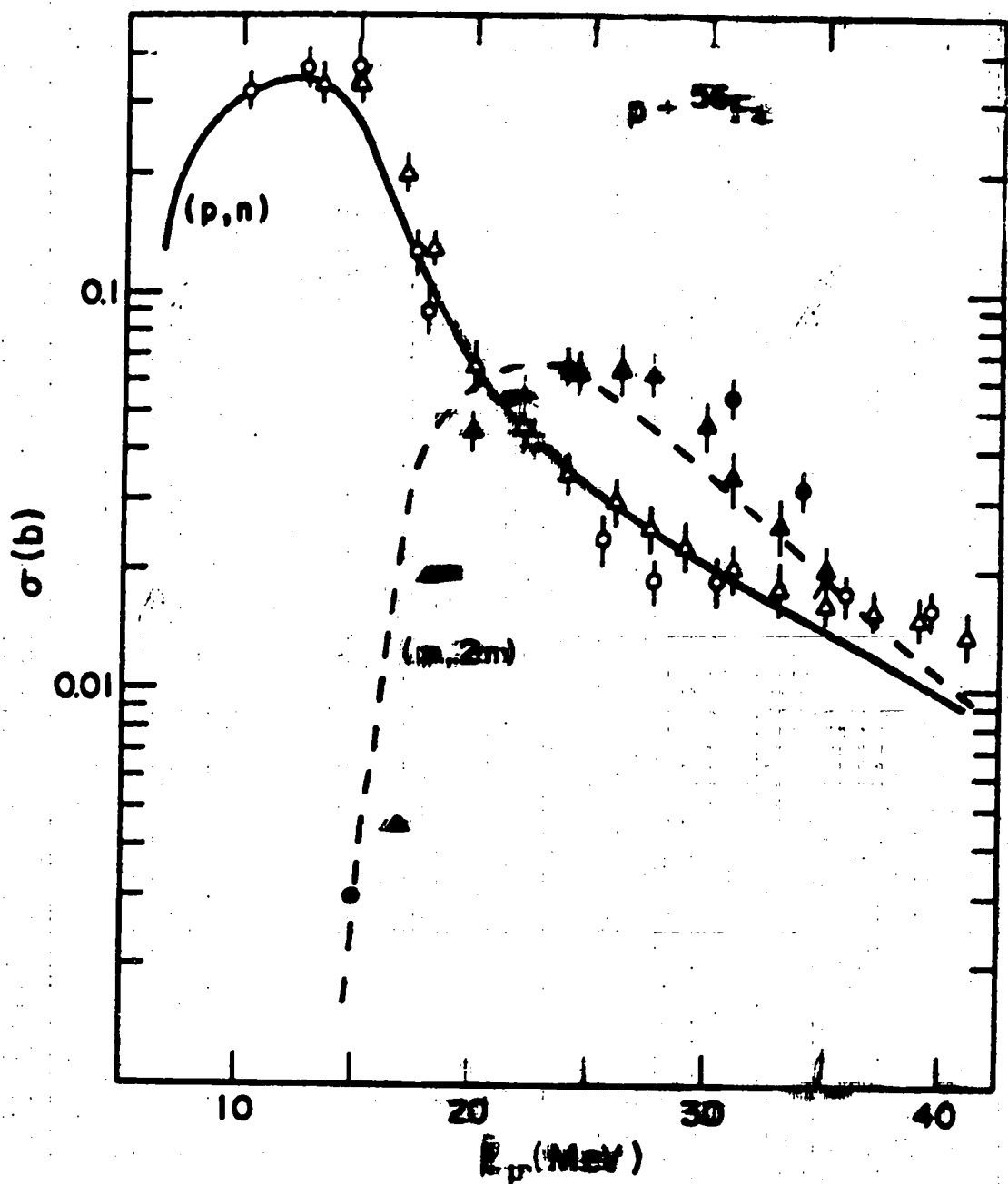


Fig. 18. Experimental and calculated (p,n) and (p,2n) cross sections for  ${}^{56}\text{Fe}$ . The calculations use parameters similar to those in the compound nucleus model.

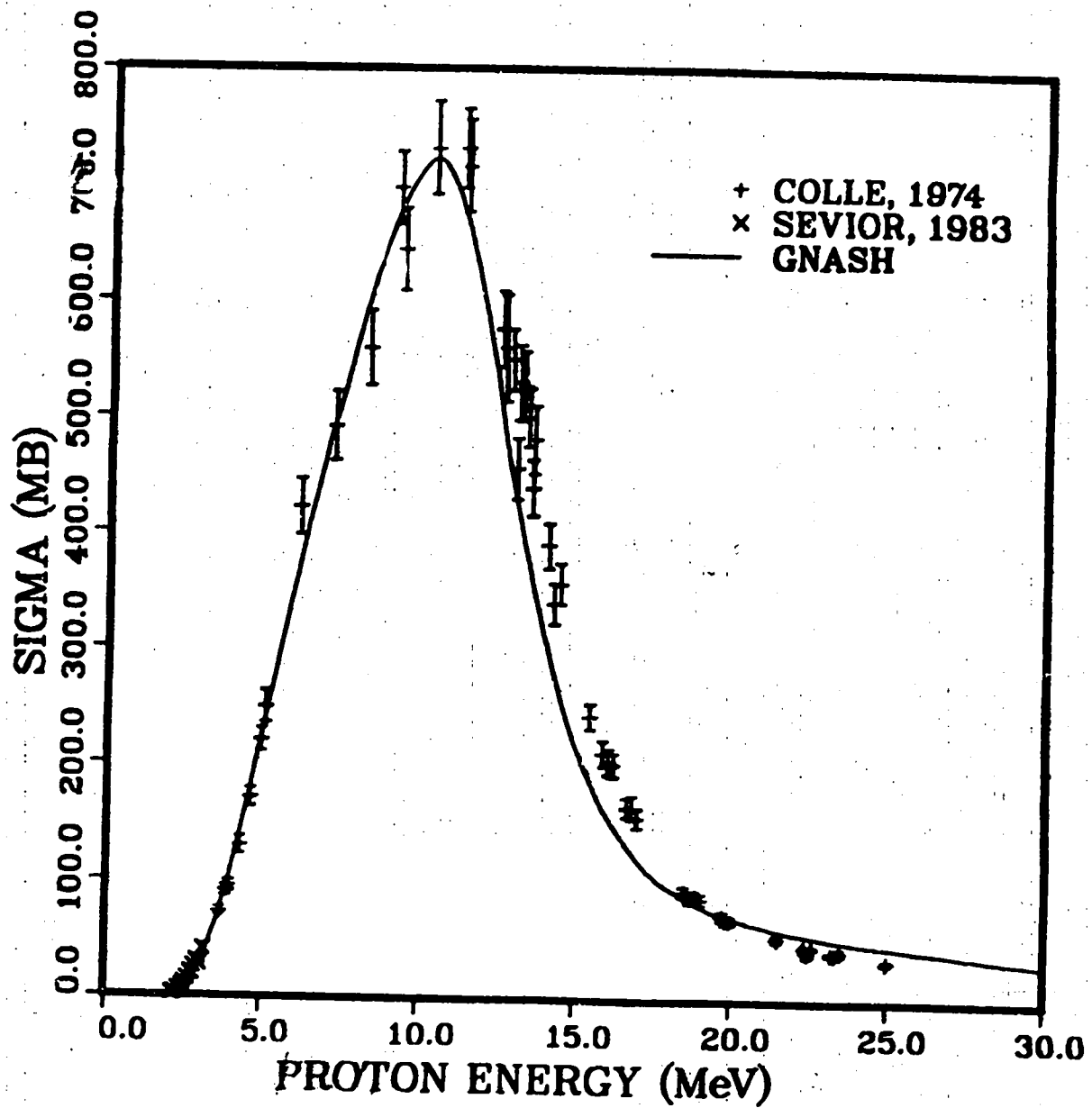
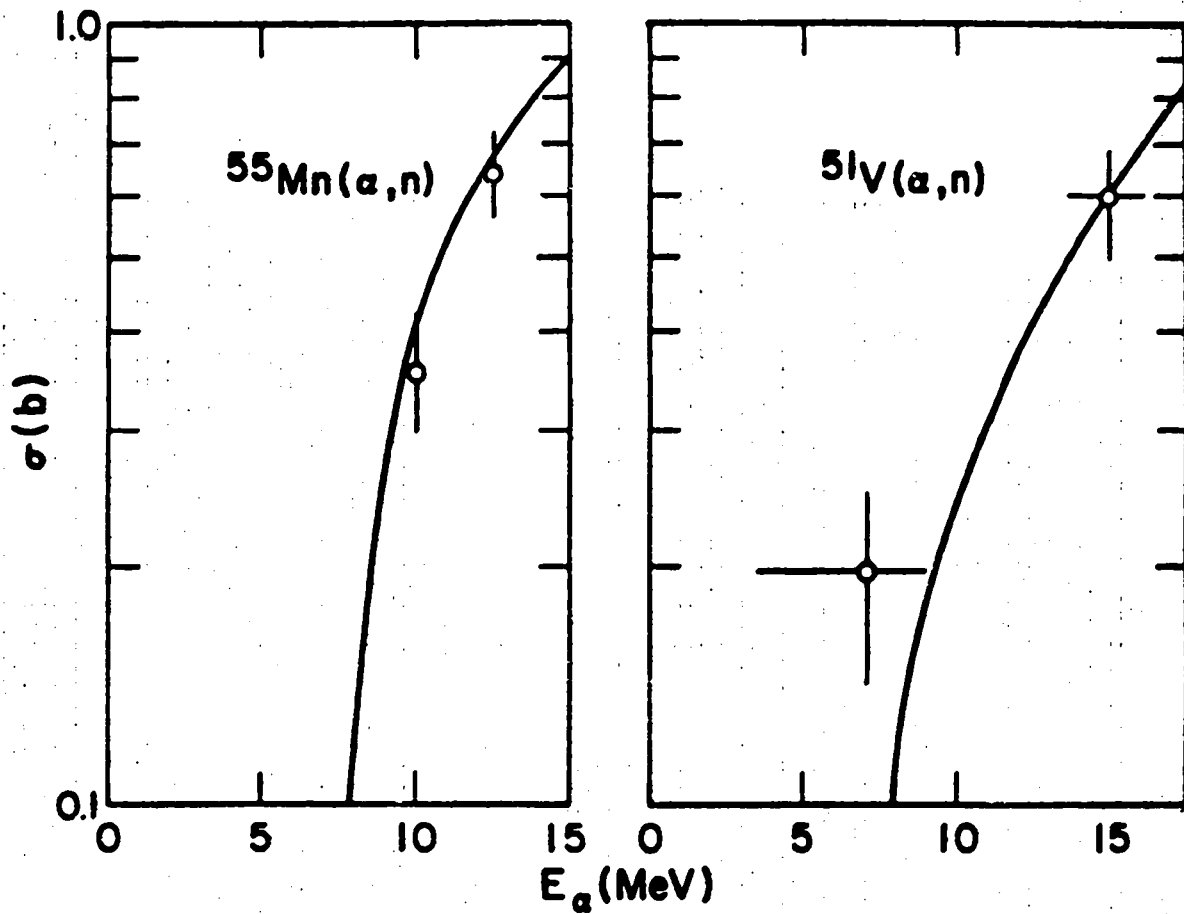


Fig. 19. Calculated and measured values of the  $^{65}\text{Cu}(p,n)^{65}\text{Zn}$  cross section.



**Fig. 20. Comparison of calculated and measured  $(\alpha, n)$  cross sections for  $^{55}\text{Mn}$  and  $^{51}\text{V}$ . The calculations use parameters similar to those utilized in the computer exercises.**



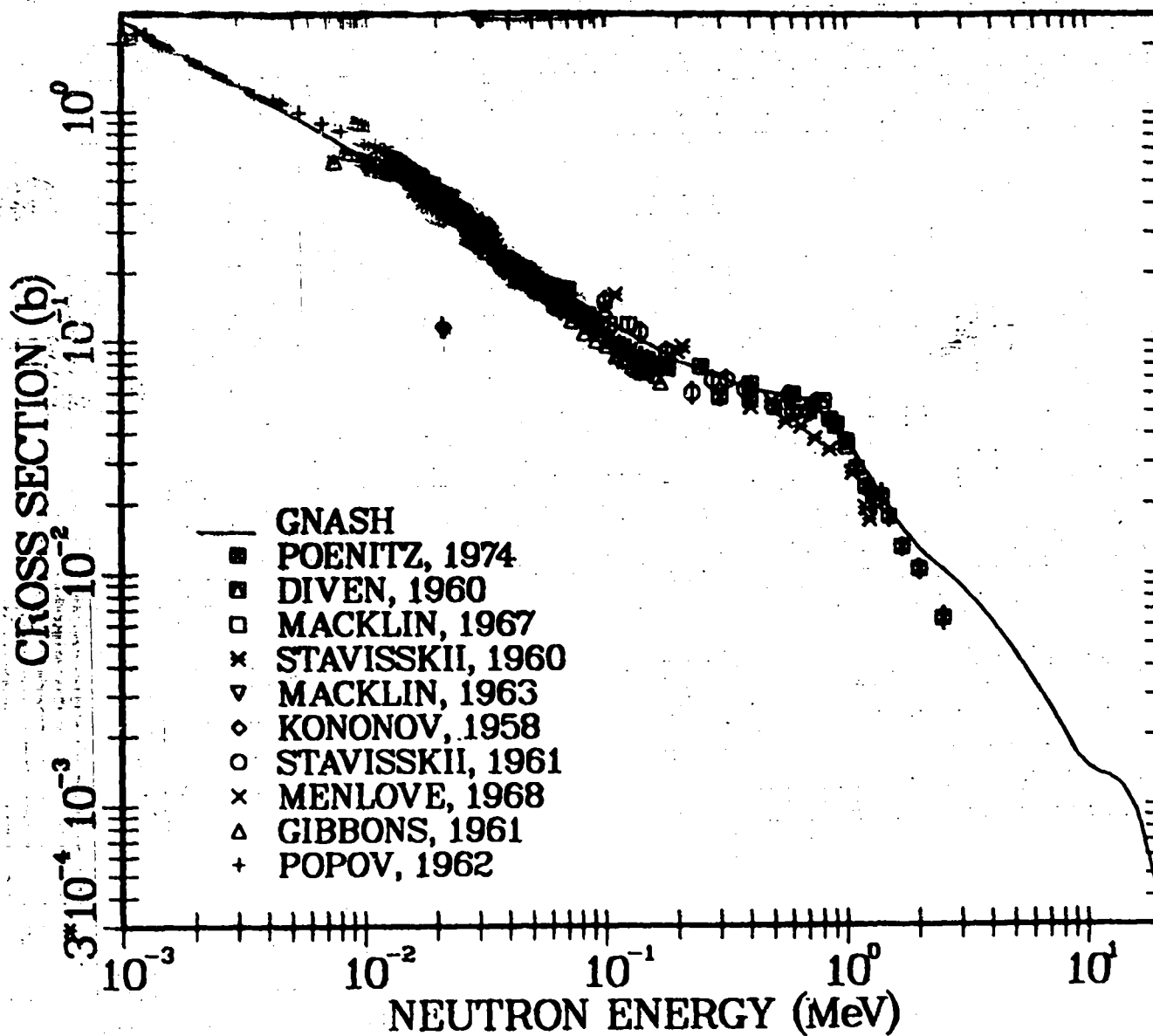


Fig. 21. Comparison of GNASH calculations of the  $^{93}\text{Nb}(n,\gamma)^{94}\text{Nb}$  cross section with experimental data. The calculations use parameters from the computer exercises.

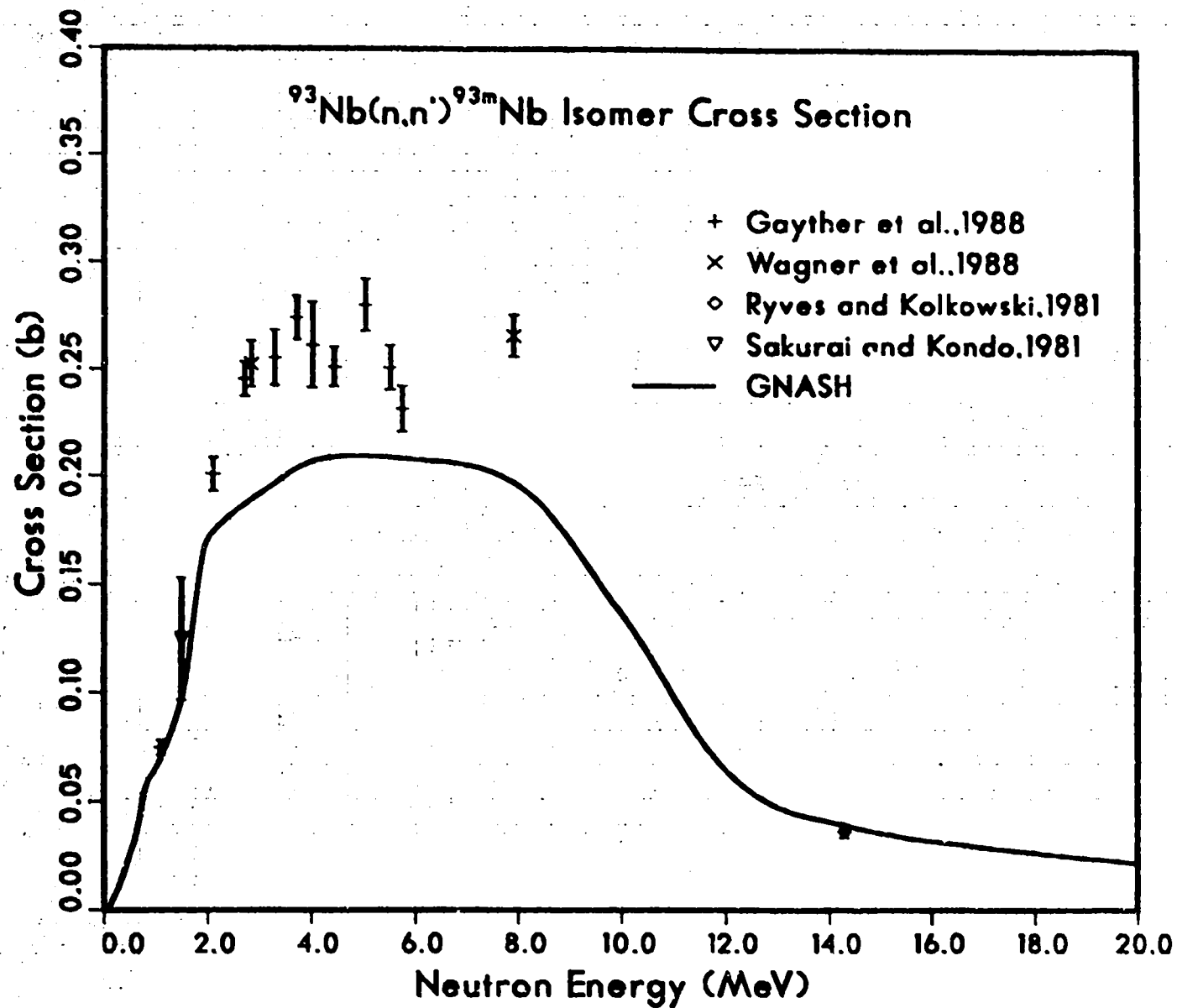


Fig. 22. Calculated and measured values of the  $^{93}\text{Nb}(n,n')$  cross section to the 13.6-y metastable state in  $^{93}\text{Nb}$ . The calculations use parameters similar to those utilized in the computer exercises.

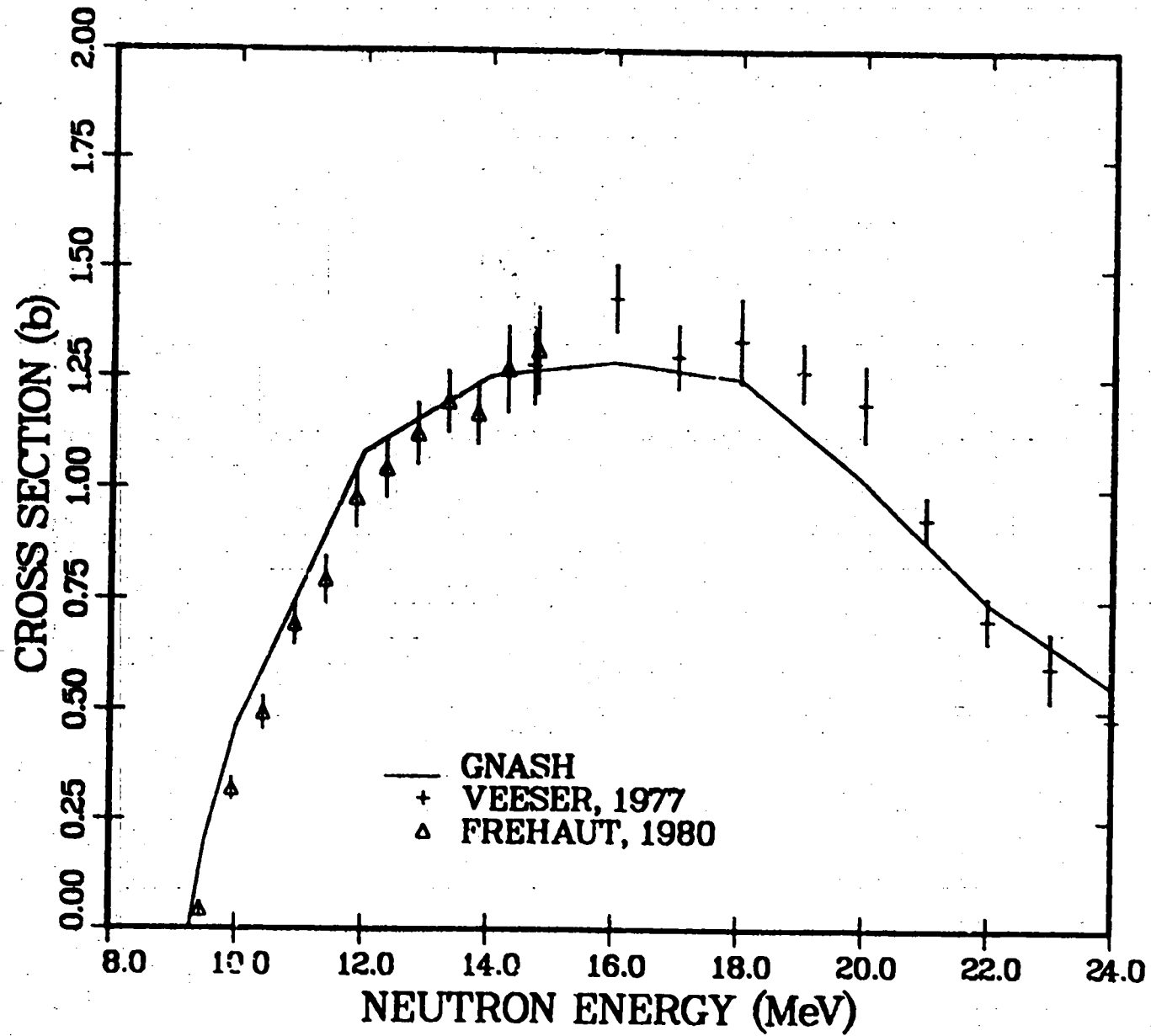


Fig. 23. Calculated and measured values of the  $^{93}\text{Nb}(n,2n)^{92}\text{Nb}$  cross section. The calculations use the same parameters that are utilized in the computer exercises.

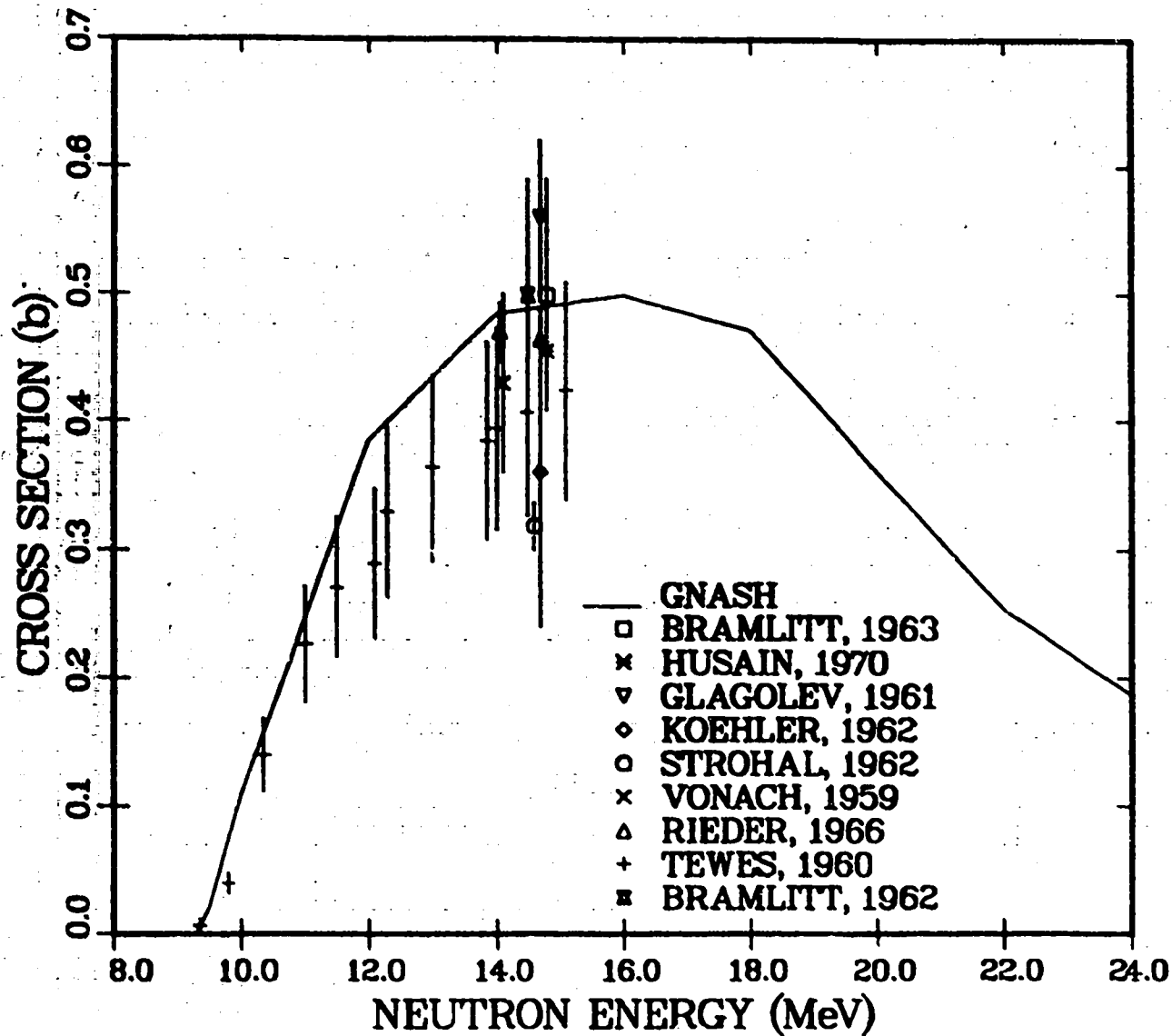


Fig. 24. Comparison of calculated values of the  $^{93}\text{Nb}(n,2n)^{92\text{m}}\text{Nb}$  ( $T_{1/2} = 10.1$  d) cross section to experimental data. The calculations use parameters from the computer exercises.

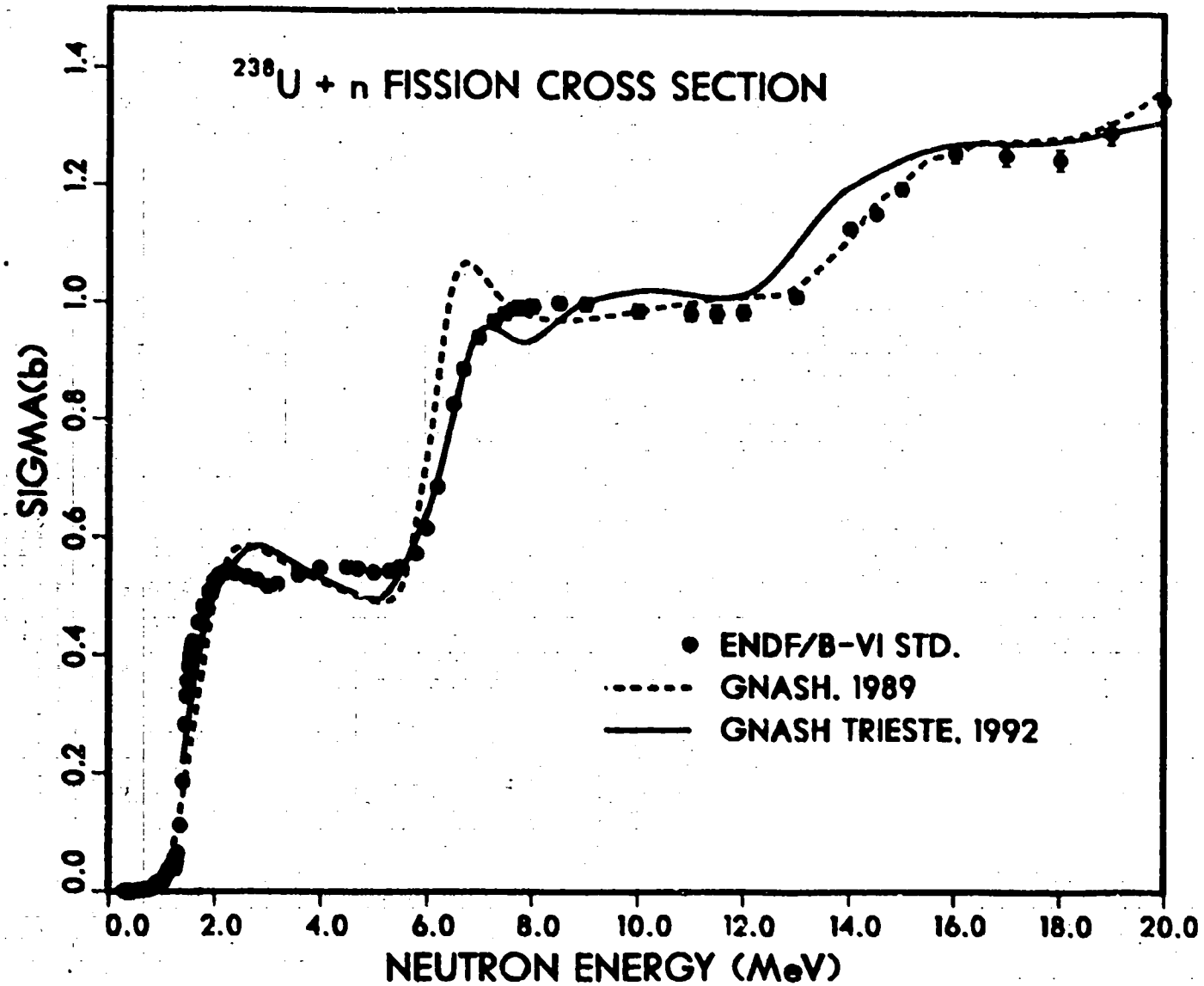


Fig. 25. Comparison of the present calculation of the  $^{238}\text{U}(n,f)$  cross section with the ENDF/B-VI standard's analysis (points) and with a GNASH analysis made in 1989 in conjunction with the ENDF/B-VI evaluation. Note that the standard's analysis is a composite of consistently analyzed experimental data.

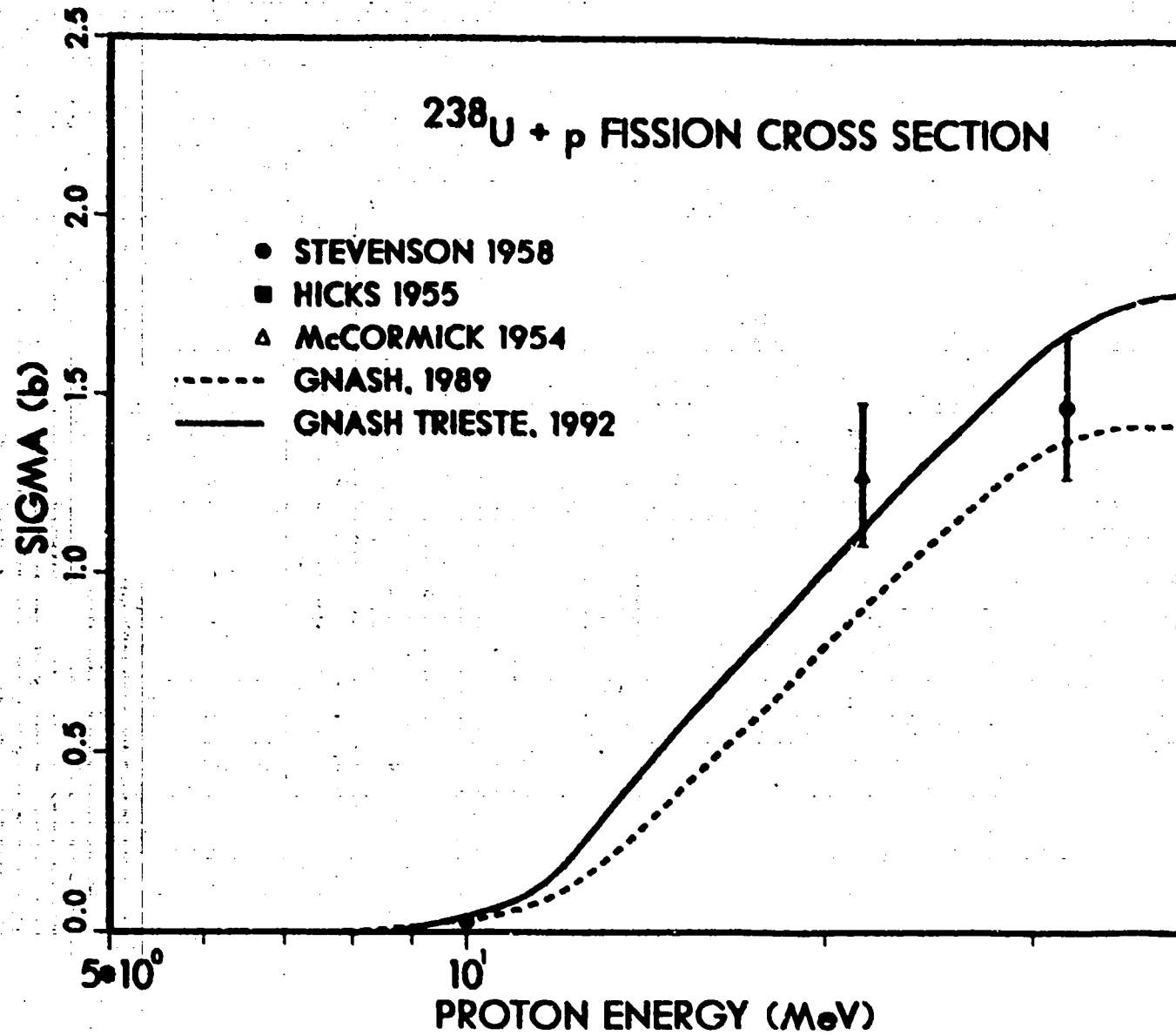


Fig. 26. Calculated and measured fission cross section from  $p + ^{238}\text{U}$  reactions. The dashed line indicates an earlier GNASH analysis,<sup>4</sup> and the solid curve was calculated using the input deck for the computer exercise.

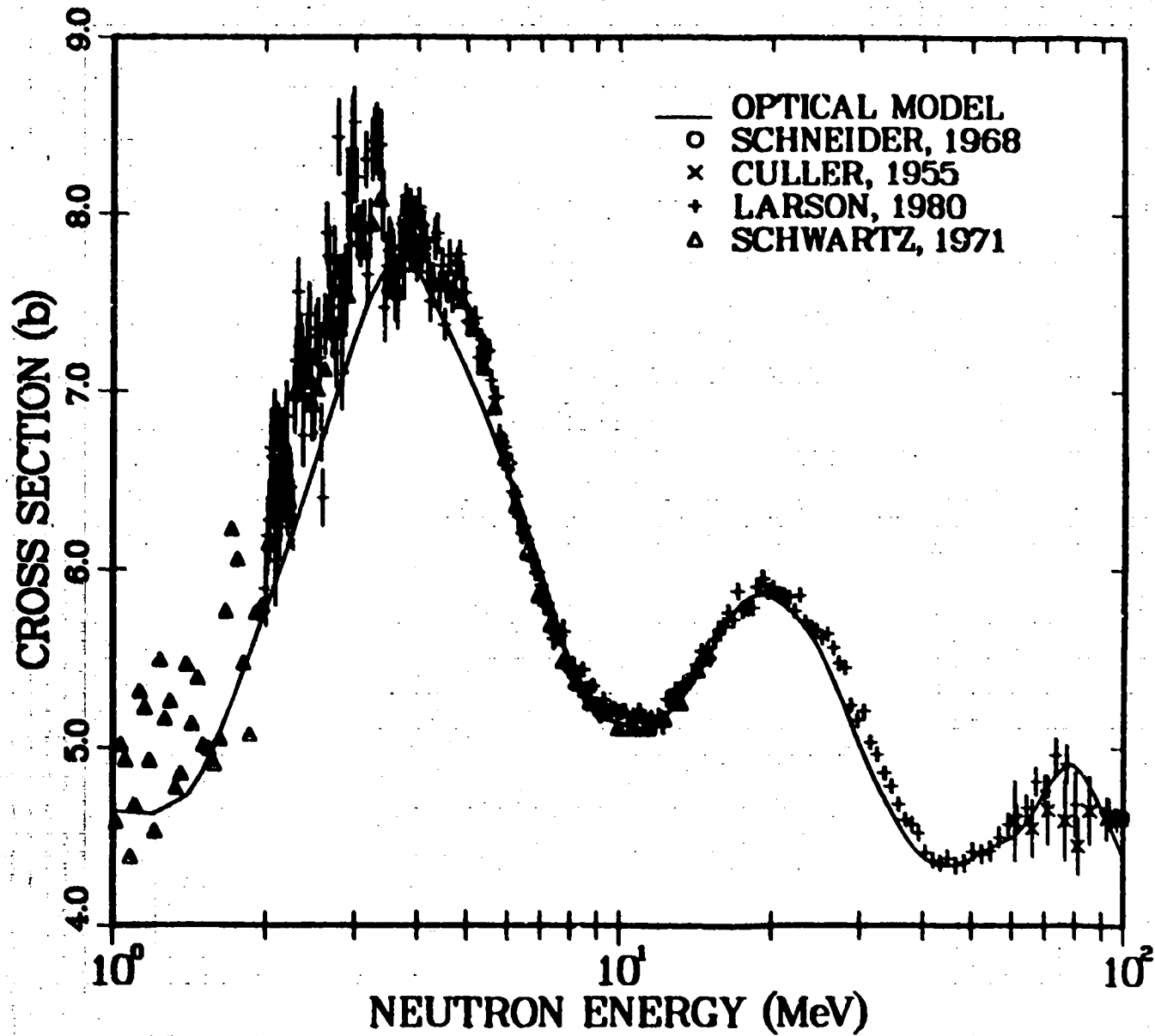


Fig. 27. Comparison of neutron total cross section measurements<sup>47</sup> for  $^{nat}\text{Pb}$  with optical model calculations for  $n + ^{208}\text{Pb}$  interactions.

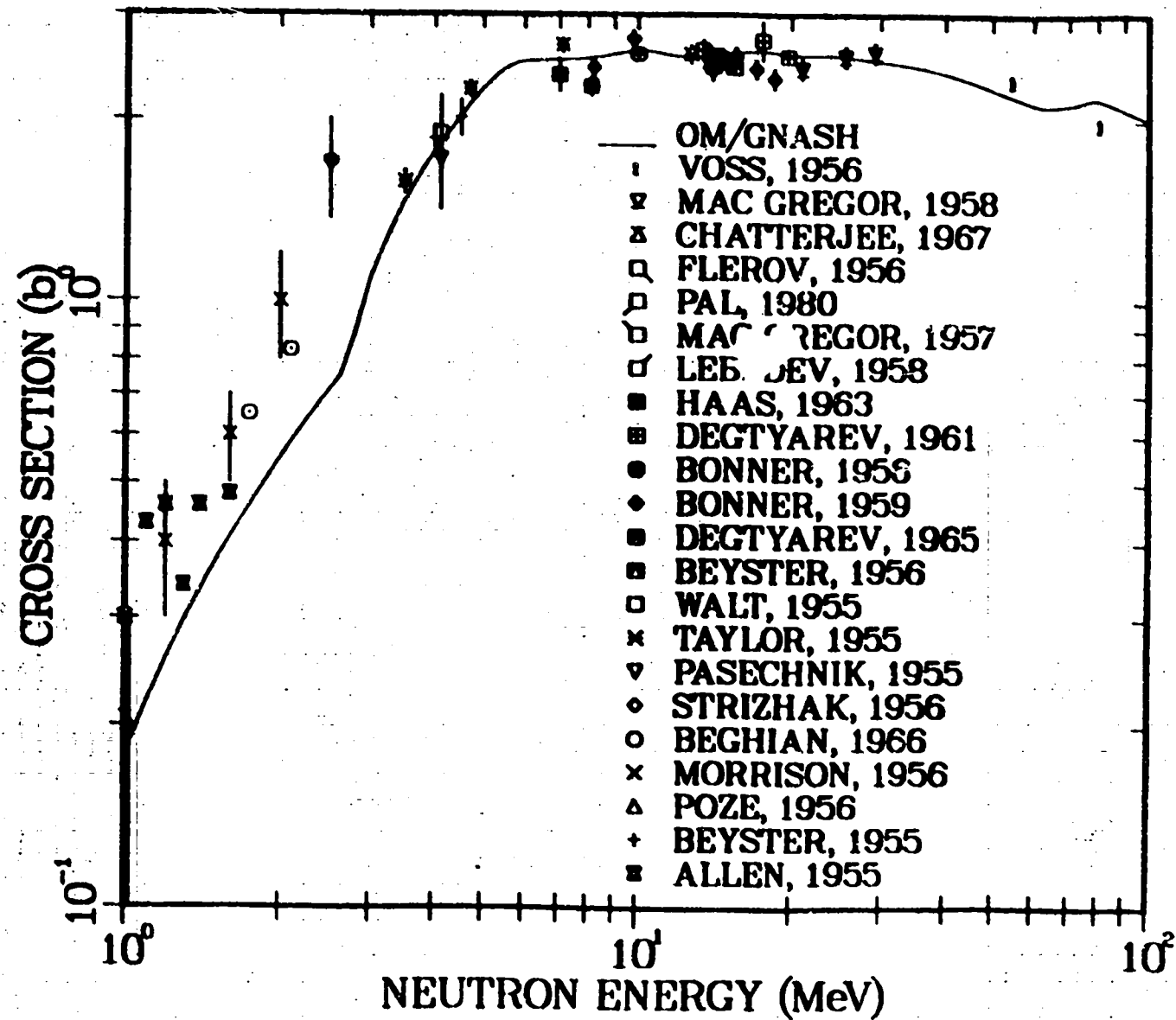


Fig. 28. Calculated and measured<sup>47</sup> nonelastic cross section for neutron reactions on <sup>nat</sup>Pb.



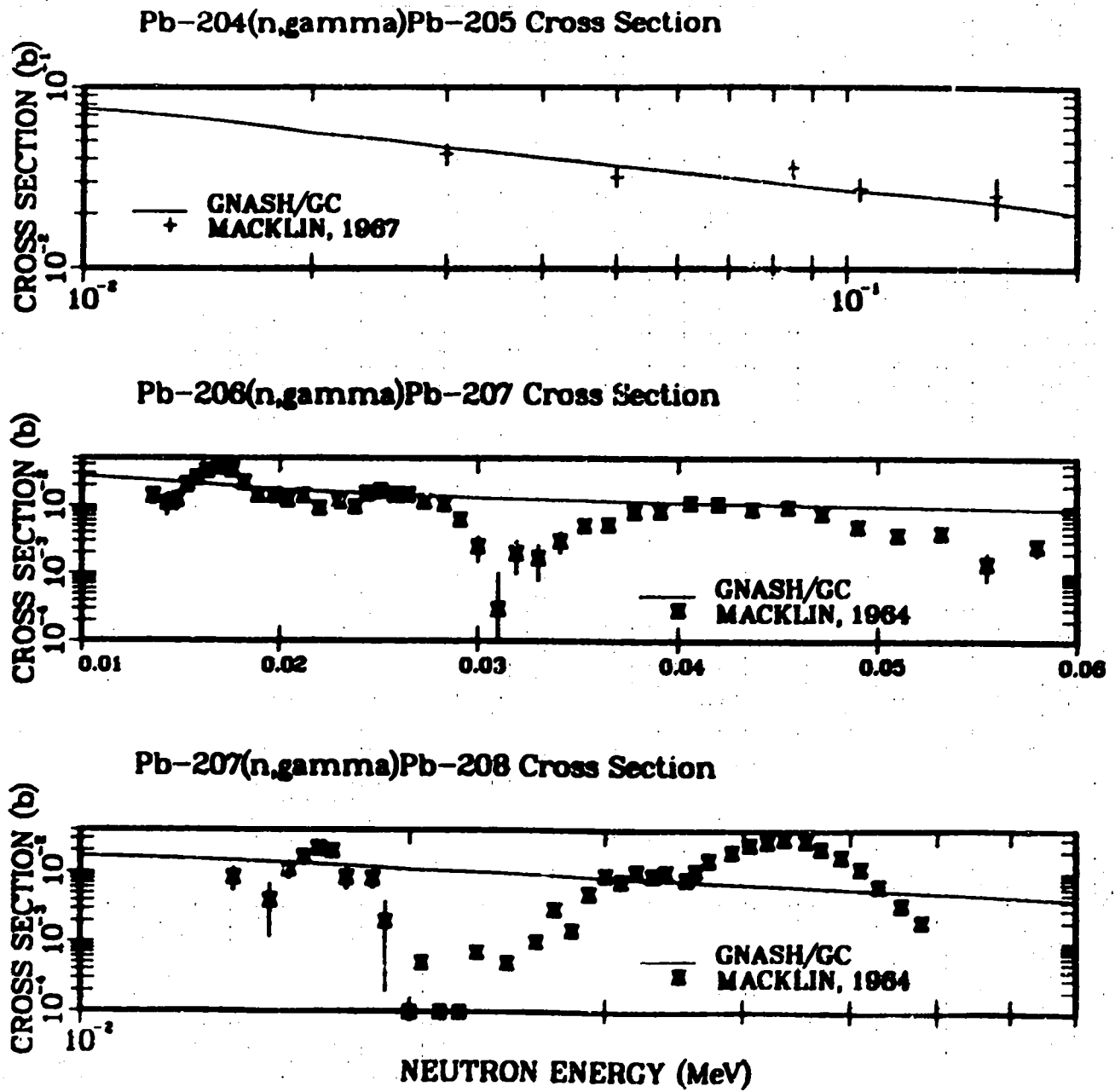
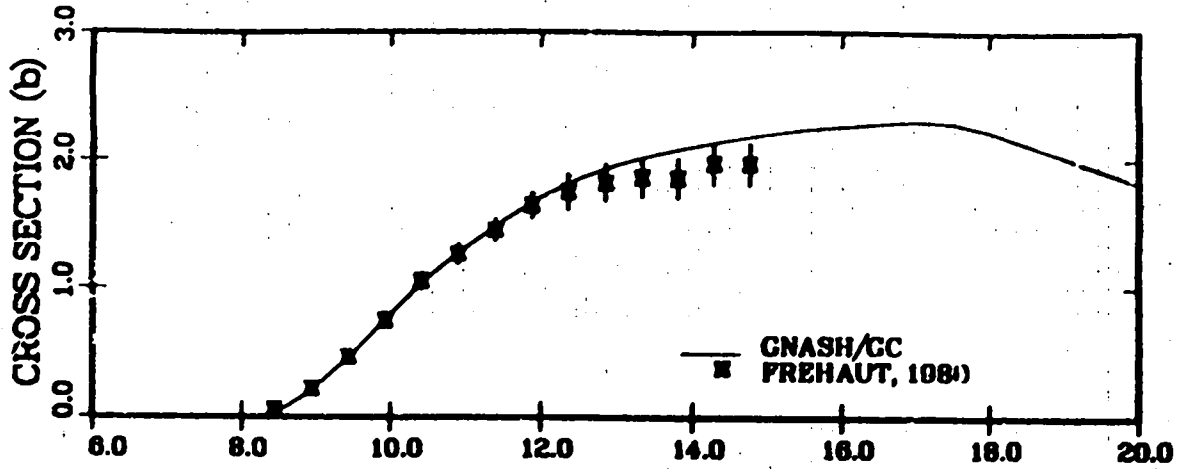


Fig. 29. Calculated and measured radiative capture cross sections for neutron reactions on  $^{204}\text{Pb}$ ,  $^{206}\text{Pb}$ , and  $^{207}\text{Pb}$ . The normalization of the gamma-ray transmission coefficients were determined by matching to these data,<sup>47</sup> as described in the text.

### Pb-206(n,2n) Cross Section



### Pb-207(n,2n) Cross Section

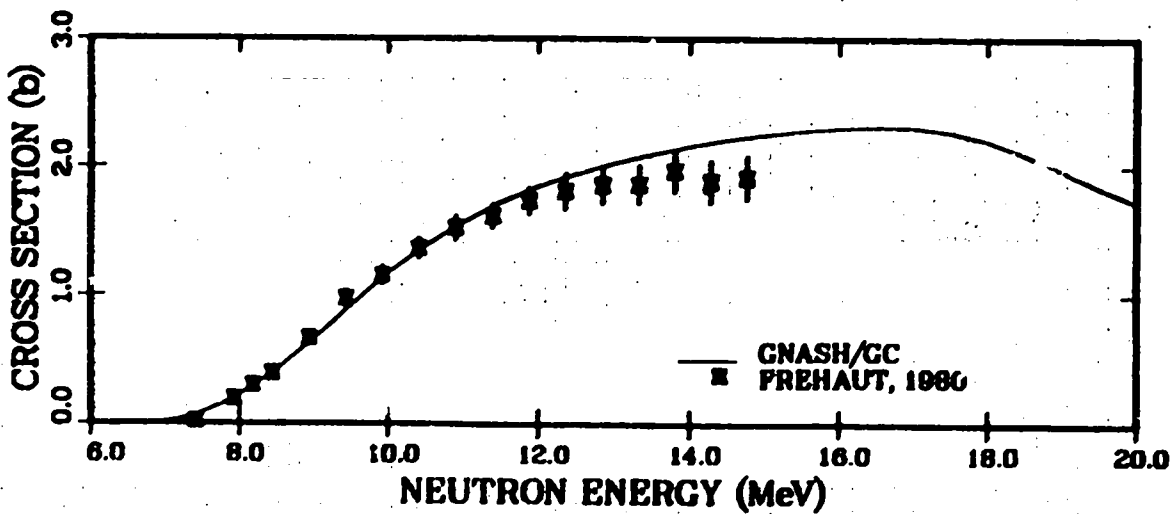


Fig. 30. Comparisons of the  $^{206}\text{Pb}(n,2n)^{205}\text{Pb}$  and  $^{207}\text{Pb}(n,2n)^{206}\text{Pb}$  cross sections calculated with the Gilbert and Cameron<sup>28</sup> level density formulation to experimental data.

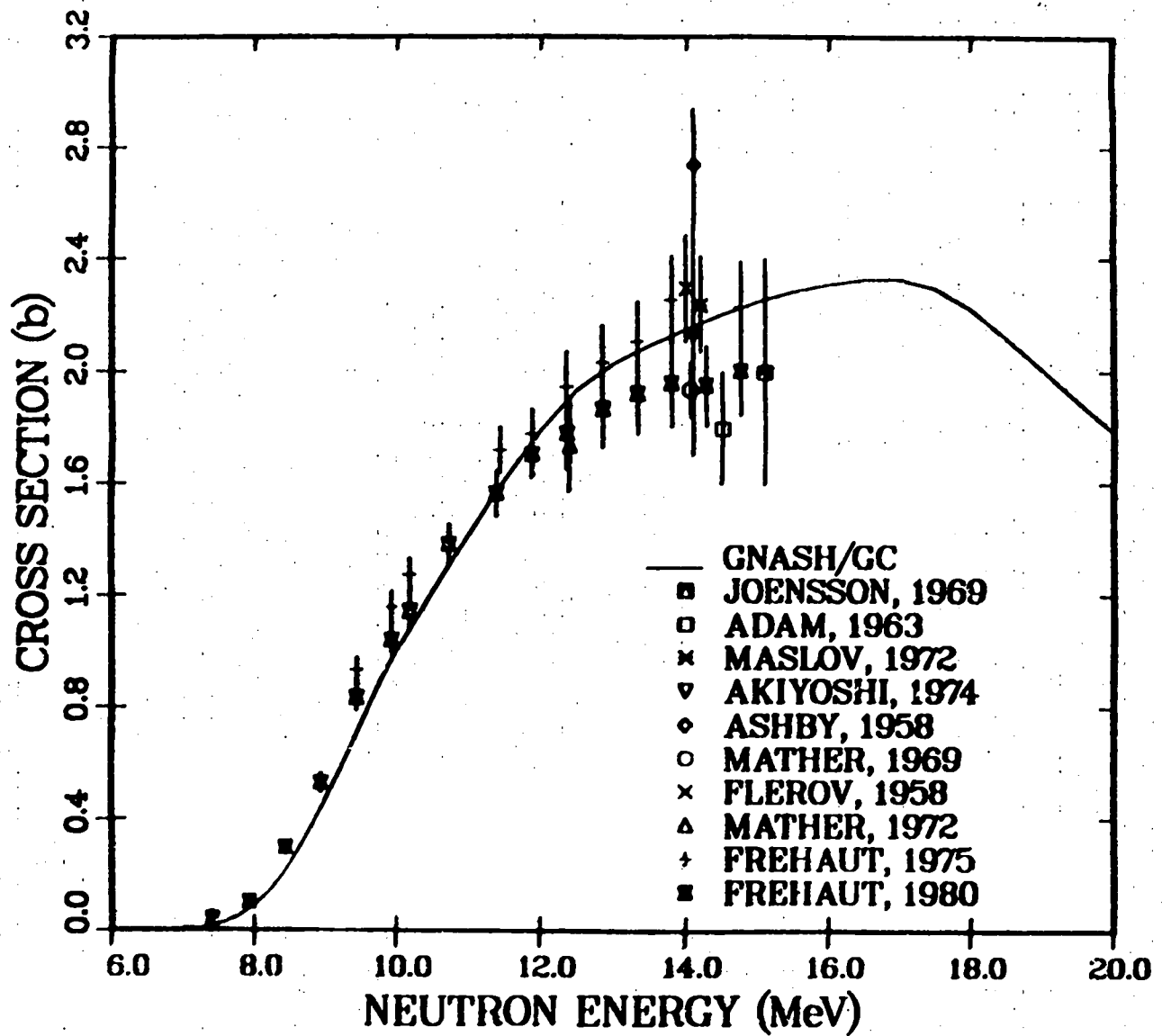
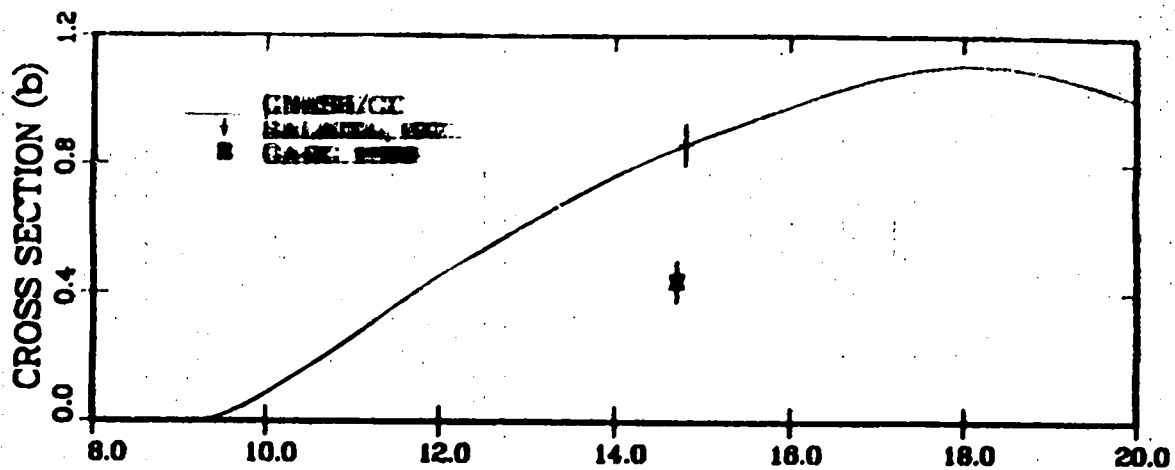


Fig. 31. Calculated and measured  $^{208}\text{Pb}(n,2n)$  cross sections. The solid curve was obtained by combining the GNASH calculations for individual isotopes using the Gilbert and Cameron level density model.<sup>28</sup>

Pb-206(n,2n)Pb-205m Cross Section



Pb-206(n,3n)Pb-204m Cross Section

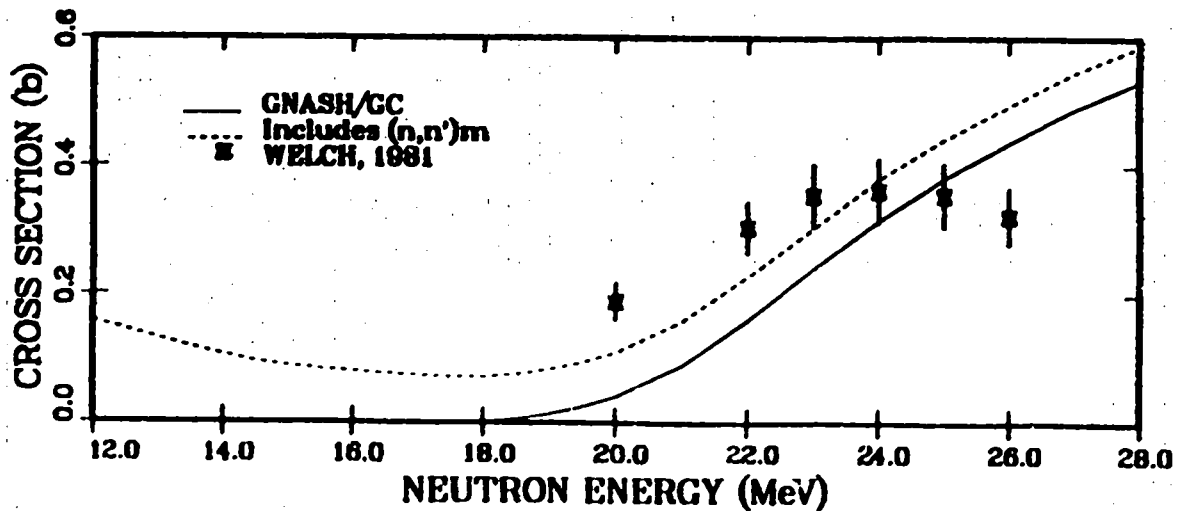


Fig. 32. Comparison of activation measurements of the  $^{206}\text{Pb}(n,2n)^{205\text{m}}\text{Pb}$  and  $^{206}\text{Pb}(n,3n)^{204\text{m}}\text{Pb}$  reactions with calculations using the Gilbert and Cameron level density representation.<sup>28</sup> The dashed curve in the lower half of the figure includes the  $^{204}\text{Pb}(n,n')^{204\text{m}}\text{Pb}$  cross section.

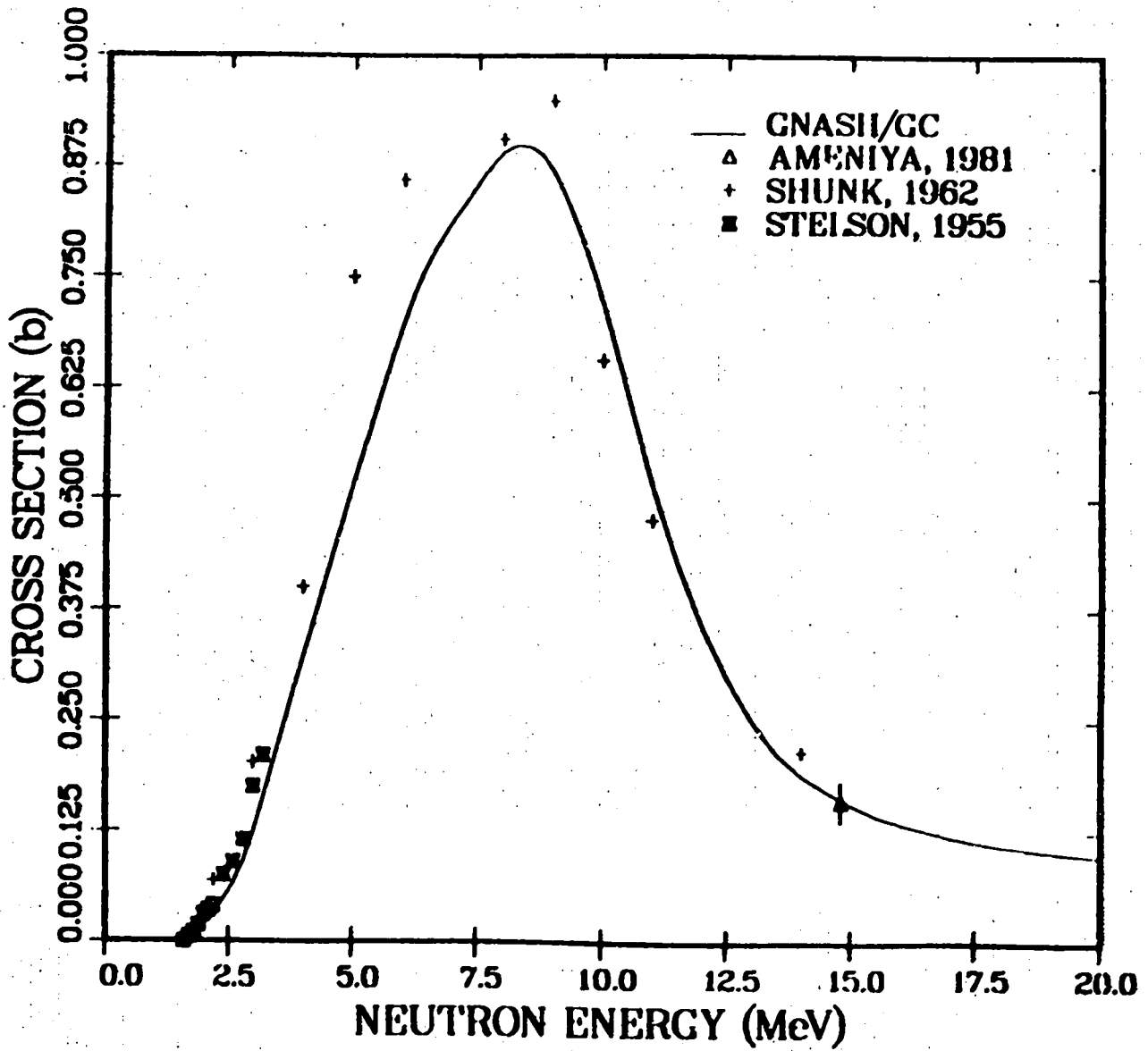
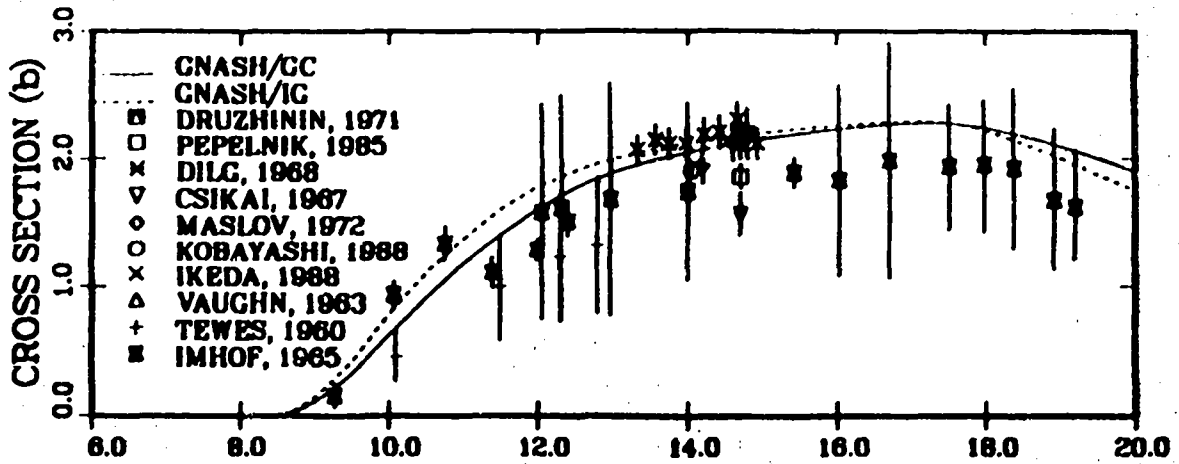


Fig. 33. Calculated and measured<sup>47</sup> values of the  $^{207}\text{Pb}(n,n')^{207\text{m}}\text{Pb}$  cross section.

Pb-204(n,2n) Cross Section



Pb-208(n,2n) Cross Section

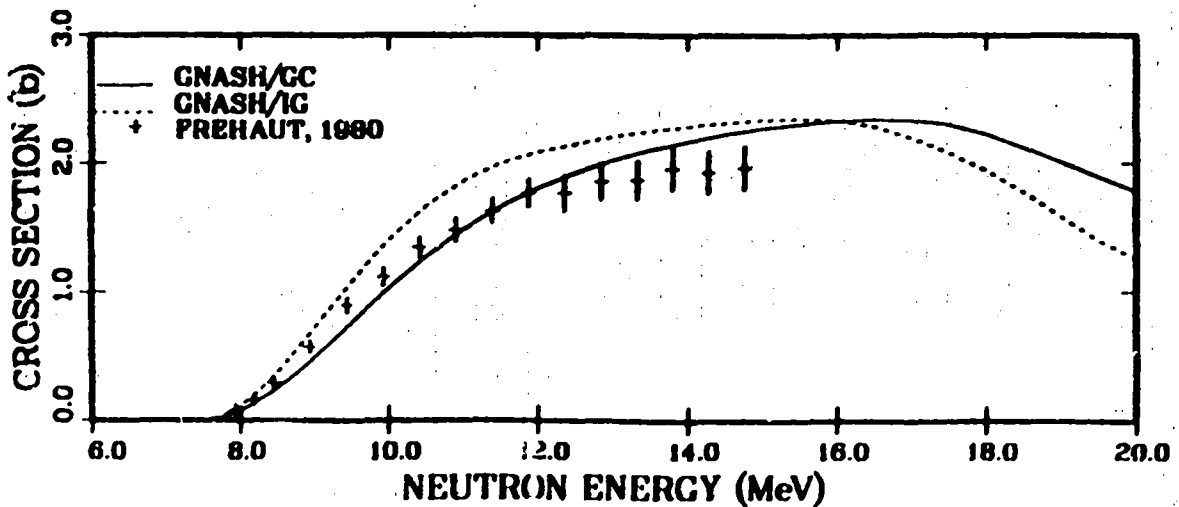


Fig. 34. Comparison of calculated and measured<sup>47</sup> values of  $^{204}\text{Pb}(n,2n)^{203}\text{Pb}$  and  $^{208}\text{Pb}(n,2n)^{207}\text{Pb}$  cross sections. The solid curve was calculated using the Gilbert and Cameron<sup>28</sup> model for level-densities and the dashed curve was obtained using the representation of Ignatyuk et al.<sup>31</sup>

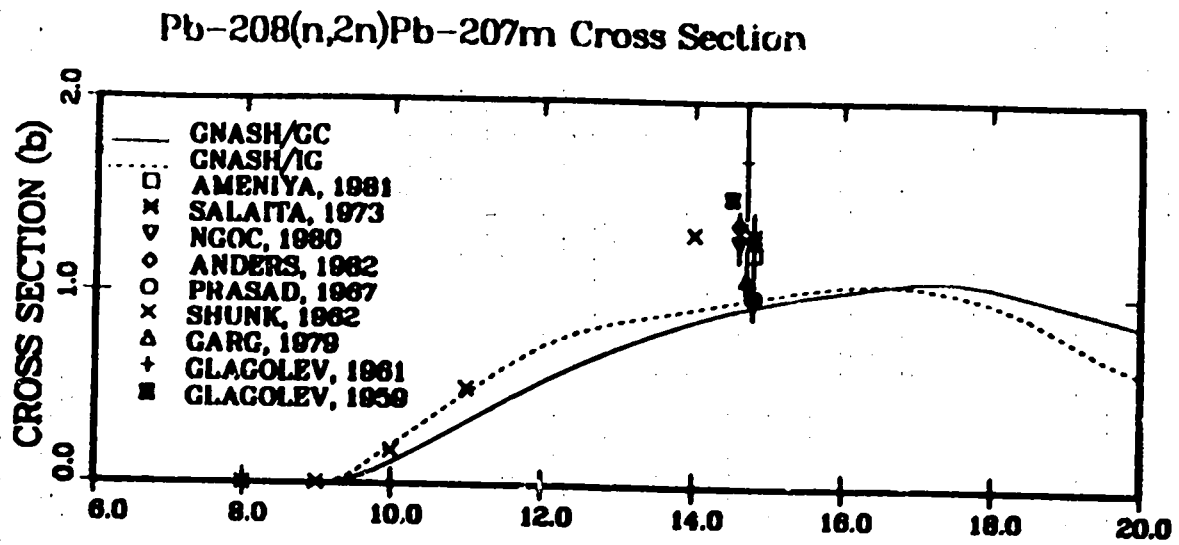


Fig. 35. Calculated and measured<sup>47</sup> values of the  $^{204}\text{Pb}(n,n')^{204m}\text{Pb}$  and  $^{208}\text{Pb}(n,2n)^{207m}\text{Pb}$  cross sections. See caption of Fig. 34 for explanation of curves.

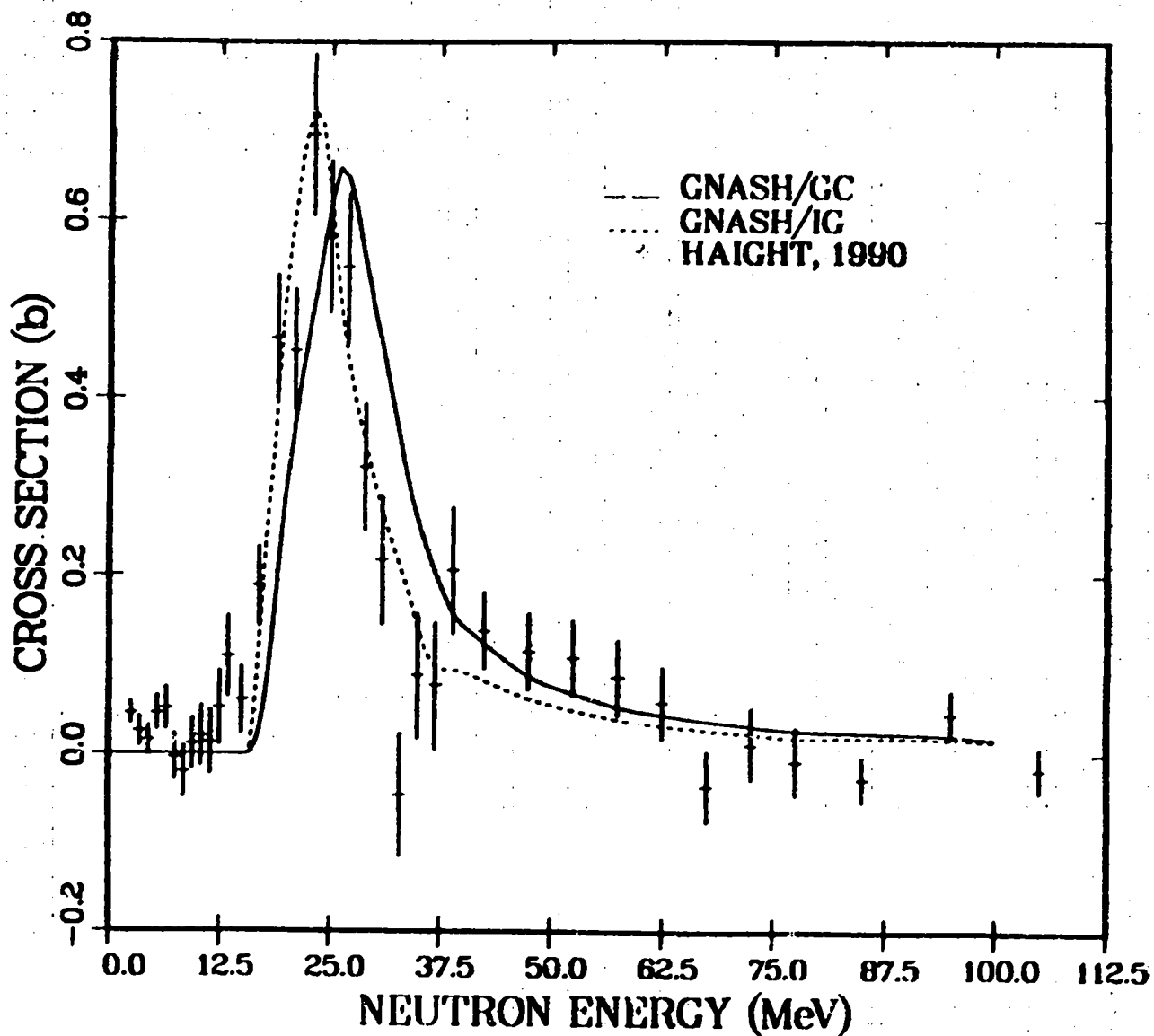


Fig. 36. Comparison of calculated and measured<sup>10</sup> values of the  $^{208}\text{Pb}(n,3n)^{206}\text{Pb}$  cross section for the 0.803-MeV gamma ray. See caption of Fig. 34 for explanation of curves.



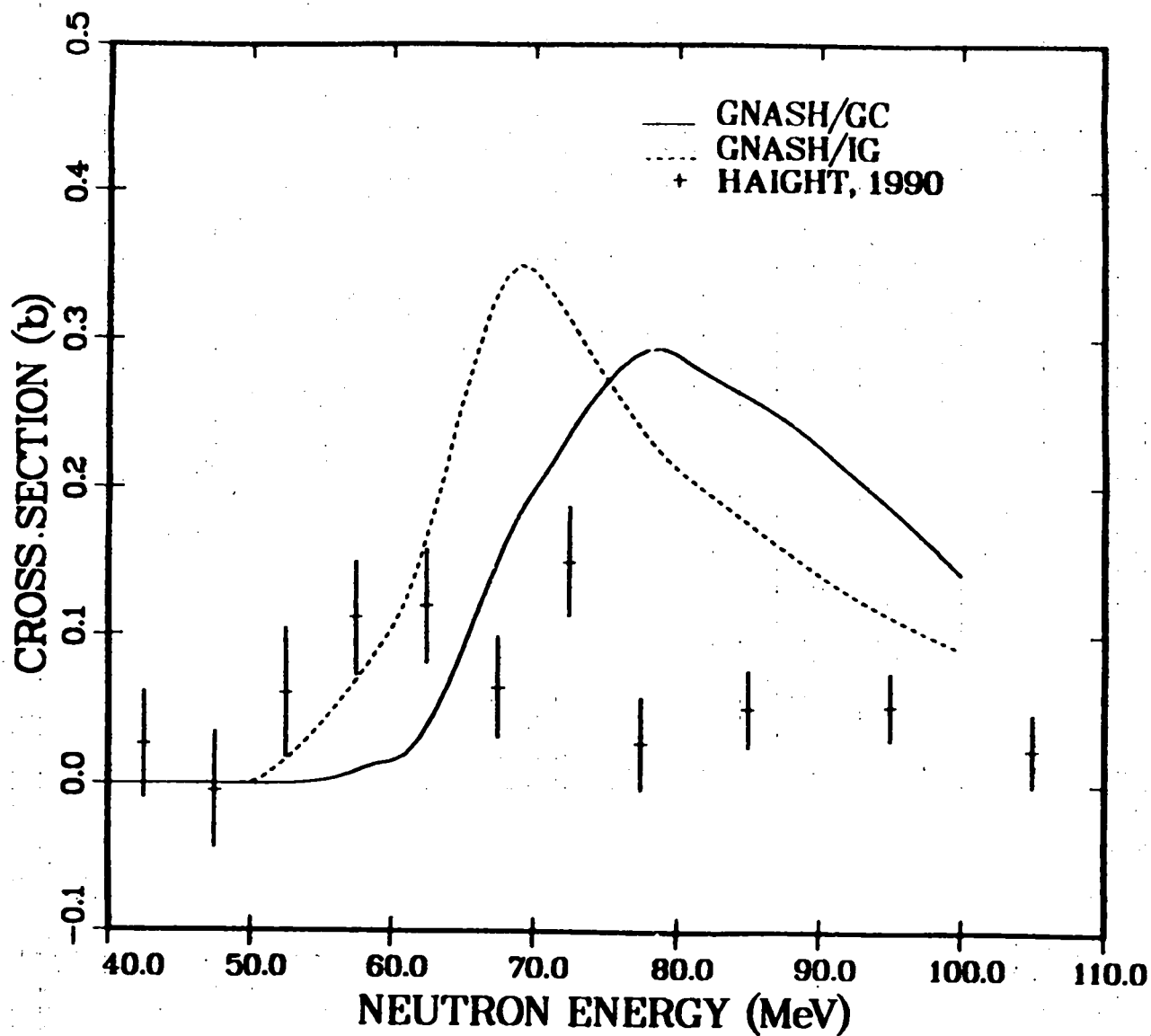


Fig. 37. Comparison of calculated and measured<sup>10</sup> values of the  $^{208}\text{Pb}(n,7n)^{202}\text{Pb}$  cross section for the 0.960-MeV gamma ray. See caption of Fig. 34 for explanation of curves.

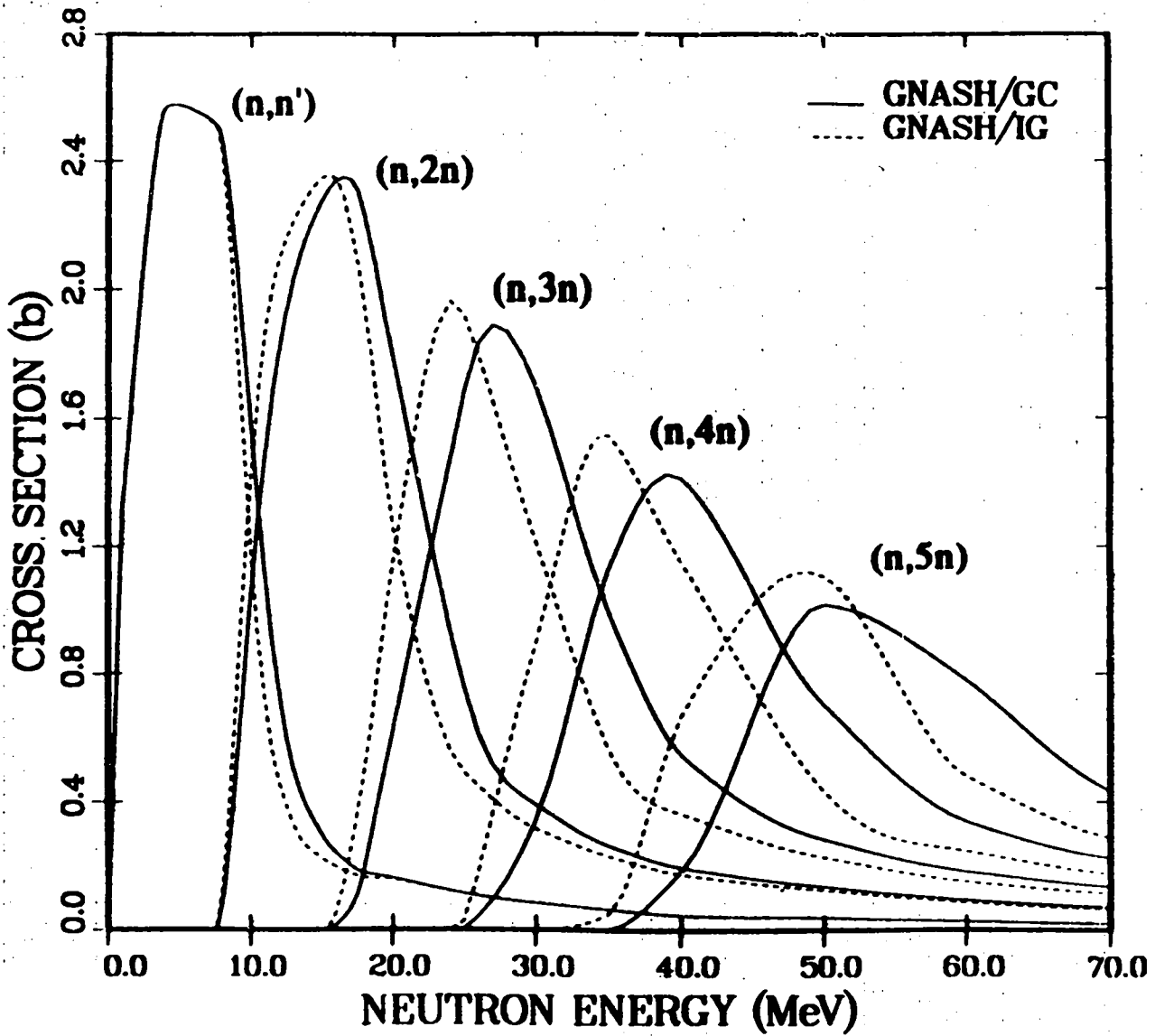


Fig. 38. Calculation of  $^{208}\text{Pb}(n,xn)$  cross sections between threshold and 70 MeV, where  $1 \leq x \leq 5$ , using the Gilbert and Cameron<sup>28</sup> (solid curves) and Ignatyuk et al.<sup>31</sup> (dashed curves) level density representations.

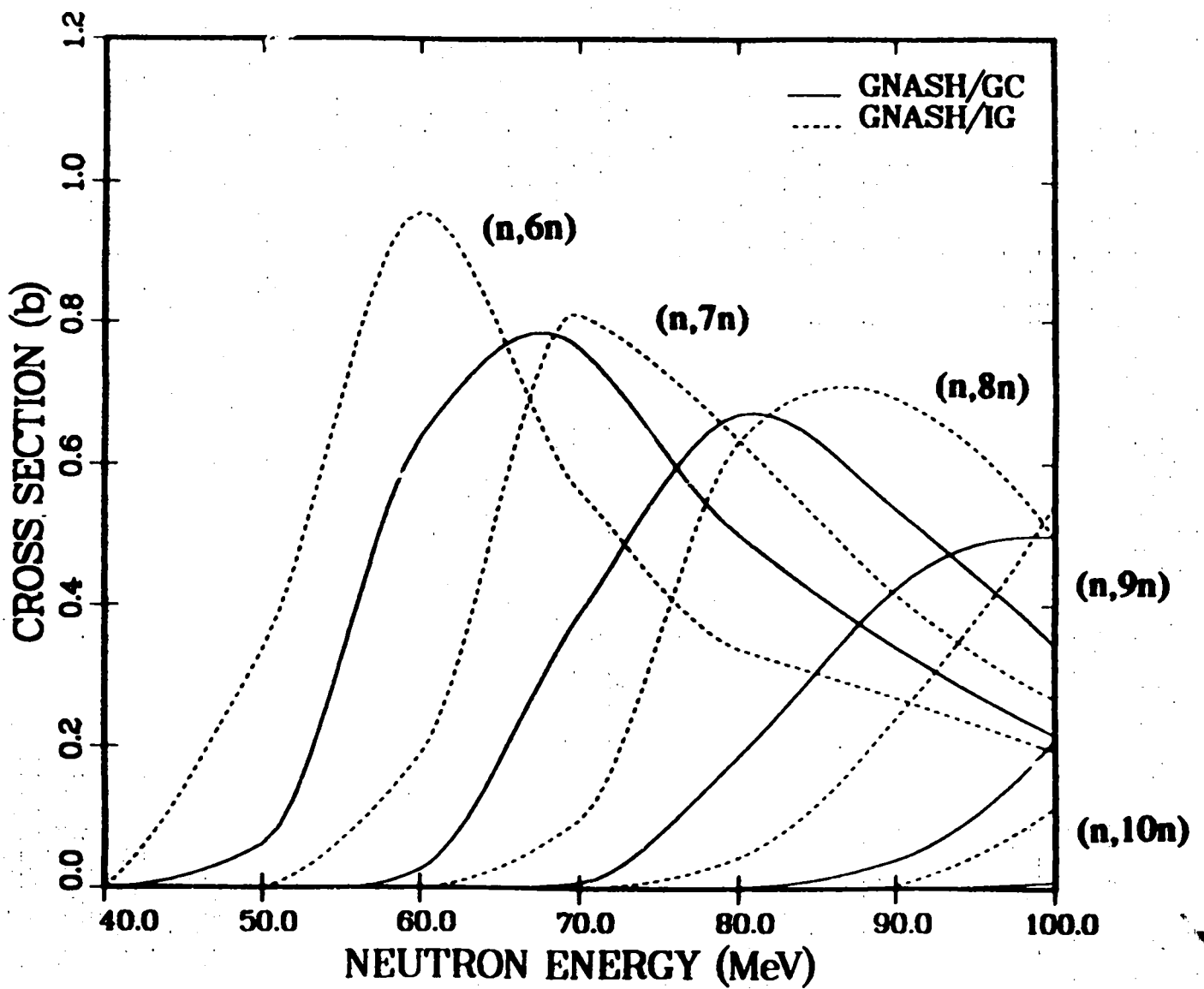


Fig. 39. Calculation of  $^{208}\text{Pb}(n,xn)$  cross sections between threshold and 100 MeV, where  $6 \leq x \leq 10$ , using the Gilbert and Cameron<sup>28</sup> (solid curves) and Ignatyuk et al.<sup>31</sup> (dashed curves) level density representations.

# APPENDIX 1

## SAMPLE OF DATA IN GROUND-STATE MASS, J<sup>n</sup> FILE (TAPE13)

Masses based on Wapstra 1986 and Moller-Nix 1986 merged files, as obtained from D. Madland (files MASS86 and MN86, respectively). Spin, parities from BCDGRD3 and Nuclear Wallet Cards. Date 10/25/88. Total entries 4795.

3846														
1	8.071380	100.5	1001	7.289029	100.5	1002	12.135824	101.0	1003	14.949913	100.5	1004	25.840000	9999.0
1005	33.790000	9999.0	2003	14.931314	100.5	2004	2.424910	100.0	2005	11.390000	-98.5	2006	17.592600	100.0
2007	26.110000	9999.0	2008	31.598000	100.0	2009	40.810000	9999.0	3004	25.120000	9999.0	3005	11.680000	-98.5
3006	14.085700	101.0	3007	14.907000	-98.5	3008	20.945600	102.0	3009	24.954100	-98.5	3010	33.840000	9999.0
3011	40.900000	9999.0	4006	18.374000	100.0	4007	15.768900	-98.5	4008	4.941710	100.0	4009	11.347700	-98.5
4010	12.607100	100.0	4011	20.174000	100.5	4012	25.077000	100.0	4013	35.000000	9999.0	4014	40.100000	100.0
5007	27.870000	9999.0	5008	22.920400	102.0	5009	12.415900	-98.5	5010	12.050990	103.0	5011	8.668200	-98.5
5012	13.369500	101.0	5013	16.562500	-98.5	5014	23.664000	9999.0	5015	28.970000	9999.0	5016	38.000000	9999.0
5017	45.270000	9999.0	6008	35.094000	100.0	6009	28.913900	-98.5	6010	15.699100	100.0	6011	10.650400	-98.5
6012	0.000000	100.0	6013	3.125030	-99.5	6014	3.019908	100.0	6015	9.873200	100.5	6016	13.694000	100.0
6017	21.035000	9999.0	6018	24.920000	100.0	6019	34.047000	9999.0	6020	40.843000	9999.0	6021	50.692000	9999.0
6022	58.506000	9999.0	6023	69.072000	9999.0	6024	78.277000	9999.0	6025	89.624000	9999.0	6026	101.992000	9999.0
6027	112.246000	9999.0	7010	39.500000	9999.0	7011	24.890000	9999.0	7012	17.338100	101.0	7013	5.345520	-99.5
7014	2.863433	101.0	7015	-0.101496	-99.5	7016	5.682100	-98.0	7017	7.871000	-99.5	7018	13.117000	9999.0
7019	15.871000	9999.0	7020	20.913000	9999.0	7021	28.076000	9999.0	7022	33.565000	9999.0	7023	41.170000	9999.0
7024	50.171000	9999.0	7025	58.697000	9999.0	7026	68.179000	9999.0	7027	76.553000	9999.0	7028	69.587000	9999.0
7029	100.506000	9999.0	7030	111.525000	9999.0	7031	122.096000	9999.0	7032	134.848000	9999.0	8012	32.060000	100.0
8013	23.113000	9999.0	8014	8.006540	100.0	8015	2.855400	-99.5	8016	-4.737037	100.0	8017	-0.809080	102.5
8018	-0.782200	100.0	8019	3.332100	102.5	8020	3.796900	100.0	8021	8.066000	9999.0	8022	9.440000	100.0
8023	18.174000	9999.0	8024	22.918000	9999.0	8025	32.568000	9999.0	8026	38.394000	9999.0	8027	47.479000	9999.0
8028	53.833000	9999.0	8029	64.240000	9999.0	8030	77.430000	9999.0	8031	84.614000	9999.0	8032	94.551000	9999.0
8033	108.875000	9999.0	9014	33.610000	9999.0	9015	16.770000	9999.0	9016	10.680000	-100.0	9017	1.951780	102.5
9018	0.873400	101.0	9019	-1.487430	100.5	9020	-0.017350	102.0	9021	-0.047500	102.5	9022	2.830000	9999.0
9023	3.350000	9999.0	9024	8.791000	9999.0	9025	12.990000	9999.0	9026	20.324000	9999.0	9027	26.089000	9999.0
9028	33.707000	9999.0	9029	39.530000	9999.0	9030	48.392000	9999.0	9031	57.107000	9999.0	9032	67.456000	9999.0
9033	74.853000	9999.0	9034	84.549000	9999.0	9035	95.734000	9999.0	10016	23.989000	100.0	10017	16.480000	-99.5
10018	5.319000	100.0	10019	1.751000	100.5	10020	-7.047800	100.0	10021	-5.737400	101.5	10022	-8.027200	100.0
10023	-5.156000	102.5	10024	-5.950000	100.0	10025	-2.060000	9999.0	10026	0.440000	100.0	10027	7.953000	9999.0
10028	11.638000	9999.0	10029	19.094000	9999.0	10030	22.880000	9999.0	10031	32.430000	9999.0	10032	38.923000	9999.0
10033	46.634000	9999.0	10034	54.725000	9999.0	10035	63.641000	9999.0	10036	72.830000	9999.0	10037	80.953000	9999.0
10037	36.700000	9999.0	11018	24.444000	9999.0	11019	12.928000	9999.0	11020	6.839000	102.0	11021	-2.189800	101.5

## APPENDIX 2

### DISCRETE LEVEL FILE (TAPE8) INPUT PARAMETERS

For each residual nucleus requiring discrete level data the following card (record) sequence is required. Note that the essential parameters that must be specified are: ID, NL, NX, EL(N), AJ(N), NT, NF,P, and CP. The other parameters may be left blank.

- (A) 1 card, FORMAT (I8, I5, F12.6): ID, NL, F
- (B) Outer loop on levels (DO-loop N = 1, NL)  
FORMAT (I6, F12.6, 2F6.1, E12.5, I6): NX, EL(N), AJ(N), AT(N), TAU, NT
- (C) Inner loop for each level (DO loop K = 1, NT)  
FORMAT (12X, I6, 2F12.6): NF, P, CP

<u>PARAMETER</u>	<u>DESCRIPTION</u>
ID	1000 * Z + A of the nucleus whose levels are being input.
NL	Number of discrete levels being input.
F	For card input, i.e., on INPUT file, set F = -1. for the last nucleus (highest ID) for which level data are input. Normally, just set F = 0.
NX	Level number (= N in DO loop), that is, NX = 1 for the ground state, NX = 2 for the first excited state, etc.
EL(N)	Energy in million electron volts (MeV) of the N <sup>th</sup> level.
AJ(N)	Spin and parity of the N <sup>th</sup> level. The sign of AJ(N) indicates the parity. For example, AJ(N) = -0. is interpreted as a J <sup>π</sup> = 0 <sup>-</sup> state.
AT(N)	Isospin of the N <sup>th</sup> level. It is not used in GNASH and can be set to zero. Note that a value of 99. sometimes appears in the file, indicating an unknown isospin.
TAU	Half life of the state in seconds. It is not used in GNASH and can be set to zero. Note that a value of 99. sometimes appears in the file, indicating an unknown half life.
NT	Number of gamma-ray branches from the N <sup>th</sup> level to lower levels.
NF	Level number indicator for a level to which a gamma-ray transition is occurring.

**P** Gamma-ray branching ratio for the transition defined by  $N \rightarrow NF$ . For bound states, the sum of  $P(N \rightarrow NF)$  over the NT transitions possible for state N is unity. For unbound states, the sum equals the total probability for decays other than particle emission.

**CP** Probability that the transitions characterized by  $P(N \rightarrow NF)$  are gamma-ray transitions. If, for example, there is a 20% probability that electron conversion is the decay mechanism, then  $CP = 0.80$ .

**SAMPLE FILES LEVEL DATA FOR <sup>93</sup>Nb**

41093	20	0.000000	0.000000	0.000000	31390
1	0.000000	4.5	99.0	0	
2	0.030820	-0.5	99.0	1	
	1	1	1.000000	1.000000	0.00000e+00
3	0.687000	-1.5	99.0	1	
	1	2	1.000000	1.000000	0.00000e+00
4	0.743910	3.5	99.0	1	
	1	1	1.000000	1.000000	0.00000e+00
5	0.808580	2.5	99.0	2	
	1	4	0.012346	1.000000	0.00000e+00
	2	1	0.987654	1.000000	0.00000e+00
6	0.810410	-1.5	99.0	1	
	1	2	1.000000	1.000000	0.00000e+00
7	0.949830	6.5	99.0	1	
	1	1	1.000000	1.000000	0.00000e+00
8	0.978940	5.5	99.0	1	
	1	1	1.000000	1.000000	0.00000e+00
9	1.082670	4.5	99.0	2	
	1	4	0.793651	1.000000	0.00000e+00
	2	1	0.206349	1.000000	0.00000e+00
10	1.253720	3.5	99.0	1	
	1	1	1.000000	1.000000	0.00000e+00
11	1.290000	-0.5	99.0	2	
	1	3	0.665290	1.000000	8.88890e+08
	2	6	0.334710	1.000000	8.88890e+08
12	1.297240	4.5	99.0	3	
	1	8	0.220513	1.000000	0.00000e+00
	2	4	0.266667	1.000000	0.00000e+00
	3	1	0.512821	1.000000	0.00000e+00
13	1.315310	-2.5	99.0	2	
	1	5	0.186992	1.000000	0.00000e+00
	2	4	0.813008	1.000000	0.00000e+00
.					
.					
.					
.					
20	1.500110	3.5	99.0	1	
	1	1	1.000000	1.000000	0.00000e+00

### APPENDIX 3

#### TRANSMISSION COEFFICIENT FILE (TAPE10)

- (A) (1 Record) FORMAT (I4, 1X, 7A8, A5 ): NPART, [BCDTC(I), I=1,8]
- (B) Outer loop on particles (DO loop N=1, |NPART|)  
(1 record per N loop) FORMAT (43X, A8, 13X, 2I4, A8): XBCD, NE, NN, K
- (C) Input energy grid for particle N (internal identifier = ID),  
(DO loop I = 2, NE, 6)  
(1-5 records per N loop) FORMAT (6E11.5, A6): [ETC(J, ID), J = I, I+5], K
- (D) Input optical model cross sections (optional) and transmission coefficients for particle N.  
Outer loop on energy (DO loop I = 2, NE) (1-8 records per energy)
- (1 record if NPART is negative) FORMAT (4E11.4) DU1, DU2, DU3, DU4  
(1-7 records per energy) FORMAT (6E11.4, A6): [TDUM(L), L = J, J+5], K

<u>Parameter</u>	<u>Description</u>
NPART	Absolute value is the number of particles for which transmission coefficients are input. Set NPART negative to also input optical model integrated cross sections at each incident energy.
BCDTC(8)	Sixty-one columns of Hollerith descriptive information.
XBCD	Alphanumeric particle identifiers in A8 format, as follows: NEUTRON , PROTON , DEUTERON, TRITON , HE-3 , ALPHA .
NE	Number of energies included in energy grid for the transmission coefficient array.
NN	Number of coefficients input at each energy.
K	Not used. Can be used as a card or record counter.
ETC(J, ID)	Energy grid for transmission coefficients. The index J specifies the energy and ID is an internal identifier that identifies the particle type, according to XBCD.
DU1	Incident particle energy in the laboratory system (MeV).
DU2	Reaction cross section from optical model calculation in barns.
DU3	Shape elastic cross section from optical model calculation in barns.
DU4	Total cross section (DU2 + DU3) from optical model calculation in barns.
TDUM(L)	Transmission coefficient array in the format used by the COMNUC code. The index L runs from 1 to NN for each energy on the grid. The coefficients are later collapsed to remove the J-dependence from spin-orbit coupling. Coefficients are stored as functions of energy for each particle.

# EXAMPLE OF TRANSMISSION COEFFICIENT INPUT DATA FOR <sup>93</sup>Nb

RECORD  
NO.

DATA

1	-3 n + nb-93 p.nagel parameters for model code compar. sc90tst2					
2	energies and penetrabilities for the neutron continuum 36 40					
3	1.0000e-03	5.0000e-03	1.0000e-02	5.0000e-02	1.0000e-01	1.5000e-01
4	3.0000e-01	5.0000e-01	7.5000e-01	1.0000e+00	1.2500e+00	1.5000e+00
5	2.0000e+00	2.5000e+00	3.0000e+00	4.0000e+00	5.0000e+00	6.0000e+00
6	7.0000e+00	8.0000e+00	9.0000e+00	1.0000e+01	1.2000e+01	1.4000e+01
7	1.6000e+01	1.8000e+01	2.0000e+01	2.5000e+01	3.0000e+01	3.5000e+01
8	4.0000e+01	4.5000e+01	5.0000e+01	5.5000e+01	6.0000e+01	
9	1.0108e-03	1.3159e+01	5.2973e+00	1.8457e+01		
10	1.9365e-02	1.6416e-04	8.7075e-09	2.3414e-04	7.6980e-09	0.0000e+00
11	0.0000e+00	0.0000e+00	0.0000e+00	0.0000e+00	0.0000e+00	0.0000e+00
12	0.0000e+00	0.0000e+00	0.0000e+00	0.0000e+00	0.0000e+00	0.0000e+00
13	0.0000e+00	0.0000e+00	0.0000e+00	0.0000e+00	0.0000e+00	0.0000e+00
14	0.0000e+00	0.0000e+00	0.0000e+00	0.0000e+00	0.0000e+00	0.0000e+00
15	0.0000e+00	0.0000e+00	0.0000e+00	0.0000e+00	0.0000e+00	0.0000e+00
16	0.0000e+00	0.0000e+00	0.0000e+00	0.0000e+00		
17	5.0542e-03	6.5544e+00	5.2197e+00	1.1774e+01		
18	4.2770e-02	1.8288e-03	4.8529e-07	2.6008e-03	4.2927e-07	4.0560e-10
19	0.0000e+00	8.3941e-10	0.0000e+00	0.0000e+00	0.0000e+00	0.0000e+00
20	0.0000e+00	0.0000e+00	0.0000e+00	0.0000e+00	0.0000e+00	0.0000e+00
21	0.0000e+00	0.0000e+00	0.0000e+00	0.0000e+00	0.0000e+00	0.0000e+00
22	0.0000e+00	0.0000e+00	0.0000e+00	0.0000e+00	0.0000e+00	0.0000e+00
23	0.0000e+00	0.0000e+00	0.0000e+00	0.0000e+00	0.0000e+00	0.0000e+00
24	0.0000e+00	0.0000e+00	0.0000e+00	0.0000e+00		
193	1.4152e+01	1.7558e+00	2.3064e+00	4.0621e+00		
194	6.8537e-01	7.9966e-01	7.1564e-01	7.6002e-01	7.5721e-01	7.7759e-01
195	9.0647e-01	6.8263e-01	9.0530e-01	5.0439e-01	6.2361e-01	6.5269e-01
196	4.7418e-01	9.6235e-02	1.1984e-02	3.5877e-01	2.7753e-02	1.5307e-03
197	1.9312e-04	2.3454e-03	2.3947e-04	2.3876e-05	2.9029e-06	2.6525e-05
198	3.0497e-06	3.4831e-07	0.0000e+00	3.5613e-07	0.0000e+00	0.0000e+00
199	0.0000e+00	0.0000e+00	0.0000e+00	0.0000e+00	0.0000e+00	0.0000e+00
200	0.0000e+00	0.0000e+00	0.0000e+00	0.0000e+00		

COMNUC ORDERING OF  $T_l^\pm$  FOR SPIN 1/2 PARTICLES, WHERE  $J = l \pm 1/2$

$T_0$	$T_1^-$	$T_2^-$	$T_1^+$	$T_2^+$	$T_3^-$
$T_4^-$	$T_3^+$	$T_4^+$	$T_5^-$	$T_6^-$	$T_5^+$
etc.					



**APPENDIX 4**  
**GNASH INPUT FILE DESCRIPTION**

- (A) (2 cards) FORMAT (10A8): TITLE(N), N = 1, 20
- (B) (1 card) FORMAT (8I4): IPRTLEV, IPRTTC, IPRTWID, IPRTSP, IPRTGC  
IPRE, IGAMCAS, ILD
- (B') Skip if ILD < 1
- (0 - NLDR cards) Format (\*): NLDR  
DO loop II = 1, NLDR  
(1 card per II) FORMAT (\*): IR, ALD(IR), ECLD(IR), XNLLD(IR),  
ECLDL(IR), XNLLDL(IR), PA(IR), SIG2(IR)
- (C) (1 card) FORMAT (10I4): INPOPT, KLIN, KTIN, NIBD, LMAXOPT, NLDIR,  
ILDIN, LPDECAY, KSPLIT, LPOP, IHELV,  
IQBETA1, ISURF, ISEADD, IBEOFF
- (D) (1 card) FORMAT (12I4): NI, NMP, LGROPT, LPEQ, NJMAX, ICAPT, IFIS,  
IBSF, ISIG2, IWFC, LDELGC, ISPCUT, LGSFINT
- (D') Skip if IFIS = 0
- (1 card) FORMAT (4I4): NBAR, IDIAF, IHFACT, KFMAX
- (E) (1 card) FORMAT (7E10.3): ZAP, ZAT, DE, FSIGCN, EGS, SPINGS, PARGS
- (E') Skip if ISPCUT = 0
- (1 card) FORMAT (2E10.3): SCUTFTR, SDFTR, OLDGC
- (F) (1 card) FORMAT (I4): NELAB
- (G) (1-3 cards) FORMAT (8E10.3): ELABS(N), N=1, NELAB

(H) (0-130 cards) Reaction-chain data. The form and complexity of this segment depend on the particular input option chosen, as follows:

(1) INPOPT = 1, 2, or 3 (0 cards)

Reaction chains are set up automatically.

(2) INPOPT = -1 (1-8 cards) (DO loop I=1, NI)

FORMAT (8E10.3): ZACN(I), XNIP(I), SWS(I), [ZZA1(IP), IP=2, NIP]

(3) INPOPT = 0 (2-130 cards)

(a) Outer DO loop I = 1, NI

(1 card per I) FORMAT (5E10.3): ZACN(I), XNIP(I), CNPI(I),  
CNPIP(I), SWS(I)

(b) Inner DO loop IP = 1, NIP

i. (1 card per IP) FORMAT (8E10.3): ZA1(IR), XNL(IR), A(IR),  
XNLGC(IR), ECGC(IR), XNLGCL(IR),  
ECGCL(IR), XMESH(IR),

where IR is a running reaction index that defines a unique I, IP, for each reaction sequence.

ii. ILDIN = 1 (Skip otherwise.)

(1 card per IP) FORMAT (3E10.3): EOIN(IR), TGCIN(IR),  
EMATIN(IR), SIG2(IR), PA(IR), EDS(IR)

(I) (1-6 cards) (DO loop MP = 1, NMP) FORMAT (8X, A1, I1, 2E10.3):  
LMGHOL(MP), LG, RE1(MP), GGDNORM(MP)

(J) [2 cards IF LGROPT=2 (Brink-Axel option), 0 cards if LGROPT=1]  
FORMAT (8E10.3) EG1, GG1, EG2, GG2, G2NORM, EG3, GG3, G3NORM  
FORMAT (8E10.3) SIGE1, EGCONM1, EGCON, GDSTEP, GDELS, GDELSL,  
GDEDELE, XNFE1

(J) [2 cards IF LGROPT=3 (Kopecky option), 0 cards if LGROPT=1]  
FORMAT (8E10.3) EG1, GG1, EG2, GG2, G2NORM, EG3, GG3, G3NORM  
FORMAT (8E10.3) SIGE1, SIGM1, EGCON, GDSTEP, GDELS, GDELSL,  
GDEDELE, XNFE1

(K) [if LPEQ=0 (0 cards), if LPEQ≥1 (1 card)]  
FORMAT (8E10.3) F2, GG, (GR(M), M=1, 6)

(L) Skip if IFIS  $\neq 1$

Outer DO Loop  $II = 1, NFISSION$  (Number of fission channels)

(1 card) FORMAT (3E10.3): EBAR(II,N),  $N = 1, NBAR$

(1 card) FORMAT (3E10.3): XBOM(II,N),  $N = 1, NBAR$

(1 card) FORMAT (3E10.3) DENFAC(II,N),  $N = 1, NBAR$

(1 card) FORMAT (2E10.3): FSTS(II), ERFIS(II)

Skip 1st Inner DO Loop if  $FSTS(II) \leq 0$ .

1st Inner DO Loop  $N = 1, IFIX(FSTS(II))$

(1 card per N) FORMAT (2E10.3): EBBF, XJPIF

END 1st Inner Loop

Skip 2nd Inner DO Loop if  $FSTS(II) \geq 0$ .

2nd Inner DO Loop  $NB = 1, NBAR$

(1 card per NB) FORMAT (I4): IBAND

Innermost DO Loop  $KB = 1, IBAND$

(1 card per KB) FORMAT (3E10.3): EBAND, XJPIBA, PIB1

END Innermost Loop

END 2nd Inner Loop

END Outer Loop

## DEFINITION OF GNASH INPUT FILE PARAMETERS

<u>Parameter</u>	<u>Description</u>
<b>TITLE</b>	Two cards of Hollerith information to describe the problem being calculated.
<b>IPRTLEV</b>	Print control for discrete level data. Set IPRTLEV = 0(1) to omit (include) print of discrete level energies, spins, parities, branching ratios, and computed cross sections.
<b>IPRTTC</b>	Print control for transmission coefficients and gamma-ray strength functions. Set IPRTTC = 0(1) to omit (include) print of input transmission coefficients and strength functions. Set IPRTTC > 1 to print coefficients at every (IPRTTC-1)th energy on the basic integration energy mesh.
<b>IPRTWID</b>	Print control for reaction decay widths. Set IPRTWID = 0(1) to omit (include) print of decay widths for each reaction channel on the basic integration energy mesh.
<b>IPRTSP</b>	Print control for calculated energy spectra, as follows: <ul style="list-style-type: none"> <li>IPRTSP = 0 to omit print of all calculated energy spectra.</li> <li>= 1 to only print composite spectra for each radiation in the calculation; that is, composite spectra from emitted gamma rays, neutrons, protons, etc.</li> <li>= 2 to print individual spectra from each decay process included in the calculation, omitting the composite spectra.</li> <li>= 3 to print both individual reaction and composite spectra.</li> </ul>
<b>IPRTGC</b>	Print control for level-density information. Set IPRTGC = 0(i) to omit (include) print of level-density parameters for each residual nucleus in the calculation. Set IPRTGC > 1 to print parameters and computer level densities at every (IPRTGC-1)th energy on the basic integration energy mesh for each residual nucleus.
<b>IPRE</b>	Print control for preequilibrium spectra and other parameters associated with the preequilibrium correction. Set IPRE = 1 to include print, 0 otherwise.
<b>IGAMCAS</b>	This option is used mainly for ENDF evaluations where discrete inelastic scattering gamma-ray lines and the continuum inelastic scattering contributions are to be kept separate: <ul style="list-style-type: none"> <li>IGAMCAS = 0 All discrete gammas are included in continuum energy spectra, as usual;</li> <li>= 1 No discrete <i>inelastic</i> gammas (pure discrete or continuum) are included in energy spectra;</li> <li>= 2 No discrete gammas <i>at all</i> are accumulated in spectra;</li> <li>IGAMCAS = 3 Both particles and gammas from pure discrete <i>inelastic</i> (only) are excluded from the spectra.</li> </ul>

- ILD** Set equal to 1 to read in level density parameters for residual nuclei in selected reactions.
- IR** Running reaction index. Each IR designates a particular I, IP combination for which level density parameters are given (see below).
- ALD** Fermi gas 'a' level density parameter for reaction IR.
- ECLD, XNLLD** XNLLD is the number of discrete levels at upper end of the excitation energy range (ECLD) where experimental level data are used. Default values are the maximum values of the level data read from TAPE 8. If only ECLD is input as zero, then ECLD is determined from XNLLD and the level data on TAPE8.
- ECLDL, XNLLDL** XNLLDL is the number of the discrete level (1 = ground state) at the lower excitation energy (ECLDL) used with XNLLD and ECLD in matching the Gilbert-Cameron temperature level density function. If only ECLDL is input as zero, then ECLDL is determined from XNLLDL and the discrete level data on TAPE8. If either XNLLDL or ECLDL is set negative, then the old method of matching to only XNLLD and ECLD is used; that is, it is assumed that XNLLDL = 0. at ECLDL =  $-\infty$ .
- SIG2(IR)** Spin-cutoff,  $\sigma^2$ , for discrete level region. Determined from discrete level data on TAPE8 if input as zero. Default is 0.
- PA(IR)** If not left blank, the pairing energy used in the Gilbert-Cameron level density will be set equal to PA(IR). If left blank, pairing energies from Cock et al. [*Aust. J. Phys.* **20**, 477 (1967)] are used.
- INPOPT** Input control for designating the input option chosen to specify the reaction chains followed in the calculation. The following options are available.
- INPOPT** = 0 is the most general input option available for specifying the reaction chains and the various parameters associated with each chain. For example, it permits (but does not require) input of level-density parameters for each residual nucleus in a calculation. See description of card input for details of reaction-chain input.
- = -1 also permits general specification of reaction chains but uses automatic features to simplify input. With this option, the code uses a built-in level-density parameterization and automatically determines parentage of each decaying compound nucleus by assuming that all previous, unassigned reactions leading to a given compound nucleus contribute to its initial populations of states.
- = 1 to automatically follow the neutron chains from the initial compound nucleus. A total of NI (see Card No. 5) compound nuclei are included, and each is permitted to decay by emission of gamma rays and neutrons.
- = 2 same as INPUT = 1 except each compound nucleus is permitted to decay by emission of gamma rays, neutrons, protons, and alpha particles.

- INPOPT = 3** same as **INPOPT = 2** except that the product nuclei that result from proton and alpha emission are themselves allowed to decay.
- KLIN** Input file designator for discrete energy-level data (= 5 for card input, = blank or 8 for input on file TAPE8). Note that TAPE8 is the recommended option.
- KTIN** Input file designator for transmission-coefficient data (= 5 for card input, = blank or 10 for input on file TAPE10). Note that TAPE10 is the recommended option.
- NIBD** Number of large-core buffers set up for storing state populations in reaction products that will further decay. The default value for NIBD is currently 10, which is also the maximum dimension.<sup>1</sup>
- LMAXOPT** Control for limiting the number of transmission coefficient ( $T_l$ ) included in a calculation by requiring that  $(2l + 1)T > T_0 \cdot 10^{-|LMAXOPT|}$ . The default value is **LMAXOPT = 5**.
- NLDIR** Control for including direct reaction cross sections for inelastic scattering from NLDIR levels. If NLDIR is greater than 0, then direct reaction cross-section information must be supplied on TAPE33 (see below) in free format form. NLDIR must include the ground state and all inelastic levels up through NLDIR, whether or not such levels have nonzero direct components. In the case of the ground state and levels with no direct component, zeroes must be entered. Add 100 to NLDIR to add in coupled-channel direct reaction cross sections, which are not used in renormalizing the reaction cross section.
- ILDIN** Input control (used only when **INOPT=0**) to directly read in  $E_0$ ,  $T$ , and  $E_m$  for the constant temperature part of the Gilbert-Cameron level density function. (The quantity  $E_m$  is the matching energy between the constant temperature and Fermi-gas parts of the function). Set **ILDIN = 1** to input these quantities; set **ILDIN = 0** to omit, which then permits these quantities to be determined automatically from the cumulative number of levels.
- LPDECAY** Control that permits discrete energy levels to particle decay. Set **LPDECAY = 0 (1)** to include (omit) particle decay from the levels. Note that if **LPDECAY = 0**, then the fraction of the population of any level that particle decays is taken as  $1.0 - \sum B_m$ , where  $\sum B_m$  is the sum of all  $\gamma$ -ray branching ratios for that level.
- KSPLIT** Number of energy bins (beginning with the highest excitation energy bin in the first compound nucleus) that utilize the improved integration scheme activated by the **XMESH (IR)** parameter described below. The default value for **KSPLIT** is 5.
- LPOP** Any calculated bin population less than  $10^{-|LPOP|}$  is assumed zero. Input of **LPOP = 0** is normally used, which sets default of 20.
- IHELV** Control to permit embedded discrete states in the continuum. Set **IHELV = 0(1)** to ignore (activate). When activated, **ECGC** and/or **XNLGC** must be read in for those reactions where the continuum cutoff is desired below the highest levels used in the calculation.

<sup>1</sup> All important dimensions are set in a **PARAMETER** statement and are therefore easily changed.

- IQBETA1** Set  $IQBETA1 = 0$  to include preequilibrium QBETA calculation, as usual. If  $IQBETA1 = 1$ , then QBETA is forced to equal 1, maximizing the neutron preequilibrium contribution.
- ISURF** Set  $ISURF = 0$  (1) to omit (include) Kalbach's surface effects correction.
- ISEADD** Set  $ISEADD = 0$  (1) to omit (include) the addition of the shape elastic cross section from TAPE10 (transmission coefficient file) in the outputted energy spectra and level excitation cross sections.
- IBEOFF** Set  $IBEOFF = 0$  (1) to include (omit) a crude kinematics and double-counting correction for identical residual nuclei.
- NI** Number of compound nuclei that are permitted to decay in the reaction chain (currently dimensioned for 10).<sup>2</sup>
- NMP** Number of gamma-ray multipolarities permitted in radiative decays (currently dimensioned for 6).<sup>2</sup>
- LGROPT** Control for indicating the model desired for calculating gamma-ray transition probabilities, as follows:
- LGROPT** = 1 for the Weisskopf model;  
                   = 2 for the Brink-Axel model;  
                   = 3 for the Kopecky-Uhl model.
- LPEQ** Preequilibrium control. Set  $LPEQ = 0$  to omit preequilibrium processes in the calculation. Set  $LPEQ=1$ (2) to use the new (old) QBETA option in the preequilibrium calculation.
- NJMAX** Maximum number of values of total angular momentum permitted in the calculation (dimensioned for 40, which is also the default value). For even-A cases,  $J_{max} = NJMAX - 1$ ; for odd-A cases,  $J_{max} = (2 * NJMAX - 1)/2$ . NJMAX also acts as a control for increasing the JRAST values for all continuum levels (see SUBROUTINE LCMLOAD). Set  $NJMAX = -NX$  to increment all JRAST levels by  $+|NX|$ . NJMAX is then reset to its default value.
- ICAPT** Gamma-ray cascade control for initial compound nucleus:
- $ICAPT = 0$  to omit full gamma-ray cascade calculation in the initial compound nucleus (all subsequent compound nuclei do include the full cascade).
- = 1 to include the full gamma-ray cascade in calculations for all compound nuclei.
- IFIS** Set  $IFIS > 0$  to activate fission option.

---

<sup>2</sup> See footnote 1.

- IBSF** Control for setting level density option as follows:
- = 0 to use the Gilbert-Cameron level density form;
  - = 1 to use the Backshifted Fermi Gas level density option. When activated, the A(IR) and PA(IR) input parameters (below) must be input to provide the BSF level density 'a' and pairing 'Δ' parameters;
  - = 2 to use the Ignatyuk level density formulation.
- ISIG2** Set ISIG2 = 1 to use  $\sigma^2$  (spin cutoff parameter SIG22) from the discrete level region, linearly interpolated from the top of the discrete levels (ECGC) to the matching energy between the Gilbert-Cameron temperature and Fermi gas regions (EMATGC), where a continuum expression for  $\sigma^2$  is employed.
- IWFC** Set IWFC = 1 to input width-fluctuation correction factors on TAPE33 (see TAPE33 description below). Set IWFC=0 to omit width-fluctuation corrections.
- LDELGC** If LDELGC = 0: Default A(IR) are taken directly from GC tables.
- If LDELGC = 1: Default A(IR) are scaled from values from the GC tables in the same manner that A(1) [main compound nucleus] varies from the GC table values.
- If LDELGC = 2: Same as 0 except default A(IR) is scaled according to which value of the spin cutoff constant is used (Gilbert-Cameron or Reffo) so that  $\langle D_0 \rangle_{GC}$  is preserved.
- ISPCUT** Set ISPCUT = 1 to change either SCUTFTR or SDFTR from their default values of 0.146 and 1.5, respectively. See below for SCUTFTR and SDFTR definitions. Set ISPCUT=0 to use defaults.
- LGSFINT** Control for angular momentum sum in renormalizing gamma-ray strength functions to  $2\pi\langle\Gamma_\gamma\rangle/\langle D_0\rangle$ , as follows:
- = 0 to include angular momentum sum, as usual;
  - = 1 to omit angular momentum sum. This option was used for testing Kopecky-Uhl option and is not recommended for general use.
- NBAR** Number of fission barriers (maximum of 3).
- IDIAF** Diagnostic print for fission where 0(1) = off (on).
- IHFACT** IHFACT \*  $\hbar\omega$  = integration range for fission barrier (default = 5).
- KFMAX** Fine step control for fission barrier integration, subdivides integration step size by KFMAX (default = 10).
- ZAP** 1000 \* Z + A for the incident particle or projectile, where Z is atomic number and A is the (integer) mass number.
- ZAT** 1000 \* Z + A for the target nucleus.



- DE** Energy increment for the basic integration energy mesh (in MeV). A current maximum of 240 energy steps is permitted.<sup>3</sup> If the chosen value of DE is too small, the code automatically increases it to satisfy the 240-step limit.
- FSIGCN** Constant multiplier applied to all calculated quantities (default value is 1.0).
- EGS** Excitation energy of the target nucleus. If left blank, target is in its ground state.
- SPINGS** Spin of the target nucleus. If left blank, the spin is taken from the value in the mass table (TAPE13).
- PARGS** Parity of the target nucleus. If left blank, the spin is taken from the value in the mass table (TAPE13).
- SCUTFTR** Spin cutoff constant, e.g., 0.0888 for original Gilbert-Cameron value or 0.146 for the Facchini and Saetta-Menichella value. The default value is 0.146.
- SDFTR** Control for integration over the spin distribution for continuum level densities:
- SDFTR = Negative to use old method of determining  $J_{max}$  from YRAST continuum formula (maximum spin at a given  $E_{\gamma}$ ).
- SDFTR = Positive to integrate to an upper limit of  $J_{max} = SDFTR * \langle J \rangle_{mean}$ .
- SDFTR = 0. to set default of SDFTR = 1.5.
- OLDGC** Set OLDGC = 1.0 to force use of the old method of level matching whereby the cumulative number of levels is determined in an integral from  $-\infty$  to excitation energy ECGC(IR). Set OLDGC = 0. or blank otherwise.
- NELAB** Number of incident neutron energies included in the calculation (maximum of 50).<sup>3</sup>
- ELABS(N)** Incident particle laboratory energies in MeV for the calculation.
- ZACN(I)**  $1000 * Z + A$  for each compound nucleus that is permitted to decay. (I is the index that specifies the decaying compound nucleus.)
- XNIP(I)** Number of decay channels included for compound nucleus ZACN(I). The minimum value is 1, and the maximum is currently 5.<sup>4</sup> The fixed-point value of XNIP(I) is NIP in the code, and the decay index IP runs from IP = 1 to NIP for each compound nucleus. IP = 1 must correspond to gamma-ray decay. Also IP = 1, IP = 2 should correspond to elastic scattering.
- SWS(I)** Value of the (experimental) gamma-ray strength function for s-wave neutrons,  $2\pi\langle\Gamma_{\gamma}\rangle/\langle D_0\rangle$ , that is used to normalize the gamma-ray transition probabilities, as follows:

<sup>3</sup> See footnote 1.

<sup>4</sup> See footnote 1.

SWS = + to individually normalize the E1, M1, E2, etc., components of the gamma-ray strength function, using the inputted RE1(MP) values to divide SWS into individual components. In this case, the inputted RE1(MP) should sum to 1.

SWS = - to perform one overall normalization of the gamma-ray strength function, using the calculated absolute E1, M1, E2, etc., components to determine their relative values. Adjustments to the calculated values can be made by means of the inputted RE1(MP), which do not need to sum to 1.0 in this case.

SWS = 0 to use absolute E1, M1, E2, etc., strength functions as calculated from the model used. Again, adjustments to the calculated  $\rho_{\gamma}$  can be made with the inputted RE1(MP), which do not need to sum to 1.0 in this case.

**ZZA1(IP)**  $1000 * Z + A$  for the radiation emitted from ZACN(I) by decay into channel IP. Note that ZZA1(I) = 0 (gamma ray) is assumed in all cases. Other possible values for IP > 1 are 1, 1001, 1002, 1003, 2003, and 2004 (the maximum of IP is currently 5).<sup>5</sup> A fission channel is designated by ZZA1(IP) = 99.

**CNPI(I)** Parentage designator that indicates the previous compound nucleus index I' whose decay leads to the formation of ZACN(I).

**CNPIP(I)** Parentage designator that indicates the previous decay index IP' that leads to the formation of ZACN(I). Note that multiple values of I and IP involved in forming a given compound nucleus are indicated in 2-digit increments in CNPI(I) and CNPIP(I). For example, CNPI(I) = 20306 and CNPIP(I) = 10405 indicates that the reactions defined by I' = 2, IP' = 1; I' = 3, IP' = 4; and I' = 6, IP' = 5 all lead to the same compound nucleus, and a single state population storage buffer will be used for that compound nucleus. This feature is automatically included when input option INPOPT = -1 is used. Note that when multiple parentage is included, the most positive Q-value reaction must appear left-most in CNPI and CNPIP.

**ZA1(IR)** Same as ZZA1(IP) described above. Note that the running reaction index IR defines a unique I, IP for each reaction sequence

**XNL(IR)** Number of discrete levels to be included in the calculation for the residual nucleus formed in reaction IR. If XNL(IR) = 0, then the total number of levels input in the Level-Data File (TAPE8: see Sec. V of LA-9647) is used.

**A(IR)** Level-density parameter, a, for use in the level density formula for the residual nucleus formed by reaction IR. Set A(IR) = 0 to use built-in values [see Eq. (14) in LA-6947] for the Gilbert-Cameron or Ignatyuk formulations.

**XNLGC(IR)**, Number of discrete levels, XNLGC(IR), at upper excitation energy limit,  
**ECGC(IR)** ECGC(IR), that are matched together with the lower limit fit values of XNLGCL(IR) and ECGCL(IR) [described below] in the code to the Gilbert-Cameron (or Ignatyuk) temperature level density. If both these parameters are set equal to 0, then the total number of levels input in the Level-Data file is used. If only ECGC(IR) is 0, then ECGC(IR) is determined from level number XNLGC(IR) in the level data from TAPE8.

<sup>5</sup> See footnote 1.

**XNLGCL(IR)**, Number of discrete levels (1 = ground state) and excitation energy at lower  
**ECGCL(IR)** unit for matching the Gilbert-Cameron (or Ignatyuk) temperature level density, as described above. If both are set equal to zero, then  $XNLGCL(IR) = 3$  is used, with the appropriate **ECGCL(IR)** from the TAPE8 level data. If only **ECGCL(IR)** is zero, then **ECGCL(IR)** is similarly determined from **XNLGCL(IR)**. If either **XNLGCL(IR)** or **ECGCL(IR)** is set negative, then the old method of matching to only **XNLGC** and **ECGC** is used; that is, it is assumed that  $XNLGCL(IR) = 0$ , at  $ECGCL(IR) = -\infty$ .

**XMESH(IR)** This is a parameter to increase the integration accuracy for low-particle emission energies in the continuum. If a non-zero, positive value is specified, then the top few (**KSPLIT**) bins in the residual nucleus reached in this reaction will be subdivided into smaller increments, each of width  $DE/XMESH(IR)$ . Thus, if  $XMESH(IR) = 10$ , then the affected bins in the residual nucleus will be divided into 10 smaller parts. This is especially useful around reaction thresholds that show a rapid rise in cross sections. This feature is only used for particle channels and in practice is only important for neutron channels.

**EOIN(IR)**  $E_0$  parameter in Gilbert-Cameron temperature level density function  $\rho(E) = e^{(E_x - E_0)/T}$ . If set to zero, **EOIN** is automatically determined by matching to discrete levels.

**TGCIN(IR)**  $T$  parameter in GC temperature expression (above). Determined automatically if input as zero.

**FMA1IN(IR)** Excitation energy at which Gilbert-Cameron temperature and Fermi gas level density functions are matched. Determined automatically if input as zero.

**EDS (IR)** If not left blank, then the value of **EDS(IR)** will determine the excitation energy of the highest known or available discrete level. This aids in keeping the matching energy,  $U_x$ , used between the constant temperature and Fermi-gas level density expression, from having a value less than the excitation energy of the highest discrete level.

**LMGHOL(MP)** Hollerith E or M to designate the  $MP^{th}$  radiative transition as electric or magnetic.

**LG** Multipole order of the  $MP^{th}$  transition.

**RE1(MP)** Relative strength of the  $MP^{th}$  transition. Set  $RE1(MP) = 0$  to use a built-in value. The summation of the **RE1(MP)** values should normally be unity when **SWS** is positive, i.e., the individual E1, M1, E2, etc. contributions are determined from the inputted **RE1(MP)**. If **SWS** is zero or negative, then the **RE1(MP)** should be (nominally) 1.0 to use absolute calculated or inputted E1, M1, E2, etc. strength functions. In the case of negative **SWS**, an overall normalization is done but the relative contributions of the  $fxl$  are determined from the absolute  $fxl$ . In both the latter cases the **RE1(MP)** can be used for minor adjustments of the absolute values, i.e., they are nominally 1.0 but one could be, e.g., 0.9 for a 10% decrease.

- GGDNORM(MP)** Normalization factor to be used with the gamma-ray strength function for the  $MP^{\text{th}}$  transition in the ZACN(I) compound nucleus if a zero value of SWS(I) is input. [Normally these normalization factors are determined in an initial run with ABS[SWS(I)] set equal to the experimental value for  $2\pi\langle\Gamma_\gamma\rangle/\langle D_0\rangle$ ]. When SWS is positive, the individual GGDNORM(MP) are in general different because each strength function is normalized according to the inputted RE1(MP). For negative SWS, only one overall normalization is obtained and the relative contributions are obtained from the inputted or calculated strength function values. If SWS(I) = 0., then the inputted values of GGDNORM(MP) are used to multiply the absolute values of the default strength functions. If both SWS(I) and GGDNORM(MP) are zero, then the GGDNORM(MP) are set equal to one, i.e., the default strength functions are used without adjustment.
- EG1,GG1** If LGROPT = 2 (Brink-Axel form) or 3 (Kopecky-Uhl), then these are the positions and widths of the giant dipole resonance (GDR). These must be provided since a default is not used.
- EG2,GG2, G2NORM** For deformed nuclei, these represent the position, width, and strength (relative to the first GDR) of a second giant dipole resonance. That is, G2NORM is given by the ratio  $\sigma_{m2}/\sigma_{m1}$  of the Lorentz photoneutron cross sections in the Berman tables.
- EG3,GG3, G3NORM** Position, width, and strength (relative to the first giant dipole resonance) of a possible "pygmy" resonance lying below the position of the main giant dipole resonance.
- SIGE1** SIGE1 is the E1 giant dipole resonance photoneutron cross section associated with the first peak of the Lorentzian (i.e.,  $\sigma_{m1}$  in the Berman tables). It is used in the preequilibrium (Chadwick) calculation of the direct-semidirect capture cross section, as well as in obtaining the absolute E1 gamma-ray strength function. If set to zero in the input, a default value of 0.3 b is used.
- EGCONM1** Energy in MeV below which the M1 giant dipole resonance strength function is constant. Set EGCONM1 to a large value (e.g.,  $\geq 50$  MeV) for constant M1 strength function (Weisskopf approximation).
- EGCON** Gamma energy below which the  $\gamma$ -ray E1 giant dipole resonance strength function is assumed constant (LGROPT=2 only).
- GDSTEP** This represents the step decrease that can be applied to the giant dipole resonance tail between gamma-ray energies of GDELS and GDELSL (LGROPT=2 only). For instance, a GDSTEP of 0.1 would result in a 10% reduction in the strength function at all gamma-ray energies between  $E_\gamma = \text{GDELSL}$  and  $E_\gamma = \text{GDELS}$ .
- GDELS, GDELSL** Upper and lower range of  $\gamma$ -ray energies to which the reduction specified by GDSTEP is applied (LGROPT=2 only).
- GDEDELE** For cases where GDSTEP > 0., GDEDELE defines the energy range over which the step rises to its full value (LGROPT=2 only). That is, the step increases linearly from 0 to GDSTEP as the gamma-ray energy decreases from GDELS + GDEDELE to GDELS. The default value for GDEDELE is 1 MeV.

**XNFE1** Set  $XNFE1 = 0$ . to use Brink-Axel giant dipole resonance model to calculate gamma-ray strength functions. If  $XNFE1 > 0$ ., then tabulated gamma-ray strength function at  $IFIX(XNFE1)$  energies is read from TAPE33. See TAPE33 description below (LGROPT=2 only).

**SIGM1** SIGM1 is the photoneutron cross section associated with a Lorentzian parameterization of the M1 gamma-ray strength function. It is used in obtaining an absolute M1 gamma-ray strength function. If set to zero in the input, a default value of 0.001 b is used.

**F2** The normalization factor (divided by 100) used with the Kalbach preequilibrium model. F2 usually has a value between 1.3 and 1.6.

**GG** The composite nucleus state density constant used in the preequilibrium model and generally defined as  $A/13$  or  $6a/\pi^2$ , where  $a$  is the level density parameter for the relevant residual nucleus.

**GR** State density constants for the residual nuclei appearing in the decay of the first compound nucleus. If left blank, then  $A/13$  will be used. Can also be related to the Gilbert-Cameron level density parameter,  $a$ , by  $g = 6a/\pi^2$ . Note:

GR(1) → neutron  
GR(2) → proton  
GR(3) →  $\alpha$  particle

GR(4) → deuteron  
GR(5) → triton  
GR(6) →  $^3\text{He}$  particle

**EBAR(II,N)** Fission barrier heights in MeV.

**XBOM(II,N)**  $\hbar\omega$ 's for each fission barrier.

**DENFAC(II,N)** Factors that directly multiply the level density at each barrier to account for symmetries.

**FSTS(II)** Number of fission transition states to be used at each barrier. Set  $FSTS(II) > 0$ . to read in the actual states and assume the spectra are identical at each barrier. Set  $FSTS(II) < 0$ . to read in the bandhead information and then code constructs the transition states.

**ERFIS(II)** Moment of inertia parameter used to construct transition states with the given bandhead information.

**EBBF, XJPIF** When transition states are read in, these specify the energy, spin, and parity for each state (sign of XJPIF is parity).

**IBAND** Number of bandheads for which bandhead information is read in.

**EBAND, XJPIBA, PIBI** Bandhead energy, spin, and parity for each bandhead read in.

APPENDIX 5

n + <sup>93</sup>Nb PROBLEM SAMPLE INPUT

RECORD

NO	DATA	COMMENTS
1	n + nb-93 calculation - gn5cp0b tcnbtr nblevtr t33nbtr	Descriptive information
2	gnipnb2 14-MeV Test Calc for IAEA - Kopecky gsf TITLE(N), N+1,20	
3	1 0 0 3 1 1 0 0 IPRTLEV, IPRTTC, IPRTWID, IPRTSP, IPRTGC, IPRE, IGANCAS, ILD	Print flags
4	-1 0 0 0 0 00 0 0 0 0 0 0 0 0 INPOPT, KLIN, KTIN, NIBD, LMAXOPT, NLDIR, ILDIN, LPDECAY, KSPLIT, LPOP, IHELV, IQBETA1, ISURF, ISBADD	Input option flag, no. of direct levels read from TAPE33. etc.
5	8 3 3 1 0 0 0 00 0 1 0 1 NI, NMP, LGROPT, LPEQ, NJMAX, ICAPT, IFIS, IBSF, ISIG2, IWFC, LDELGC, ISPCUT	No. of comp'd nuclei, no. of $\gamma$ -ray multipolarities, $\gamma$ -ray transmission coef, option, preequilibrium flag, etc.
6	1. 41093. 1.00 ZAP, ZAT, DE	Incident particle and target specification.
7	0.0888 0. 0. SCUTFTR, SDFTR, OLDGC	Spin cutoff constant specification.
8	+01 NELAB	No. incident energies
9	14. 0.0 0.0 0.0 0.0 0.0 ELABS(N), N=1, NELAB	Incident energies.

414

APPENDIX 5 (CONT'D)

RECORD NO	DATA						COMMENTS
10	41094.	4.	-0.0118	1.	1001.	2004.	First CN and its decays.
11	41093.	4.	-0.0	1.	1001.	2004.	Second CN and its decays.
12	41092.	4.	-0.0	1.	1001.	2004.	Third CN and its decays.
13	40093.	4.	-0.0	1.	1001.	2004.	Fourth CN and its decays.
14	40092.	4.	-0.0	1.	1001.	2004.	Fifth CN and its decays.
15	40091.	4.	-0.0	1.	1001.	2004.	Sixth CN and its decays.
16	39090.	4.	-0.0	1.	1001.	2004.	Seventh CN and its decays.
17	39089.	4.	-0.0	1.	1001.	2004.	Eighth CN and its decays.
	ZACN(I), XNIP(I), SWS(I), [ZZA1(IP), IP=2, NIP]						
18		e1 0.0000	0.0000				E1 gamma ray: defaults used.
19		m1 0.00000	0.0000				M1 gamma ray: defaults used.
20		e2 0.00000	0.0000				E2 gamma ray: defaults used.
	LMGHOL(MP), LG, RE1(MP), GGDNORM(MP)						
21	16.59	5.05	0.0	0.0	0.0	0.0	GDR shape parameters.
	EG1,	GG1,	EG2,	GG2,	G2NORM,	EG3	
22	0.2	0.0	0.0	0.0	0.0	0.0	GDR E1 photoneutron cross section, more shape parameters
	SIGB1,	SIGM1,	EGCON,	GDSTEP,	GDELS,	GDELSSL	
23	1.35	7.15	0.00	0.00	0.00	0.00	Preequilibrium norm and composite system state density.
	F2,	GG,	[GR(M), M=1, 6]				

## APPENDIX 6

### TAPE33 INPUT DESCRIPTION

A. Case where XNFE1 > 0.

Read (\*) (EFE1(I), FE1(I), I = 1, IFIX(XNFE1))

where:

XNFE1 = number of entries in table (see App. 4).

EFE1(I), FE1(I) = table of  $\gamma$ -ray energies and E1 relative  $\gamma$ -ray strength function values.

B. Case where NLDIR > 0.

Read (\*) (ELDIR(J), J = 1, NLDIR)

Read (\*) NEDD

Read (\*) EMSHD(J), J = 1, NEDD)

DO J = 1, NLDIR

READ (\*) (XSD(I,J), I = 1, NEDD)

END Loop

where:

NLDIR = number of direct reaction levels to be read. See App. 4 for details. Note that if NLDIR > 100 (that is, for coupled-channel data), then NLDIR = NLDIR - 100.

ELDIR (J) = excitation energies of levels for which direct cross sections will be read (start with ground state and skip no levels--read zeros if necessary).

NEDD = number of incident particle energies for which direct cross sections are read.

EMSHD(J) = incident energy mesh over which direct cross sections are supplied.

XSD(I,J) = direct reaction cross sections read for each level (J) and incident energy (I).



C. Case where IWFC > 0

Read (\*) NEWFC

```
DO I = 1, NEWFC
  Read (*) EWFC(I), (WFC1(I,IID), IID = 1,7)
END Loop
```

```
DO I = 1, NEWFC
  Read (*) EWFC'(I), (WFC2(I,IID), IID = 1,7)
END Loop
```

where:

NEWFC = number of incident energies for reading width-fluctuation corrections.

EWFC(I) = incident energy mesh over which width-fluctuation corrections are read.

WFC1(I,IID) = ratio of  $\sigma_{\text{corrected}}/\sigma_{\text{uncorrected}}$  for ground-state reactions with IID = 1 (neutrons), = 2 (protons) = 3 (deuterons), = 4 (tritons) = 5 ( $^3\text{He}$ ), = 6 (alphas), = 7 (gamma rays).

WFC2(I,IID) = same as WFC1 except for reactions leaving the residual nucleus in excited states. Note that zeros for both WFC1 and WFC2 are converted to 1.0.

APPENDIX 7

SELECTED PORTIONS OF MAIN OUTPUT FILE FROM  $n + {}^{93}\text{Nb}$  CALCULATION

1. Input Print Section

A. Mass File (TAPE13) Description

MASS DATA INPUT TO SUBROUTINE ENERGY  
Masses based on Wapstra 1986 and Moller-Nix 1986 merged files, as obtained  
from D. Madland (files MASS86 and MN86, respectively). Spin, parities from  
BCDGRD3 and Nuclear Wallet Cards. Date 10/25/88. Total entries 4795.

B. Input File Information

$n + \text{Nb-93}$  calculation - gn5cp0b tcnbtr nblevtr t33nbtr  
gnipnb2 14-MeV Test Calc for IAEA - Kopecky gsf

the date and time of this calculation are 11/06/91 16:20:32  
GNASH Version and Date: GN5X0b, 1 Nov. 1991 - Version for Trieste (3/92) course.

iprtlev= 1 iprttc= 0 iprtwid= 0 iprtsp= 3 iprtgc= 1 ipre= 1 igamcas= 0  
inpopt=-1 klin= 8 ktin=10 nibd= 0 lmaxopt= 0 iseadd= 0

nldir= 0 ildin= 0 ild= 0 lpop= 0  
lpdecay = 0 (0 = on, 1 = off) ksplite = 5 ihelv = 0 iqbeta1= 0 isurf= 0 ibeoff= 0  
ibsf= 0 isig2= 0 iwfc= 1 ldelgc= 0 ispcut= 1 lgsfint= 0  
number of lcm buffers is 10

maximum number of energy bins is 100  
approximate storage requirements for 1-, 2-, 3-dimensional variables in common = 4611 33094 187616  
total storage requirements of common variables = 225321

nldim= 10 nipdim= 6 njdim= 40 nkdim= 100 nldim= 36 niddim= 7 nlevdim= 60  
needim= 38 ngrdim= 100 nmpdim= 6 nfedim= 25 nfissn=10 nibdim= 10 nfaccim= 51  
nupdim= 40 neddim= 40 ks= 35

ni= 8 nmp= 3 lgropt= 3 lpeq= 1 njmax= 40 icapt= 0  
jrst level increment = 0

zap= 1. zat=41093. de= 1.000 mev xmt= 92.90638 amu sp= 7.229 mev ecutoff= 0.10 mev  
acn= 0.000 /mev fsigcn= 1.000 defcn=0. spint = 4.5 pit= 1.  
scutftr= 0.08880 sdftr= 1.50 ioldgc= 0

incident energies (mev) = 1.400e+01

1. Input Print Section (cont'd)

C. Reaction Labeling, Reaction Parentage, Masses, Buffer Numbers

i	zacr	nip	parent	s-wave	ip	ir	zal	za2	xmr	s	nlev	def	a	nlgc	edge	buffer
---	---	---	(line 2)	strength, energy	---	---	---	---	(amu)	(mev)	---	---	(/mev)	---	(mev)	number
1	41094.	4.		-1.180e-02 7.229												
i=			1. ip=	1.	1	1	0.	41094.	93.907	0.000	0.	0.0.000		0.	0.000	1
					2	2	1.	41093.	92.906	7.229	0.	0.0.000		0.	0.000	
					3	3	1001.	40093.	92.906	6.537	0.	0.0.000		0.	0.000	
					4	4	2004.	39090.	89.907	2.305	0.	0.0.000		0.	0.000	
2	41093.	4.		0.000e+00 8.830												
i=			1. ip=	2.	1	5	0.	41093.	92.906	0.000	0.	0.0.000		0.	0.000	
					2	6	1.	41092.	91.907	8.830	0.	0.0.000		0.	0.000	
					3	7	1001.	40092.	91.905	6.042	0.	0.0.000		0.	0.000	5
					4	8	2004.	39089.	88.906	1.933	0.	0.0.000		0.	0.000	8
3	41092.	4.		0.000e+00 7.883												
i=			2. ip=	2.	1	9	0.	41092.	91.907	0.000	0.	0.0.000		0.	0.000	3
					2	10	1.	41091.	90.907	7.883	0.	0.0.000		0.	0.000	0
					3	11	1001.	40091.	90.906	5.847	0.	0.0.000		0.	0.000	6
					4	12	2004.	39088.	87.910	4.582	0.	0.0.000		0.	0.000	0
4	40093.	4.		0.000e+00 6.734												
i=			1. ip=	3.	1	13	0.	40093.	92.906	0.000	0.	0.0.000		0.	0.000	4
					2	14	1.	40092.	91.905	6.734	0.	0.0.000		0.	0.000	5
					3	15	1001.	39092.	91.909	9.576	0.	0.0.000		0.	0.000	0
					4	16	2004.	38089.	88.907	3.334	0.	0.0.000		0.	0.000	0
5	40092.	4.		0.000e+00 8.635												
i=			204. ip=	302.	1	17	0.	40092.	91.905	0.000	0.	0.0.000		0.	0.000	5
					2	18	1.	40091.	90.906	8.635	0.	0.0.000		0.	0.000	6
					3	19	1001.	39091.	90.907	9.397	0.	0.0.000		0.	0.000	0
					4	20	2004.	38088.	87.906	2.966	0.	0.0.000		0.	0.000	0
6	40091.	4.		0.000e+00 7.195												
i=			305. ip=	302.	1	21	0.	40091.	90.906	0.000	0.	0.0.000		0.	0.000	6
					2	22	1.	40090.	89.905	7.195	0.	0.0.000		0.	0.000	0
					3	23	1001.	39090.	89.907	8.694	0.	0.0.000		0.	0.000	7
					4	24	2004.	38087.	86.909	5.443	0.	0.0.000		0.	0.000	0
7	39090.	4.		0.000e+00 6.857												
i=			106. ip=	403.	1	25	0.	39090.	89.907	0.000	0.	0.0.000		0.	0.000	7
					2	26	1.	39089.	88.906	6.857	0.	0.0.000		0.	0.000	8
					3	27	1001.	38089.	88.907	7.567	0.	0.0.000		0.	0.000	0
					4	28	2004.	37086.	85.911	6.170	0.	0.0.000		0.	0.000	0
8	39089.	4.		0.000e+00 11.480												
i=			207. ip=	402.	1	29	0.	39089.	88.906	0.000	0.	0.0.000		0.	0.000	8
					2	30	1.	39088.	87.910	11.480	0.	0.0.000		0.	0.000	0
					3	31	1001.	38088.	87.906	7.075	0.	0.0.000		0.	0.000	0
					4	32	2004.	37085.	84.912	7.964	0.	0.0.000		0.	0.000	0

## 2. Gamma-Ray Strength Functions

START OF SPECTRA SUBROUTINE

Time From Start Of This Energy = 0.007 Sec. Total Elapsed Time = 5.164 Sec.

+++ gilcam subroutine unable to match discrete levels with level density function for residual nucleus in reaction ir = 15 +++

+++ gilcam subroutine unable to match discrete levels with level density function for residual nucleus in reaction ir = 22 +++

START OF I = 1 LOOP IN SUBROUTINE SPECTRA

Time From Start Of This Energy = 0.086 Sec. Total Elapsed Time = 5.243 Sec.

jmaxcn = 16

sigrtot= 1.7559e+00 sigdwba= 0.0000e+00 sigcn= 1.7559e+00 ratcndw= 1.0000e+00

Gamma-Ray Strength Function Normalization: i= 1 lgropt= 3 lgsfint= 0

Radiation	RE1	Constant	Strngth Funct
e1	1.0000e+00	2.5536e+00	3.5862e-03
m1	1.0000e+00	2.5536e+00	7.3044e-04
e2	1.0000e+00	2.5536e+00	3.0438e-04

EXP. SWS(i) = -1.1800e-02 GNASH SWS = 4.6210e-03 NORMALIZED SWS = 1.1800e-02

GIANT DIPOLE RESONANCE PARAMETERS USED IN CALCULATIONS:

RADIATION	EGR	GGR	SIGPHOTN
E1	16.5900	5.0500	2.000e-01
E1	0.0000	0.0000	0.000e+00
E1	0.0000	0.0000	0.000e+00
M1	9.0202	4.0000	1.000e-03
E2	13.8603	4.9831	2.148e-03

### 3. Preequilibrium Cross Sections

spectra after preequilibrium for id = 1

i	e (mev)	preequil (b/mev)	mod equil (b/mev)	total (b/mev)
1	1.000	0.7574e-01	0.4102e+00	0.4860e+00
2	2.000	0.8790e-01	0.2260e+00	0.3139e+00
3	3.000	0.8704e-01	0.1317e+00	0.2187e+00
4	4.000	0.7974e-01	0.6590e-01	0.1456e+00
5	5.000	0.7302e-01	0.2978e-01	0.1028e+00
6	6.000	0.6644e-01	0.1257e-01	0.7901e-01
7	7.000	0.5903e-01	0.4911e-02	0.6394e-01
8	8.000	0.5125e-01	0.1824e-02	0.5307e-01
9	9.000	0.4362e-01	0.6697e-03	0.4429e-01
10	10.000	0.3630e-01	0.2383e-03	0.3654e-01
11	11.000	0.2919e-01	0.8315e-04	0.2928e-01
12	12.000	0.2206e-01	0.3938e-05	0.2206e-01
13	13.000	0.1462e-01	0.1096e-04	0.1463e-01
14	14.000	0.6509e-02	0.1392e-05	0.6510e-02

spectra after preequilibrium for id = 2

i	e (mev)	preequil (b/mev)	mod equil (b/mev)	total (b/mev)
1	1.000	0.1418e-10	0.3724e-09	0.3866e-09
2	2.000	0.6732e-06	0.1219e-04	0.1286e-04
3	3.000	0.5373e-04	0.6181e-03	0.6718e-03
4	4.000	0.5721e-03	0.3846e-02	0.4418e-02
5	5.000	0.2363e-02	0.8525e-02	0.1089e-01
6	6.000	0.5404e-02	0.9694e-02	0.1510e-01
7	7.000	0.8165e-02	0.6718e-02	0.1488e-01
8	8.000	0.9692e-02	0.3337e-02	0.1303e-01
9	9.000	0.1011e-01	0.1342e-02	0.1145e-01
10	10.000	0.9733e-02	0.4437e-03	0.1018e-01
11	11.000	0.8879e-02	0.1240e-03	0.9003e-02
12	12.000	0.7546e-02	0.2720e-04	0.7573e-02
13	13.000	0.5891e-02	0.2746e-05	0.5894e-02
14	14.000	0.3882e-02	0.5367e-06	0.3883e-02
15	15.000	0.7203e-03	0.4400e-06	0.7207e-03

spectra after preequilibrium for id = 6

i	e (mev)	preequil (b/mev)	mod equil (b/mev)	total (b/mev)
1	1.000	0.0000e+00	0.0000e+00	0.0000e+00
2	2.000	0.0000e+00	0.0000e+00	0.0000e+00
3	3.000	0.0000e+00	0.0000e+00	0.0000e+00
4	4.000	0.2509e-11	0.8708e-10	0.8959e-10

5	5.000	0.1119e-08	0.3050e-07	0.3161e-07
6	6.000	0.7238e-07	0.1465e-05	0.1537e-05
7	7.000	0.1545e-05	0.2149e-04	0.2304e-04
8	8.000	0.1661e-04	0.1456e-03	0.1622e-03
9	9.000	0.1103e-03	0.5559e-03	0.6600e-03
10	10.000	0.4846e-03	0.1314e-02	0.1399e-02
11	11.000	0.1565e-02	0.2137e-02	0.3021e-02
12	12.000	0.2542e-02	0.1647e-02	0.4189e-02
13	13.000	0.3342e-02	0.9843e-03	0.4326e-02
14	14.000	0.3588e-02	0.4565e-03	0.4044e-02
15	15.000	0.3234e-02	0.1720e-03	0.3406e-02
16	16.000	0.2529e-02	0.5446e-04	0.2583e-02
17	17.000	0.1643e-02	0.5196e-05	0.1648e-02
18	18.000	0.8043e-03	0.6338e-05	0.8106e-03
19	19.000	0.2277e-03	0.1935e-05	0.2297e-03

START OF I = 2 LOOP IN SUBROUTINE SPECTRA  
Time From Start Of This Energy = 0.655 Sec. Total Elapsed Time = 5.812 Sec.

Gamma-Ray Strength Function Normalization: i= 2 lgropt= 3 lgsfint= 0

•  
•  
•

Average Gamma Energy\*\*2.5 = 7.62071e+00 MeV\*\*2.5  
Gamma Fraction Above 5 MeV = 0.01320

**4. Preequilibrium Ratios**

pe fract bin energies	1.000	2.000	3.000	4.000	5.000	6.000	7.000	8.000	9.000	10.000
neutron	5.990e-02	1.492e-01	2.591e-01	4.319e-01	6.823e-01	8.409e-01	9.232e-01	9.656e-01	9.849e-01	9.935e-01
	9.972e-01	9.972e-01	9.972e-01	9.972e-01	9.972e-01					
proton	1.961e-05	1.047e-02	3.799e-02	1.109e-01	2.025e-01	3.488e-01	5.451e-01	7.433e-01	8.826e-01	9.564e-01
	9.862e-01	9.964e-01	9.964e-01	9.964e-01	9.964e-01	9.964e-01				
alpha	0.000e+00	0.000e+00	0.000e+00	4.286e-06	8.769e-05	7.072e-04	3.442e-03	3.925e-02	9.842e-02	2.042e-01
	3.876e-01	6.008e-01	7.725e-01	8.871e-01	9.495e-01	9.789e-01	9.789e-01	9.789e-01	9.789e-01	9.789e-01

END OF I LOOP IN SUBROUTINE SPECTRA  
Time From Start Of This Energy = 3.074 Sec. Total Elapsed Time = 8.231 Sec.

## 5. Binary Integrated Cross Sections

n + nb-93 calculation - gn5cp0b tcnbtr nblevtr t33nbtr  
gnipnb2 14-MeV Test Calc for IAEA - Kopecky gsf

lab neutron energy = 1.4000e+01 mev  
 total x/s (barns) = 4.0771e+00  
 elast. x/s (barns) = 2.3260e+00  
 nonelastic x/s (barns) = 1.7511e+00  
 total reaction x/s (barns) = 1.7565e+00  
 shape elastic x/s (barns) = 2.3206e+00  
 compd elastic x/s (barns) = 5.4055e-03  
 direct reaction x/s (barns) = 0.0000e+00  
 compd reaction x/s (barns) = 1.7565e+00  
 radiat. capture x/s (barns) = 5.0491e-03  
 semidir capture x/s (barns) = 8.1679e-04  
 discrete inelas x/s (barns) = 3.7795e-02

TAPE10 (Spherical Optical Model)  
 TAPE10 shape el. x/s + GNASH com. el. x/s  
 TAPE10 react. x/s - GNASH com. elas. x/s  
 TAPE10  
 TAPE10  
 GNASH  
 (Nothing input on TAPE33)  
 TAPE10 total react. x/s - direct reac. x/s  
 Not applicable (ICAPT = 0)  
 Direct-semidirect calculation  
 GNASH

binary reaction summaries (compound nucleus only)

reaction product	sigma (barns)	
reaction	1.7559e+00	GNASH only
gammaray	4.2323e-03	
neutron	1.6719e+00	
proton	6.5615e-02	
helium-4	1.4192e-02	

----- pre-equilibrium summary -----

ip = 2 id = 1 outgoing particle = neutron  
 initial exciton number = 3 preq normalization = 5.00000e-04  
 compound x-sec(barns) = 8.83916e-01 preeq x-sec(barns) = 7.32454e-01

ip = 3 id = 2 outgoing particle = proton  
 initial exciton number = 3 preq normalization = 5.00000e-04  
 compound x-sec(barns) = 3.46911e-02 preeq x-sec(barns) = 7.30150e-02

ip = 4 id = 6 outgoing particle = helium-4  
 initial exciton number = 3 preq normalization = 5.00000e-03  
 compound x-sec(barns) = 7.50336e-03 preeq x-sec(barns) = 2.00869e-02

# 6. Individual Reaction Emission Spectra

spectra from individual reactions

	zacr=41094	zacr=41094	zacr=41094	zacr=41094	zacr=41093	zacr=41093	zacr=41093	zacr=41093	zacr=41092	zacr=41092
	zal= 0	zal= 1	zal= 1001	zal= 2004	zal= 0	zal= 1	zal= 1001	zal= 2004	zal= 0	zal= 1
	za2=41094	za2=41093	za2=40093	za2=39090	za2=41093	za2=41092	za2=40092	za2=39099	za2=41092	za2=41091
	sigma	sigma	sigma	sigma	sigma	sigma	sigma	sigma	sigma	sigma
	(barns)	(barns)	(barns)	(barns)	(barns)	(barns)	(barns)	(barns)	(barns)	(barns)
level decay c/s=	1.32556-7	0.00000-0	0.00000+0	0.00000+0	5.22922-1	0.00000+0	0.00000+0	0.00000+0	1.53579-8	0.00000+0
level excit c/s=	1.91602-7	4.32009-2	1.04975-2	2.68803-3	9.50230-1	5.40385-1	2.51032-3	2.11460-3	2.71971-8	0.00000+0
total prod. c/s=	5.17056-3	1.61637+0	1.07706-1	2.75902-2	1.28032+0	1.18394+0	2.81466-3	2.20764-3	2.30943+0	0.00000+0
avg.energy (mev)	9.52305+0	3.54085+0	8.44629+0	1.33629+1	2.04948+0	1.35163+0	4.37403+0	6.95636+0	1.25661+0	0.00000+0
k	energy (mev)	sigma (b/mev)	sigma (b/mev)	sigma (b/mev)	sigma (b/mev)	sigma (b/mev)	sigma (b/mev)	sigma (b/mev)	sigma (b/mev)	sigma (b/mev)
1	1.00000	3.65114-5	4.85984-1	3.8662-10	0.00000+0	6.04835-1	7.51555-1	7.22566-7	0.00000+0	1.63397-0
2	2.00000	1.45520-4	3.13903-1	1.26615-5	0.00000+0	2.51869-1	2.72429-1	5.14191-5	0.00000+0	4.09269-1
3	3.00000	2.51728-4	2.18710-1	6.71825-4	0.00000+0	2.07668-1	1.16799-1	7.42388-4	3.02732-9	1.97184-1
4	4.00000	3.23787-4	1.45644-1	4.41842-3	8.9586-11	1.12664-1	3.89312-2	7.38862-4	5.77493-7	5.72896-2
5	5.00000	3.71382-4	1.02801-1	1.08882-2	3.16140-8	5.64009-2	4.22537-3	7.80782-4	1.26791-5	6.71657-3
6	6.00000	4.08206-4	7.90089-2	1.50981-2	1.53742-6	2.69978-2	0.00000+0	3.92857-4	1.00705-4	0.00000+0
7	7.00000	4.36704-4	6.39373-2	1.48828-2	2.30398-5	1.18668-2	0.00000+0	9.66599-5	4.25744-4	0.00000+0
8	8.00000	4.63333-4	5.30733-2	1.30291-2	1.62188-4	6.43261-3	0.00000+0	1.09676-5	2.61039-4	0.00000+0
9	9.00000	4.28213-4	4.42945-2	1.14539-2	6.66213-4	1.37203-3	0.00000+0	0.00000+0	4.54398-4	0.00000+0
10	10.00000	3.58961-4	3.65360-2	1.01771-2	1.79882-3	1.04521-4	0.00000+0	0.00000+0	5.74975-4	0.00000+0
11	11.00000	3.05302-4	2.92776-2	9.00177-3	3.70207-3	5.01149-5	0.00000+0	0.00000+0	3.35605-4	0.00000+0
12	12.00000	2.67047-4	2.20638-2	7.57308-3	4.18896-3	2.80156-5	0.00000+0	0.00000+0	4.19143-5	0.00000+0
13	13.00000	2.38743-4	1.46266-2	5.89423-3	4.32617-3	8.65087-6	0.00000+0	0.00000+0	0.00000+0	0.00000+0
14	14.00000	2.20218-4	6.51042-3	3.88251-3	4.04403-3	9.51975-7	0.00000+0	0.00000+0	0.00000+0	0.00000+0
15	15.00000	2.10896-4	0.00000+0	7.20721-4	3.40572-3	0.00000+0	0.00000+0	0.00000+0	0.00000+0	0.00000+0
16	16.00000	1.97704-4	0.00000+0	0.00000+0	2.58339-3	0.00000+0	0.00000+0	0.00000+0	0.00000+0	0.00000+0
17	17.00000	1.72024-4	0.00000+0	0.00000+0	1.64772-3	0.00000+0	0.00000+0	0.00000+0	0.00000+0	0.00000+0
18	18.00000	1.32718-4	0.00000+0	0.00000+0	8.10641-4	0.00000+0	0.00000+0	0.00000+0	0.00000+0	0.00000+0
19	19.00000	9.68041-5	0.00000+0	0.00000+0	2.29664-4	0.00000+0	0.00000+0	0.00000+0	0.00000+0	0.00000+0
20	20.00000	7.13414-5	0.00000+0	0.00000+0	0.00000+0	0.00000+0	0.00000+0	0.00000+0	0.00000+0	0.00000+0
21	21.00000	3.34145-5	0.00000+0	0.00000+0	0.00000+0	0.00000+0	0.00000+0	0.00000+0	0.00000+0	0.00000+0



# 6. Individual Reaction Emission Spectra (cont'd)

spectra from individual reactions

	zacr=41092 zal= 1001 za2=40091	zacr=41092 zal= 2004 za2=39068	zacr=40093 zal= 0 za2=40093	zacr=40093 zal= 1 za2=40092	zacr=40093 zal= 1001 za2=39092	zacr=40093 zal= 2004 za2=38089	zacr=40092 zal= 0 za2=40092	zacr=40092 zal= 1 za2=40091	zacr=40092 zal= 1001 za2=39091	zacr=40092 zal= 2004 za2=38088
	sigma (barns)	sigma (barns)	sigma (barns)	sigma (barns)	sigma (barns)	sigma (barns)	sigma (barns)	sigma (barns)	sigma (barns)	sigma (barns)
level decay c/s=	0.00000+0	0.00000+0	4.56551-2	0.00000+0	0.00000+0	0.00000+0	5.05764-2	0.00000+0	0.00000+0	0.00000+0
level excit c/s=	0.00000+0	0.00000+0	9.88175-2	2.33909-2	3.1381-11	2.89219-7	7.84296-2	0.00000+0	0.00000+0	4.3174-18
total prod. c/s=	0.00000+0	0.00000+0	2.02370-1	2.56031-2	3.4014-11	2.89220-7	5.26654-2	0.00000+0	0.00000+0	4.3174-18
avg.energy (mev)	0.00000+0	0.00000+0	1.65171+0	9.01371-1	2.33703+0	6.32665+0	7.97214-1	0.00000+0	0.00000+0	4.00000+0
k	energy (mev)	sigma (b/mev)	sigma (b/mev)	sigma (b/mev)	sigma (b/mev)	sigma (b/mev)	sigma (b/mev)	sigma (b/mev)	sigma (b/mev)	sigma (b/mev)
1	1.00000	0.00000+0	0.00000+0	1.08402-1	2.28511-2	1.5340-14	0.00000+0	5.09632-2	0.00000+0	0.00000+0
2	2.00000	0.00000+0	0.00000+0	4.78133-2	2.35635-3	2.2517-11	0.00000+0	1.40918-3	0.00000+0	0.00000+0
3	3.00000	0.00000+0	0.00000+0	3.23330-2	3.57272-4	1.1480-11	8.2993-11	2.30487-4	0.00000+0	0.00000+0
4	4.00000	0.00000+0	0.00000+0	9.94107-3	3.70817-5	1.5068-15	7.78587-9	5.91966-5	0.00000+0	4.3174-18
5	5.00000	0.00000+0	0.00000+0	2.95387-3	1.34657-6	0.00000+0	4.64960-8	3.27602-6	0.00000+0	0.00000+0
6	6.00000	0.00000+0	0.00000+0	7.19801-4	7.40859-9	0.00000+0	1.06292-7	3.45796-8	0.00000+0	0.00000+0
7	7.00000	0.00000+0	0.00000+0	1.81662-4	6.9349-14	0.00000+0	1.01017-7	6.7320-13	0.00000+0	0.00000+0
8	8.00000	0.00000+0	0.00000+0	2.47779-5	0.00000+0	0.00000+0	2.68057-8	0.00000+0	0.00000+0	0.00000+0
9	9.00000	0.00000+0	0.00000+0	7.47020-7	0.00000+0	0.00000+0	7.3963-10	0.00000+0	0.00000+0	0.00000+0
10	10.00000	0.00000+0	0.00000+0	1.55967-7	0.00000+0	0.00000+0	3.3469-14	0.00000+0	0.00000+0	0.00000+0
11	11.00000	0.00000+0	0.00000+0	3.38871-8	0.00000+0	0.00000+0	0.00000+0	0.00000+0	0.00000+0	0.00000+0
12	12.00000	0.00000+0	0.00000+0	2.40195-9	0.00000+0	0.00000+0	0.00000+0	0.00000+0	0.00000+0	0.00000+0
13	13.00000	0.00000+0	0.00000+0	2.4217-11	0.00000+0	0.00000+0	0.00000+0	0.00000+0	0.00000+0	0.00000+0
14	14.00000	0.00000+0	0.00000+0	4.2864-16	0.00000+0	0.00000+0	0.00000+0	0.00000+0	0.00000+0	0.00000+0
15	15.00000	0.00000+0	0.00000+0	0.00000+0	0.00000+0	0.00000+0	0.00000+0	0.00000+0	0.00000+0	0.00000+0
16	16.00000	0.00000+0	0.00000+0	0.00000+0	0.00000+0	0.00000+0	0.00000+0	0.00000+0	0.00000+0	0.00000+0
17	17.00000	0.00000+0	0.00000+0	0.00000+0	0.00000+0	0.00000+0	0.00000+0	0.00000+0	0.00000+0	0.00000+0
18	18.00000	0.00000+0	0.00000+0	0.00000+0	0.00000+0	0.00000+0	0.00000+0	0.00000+0	0.00000+0	0.00000+0
19	19.00000	0.00000+0	0.00000+0	0.00000+0	0.00000+0	0.00000+0	0.00000+0	0.00000+0	0.00000+0	0.00000+0
20	20.00000	0.00000+0	0.00000+0	0.00000+0	0.00000+0	0.00000+0	0.00000+0	0.00000+0	0.00000+0	0.00000+0
21	21.00000	0.00000+0	0.00000+0	0.00000+0	0.00000+0	0.00000+0	0.00000+0	0.00000+0	0.00000+0	0.00000+0

### 6. Individual Reaction Emission Spectra (cont'd)

spectra from individual reactions

	zacr=40091	zacr=40091	zacr=40091	zacr=40091	zacr=39090	zacr=39090	zacr=39090	zacr=39090	zacr=39090	zacr=39090
	zal= 0	zal= 1	zal= 1001	zal= 2004	zal= 0	zal= 1	zal= 1001	zal= 2004	zal= 0	zal= 1
	za2=40091	za2=40090	za2=39090	za2=38087	za2=39090	za2=39089	za2=38089	za2=37086	za2=39089	za2=39089
	sigma	sigma	sigma	sigma	sigma	sigma	sigma	sigma	sigma	sigma
	(barns)	(barns)	(barns)	(barns)	(barns)	(barns)	(barns)	(barns)	(barns)	(barns)
level decay c/s=	0.00000+0	0.00000+0	0.00000+0	0.00000+0	3.96736-2	0.00000+0	0.00000+0	0.00000+0	5.25221-3	0.00000+0
level excit c/s=	0.00000+0	0.00000+0	0.00000+0	0.00000+0	6.27506-2	4.49372-3	2.30894-8	1.2043-12	1.19570-2	0.00000+0
total prod. c/s=	0.00000+0	0.00000+0	0.00000+0	0.00000+0	7.50014-2	4.51333-3	2.30895-8	1.3892-12	5.45696-3	0.00000+0
avg.energy (mev)	0.00000+0	0.00000+0	0.00000+0	0.00000+0	1.63507+0	9.25579-1	3.08200+0	9.514+0	1.00316+0	0.00000+0
k	energy (mev)	sigma (b/mev)	sigma (b/mev)	sigma (b/mev)	sigma (b/mev)	sigma (b/mev)	sigma (b/mev)	sigma (b/mev)	sigma (b/mev)	sigma (b/mev)
1	1.00000	0.00000+0	0.00000+0	0.00000+0	4.43674-2	3.95193-3	2.1639-11	0.00000+0	4.34345-2	0.00000+0
2	2.00000	0.00000+0	0.00000+0	0.00000+0	1.37726-2	4.76426-4	2.87339-9	0.00000+0	9.35155-4	0.00000+0
3	3.00000	0.00000+0	0.00000+0	0.00000+0	9.61974-3	7.94331-5	1.57562-8	0.00000+0	6.81672-5	0.00000+0
4	4.00000	0.00000+0	0.00000+0	0.00000+0	4.50022-3	5.39036-6	4.06712-9	1.4362-14	9.51506-6	0.00000+0
5	5.00000	0.00000+0	0.00000+0	0.00000+0	1.76102-3	1.54040-7	3.6495-10	4.2163-13	6.07312-7	0.00000+0
6	6.00000	0.00000+0	0.00000+0	0.00000+0	7.23536-4	2.82176-9	6.1257-12	6.4468-13	2.47361-5	0.00000+0
7	7.00000	0.00000+0	0.00000+0	0.00000+0	2.49790-4	1.8888-11	9.1518-15	2.4420-13	3.5304-10	0.00000+0
8	8.00000	0.00000+0	0.00000+0	0.00000+0	6.63247-6	1.6096-14	0.00000+0	1.3984-14	9.5048-13	0.00000+0
9	9.00000	0.00000+0	0.00000+0	0.00000+0	3.77779-7	0.00000+0	0.00000+0	1.6629-16	0.00000+0	0.00000+0
10	10.00000	0.00000+0	0.00000+0	0.00000+0	5.63988-8	0.00000+0	0.00000+0	0.00000+0	0.00000+0	0.00000+0
11	11.00000	0.00000+0	0.00000+0	0.00000+0	6.28149-9	0.00000+0	0.00000+0	0.00000+0	0.00000+0	0.00000+0
12	12.00000	0.00000+0	0.00000+0	0.00000+0	3.0198-10	0.00000+0	0.00000+0	0.00000+0	0.00000+0	0.00000+0
13	13.00000	0.00000+0	0.00000+0	0.00000+0	1.0075-11	0.00000+0	0.00000+0	0.00000+0	0.00000+0	0.00000+0
14	14.00000	0.00000+0	0.00000+0	0.00000+0	1.3045-13	0.00000+0	0.00000+0	0.00000+0	0.00000+0	0.00000+0
15	15.00000	0.00000+0	0.00000+0	0.00000+0	2.1450-16	0.00000+0	0.00000+0	0.00000+0	0.00000+0	0.00000+0
16	16.00000	0.00000+0	0.00000+0	0.00000+0	0.00000+0	0.00000+0	0.00000+0	0.00000+0	0.00000+0	0.00000+0
17	17.00000	0.00000+0	0.00000+0	0.00000+0	0.00000+0	0.00000+0	0.00000+0	0.00000+0	0.00000+0	0.00000+0
18	18.00000	0.00000+0	0.00000+0	0.00000+0	0.00000+0	0.00000+0	0.00000+0	0.00000+0	0.00000+0	0.00000+0
19	19.00000	0.00000+0	0.00000+0	0.00000+0	0.00000+0	0.00000+0	0.00000+0	0.00000+0	0.00000+0	0.00000+0
20	20.00000	0.00000+0	0.00000+0	0.00000+0	0.00000+0	0.00000+0	0.00000+0	0.00000+0	0.00000+0	0.00000+0
21	21.00000	0.00000+0	0.00000+0	0.00000+0	0.00000+0	0.00000+0	0.00000+0	0.00000+0	0.00000+0	0.00000+0

# 6. Individual Reaction Emission Spectra (cont'd)

spectra from individual reactions

zacr=39089    zacr=39089  
 zal= 1001    zal= 2004  
 za2=38088    za2=37085

-----  
           sigma        sigma  
           (barns)      (barns)  
 level decay c/s= 0.0000+0    0.0000+0  
 level excit c/s= 2.2085-19    0.0000+0  
 total prod. c/s= 2.2085-19    0.0000+0  
 -----  
 avg.energy (mev) 7.5000-1    0.0000+0  
 -----

k	energy (mev)	sigma (b/mev)	sigma (b/mev)
1	1.00000	2.2085-19	0.0000+0
2	2.00000	0.0000+0	0.0000+0
3	3.00000	0.0000+0	0.0000+0
4	4.00000	0.0000+0	0.0000+0
5	5.00000	0.0000+0	0.0000+0
6	6.00000	0.0000+0	0.0000+0
7	7.00000	0.0000+0	0.0000+0
8	8.00000	0.0000+0	0.0000+0
9	9.00000	0.0000+0	0.0000+0
10	10.00000	0.0000+0	0.0000+0
11	11.00000	0.0000+0	0.0000+0
12	12.00000	0.0000+0	0.0000+0
13	13.00000	0.0000+0	0.0000+0
14	14.00000	0.0000+0	0.0000+0
15	15.00000	0.0000+0	0.0000+0
16	16.00000	0.0000+0	0.0000+0
17	17.00000	0.0000+0	0.0000+0
18	18.00000	0.0000+0	0.0000+0
19	19.00000	0.0000+0	0.0000+0
20	20.00000	0.0000+0	0.0000+0
21	21.00000	0.0000+0	0.0000+0

# 7. Composite Particle and Gamma-Ray Production Spectra

## composite spectra

	neutron spectrum	proton spectrum	deuteron spectrum	triton spectrum	helium-3 spectrum	helium-4 spectrum	gammaray spectrum	g.neutron spectrum
	sigma (barns)	sigma (barns)	sigma (barns)	sigma (barns)	sigma (barns)	sigma (barns)	sigma (barns)	sigma (barns)
total prod. c/s=	2.83043+0	1.10521-1	0.00000+0	0.00000+0	0.00000+0	2.97982-2	3.93031+0	0.00000+0
avg.energy (mev)	2.60963+0	8.34258+0	0.00000+0	0.00000+0	0.00000+0	1.30364+1	1.54683+0	0.00000+0
k	energy (mev)	sigma (b/mev)	sigma (b/mev)	sigma (b/mev)	sigma (b/mev)	sigma (b/mev)	sigma (b/mev)	sigma (b/mev)
1	1.00000	1.26434+0	7.22974-7	0.00000+0	0.00000+0	0.00000+0	0.00000+0	2.45192+0
2	2.00000	5.89164-1	6.42834-5	0.00000+0	0.00000+0	0.00000+0	0.00000+0	7.25234-1
3	3.00000	3.35946-1	1.41423-3	0.00000+0	0.00000+0	0.00000+0	3.11032-9	4.47355-1
4	4.00000	1.84617-1	5.15728-3	0.00000+0	0.00000+0	0.00000+0	5.85368-7	1.84787-1
5	5.00000	1.07028-1	1.16690-2	0.00000+0	0.00000+0	0.00000+0	1.27572-5	6.82077-2
6	6.00000	7.90089-2	1.54910-2	0.00000+0	0.00000+0	0.00000+0	1.02349-4	2.88494-2
7	7.00000	6.39373-2	1.49795-2	0.00000+0	0.00000+0	0.00000+0	4.48885-4	1.27349-2
8	8.00000	5.30733-2	1.30400-2	0.00000+0	0.00000+0	0.00000+0	4.23253-4	6.92736-3
9	9.00000	4.42945-2	1.14539-2	0.00000+0	0.00000+0	0.00000+0	1.12061-3	1.80137-3
10	10.00000	3.65360-2	1.01771-2	0.00000+0	0.00000+0	0.00000+0	2.37380-3	4.63694-4
11	11.00000	2.92776-2	9.00327-3	0.00000+0	0.00000+0	0.00000+0	4.03768-3	3.55457-4
12	12.00000	2.20638-2	7.57308-3	0.00000+0	0.00000+0	0.00000+0	4.23090-3	2.95065-4
13	13.00000	1.46266-2	5.89423-3	0.00000+0	0.00000+0	0.00000+0	4.32617-3	2.47394-4
14	14.00000	6.51042-3	3.88251-3	0.00000+0	0.00000+0	0.00000+0	4.04403-3	2.21170-4
15	15.00000	0.00000+0	7.20721-4	0.00000+0	0.00000+0	0.00000+0	3.40572-3	2.10896-4
16	16.00000	0.00000+0	0.00000+0	0.00000+0	0.00000+0	0.00000+0	2.58339-3	1.97704-4
17	17.00000	0.00000+0	0.00000+0	0.00000+0	0.00000+0	0.00000+0	1.64772-3	1.72024-4
18	18.00000	0.00000+0	0.00000+0	0.00000+0	0.00000+0	0.00000+0	8.10641-4	1.32718-4
19	19.00000	0.00000+0	0.00000+0	0.00000+0	0.00000+0	0.00000+0	2.29664-4	9.68041-5
20	20.00000	0.00000+0	0.00000+0	0.00000+0	0.00000+0	0.00000+0	0.00000+0	7.13414-5
21	21.00000	0.00000+0	0.00000+0	0.00000+0	0.00000+0	0.00000+0	3.34145-5	0.00000+0

## 8. Discrete Level Cross Sections

### A. Primary Capture Gamma-Ray Cross Sections

primary capture gamma ray cross sections in barns

level no	level energy	gamma energy	cross section
1	0.00000	21.07882	4.42937e-09
2	0.04095	21.03787	2.28466e-09
3	0.05872	21.02009	3.15975e-09
4	0.07869	21.00014	4.91731e-09
5	0.11340	20.96541	3.92099e-09
6	0.14035	20.93946	1.82744e-09
7	0.30161	20.77721	1.86085e-09
8	0.31185	20.76697	3.24993e-09
9	0.33417	20.74465	2.36042e-09
10	0.39627	20.68254	2.73233e-09
11	0.45021	20.62861	2.74995e-09
12	0.63166	20.44716	3.37798e-09
13	0.64092	20.43790	4.17202e-09
14	0.66574	20.41308	2.45771e-09
15	0.78493	20.29389	2.49603e-09
16	0.79294	20.28588	2.49867e-09
17	0.81784	20.26098	2.82093e-09
18	0.82090	20.25792	3.46201e-09
19	0.89574	20.18308	2.53337e-09
20	0.92400	20.15482	1.67524e-09

### B. Capture Gamma-Ray Cascade Cross Sections (Only meaningful for ICAPT-1)

i= 1 ip= 1 ir= 1 za1= 0 za2=41094 separation energy = 0.000 mev accumulated separation energy = 0.000 mev  
 number of level in residual nucleus = 20 number of gamma rays = 40 residual nucleus id =41094

level no	level energy (mev)	spin, parity	production cross section (barns)	number of transitions	final level no	final energy (mev)	transition probability	conditional probability	gamma number	gamma energy (mev)	production cross section (barns)
1	0.0000	+ 6.0	5.9047e-08	0							
2	0.0410	+ 3.0	3.7850e-08	1	1	0.0000	1.0000	1.0000	1	0.0410	3.7850e-08
3	0.0587	+ 4.0	9.9871e-09	2	1	0.0000	0.1106	1.0000	2	0.0587	1.1050e-09
					2	0.0410	0.8894	1.0000	3	0.0178	8.8822e-09
4	0.0787	+ 7.0	6.7156e-09	1	1	0.0000	1.0000	1.0000	4	0.0787	6.7156e-09
5	0.1134	+ 5.0	8.8635e-09	2	1	0.0000	0.9709	1.0000	5	0.1134	8.6053e-09
					3	0.0587	0.0291	1.0000	6	0.0547	2.5816e-10
6	0.1404	- 2.0	1.9466e-08	1	2	0.0410	1.0000	1.0000	7	0.0994	1.9466e-08
7	0.3016	- 2.0	3.4898e-09	1	6	0.1404	1.0000	1.0000	8	0.1613	3.4898e-09
8	0.3118	+ 4.0	4.2633e-09	1	3	0.0587	1.0000	1.0000	9	0.2531	4.2633e-09
9	0.3342	+ 3.0	4.8536e-09	2	2	0.0410	0.9671	1.0000	10	0.2932	4.6940e-09
					6	0.1404	0.0329	1.0000	11	0.1938	1.5960e-10
10	0.3963	- 3.0	6.2927e-09	3	2	0.0410	0.0290	1.0000	12	0.3553	1.8240e-10
					3	0.0587	0.2464	1.0000	13	0.3376	1.5504e-09
					6	0.1404	0.7246	1.0000	14	0.2559	4.5600e-09

**C. Level Excitation Cross Sections from Particle and Gamma-Ray Reactions;  
Discrete Gamma-Ray Cross Sections; Isomer Production Cross Sections**

i= 1 ip= 2 ir= 2 zal= 1 za2=41093 separation energy = 7.229 mev accumulated separation energy = 0.000 mev  
number of levels in residual nucleus = 20

level no	level energy (mev)	spin, parity	iso-spin	production cross section (barns)
1	0.0000	+ 4.5	99.0	5.4055e-03
2	0.0308	- 0.5	99.0	1.1050e-03
3	0.6870	- 1.5	99.0	5.9902e-04
4	0.7439	+ 3.5	99.0	1.1945e-03
5	0.8086	+ 2.5	99.0	8.9807e-04
6	0.8104	- 1.5	99.0	5.9337e-04
7	0.9498	+ 6.5	99.0	1.8318e-03
8	0.9789	+ 5.5	99.0	1.6664e-03
9	1.0827	+ 4.5	99.0	1.4354e-03
10	1.2537	+ 3.5	99.0	1.1520e-03
11	1.2900	- 0.5	99.0	2.8631e-04
12	1.2972	+ 4.5	99.0	1.4146e-03
13	1.3153	- 2.5	99.0	8.5343e-04
14	1.3200	- 2.5	99.0	8.5312e-04
15	1.3352	+ 8.5	99.0	1.8486e-03
16	1.3698	- 0.5	99.0	1.1941e-03
17	1.3956	+ 2.5	99.0	3.6091e-03
18	1.4834	+ 3.5	99.0	4.7560e-03
19	1.4911	+ 7.5	99.0	7.7543e-03
20	1.5001	+ 3.5	99.0	4.7503e-03

i= 1 ip= 3 ir= 3 zal=1001 za2=40093 separation energy = 6.537 mev accumulated separation energy = 0.000 mev  
number of levels in residual nucleus = 15

level no	level energy (mev)	spin, parity	iso-spin	production cross section (barns)
1	0.0000	+ 2.5	99.0	7.2072e-04
2	0.2668	+ 1.5	99.0	2.0380e-03
3	0.9471	+ 0.5	99.0	9.2682e-04
4	1.0180	+ 0.5	99.0	9.1773e-04
5	1.1685	+ 0.5	99.0	2.6657e-04

6	1.2220 +	0.5	99.0	2.6453e-04
7	1.4253 +	1.5	99.0	5.1848e-04
8	1.4504 +	1.5	99.0	5.1657e-04
9	1.4640 +	3.5	99.0	1.0565e-02
10	1.4701 +	2.5	99.0	7.8275e-04
11	1.5980 +	2.5	99.0	7.6831e-04
12	1.6500 +	1.5	99.0	5.0144e-04
13	1.8267 +	2.5	99.0	7.4266e-04
14	1.9095 +	0.5	99.0	2.3838e-04
15	1.9185 +	0.5	99.0	2.3804e-04

i= 1 ip= 4 ir= 4 zal=2004 za2=39090 separation energy = 2.305 mev accumulated separation energy = 0.000 mev  
number of levels in residual nucleus = 15

level no	level energy (mev)	spin, parity	iso- spin	production cross section (barns)
1	0.0000 -	2.0	99.0	9.9405e-05
2	0.2025 -	3.0	99.0	1.3026e-04
3	0.6820 +	7.0	99.0	2.1819e-04
4	0.7767 +	2.0	99.0	9.9026e-05
5	0.9540 +	3.0	99.0	1.3250e-04
6	1.0470 +	5.0	99.0	1.8426e-04
7	1.1900 +	4.0	99.0	1.5708e-04
8	1.2150 +	0.0	99.0	1.9574e-05
9	1.2980 +	6.0	99.0	4.8323e-04
10	1.3710 -	1.0	99.0	1.4144e-04
11	1.4170 -	3.0	99.0	3.0976e-04
12	1.5700 -	1.0	99.0	1.3779e-04
13	1.6410 -	1.0	99.0	1.3645e-04
14	1.7600 -	2.0	99.0	2.2035e-04
15	1.8130 -	2.0	99.0	2.1870e-04



i= 2 ip= 1 ir= 5 zal= 0 za2=41093 separation energy = 0.000 mev accumulated separation energy = 7.229 mev  
 number of level in residual nucleus = 20 number of gamma rays = 32 residual nucleus id =41093

level no	level energy (mev)	spin, parity	production cross section (barns)	number of transitions	final level no	final energy (mev)	transition probability	conditional probability	gamma number	gamma energy (mev)	production cross section (barns)
1	0.0000	+ 4.5	4.2741e-01	0							
2	0.0308	- 0.5	5.5461e-02	1	1	0.0000	1.0000	1.0000	1	0.0308	5.5461e-02
3	0.6870	- 1.5	1.6525e-02	1	2	0.0308	1.0000	1.0000	2	0.6562	1.6525e-02
4	0.7439	+ 3.5	6.8415e-02	1	1	0.0000	1.0000	1.0000	3	0.7439	6.8415e-02
5	0.8086	+ 2.5	3.1563e-02	2	4	0.7439	0.0123	1.0000	4	0.0647	3.8967e-04
					1	0.0000	0.9877	1.0000	5	0.8086	3.1173e-02
6	0.8104	- 1.5	2.3779e-02	1	2	0.0308	1.0000	1.0000	6	0.7796	2.3779e-02
7	0.9498	+ 6.5	1.0068e-01	1	1	0.0000	1.0000	1.0000	7	0.9498	1.0068e-01
8	0.9789	+ 5.5	3.5444e-02	1	1	0.0000	1.0000	1.0000	8	0.9789	3.5444e-02
9	1.0827	+ 4.5	2.2303e-02	2	4	0.7439	0.7937	1.0000	9	0.3388	1.7701e-02
					1	0.0000	0.2063	1.0000	10	1.0827	4.6022e-03
10	1.2537	+ 3.5	1.4483e-02	1	1	0.0000	1.0000	1.0000	11	1.2537	1.4483e-02
11	1.2900	- 0.5	2.7124e-03	2	3	0.6870	0.6653	1.0000	12	0.6030	1.8045e-03
					6	0.8104	0.3347	1.0000	13	0.4796	9.0787e-04
12	1.2972	+ 4.5	1.5956e-02	3	8	0.9789	0.2205	1.0000	14	0.3183	3.5185e-03
					4	0.7439	0.2667	1.0000	15	0.5533	4.2549e-03
					1	0.0000	0.5128	1.0000	16	1.2972	8.1826e-03

i= 2 ip= 2 ir= 6 zal= 1 za2=41092  
number of levels in residual nucleus = 20

separation energy = 8.830 mev accumulated separation energy = 7.229 mev

level no	level energy (mev)	spin, parity	iso-spin	production cross section (barns)
1	0.0000 +	7.0	99.0	1.9347e-01
2	0.1355 +	2.0	99.0	1.7726e-02
3	0.2259 -	2.0	99.0	1.8010e-02
4	0.2856 +	3.0	99.0	2.4910e-02
5	0.3574 +	5.0	99.0	5.1694e-02
6	0.3898 -	3.0	99.0	2.7278e-02
7	0.4802 +	4.0	99.0	3.2313e-02
8	0.5012 +	6.0	99.0	6.8847e-02
9	0.9751 +	0.0	99.0	1.2298e-03
10	1.0894 -	1.0	99.0	3.2063e-03
11	1.1501 -	1.0	99.0	3.0882e-03
12	1.3098 +	5.0	99.0	1.8714e-02
13	1.3240 -	2.0	99.0	5.2876e-03
14	1.3455 +	2.0	99.0	5.0643e-03
15	1.3740 +	5.0	99.0	1.7855e-02
16	1.4102 +	5.0	99.0	1.7366e-02
17	1.4144 +	3.0	99.0	7.6835e-03
18	1.4228 -	4.0	99.0	1.3055e-02
19	1.4679 +	4.0	99.0	1.1109e-02
20	1.4815 +	1.0	99.0	2.4809e-03

i= 2 ip= 3 ir= 7 zal=1001 za2=40092  
number of levels in residual nucleus = 15

separation energy = 6.042 mev accumulated separation energy = 7.229 mev

level no	level energy (mev)	spin, parity	iso-spin	production cross section (barns)
1	0.0000 +	0.0	99.0	7.0798e-04
2	0.9345 +	2.0	99.0	4.3840e-04
3	1.3828 +	0.0	99.0	3.6447e-05
4	1.4954 +	4.0	99.0	4.5113e-04
5	1.8473 +	2.0	99.0	1.0302e-04
6	2.0667 +	2.0	99.0	7.3388e-05
7	2.1500 +	5.0	99.0	2.4172e-04
8	2.3397 -	3.0	99.0	7.1828e-05

9	2.3983	+	4.0	99.0	9.9334e-05
10	2.4860	-	5.0	99.0	1.2457e-04
11	2.7435	-	4.0	99.0	4.7837e-05
12	2.8197	+	2.0	99.0	1.6958e-05
13	2.8640	+	4.0	99.0	3.9752e-05
14	2.9036	+	0.0	99.0	2.5233e-06
15	2.9095	+	5.0	99.0	5.5422e-05

i= 2 ip= 4 ir= 8 zal=2004 za2=39089  
 number of levels in residual nucleus = 13

separation energy = 1.933 mev accumulated separation energy = 7.229 mev

level no	level energy (mev)	spin, parity	iso-spin	production cross section (bar.is)
1	0.0000	- 0.5	99.0	7.5099e-04
2	0.9092	+ 4.5	99.0	1.0289e-03
3	1.5070	- 1.5	99.0	7.8035e-05
4	1.7445	- 2.5	99.0	7.4772e-05
5	2.2220	+ 2.5	99.0	3.4051e-05
6	2.5300	+ 3.5	99.0	2.7217e-05
7	2.5665	+ 5.5	99.0	6.3064e-05
8	2.6220	+ 4.5	99.0	3.4557e-05
9	2.8710	+ 3.5	99.0	1.0660e-05
10	2.8810	- 1.5	99.0	3.8300e-06
11	3.0670	- 1.5	99.0	3.0124e-06
12	3.1060	- 1.5	99.0	2.8421e-06
13	3.1380	- 1.5	99.0	2.7014e-06

i= 3 ip= 1 ir= 9 zal= 0 za2=41092 separation energy = 0.000 mev accumulated separation energy = 16.060 mev  
 number of level in residual nucleus = 20 number of gamma rays = 35 residual nucleus id =41092

level no	level energy (mev)	spin, parity	production cross section (barns)	number of transitions	final level no	final energy (mev)	transition probability	conditional probability	gamma number	gamma energy (mev)	production cross section (barns)
1	0.0000 +	7.0	1.1839e-00	0							
2	0.1355 +	2.0	4.5079e-01	1	1	0.0000	1.0000	1.0000	1	0.1355	4.5079e-01
3	0.2259 -	2.0	2.0753e-01	1	2	0.1355	1.0000	1.0000	2	0.0904	2.0753e-01
4	0.2856 +	3.0	1.6001e-01	1	2	0.1355	1.0000	1.0000	3	0.1501	1.6001e-01
5	0.3574 +	5.0	1.5255e-01	1	1	0.0000	1.0000	1.0000	4	0.3574	1.5255e-01
6	0.3898 -	3.0	1.2608e-01	3	4	0.2856	0.0096	1.0000	5	0.1042	1.2123e-03
					3	0.2259	0.9615	1.0000	6	0.1639	1.2123e-01
					2	0.1355	0.0288	1.0000	7	0.2543	3.6370e-03
7	0.4802 +	4.0	9.0950e-02	2	5	0.3574	0.2424	1.0000	8	0.1228	2.2049e-02
					4	0.2856	0.7576	1.0000	9	0.1946	6.8902e-02
8	0.5012 +	6.0	1.6942e-01	1	1	0.0000	1.0000	1.0000	10	0.5012	1.6942e-01
9	0.9751 +	0.0	2.9595e-03	1	3	0.2259	1.0000	1.0000	11	0.7492	2.9595e-03
10	1.0894 -	1.0	7.3403e-03	3	4	0.2856	0.2000	1.0000	12	0.8038	1.4681e-03
					3	0.2259	0.5405	1.0000	13	0.6635	3.9678e-03
					2	0.1355	0.2595	1.0000	14	0.9539	1.9045e-03

# 9. Level Density Parameters and Matching Results

## level density parameters

i	ip	ir	izal	iza2	a	temp	e0	ematch	ecut	levels	ecut1	levels	sig2	q	pair	d0
					(/mev)	(mev)	(mev)	(mev)	(mev)	at	ecut	at	ecut1	(mev)	(mev)	(ev)
1	1	1	C	41094	11.814	0.743	-1.443	3.741	0.9381	20.	0.0687	3.	0.000	7.2292	-0.240	8.049e+01
1	2	2	1	41093	10.758	0.956	-1.756	7.540	1.5046	20.	0.7155	3.	0.000	0.0000	0.880	1.856e+02
1	3	3	1001	40093	11.901	0.597	0.300	2.656	1.9231	15.	0.9825	3.	0.000	0.6919	0.590	1.447e+03
1	4	4	2004	39090	9.759	0.769	-0.280	3.331	1.8395	15.	0.7294	3.	0.000	4.9247	0.300	2.028e+03
2	1	5	0	41093	10.758	0.956	-1.756	7.540	1.5046	20.	0.7155	3.	0.000	0.0000	0.880	1.856e+02
2	2	6	1	41092	10.153	0.878	-1.248	5.109	1.4883	20.	0.2557	3.	0.000	-8.8305	0.270	2.490e+02
2	3	7	1001	40092	10.854	0.721	1.022	4.808	2.9124	15.	1.4391	3.	0.000	-6.0423	1.710	2.869e+02
2	4	8	2004	39089	9.365	0.996	0.619	1.597	3.1540	13.	1.6257	3.	0.000	-1.9326	1.220	4.862e+01
3	1	9	0	41092	10.153	0.878	-1.248	5.109	1.4883	20.	0.2557	3.	0.000	-8.8305	0.270	2.490e+02
3	2	10	1	41091	9.751	0.952	-0.713	6.805	2.0802	15.	1.1134	3.	0.000	-16.7135	1.190	4.463e+01
3	3	11	1001	40091	10.252	0.831	-0.098	5.314	2.4089	15.	1.6742	3.	0.000	-14.6774	1.100	4.388e+03
3	4	12	2004	39088	10.471	0.872	-1.367	5.297	1.2815	15.	0.5337	3.	0.000	-13.4128	0.290	1.237e+02
4	1	13	0	40093	11.901	0.597	0.300	2.656	1.9231	15.	0.9825	3.	0.000	0.6919	0.590	1.447e+03
4	2	14	1	40092	10.854	0.721	1.022	4.808	2.9124	15.	1.4391	3.	0.000	-6.0423	1.710	2.869e+02
4	3	15	1001	39092	11.385	0.873	0.000	0.088	0.0000	1.	*****	0.	0.000	-8.8844	-0.210	5.411e+02
4	4	16	2004	38089	10.043	1.011	0.523	1.583	3.2768	15.	1.7067	3.	0.000	-2.6423	1.250	1.298e+04
5	1	17	0	40092	10.854	0.721	1.022	4.808	2.9124	15.	1.4391	3.	0.000	-6.0423	1.710	2.869e+02
5	2	18	1	40091	10.252	0.831	-0.098	5.314	2.4089	15.	1.6742	3.	0.000	-14.6774	1.100	4.388e+03
5	3	19	1001	39091	10.352	0.784	0.000	4.541	0.0000	1.	*****	0.	0.000	-15.4398	0.910	4.107e+02
5	4	20	2004	38088	9.647	1.005	1.507	2.527	4.3125	15.	2.9763	3.	0.000	-9.0078	2.170	1.134e+02
6	1	21	0	40091	10.252	0.831	-0.098	5.314	2.4089	15.	1.6742	3.	0.000	-14.6774	1.100	4.388e+03
6	2	22	1	40090	9.850	1.100	-1.728	2.348	4.5994	15.	2.2525	3.	0.000	-21.8720	2.020	4.069e+01
6	3	23	1001	39090	9.759	0.769	-0.280	3.331	1.8395	15.	0.7294	3.	0.000	-23.3712	0.300	2.028e+03
6	4	24	2004	38087	10.734	0.775	0.892	1.599	2.9935	15.	1.0510	3.	0.000	-20.1205	1.240	1.049e+03
7	1	25	0	39090	9.759	0.769	-0.280	3.331	1.8395	15.	0.7294	3.	0.000	4.9247	0.300	2.028e+03
7	2	26	1	39089	9.365	0.996	0.619	1.597	3.1540	13.	1.6257	3.	0.000	-1.9326	1.220	4.862e+01
7	3	27	1001	38089	10.043	1.011	0.523	1.583	3.2768	15.	1.7067	3.	0.000	-2.6423	1.250	1.298e+04
7	4	28	2004	37086	10.761	0.608	0.000	0.544	0.0000	1.	*****	0.	0.000	-1.2449	0.040	5.963e+01
8	1	29	0	39089	9.365	0.996	0.619	1.597	3.1540	13.	1.6257	3.	0.000	-1.9326	1.220	4.862e+01
8	2	30	1	39088	10.471	0.872	-1.367	5.297	1.2815	15.	0.5337	3.	0.000	-13.4128	0.290	1.237e+02
8	3	31	1001	38088	9.647	1.005	1.507	2.527	4.3125	15.	2.9763	3.	0.000	-9.0078	2.170	1.134e+02
8	4	32	2004	37085	11.602	0.787	0.000	6.010	0.0000	1.	*****	0.	0.000	-9.8961	1.500	2.350e+01

9. PRINT OF LEVEL DENSITY PARAMETERS AND MATCHING RESULTS (CONT'D)

i	ip	ir	iza1	iza2	pn (mev)	pz (mev)	sn (mev)	sz (mev)	s (mev)	sac (mev)	id	sepn (mev)	spint
1	1	1	0	41094	-0.50	0.26	14.90	-16.68	0.000	0.000	7	7.2292	4.5
1	2	2	1	41093	0.62	0.26	13.81	-16.68	7.229	0.000	1	8.8305	7.0
1	3	3	1001	40093	-0.50	1.09	14.90	-16.43	6.537	0.000	2	6.7342	0.0
1	4	4	2004	39090	0.01	0.29	13.23	-16.89	2.305	0.000	6	6.8573	0.5
2	1	5	0	41093	0.62	0.26	13.81	-16.68	0.000	7.229	7	8.8305	7.0
2	2	6	1	41092	0.01	0.26	13.23	-16.68	8.830	7.229	1	7.8820	4.5
2	3	7	1001	40092	0.62	1.09	13.81	-16.43	6.042	7.229	2	8.6351	2.5
2	4	8	2004	39089	0.93	0.29	12.88	-16.89	1.933	7.229	6	11.4602	4.0
3	1	9	0	41092	0.01	0.26	13.23	-16.68	0.000	16.060	7	7.8830	4.5
3	2	10	1	41091	0.93	0.26	12.88	-16.68	7.883	16.060	1	12.0524	8.0
3	3	11	1001	40091	0.01	1.09	13.23	-16.43	5.847	16.060	2	7.1946	0.0
3	4	12	2004	39088	0.00	0.29	14.38	-16.89	4.582	16.060	6	9.3514	0.5
4	1	13	0	40093	-0.50	1.09	14.90	-16.43	0.000	6.537	7	6.7342	0.0
4	2	14	1	40092	0.62	1.09	13.81	-16.43	6.734	6.537	1	8.6351	2.5
4	3	15	1001	39092	-0.50	0.29	14.90	-16.89	9.576	6.537	2	6.5554	0.5
4	4	16	2004	38089	0.01	1.24	13.23	-16.41	3.334	6.537	6	6.3656	0.0
5	1	17	0	40092	0.62	1.09	13.81	-16.43	0.000	13.272	7	8.6351	2.5
5	2	18	1	40091	0.01	1.09	13.23	-16.43	8.635	13.272	1	7.1946	0.0
5	3	19	1001	39091	0.62	0.29	13.81	-16.89	9.397	13.272	2	7.9315	2.0
5	4	20	2004	38088	0.93	1.24	12.88	-16.41	2.966	13.272	6	11.1127	4.5
6	1	21	0	40091	0.01	1.09	13.23	-16.43	0.000	21.907	7	7.1946	0.0
6	2	22	1	40090	0.93	1.09	12.88	-16.43	7.195	21.907	1	11.9709	4.5
6	3	23	1001	39090	0.01	0.29	13.23	-16.89	8.694	21.907	2	6.8573	0.5
6	4	24	2004	38087	0.00	1.24	14.38	-16.41	5.443	21.907	6	8.4281	0.0
7	1	25	0	39090	0.01	0.29	13.23	-16.89	0.000	2.305	7	6.8573	0.5
7	2	26	1	39089	0.93	0.29	12.88	-16.89	6.857	2.305	1	11.4602	4.0
7	3	27	1001	38089	0.01	1.24	13.23	-16.41	7.567	2.305	2	6.3656	0.0
7	4	28	2004	37086	0.00	0.04	14.38	-16.22	6.170	2.305	6	8.6512	2.5
8	1	29	0	39089	0.93	0.29	12.88	-16.89	0.000	9.162	7	11.4802	4.0
8	2	30	1	39088	0.00	0.29	14.38	-16.89	11.480	9.162	1	9.3514	0.5
8	3	31	1001	38088	0.93	1.24	12.88	-16.41	7.075	9.162	2	11.1127	4.5
8	4	32	2004	37085	1.46	0.04	15.62	-16.22	7.964	9.162	6	10.4878	2.0

APPENDIX 8

n + <sup>238</sup>U PROBLEM SAMPLE INPUT

**RECORD**

<u>NO</u>	<u>DATA</u>	<u>COMMENTS</u>
1	U238 + n fission calculation - gn5cp0b tcu8tr ulevtr	Descriptive comments
2	gnipu8 14-MeV Test Calc for IAEA (Exc.Funct.Exer.) TITLE(N), N+1,20	
3	1 0 0 3 1 01 0 0 IPRTLEV, IPRTTC, IPRTWID, IPRTSP, IPRTGC, IPRE, IGAMCAS, ILD	Print flags
4	0 0 0 0 0 119 1 1 0 0 0 0 1 INPOPT, KLIN, KLIN, NIBD, LMAXOPT, NLDIR, ILDIN, LPDECAY, KSPLIT, LPOP, IHELV, IQBETA1, ISURF, ISEADD	Input setup option, no. of direct levels read from from TAPE33
5	3 3 2 1 0 0 1 0 0 0 0 1 NI, NMP, LGROPT, LPEQ, NJMAX, ICAPT, IFIS, IBSF, ISIG2, IWFC, LDELGC, ISPCUT	Set no. of CN's, $\gamma$ -ray multi- polarities, $\gamma$ -ray SF option, preeq. flag, etc.
6	2 0 4 5 NBAR, IDIAF, IHFACT, KPMAX	No. of fission barriers
7	1. 92238. 0.50 ZAP, ZAT, DE	Projectile and target description, energy bin width.
8	0.0888 -1.0 1.0 SCUTFTR, SDFTR, OLDGC	Spin cutoff constant specification.
9	01 NELAB	No. of incident energies
10	12.0 0.00 0.00 0.00 0.00 ELABS(N), N=1, NELAB	Incident energy

**RECORD**

<u>NO</u>	<u>DATA</u>						<u>COMMENTS</u>
11	92239.	3.	0.	0.	+0.00630		First CN, no. decays, gamma-ray strength funct. norm.
	ZACN,	XNIP,	CNPI,	CNPIP,	SWS		
12	0.	0.	29.088	0.	0.	0.	Gamma emission
	ZA1,	XNL,	A,	XNLGC,	BCGC,	XNLGCL,	
13	0.	0.	0.	0.	0.	0.	
	EOIN,	TGCIN,	EMATIN,	SIG2,	PA,	EDS	
14	1.	0.	29.482	17.	1.000	0.	Neutron emission
	ZA1,	XNL,	A,	XNLGC,	BCGC,	XNLGCL,	
15	0.	0.	0.	0.	1.36	0.	
	EOIN,	TGCIN,	EMATIN,	SIG2,	PA,	EDS	
16	99.	0.	29.088	0.	0.	0.	Fission channel
	ZA1,	XNL,	A,	XNLGC,	BCGC,	XNLGCL,	
17	0.	0.	0.	0.	0.	0.	
	EOIN,	TGCIN,	EMATIN,	SIG2,	PA,	EDS	
18	92238.	3.	1.	2.	-0.		Second CN, no. decays, parent reaction indicators (I, IP)
19	0.	0.	29.482	17.	1.000	0.	Gamma emission
20	0.	0.	0.	0.	1.36	0.	
21	1.	10.	29.766	0.	0.	0.	Neutron emission
22	0.	0.	0.	0.	0.74	0.	
23	99.	0.	29.482	17.	1.000	0.	Fission channel
24	0.	0.	0.	0.	1.36	0.	
25	92237.	3.	2.	2.	-0.		Third CN no. decays, parent reaction indicators
26	0.	10.	29.766	0.	0.	0.	Gamma emission
27	0.	0.	0.	0.	0.74	0.	
28	1.	0.	28.532	0.	0.	0.	Neutron emission
29	0.	0.	0.	0.	1.40	0.	



**RECORD**

NO		DATA					COMMENTS
30	99.	0.	29.766	0.	0.	0.	Fission channel
31	0.	0.	0.	0.	0.74	0.	
32		e1 0.9	.5763				E1 gamma-ray norm.
33		m1 0.1	25.76				M1 gamma-ray norm.
34		e2 0.	27.06				E2 gamma-ray norm.
LNQHOL (MP), LG, RE1 (MP), GGDNORM (MP)							
35	10.77	2.37	13.80	5.13	1.476		Gamma-ray shape parameters
	EG1,	GG1,	EG2,	GG2,	G2NORM		
36	0.3	0.	0.500	0.	0.	0.	GDR E1 photoneutron cross section.
	SIGE1,	SIGN1,	EGCON,	GDSTEP,	GDELS,	GDELSL	
37	1.3	17.92					Preequilibrium norm. and composite system state density
	F2,	GG					
38	6.24	5.99					Barrier heights <sup>239</sup> U
	EBAR(1),	EBAR(2)					
39	1.00	.50					Barrier widths <sup>239</sup> U
	XBOM(1),	XBOM(2)					
40	12.	2.					Barrier enhancements <sup>239</sup> U
	DENFAC(1),	DENFAC(2)					
41	+036.						No. transition states to directly read for <sup>239</sup> U
	FSTS						
42	.0015	-0.5					1st transition state
43	.012	-1.5					2nd transition state
44	.032	-2.5					3rd transition state
45	.06	-3.5					4th transition state

**RECORD****NO****DATA****COMMENTS**

46	.096	-4.5
47	.14	-5.5
48	.192	-6.5
49	.252	-7.5
50	.0015	0.5
51	.013	1.5
52	.033	2.5
53	.061	3.5
54	.097	4.5
55	.141	5.5
56	.193	6.5
57	.253	7.5
58	.1	1.5
59	.12	2.5
60	.148	3.5
61	.184	4.5
62	.228	5.5
63	.28	6.5
64	.1	-1.5
65	.12	-2.5
66	.148	-3.5
67	.184	-4.5
68	.19	0.5
69	.202	1.5
70	.222	2.5
71	.25	3.5
72	.286	4.5
73	.195	-0.5
74	.207	-1.5
75	.227	-2.5
76	.255	-3.5
77	.291	-4.5

**BBBF,****XJPIF**

36th transition state

**RECORD**

**NO**

**DATA**

**COMMENTS**

NO	DATA	COMMENTS
78	5.77            5.31 EBAR(1),    EBAR(2)	Barrier heights 238U
79	0.50            .50 XBOM(1),    XBOM(2)	Barrier widths 238U
80	3.5             2.0 DENFAC(1), DENFAC(2)	Barrier enhancements 238U
81	-1. FSTS	Flag indicating bandhead data
82	4 IBAND	No. transition state bandheads, barrier A 238U
83	0.            0.            1.	Begin bandhead data barrier A
84	0.3           0.           -1.	
85	0.7           2.	
86	0.9           -1.	
	EBAND,        XJPIBA,        PIB	
87	4 IBAND	No. bandheads, barrier B 238U bandheads, barrier A 238U
88	0.            0.            1.	Begin bandhead data barrier B
89	0.3           0.           -1.	
90	0.7           2.	
91	0.9           -1.	
	EBAND,        XJPIBA,        PIB	
92	6.03           5.63	Begin barrier parameters, 237U
93	0.50           .50	
94	01.8           1.8	
95	-1.	

143

**RECORD****NO****DATA****COMMENTS**

96	5			Begin transition state data, barrier A, <sup>237</sup> U
97	0.	0.5		
98	0.	1.5		
99	0.047	-3.5		
100	0.054	-2.5		
101	0.114	5.5		
102	5			Begin transition state data, barrier B, <sup>237</sup> U
103	0.	0.5		
104	0.001	5.5		
105	0.013	1.5		
106	0.017	-2.5		
107	0.110	-3.5		

APPENDIX 9

SELECTED PORTIONS OF OUTPUT FILE FROM n + <sup>238</sup>U CALCULATION

1. Input Data

U238 + n fission calculation - gn5cp0b tcu8tr ulevtr t33nutr  
gnipu8 14-MeV Test Calc for IAEA (Exc.Funct.Exercise)

the date and time of this calculation are 11/06/91 15:28:41  
GNASH Version and Date: GN5X0b, 1 Nov. 1991 - Version for Trieste (3/92) course.  
iprtlev= 1 iprttc= 0 iprtwid= 0 iprtsp= 3 iprtgc= 1 ipre= 1 igamcas= 0  
inpopt= 0 klin= 8 ktin=10 nibd= 0 lmaxopt= 0 iseadd= 0  
nldir= 119 ildin= 1 ild= 0 lpop= 0  
lpdecay = 1 (0 = on, 1 = off) ksplit = 5 ihelv = 0 iqbeta= 0 isurf= 1 ibeoff= 1  
ibsf= 0 isig2= 0 iwfc= 0 ldelgc= 0 ispcut= 1 lgsfint= 0  
number of lcm buffers is 10  
maximum number of energy bins is 100  
approximate storage requirements for 1-, 2-, 3-dimensional variables in common = 4611 33094 187616  
total storage requirements of common variables = 225321  
nidim= 10 nipdim= 6 njdim= 40 nkdim= 100 nldim= 36 niddim= 7 nlevdim= 60  
needim= 38 ngrdim= 100 nmpdim= 6 nfedim= 25 nfisn=10 nibdim= 10 nfadim= 51  
nupdim= 40 neddim= 40 ks= 35  
ni= 5 nmp= 3 lgropt= 2 lpeq= 1 njmax= 40 icapt= 0  
jrst level increment = 0  
zap= 1. zat=92238. de= 0.500 mev xmt= 238.05078 amu sp= 4.806 mev ecutoff= 0.10 mev  
acn= 29.088 /mev fsigcn= 1.000 defcn=1. spint = 0.0 pit= 1.  
scutftr= 0.08880 sdftr= 0.00 ioldgc= 1  
  
incident energies (mev) = 1.200e+01

145

## 2. Reaction Labeling, Reaction Parentage, Masses, Buffer Numbers

i	zacr	nip	parent (line 2)	s-wave strength, energy	ip	ir	zal	za2	xmr (amu)	s (mev)	nlev	def	a (/mev)	nlgc	ecgc (mev)	buffer number
1	92239.	3.		6.300e-03 4.806												
	i=		1. ip=	1.	1	1	0.	92239.	239.054	0.000	0.	1.	29.1	0.	0.000	1
					2	2	1.	92238.	238.051	4.806	0.	1.	29.5	17.	1.000	2
					3	3	99.	92239.	239.054	0.000	0.	1.	29.1	0.	0.000	0
2	92238.	3.		0.000e+00 6.153												
	i=		1. ip=	2.	1	4	0.	92238.	238.051	0.000	0.	1.	29.5	17.	1.000	2
					2	5	1.	92237.	237.049	6.153	10.	1.	29.8	0.	0.000	3
					3	6	99.	92238.	238.051	0.000	0.	1.	29.5	17.	1.000	0
3	92237.	3.		0.000e+00 5.126												
	i=		2. ip=	2.	1	7	0.	92237.	237.049	0.000	10.	1.	29.8	0.	0.000	3
					2	8	1.	92236.	236.046	5.126	0.	1.	28.5	0.	0.000	4
					3	9	99.	92237.	237.049	0.000	0.	1.	29.8	0.	0.000	0
4	92236.	3.		0.000e+00 6.545												
	i=		3. ip=	2.	1	10	0.	92236.	236.046	0.000	0.	1.	28.5	0.	0.000	4
					2	11	1.	92235.	235.044	6.545	0.	1.	29.0	0.	0.000	5
					3	12	99.	92236.	236.046	0.000	0.	1.	28.5	0.	0.000	0
5	92235.	2.		0.000e+00 5.298												
	i=		4. ip=	2.	1	13	0.	92235.	235.044	0.000	0.	1.	29.0	0.	0.000	5
					2	14	99.	92235.	235.044	0.000	0.	1.	29.0	0.	0.000	0

### 3. Fission Barrier Parameters

-----multi hump fission barrier parameters-----

za-fis	ebar1	ebar2	ebar3	hbar1	hbar2	hbar3	denfac1	denfac2	denfac3	hfcc
92239.	6.2400	5.9900	0.0000	1.00	0.50	0.00	12.00	2.00	0.00	

fission transition states for za = 92239. barrier number 1

e(mev)	barrier height(mev)	j-pi
0.0015	6.2415	-0.5
0.0120	6.2520	-1.5
0.0320	6.2720	-2.5
0.0600	6.3000	-3.5
0.0960	6.3360	-4.5
0.1400	6.3800	-5.5
0.1920	6.4320	-6.5
0.2520	6.4920	-7.5
0.0015	6.2415	0.5
0.0130	6.2530	1.5
0.0330	6.2730	2.5
0.0610	6.3010	3.5
0.0970	6.3370	4.5
0.1410	6.3810	5.5
0.1930	6.4330	6.5
0.2530	6.4930	7.5
0.1000	6.3400	1.5
0.1200	6.3600	2.5
0.1480	6.3880	3.5
0.1840	6.4240	4.5
0.2280	6.4680	5.5
0.2800	6.5200	6.5
0.1000	6.3400	-1.5
0.1200	6.3600	-2.5
0.1480	6.3880	-3.5
0.1840	6.4240	-4.5
0.1900	6.4300	0.5
0.2020	6.4420	1.5
0.2220	6.4620	2.5
0.2500	6.4900	3.5
0.2860	6.5260	4.5

for barrier 1 the continuum begins at 0.292e+00 mev  
 there are 36. transition states up to an energy of 0.291e+00 mev

### 3. Fission Barrier Parameters (Cont'd)

fission transition states for za = 92239. barrier number 2

e(mev)	barrier height(mev)	j-pi
0.0015	5.9915	-0.5
0.0120	6.0020	-1.5
0.0320	6.0220	-2.5
0.0600	6.0500	-3.5
0.0960	6.0860	-4.5
0.1400	6.1300	-5.5
0.1920	6.1820	-6.5
0.2520	6.2420	-7.5
0.0015	5.9915	0.5
0.0130	6.0030	1.5
0.0330	6.0230	2.5
0.0610	6.0510	3.5
0.0970	6.0870	4.5
0.1410	6.1310	5.5
0.1930	6.1830	6.5
0.2530	6.2430	7.5
0.1000	6.0900	1.5
0.1200	6.1100	2.5
0.1480	6.1380	3.5
0.1840	6.1740	4.5
0.2280	6.2180	5.5
0.2800	6.2700	6.5
0.1000	6.0900	-1.5
0.1200	6.1100	-2.5
0.1480	6.1380	-3.5
0.1840	6.1740	-4.5
0.1900	6.1800	0.5
0.2020	6.1920	1.5
0.2220	6.2120	2.5
0.2500	6.2400	3.5
0.2860	6.2760	4.5
0.1950	6.1850	-0.5
0.2070	6.1970	-1.5
0.2270	6.2170	-2.5
0.2550	6.2450	-3.5
0.2910	6.2810	-4.5

for barrier 2 the continuum begins at 0.292e+00 mev  
 there are 36. transition states up to an energy of 0.291e+00 mev



### 3. Fission Barrier Parameters (Cont'd)

-----multi hump fission barrier parameters-----

za-fis	ebar1	ebar2	ebar3	hbar1	hbar2	hbar3	denfac1	denfac2	denfac3	hfact
92238.	5.7700	5.3100	0.0000	0.50	0.50	0.00	3.50	2.00	0.00	

fission transition states for za = 92238. barrier number 1

e(mev)	barrier height(mev)	j-pi
0.0000	5.7700	0.0
0.0240	5.7940	2.0
0.0800	5.8500	4.0
0.1680	5.9380	6.0
0.2880	6.0580	8.0
0.4400	6.2100	10.0
0.3000	6.0700	-1.0
0.3240	6.0940	-3.0
0.3800	6.1500	-5.0
0.4680	6.2380	-7.0
0.5880	6.3580	-9.0
0.7000	6.4700	2.0
0.7240	6.4940	3.0
0.7560	6.5260	4.0
0.7960	6.5660	5.0
0.8440	6.6140	6.0
0.9000	6.6700	7.0
0.9640	6.7340	8.0
1.0360	6.8060	9.0
1.1160	6.8860	10.0
0.9000	6.6700	-1.0
0.9160	6.6860	-2.0
0.9400	6.7100	-3.0
0.9720	6.7420	-4.0
1.0120	6.7820	-5.0
1.0600	6.8300	-6.0
1.1160	6.8860	-7.0
1.1800	6.9500	-8.0
1.2520	7.0220	-9.0
1.3320	7.1020	-10.0

for barrier 1 the continuum begins at 0.133e+01 mev  
 there are 30. transition states up to an energy of 0.133e+01 mev

### 3. Fission Barrier Parameters (Cont'd)

fission transition states for za =		92238. barrier number	2
e (mev)	barrier height (mev)	j-pi	
0.0000	5.3100	0.0	
0.0240	5.3340	2.0	
0.0800	5.3900	4.0	
0.1680	5.4780	6.0	
0.2880	5.5980	8.0	
0.4400	5.7500	10.0	
0.3000	5.6100	-1.0	
0.3240	5.6340	-3.0	
0.3800	5.6900	-5.0	
0.4680	5.7780	-7.0	
0.5880	5.8980	-9.0	
0.7000	6.0100	2.0	
0.7240	6.0340	3.0	
0.7560	6.0660	4.0	
0.7960	6.1060	5.0	
0.8440	6.1540	6.0	
0.9000	6.2100	7.0	
0.9640	6.2740	8.0	
1.0360	6.3460	9.0	
1.1160	6.4260	10.0	
0.9000	6.2100	-1.0	
0.9160	6.2360	-2.0	
0.9400	6.2500	-3.0	
0.9720	6.2820	-4.0	
1.0120	6.3220	-5.0	
1.0600	6.3700	-6.0	
1.1160	6.4260	-7.0	
1.1800	6.4900	-8.0	
1.2520	6.5620	-9.0	
1.3320	6.6420	-10.0	

for barrier 2 the continuum begins at 0.133e+01 mev  
 there are 30. transition states up to an energy of 0.133e+01 mev

#### 4. Direct Reaction Cross Section Data

DIRECT REACTION/PREEQUILIBRIUM PRINT SECTION  
 STILL I=1 LOOP IN SUBROUTINE SPECTRA/PRECMP

\*\*\*\*\* elab = 12.00 mev \*\*\*\*\*

direct xsec input

nl	elev(mev)	x-sec(b)
1	0.00000	0.00000e+00
2	0.04491	2.60060e-01
3	0.14841	5.18632e-02
4	0.30721	8.76205e-03
5	0.51830	9.98163e-04
6	0.68010	0.00000e+00
7	0.73190	1.66996e-02
8	0.77570	0.00000e+00
9	0.82670	0.00000e+00
10	0.92570	0.00000e+00
11	0.93080	0.00000e+00
12	0.95020	0.00000e+00
13	0.96630	0.00000e+00
14	0.96730	5.12099e-04
15	0.99300	0.00000e+00
16	0.99750	5.94030e-03
17	1.03730	1.90750e-03
18	1.05660	0.00000e+00
19	1.05950	3.96579e-03

Coupled-channel reactions: Levels 2-5  
 Sum of cross sections = 0.3217 b

DWBA reactions: Levels 7, 14, 16, 17, 19  
 Sum of cross sections = 0.02902 b

Sum of all direct cross sections = 0.3507 b

## 5. Preequilibrium Information

preequilibrium spectra calculated with precoc

occupation probabilities p0= 2 h0= 1  
target z= 92. n=146. proj z= 0 n= 1  
g= 17.920 e= 17.250  
scale factor = 1.300 strength left= 0.654  
number of iterations= 1.870e+02 elapsed time 4.573e-09psec

p	h	cpi(p,h)	equi(p,h)
1	0	4.191e-09	2.012e-14
2	1	1.082e-07	1.534e-12
3	2	2.136e-05	1.946e-09
4	3	6.948e-04	4.679e-07
5	4	8.378e-03	3.358e-05
6	5	4.982e-02	9.075e-04
7	6	1.390e-01	1.058e-02
8	7	2.006e-01	5.786e-02
9	8	1.599e-01	1.562e-01
10	9	7.307e-02	2.141e-01
11	10	1.937e-02	1.503e-01
12	11	2.950e-03	5.376e-02
13	12	2.490e-04	9.568e-03
14	13	1.083e-05	8.144e-04
15	14	2.112e-07	3.118e-05
16	15	1.361e-09	4.916e-07
17	16	1.069e-12	2.812e-09

particle spectra z= 0 n= 1  
first emission at p= 1  
target z= 92. n=146. proj z= 0 n= 1  
p0= 2 n0= 1 g=17.920 e=17.250  
reaction cross section = 2.7888 b  
number of iterations= 1.870e+02 elapsed time 4.573e-09psec  
scale factor = 1.300 strength left= 0.654  
closed form sum starts at p= 2

5. Preequilibrium Information (Cont'd)

spectra after preequilibrium for id = 1				
i	e(mev)	preequil(b/mev)	mod equil(b/mev)	total(b/mev)
1	0.500	0.8954e-01	0.1035e+01	0.1124e+01
2	1.000	0.1243e+00	0.7487e+00	0.2730e+00
3	1.500	0.1473e+00	0.5230e+00	0.6704e+00
4	2.000	0.1534e+00	0.3094e+00	0.4628e+00
5	2.500	0.1479e+00	0.1598e+00	0.3078e+00
6	3.000	0.1376e+00	0.7721e-01	0.2149e+00
7	3.500	0.1274e+00	0.3562e-01	0.1630e+00
8	4.000	0.1176e+00	0.1576e-01	0.1333e+00
9	4.500	0.1081e+00	0.6677e-02	0.1148e+00
10	5.000	0.9997e-01	0.2726e-02	0.1027e+00
11	5.500	0.9244e-01	0.1065e-02	0.9351e-01
12	6.000	0.8540e-01	0.3962e-03	0.8580e-01
13	6.500	0.7917e-01	0.1405e-03	0.7931e-01
14	7.000	0.7356e-01	0.4704e-04	0.7361e-01
15	7.500	0.6797e-01	0.1510e-04	0.6798e-01
16	8.000	0.6201e-01	0.4804e-05	0.6202e-01
17	8.500	0.5563e-01	0.1511e-05	0.5564e-01
18	9.000	0.4894e-01	0.4700e-06	0.4894e-01
19	9.500	0.4195e-01	0.1443e-06	0.4195e-01
20	10.000	0.3467e-01	0.4188e-07	0.3467e-01
21	10.500	0.2716e-01	0.1755e-09	0.2716e-01
22	11.000	0.1935e-01	0.4147e-08	0.1935e-01
23	11.500	0.1109e-01	0.5985e-09	0.1109e-01
24	12.000	0.7561e-02	0.4901e-09	0.7561e-02

pfract,sigr,psum,csum,spp(3,1) 6.499e-01 2.789e+00 9.763e-01 2.786e+00 1.083e+00  
i.pfract,spfis,spp 1 6.499e-01 1.083e+00 7.041e-01

## 6. Binary Cross Sections

1U238 + fission calculation - gn5cp0b tcu8tr ulevtr t33nutr  
 gnipu8 4-MeV Test Calc for IAEA (Exc.Funct.Exercise)

lab neutron energy = 1.2000e+01 mev	total x/s (barns) = 5.6771e+00	TAPE10 (Coupled Channel Opt. Mod.)
	elastic x/s (barns) = 2.5761e+00	TAPE10 shape el. x/s + GNASH com. elas x/s
	nonelastic x/s (barns) = 3.1011e+00	TAPE10 react. x/s - GNASH com. elas. x/s
	total reaction x/s (barns) = 3.1014e+00	TAPE10
	shape elastic x/s (barns) = 2.5757e+00	TAPE10
	compd elastic x/s (barns) = 3.3552e-04	GNASH
	direct reaction x/s (barns) = 3.5071e-01	Coupled-chan. + DWBA (TAPE33)
	compd reaction x/s (barns) = 2.7507e+00	TAPE10 total reac. x/s - direct reac. x/s
	radiat. capture x/s (barns) = 4.0720e-03	Not applicable (ICAPT = 0)
	semidir capture x/s (barns) = 1.0707e-03	Direct-semidirect calculation
	discrete inelas x/s (barns) = 3.7266e-01	GNASH

binary reaction summaries (compound nucleus only)

reaction product	sigma (barns)	
reaction	2.7888e+00	(Also includes DWBA component of direct reaction cross sections)
gammaray	3.0013e-03	
neutron	2.2442e+00	
fission	5.4165e-01	

----- pre-equilibrium summary -----

ip = 2 id = 1 outgoing particle = neutron  
 initial exciton number = 3 preq normalization = 5.00000e-04  
 compound x-sec(barns) = 1.45772e+00 preeq x-sec(barns) = 9.80034e-01

# 7. Individual Reaction Spectra for n + <sup>238</sup>U Calculation

spectra from individual reactions

	zacr=92239 zal= 0 za2=92239	zacr=92239 zal= 1 za2=92238	zacr=92239 zal= 99 za2=92239	zacr=92238 zal= 0 za2=92238	zacr=92238 zal= 1 za2=92237	zacr=92238 zal= 99 za2=92238	zacr=92237 zal= 0 za2=92237	zacr=92237 zal= 1 za2=92236	zacr=92237 zal= 99 za2=92237	zacr=92236 zal= 0 za2=92236
level decay c/s=	5.2137-12	0.00000+0	0.00000+0	1.46594+0	0.00000+0	0.00000+0	3.46647+0	0.00000+0	0.00000+0	4.70731-2
level excit c/s=	8.5503-12	3.72993-1	0.00000+0	2.14281+0	7.36047-2	0.00000+0	4.67146+0	2.94585-2	0.00000+0	7.65317-2
total prod. c/s=	4.66092-3	2.78846+0	3.52036-1	2.17018+0	1.45491+0	6.46382-1	6.60592+0	2.94585-2	2.09626-1	4.70731-2
avg.energy (mev)	6.99646+0	3.68726+0	3.75000-1	8.62285-1	7.49491-1	3.75000-1	8.21130-1	3.75000-1	3.75000-1	3.75000-1
k	energy (mev)	sigma (b/mev)	sigma (b/mev)	sigma (b/mev)	sigma (b/mev)	sigma (b/mev)	sigma (b/mev)	sigma (b/mev)	sigma (b/mev)	sigma (b/mev)
1	0.50000	1.27829-5	1.12427+0	7.04072-1	2.85162+0	1.71257+0	1.29276+0	8.07713-0	5.89171-2	4.19252-1
2	1.00000	1.10713-4	8.73025-1	0.00000+0	4.20288-1	7.36819-1	0.00000+0	2.26384+0	0.00000+0	0.00000+0
3	1.50000	3.02899-4	6.70373-1	0.00000+0	3.87178-1	3.04396-1	0.00000+0	1.40675+0	0.00000+0	0.00000+0
4	2.00000	5.16237-4	4.62830-1	0.00000+0	3.36220-1	1.07992-1	0.00000+0	2.06143-1	0.00000+0	0.00000+0
5	2.50000	6.78175-4	3.07764-1	0.00000+0	1.86311-1	3.43426-2	0.00000+0	4.00242-1	0.00000+0	0.00000+0
6	3.00000	7.55151-4	2.14862-1	0.00000+0	9.04675-2	1.01063-2	0.00000+0	1.70035-1	0.00000+0	0.00000+0
7	3.50000	7.40908-4	1.62992-1	0.00000+0	3.99979-2	2.74381-3	0.00000+0	6.26248-2	0.00000+0	0.00000+0
8	4.00000	6.84684-4	1.33312-1	0.00000+0	1.57129-2	6.71290-4	0.00000+0	1.93064-2	0.00000+0	0.00000+0
9	4.50000	5.86023-4	1.14811-1	0.00000+0	6.90976-3	1.39829-4	0.00000+0	5.01271-3	0.00000+0	0.00000+0
10	5.00000	4.76015-4	1.02695-1	0.00000+0	2.90826-3	2.87892-5	0.00000+0	7.43927-4	0.00000+0	0.00000+0
11	5.50000	3.69524-4	9.35059-2	0.00000+0	1.13511-3	3.67361-6	0.00000+0	1.04140-5	0.00000+0	0.00000+0
12	6.00000	2.75524-4	8.57981-2	0.00000+0	3.96423-4	1.74626-7	0.00000+0	2.89300-7	0.00000+0	0.00000+0
13	6.50000	1.99670-4	7.93104-2	0.00000+0	1.32094-4	0.00000+0	0.00000+0	0.00000+0	0.00000+0	0.00000+0
14	7.00000	1.44699-4	7.36116-2	0.00000+0	5.33627-5	0.00000+0	0.00000+0	0.00000+0	0.00000+0	0.00000+0
15	7.50000	1.09532-4	6.79830-2	0.00000+0	2.07300-5	0.00000+0	0.00000+0	0.00000+0	0.00000+0	0.00000+0
16	8.00000	9.08910-5	6.20181-2	0.00000+0	8.25609-6	0.00000+0	0.00000+0	0.00000+0	0.00000+0	0.00000+0
17	8.50000	8.61038-5	5.56360-2	0.00000+0	3.36838-6	0.00000+0	0.00000+0	0.00000+0	0.00000+0	0.00000+0
18	9.00000	9.46976-5	4.89406-2	0.00000+0	1.34517-6	0.00000+0	0.00000+0	0.00000+0	0.00000+0	0.00000+0
19	9.50000	1.18936-4	4.19506-2	0.00000+0	5.27644-7	0.00000+0	0.00000+0	0.00000+0	0.00000+0	0.00000+0
20	10.00000	1.61364-4	3.46680-2	0.00000+0	1.99914-7	0.00000+0	0.00000+0	0.00000+0	0.00000+0	0.00000+0
21	10.50000	2.09821-4	2.71555-2	0.00000+0	9.83935-8	0.00000+0	0.00000+0	0.00000+0	0.00000+0	0.00000+0
22	11.00000	2.28213-4	7.74007-2	0.00000+0	3.04278-8	0.00000+0	0.00000+0	0.00000+0	0.00000+0	0.00000+0
23	11.50000	2.18291-4	3.06087-2	0.00000+0	7.25869-9	0.00000+0	0.00000+0	0.00000+0	0.00000+0	0.00000+0
24	12.00000	2.13974-4	6.31406-1	0.00000+0	5.2241-10	0.00000+0	0.00000+0	0.00000+0	0.00000+0	0.00000+0
25	12.50000	2.23879-4	0.00000+0	0.00000+0	0.00000+0	0.00000+0	0.00000+0	0.00000+0	0.00000+0	0.00000+0

# 8. Composite Spectra for Emission Particles and Gamma Rays

## composite spectra

	neutron spectrum	proton spectrum	fission spectrum	triton spectrum	helium-3 spectrum	helium-4 spectrum	gammaray spectrum	g, neutrn spectrum
	sigma (barns)	sigma (barns)	sigma (barns)	sigma (barns)	sigma (barns)	sigma (barns)	sigma (barns)	sigma (barns)
total prod. c/s	4.27283+0	0.00000+0	1.20804+0	0.00000+0	0.00000+0	0.00000+0	8.82784+0	0.00000+0
avg. energy (mev)	2.66410+0	0.00000+0	3.75000-1	0.00000+0	0.00000+0	0.00000+0	8.32129-1	0.00000+0
energy (mev)	sigma (b/mev)	sigma (b/mev)	sigma (b/mev)	sigma (b/mev)	sigma (b/mev)	sigma (b/mev)	sigma (b/mev)	sigma (b/mev)
0.00000	2.89576-1	0.00000+0	2.41609+0	0.00000+0	0.00000+0	0.00000+0	1.10229+1	0.00000+0
0.50000	1.6099-1	0.00000+0	0.00000+0	0.00000+0	0.00000+0	0.00000+0	2.68424+0	0.00000+0
1.00000	9.7474-1	0.00000+0	0.00000+0	0.00000+0	0.00000+0	0.00000+0	1.79424+0	0.00000+0
1.50000	5.777-1	0.00000+0	0.00000+0	0.00000+0	0.00000+0	0.00000+0	1.14268+0	0.00000+0
2.00000	3.4113-1	0.00000+0	0.00000+0	0.00000+0	0.00000+0	0.00000+0	5.87231-1	0.00000+0
2.50000	2.4469-1	0.00000+0	0.00000+0	0.00000+0	0.00000+0	0.00000+0	2.61258-1	0.00000+0
3.00000	1.6236-1	0.00000+0	0.00000+0	0.00000+0	0.00000+0	0.00000+0	1.03373-1	0.00000+0
3.50000	1.0984-1	0.00000+0	0.00000+0	0.00000+0	0.00000+0	0.00000+0	3.67039-2	0.00000+0
4.00000	7.4951-2	0.00000+0	0.00000+0	0.00000+0	0.00000+0	0.00000+0	1.25085-2	0.00000+0
4.50000	5.02724-2	0.00000+0	0.00000+0	0.00000+0	0.00000+0	0.00000+0	4.12820-3	0.00000+0
5.00000	3.35095-2	0.00000+0	0.00000+0	0.00000+0	0.00000+0	0.00000+0	1.51505-3	0.00000+0
5.50000	2.157983-2	0.00000+0	0.00000+0	0.00000+0	0.00000+0	0.00000+0	6.72236-4	0.00000+0
6.00000	1.393104-2	0.00000+0	0.00000+0	0.00000+0	0.00000+0	0.00000+0	3.31764-4	0.00000+0
6.50000	8.736116-2	0.00000+0	0.00000+0	0.00000+0	0.00000+0	0.00000+0	1.98062-4	0.00000+0
7.00000	5.679830-2	0.00000+0	0.00000+0	0.00000+0	0.00000+0	0.00000+0	1.30262-4	0.00000+0
7.50000	3.620181-2	0.00000+0	0.00000+0	0.00000+0	0.00000+0	0.00000+0	9.91470-5	0.00000+0
8.00000	2.356360-2	0.00000+0	0.00000+0	0.00000+0	0.00000+0	0.00000+0	6.94722-5	0.00000+0
8.50000	1.5489406-2	0.00000+0	0.00000+0	0.00000+0	0.00000+0	0.00000+0	4.60428-5	0.00000+0
9.00000	1.019506-2	0.00000+0	0.00000+0	0.00000+0	0.00000+0	0.00000+0	3.19464-4	0.00000+0
9.50000	6.746680-2	0.00000+0	0.00000+0	0.00000+0	0.00000+0	0.00000+0	2.151564-4	0.00000+0
10.00000	4.571555-2	0.00000+0	0.00000+0	0.00000+0	0.00000+0	0.00000+0	1.499919-4	0.00000+0
10.50000	3.174007-2	0.00000+0	0.00000+0	0.00000+0	0.00000+0	0.00000+0	1.028243-4	0.00000+0
11.00000	2.206087-2	0.00000+0	0.00000+0	0.00000+0	0.00000+0	0.00000+0	1.518298-4	0.00000+0
11.50000	1.531406-1	0.00000+0	0.00000+0	0.00000+0	0.00000+0	0.00000+0	1.013974-4	0.00000+0
12.00000	0.000000+0	0.00000+0	0.00000+0	0.00000+0	0.00000+0	0.00000+0	7.023879-4	0.00000+0
12.50000	0.000000+0	0.00000+0	0.00000+0	0.00000+0	0.00000+0	0.00000+0	4.840376-4	0.00000+0
13.00000	0.000000+0	0.00000+0	0.00000+0	0.00000+0	0.00000+0	0.00000+0		



9. Level Density Information for n + <sup>238</sup>U Calculation

level density parameters

i	ip	ir	izal	iza2	a (/mev)	temp (mev)	e0 (mev)	ematch (mev)	ecut (mev)	levels at	ecut1 (mev)	levels at	sig2	q (mev)	pair (mev)	d0 (ev)
1	1	1	0	92239	29.088	0.343	-0.288	2.751	0.7572	21.	.....	0.	0.000	4.8065	0.470	2.030e-01
1	2	2	1	92238	29.482	0.404	-0.144	4.850	1.0000	17.	.....	0.	0.000	0.0000	1.360	3.501e-00
1	3	3	99	92239	29.088	0.421	-1.219	4.263	0.2910	36.	.....	0.	0.000	0.0000	0.470	0.000e-00
1	3	3	99	92239	29.088	0.421	-1.219	4.263	0.2910	36.	.....	0.	0.000	0.0000	0.470	0.000e-00
2	1	4	0	92238	29.482	0.404	-0.144	4.850	1.0000	17.	.....	0.	0.000	0.0000	1.360	3.501e-00
2	2	5	1	92237	29.766	0.390	-0.625	3.999	0.2740	10.	.....	0.	0.000	-6.1528	0.740	1.470e-01
2	3	6	99	92238	29.482	0.404	-0.144	4.850	1.0000	17.	.....	0.	0.000	0.0000	1.360	0.000e-00
2	3	6	99	92238	29.482	0.404	-0.144	4.850	1.0000	17.	.....	0.	0.000	0.0000	1.360	0.000e-00
3	1	7	0	92237	29.766	0.390	-0.625	3.999	0.2740	10.	.....	0.	0.000	-6.1528	0.740	1.470e-01
3	2	8	1	92236	28.532	0.425	-0.264	5.176	1.1044	25.	.....	0.	0.000	-11.2786	1.400	7.335e-01
3	3	9	99	92237	29.766	0.425	-1.107	4.747	0.5020	44.	.....	0.	0.000	0.0000	0.740	0.000e-00
3	3	9	99	92237	29.766	0.425	-1.107	4.747	0.5020	44.	.....	0.	0.000	0.0000	0.740	0.000e-00
4	1	10	0	92236	28.532	0.425	-0.264	5.176	1.1044	25.	.....	0.	0.000	-11.2786	1.400	7.335e-01
4	2	11	1	92235	28.997	0.405	-0.824	4.057	0.5099	27.	.....	0.	0.000	-17.8237	0.630	1.000e-01
4	3	12	99	92236	28.532	0.410	-0.063	4.862	1.3320	30.	.....	0.	0.000	0.0000	1.400	0.000e-00
4	3	12	99	92236	28.532	0.410	-0.063	4.862	1.3320	30.	.....	0.	0.000	0.0000	1.400	0.000e-00
5	1	13	0	92235	28.997	0.405	-0.824	4.057	0.5099	27.	.....	0.	0.000	-17.8237	0.630	1.000e-01
5	2	14	99	92235	28.997	0.419	-1.018	4.360	0.5960	47.	.....	0.	0.000	0.0000	0.630	0.000e-00
5	2	14	99	92235	28.997	0.419	-1.018	4.360	0.5960	47.	.....	0.	0.000	0.0000	0.630	0.000e-00

i	ip	ir	izal	iza2	pn (mev)	pz (mev)	sn (mev)	sz (mev)	s (mev)	sac (mev)	id	sepn (mev)	spint
1	1	1	0	92239	-0.22	0.69	5.49	-5.04	0.000	0.000	7	4.8065	0.0
1	2	2	1	92238	0.26	0.69	5.28	-5.04	4.806	0.000	1	6.1528	0.5
1	3	3	99	92239	-0.22	0.69	5.49	-5.04	0.000	0.000	99	4.8065	0.0
2	1	4	0	92238	0.26	0.69	5.28	-5.04	0.000	4.806	7	6.1528	0.5
2	2	5	1	92237	0.05	0.69	4.93	-5.04	6.153	4.806	1	5.1258	0.0
2	3	6	99	92238	0.26	0.69	5.28	-5.04	0.000	4.806	99	6.1528	0.5
3	1	7	0	92237	0.05	0.69	4.93	-5.04	0.000	10.959	7	5.1258	0.0
3	2	8	1	92236	0.45	0.69	5.03	-5.04	5.126	10.959	1	6.5452	3.5
3	3	9	99	92237	0.05	0.69	4.93	-5.04	0.000	10.959	99	5.1258	0.0
4	1	10	0	92236	0.45	0.69	5.03	-5.04	0.000	16.085	7	6.5452	3.5
4	2	11	1	92235	-0.06	0.69	5.09	-5.04	6.545	16.085	1	5.2978	0.0
4	3	12	99	92236	0.45	0.69	5.03	-5.04	0.000	16.085	99	6.5452	3.5
5	1	13	0	92235	-0.06	0.69	5.09	-5.04	0.000	22.630	7	5.2978	0.0
5	2	14	99	92235	-0.06	0.69	5.09	-5.04	0.000	22.630	99	5.2978	0.0